

5-14-2010

## Numerical Simulation of Unsteady Hydrodynamics in the Lower Mississippi River

Mallory Davis  
*University of New Orleans*

Follow this and additional works at: <https://scholarworks.uno.edu/td>

---

### Recommended Citation

Davis, Mallory, "Numerical Simulation of Unsteady Hydrodynamics in the Lower Mississippi River" (2010).  
*University of New Orleans Theses and Dissertations*. 1126.  
<https://scholarworks.uno.edu/td/1126>

This Thesis is protected by copyright and/or related rights. It has been brought to you by ScholarWorks@UNO with permission from the rights-holder(s). You are free to use this Thesis in any way that is permitted by the copyright and related rights legislation that applies to your use. For other uses you need to obtain permission from the rights-holder(s) directly, unless additional rights are indicated by a Creative Commons license in the record and/or on the work itself.

This Thesis has been accepted for inclusion in University of New Orleans Theses and Dissertations by an authorized administrator of ScholarWorks@UNO. For more information, please contact [scholarworks@uno.edu](mailto:scholarworks@uno.edu).

# Numerical Simulation of Unsteady Hydrodynamics in the Lower Mississippi River

A Thesis

Submitted to the Graduate Faculty of the  
University of New Orleans  
in partial fulfillment of the  
requirements for the degree of

Master of Science  
in  
Civil & Environmental Engineering  
Hydraulic Engineering

by

Mallory Davis

B.S. University of New Orleans, 2008

May 2010

Copyright 2010, Mallory Davis

## **Acknowledgements**

The author wishes to thank Dr. J. Alex McCorquodale for his excellent guidance and patience. He had complete confidence in this project and gave his full support throughout. The author would also like to thank her mother for enduring the past few years and most especially the last few months during the creation of this thesis. There have been many long nights and leftover dinners, but she has graciously put up with it all. Thanks are extended to Joao Pereira for his animated conversations and technical debates, as well as his surplus of journal articles. Thanks are also extended to Jenni Schindler for her patience with the author's sometimes silly questions and for her never-ending friendship. The author would also like to acknowledge her good friend Lesley Cedotal for her constant support, confidence, and indispensable conversation that the author could not have lived without. Special thanks go to Geoff Rodrigue for his support and patience, as well as his generous formatting assistance. Lastly, the author wishes to thank her grandparents for their unyielding love and support during tough times. This study was funded by the Lake Pontchartrain Basin Foundation.



## Table of Contents

Copyright .....	ii
List of Figures .....	vi
List of Tables .....	xii
Abstract .....	xiv
Chapter 1: Introduction .....	1
Objectives .....	4
General Approach .....	4
Background and Literature Review .....	6
Description of Numerical Models .....	6
Potential Numerical Models .....	7
Numerical Modeling of the Lower Mississippi River .....	9
Chapter 2: Mississippi River .....	11
The Modeled Reach .....	13
Existing Diversions .....	16
Future Diversions .....	17
Miscellaneous .....	18
Barataria Basin .....	19
Chapter 3: Description of HEC-RAS Model .....	23
Overview .....	23
Geometric Data Editor .....	23
Unsteady Flow Data Editor .....	24
Unsteady Flow Analysis Editor .....	24
Governing Equations .....	25
Conservation of Mass (Continuity) .....	25
Conservation of Momentum .....	28
Finite Difference Method .....	33
Hydraulic Structures Equations .....	34
Chapter 4: Model Development .....	38
Geometry Data .....	38
Geometry Issues in HEC-RAS .....	39
Geometry Issues with Available Data .....	47
Hydraulic Structures .....	55
Channel Roughness .....	65
Unsteady Flow Data .....	66
Initial Conditions .....	66
Boundary Conditions .....	68
Specific Model Limitations .....	70

Chapter 5: Hydrodynamics Simulations .....	71
Calibration.....	71
Validation.....	80
Model Limitations.....	83
Chapter 6: Applications .....	86
Modeling Schemes.....	86
Results.....	87
Relative Sea Level Rise Study .....	87
West Bay Closure Study .....	98
Changes to the Delta Distributaries Study .....	106
Proposed Diversions Study .....	109
Proposed Diversions Combined with Changes to the Delta Distributaries Study .....	125
Chapter 7: Discussion .....	141
Relative Sea Level Rise Study .....	141
West Bay Closure Study .....	141
Proposed Diversions Study .....	142
Changes to the Delta Distributaries Study .....	142
Sources of Error .....	142
Chapter 8: Conclusions and Recommendations for Future Research.....	145
References.....	147
Appendix A: Junction Data.....	151
Appendix B: 2003 Barataria Basin LIDAR/bathymetry Image.....	169
Appendix C: Lacey Regime Equations.....	171
Appendix D: Initial Conditions.....	176
Appendix E: Acoustic Doppler Current Profiler Charts (Pratt, 2009).....	188
Appendix F: Boundary Conditions .....	191
Appendix G: Manning's $n$ Values .....	204
Appendix H: Passes Discharge Records .....	269
Appendix I: Flow Roughness Factors.....	284
Vita.....	286

## List of Figures

Figure 1-1: MODIS Satellite Image of Mississippi River Sediment Plume (Visible Earth, 2010) .....	1
Figure 1-2: Planning Units for the Multiple Lines of Defense Strategy (LPBF, 2008).....	3
Figure 1-3: Proposed MR Diversions and Channel Modifications for Planning Unit 1 from the Multiple Lines of Defense Strategy (LPBF, 2008) .....	3
Figure 1-4: Proposed MR Diversions for Planning Unit 2 from the Multiple Lines of Defense Strategy (LPBF, 2008) .....	4
Figure 1-5: HEC-RAS Model Schematic Overlaying Satellite Imagery (Pereira <i>et al.</i> 2010) .....	5
Figure 2-1: Google Earth Image of Old River Control structures (2010).....	12
Figure 2-2: Google Earth Image of Pass a Loutr� and North Pass from 2004 (2010).....	14
Figure 2-3: Google Earth Image of Pass a Loutr� and North Pass from 2007 (2010).....	15
Figure 2-4: HEC-RAS Image of Mississippi River Bird’s Foot Delta .....	16
Figure 2-5: Google Earth Image of Cuts at Fort St. Philip (2010) .....	17
Figure 2-6: Google Earth Image of Raccourci Island, Small Bayous, and Overland Storage Areas (2010) .....	19
Figure 2-7: Google Earth Image of Barataria Basin (2010) .....	21
Figure 2-8: HEC-RAS Image of Barataria Basin .....	22
Figure 3-1: Representative Control Volume for Conservation of Mass (Continuity) .....	25
Figure 3-2: Representative Control Volume for Conservation of Momentum.....	28
Figure 3-3: Computational Grid for the Box Scheme.....	34
Figure 3-4: Sluice Gate with Broad Crested Spillway.....	35
Figure 4-1: Google Earth Image of Davis Pond Freshwater Diversion Channel (2010) ...	39
Figure 4-2: Tecplot Image of Lac Des Allemands from 2003 LIDAR/bathymetry .....	41

Figure 4-3: HEC-RAS Image of Des Allemands Channels and Others .....	42
Figure 4-4: Google Earth Image of The Pen (2010) .....	43
Figure 4-5: Tecplot Image of Lake Cataouatche, Lake Salvador, Bayou Rigolettes, Bayou Perot, The Pen, Barataria Bay Waterway, ICCW, and Dixie Delta Canal from 2003 LIDAR/bathymetry .....	44
Figure 4-6: Tecplot Image of Bayou Perot, Bayou Rigolettes, Little Lake, Barataria Bay Waterway, Barataria Bay, and Wilkinson Canal from 2003 LIDAR/bathymetry .....	46
Figure 4-7: Tecplot Image of Barataria Bay from 2003 LIDAR/bathymetry .....	47
Figure 4-8: HEC-RAS Image of Bayou Lamoque North, Bayou Lamoque South, and Bayou Lamoque Channels.....	48
Figure 4-9: HEC-RAS Image of Fort St. Philip Equivalent Channel. ....	49
Figure 4-10: HEC-RAS Image of Caernarvon Channel .....	50
Figure 4-11: Google Earth Image of Cubit’s Gap with Main Pass, Avulsions, and Smaller Passes (2010) .....	51
Figure 4-12: HEC-RAS Image of Original Main Pass Channel .....	52
Figure 4-13: HEC-RAS Image of Altered Main Pass Channel .....	53
Figure 4-14: Google Earth Image of Grand Pass and Tiger Pass (2010).....	54
Figure 4-15: HEC-RAS Image of the West Bay Sediment Diversion Channel .....	55
Figure 4-16: HEC-RAS Image of the Bonnet Carré Spillway.....	56
Figure 4-17: 2008 Bohemia Spillway Roadway and Culvert Breach (LPBF, 2008).....	57
Figure 4-18: HEC-RAS Image of Upstream Section of Bohemia Spillway.....	58
Figure 4-19: HEC-RAS Image of Middle Section of Bohemia Spillway.....	59
Figure 4-20: HEC-RAS Image of Downstream Section of Bohemia Spillway.....	59
Figure 4-21: HEC-RAS Image of Bayou Lamoque North Gates .....	60
Figure 4-22: HEC-RAS Image of Bayou Lamoque South Gates .....	61
Figure 4-23: HEC-RAS Image of the Davis Pond Freshwater Diversion .....	62

Figure 4-24: HEC-RAS Image of the Caernarvon Freshwater Diversion .....	63
Figure 4-25: HEC-RAS Image of Raccourci Island Storage Area and Weir (Plan View) ....	64
Figure 4-26: HEC-RAS Image of Raccourci Island Weir (Cross-section View) .....	64
Figure 5-1: Google Earth Image of the ICCW Lock at Harvey (2010) .....	72
Figure 5-2: Google Earth Image of the ICCW Lock at Chalmette (2010) .....	73
Figure 5-3: Google Earth Image of the West Bay Sediment Diversion (2010) .....	74
Figure 5-4: Carrollton Stage Comparison for 2007 Calibration (Original) .....	76
Figure 5-5: Carrollton Stage Comparison for 2007 Calibration (Manning's $n$ Adjusted) ..	77
Figure 5-6: Carrollton Stage Comparison for 2007 Calibration (Flow Roughness Factors Included) .....	78
Figure 5-7: Carrollton Stage Comparison for 2007 Calibration (Tides and Salinity Included) .....	79
Figure 5-8: Carrollton Stage Comparison for 2003 Validation .....	81
Figure 5-9: Carrollton Stage Comparison for 1999-2000 Validation .....	82
Figure 5-10: Carrollton Stage Comparison for 2007-2008 Simulation .....	83
Figure 5-11: Discharge Comparison for the 2008 Bonnet Carré Spillway Opening .....	85
Figure 6-1: Shear Stress Comparison for Violet (2007) .....	87
Figure 6-2: Shear Stress Comparison for Belle Chasse (2007) .....	88
Figure 6-3: Shear Stress Comparison for Myrtle Grove (2007) .....	89
Figure 6-4: Shear Stress Comparison for West Pointe a la Hache (2007) .....	90
Figure 6-5: Bed Material Transport ( $q_s$ ) Comparison for Violet (2007) .....	91
Figure 6-6: Bed Material Transport ( $q_s$ ) Comparison for Belle Chasse (2007) .....	92
Figure 6-7: Bed Material Transport ( $q_s$ ) Comparison for Myrtle Grove (2007) .....	93

Figure 6-8: Bed Material Transport ( $q_s$ ) Comparison for West Pointe a la Hache (2007) ....	94
Figure 6-9: Rating Curve Comparison for Violet (2007) .....	95
Figure 6-10: Rating Curve Comparison for Belle Chasse (2007).....	96
Figure 6-11: Rating Curve Comparison for Myrtle Grove (2007) .....	97
Figure 6-12: Rating Curve Comparison for West Pointe a la Hache (2007) .....	98
Figure 6-13: Flow Comparison for Baptiste Collette with West Bay Closed (2007_WB) ...	99
Figure 6-14: Flow Comparison for Fort St. Philip with West Bay Closed (2007_WB)..	100
Figure 6-15: Flow Comparison for Grand Pass with West Bay Closed (2007_WB) .....	101
Figure 6-16: Flow Comparison for Main Pass with West Bay Closed (2007_WB).....	102
Figure 6-17: Flow Comparison for Pass a Loutr� with West Bay Closed (2007_WB)...	103
Figure 6-18: Flow Comparison for South Pass with West Bay Closed (2007_WB).....	104
Figure 6-19: Flow Comparison for Southwest Pass with West Bay Closed (2007_WB) .....	105
Figure 6-20: HEC-RAS Image of South Pass Closure Weir (2007_WB_SP).....	106
Figure 6-21: HEC-RAS Image of Southwest Pass Closure Weir (2007_WB_SWP).....	107
Figure 6-22: HEC-RAS Image of Wide Cross-section for Buras Channel (RS 1).....	110
Figure 6-23: Stage Comparison at Baton Rouge for the Addition of the Buras Diversion (2007_WB_B).....	111
Figure 6-24: Stage Comparison at Carrollton for the Addition of the Buras Diversion (2007_WB_B).....	112
Figure 6-25: Stage Comparison at Venice for the Addition of the Buras Diversion (2007_WB_B)	113
Figure 6-26: HEC-RAS Image of Jesuit Bend Diversion Structure .....	114
Figure 6-27: Stage Comparison at Baton Rouge for the Addition of the Jesuit Bend Diversion (2007_WB_JB_B).....	115

Figure 6-28: Stage Comparison at Carrollton for the Addition of the Jesuit Bend Diversion (2007_WB_JB_B).....	116
Figure 6-29: Stage Comparison at Venice for the Addition of the Jesuit Bend Diversion (2007_WB_JB_B).....	117
Figure 6-30: HEC-RAS Image of Myrtle Grove Diversion Structure .....	118
Figure 6-31: Stage Comparison at Baton Rouge for the Addition of the Myrtle Grove Diversion (2007_WB_JB_MG_B) .....	119
Figure 6-32: Stage Comparison at Carrollton for the Addition of the Myrtle Grove Diversion (2007_WB_JB_MG_B). .....	120
Figure 6-33: Stage Comparison at Venice for the Addition of the Myrtle Grove Diversion (2007_WB_JB_MG_B) .....	121
Figure 6-34: HEC-RAS Image of Deer Range Diversion Structure.....	122
Figure 6-35: Stage Comparison at Baton Rouge for the Addition of the Deer Range Diversion (2007_WB_JB_MG_DR_B).....	123
Figure 6-36: Stage Comparison at Carrollton for the Addition of the Deer Range Diversion (2007_WB_JB_MG_DR_B).....	124
Figure 6-37: Stage Comparison at Venice for the Addition of the Deer Range Diversion (2007_WB_JB_MG_DR_B).....	125
Figure 6-38: Stage Comparison at Baton Rouge for the Closure of South Pass and the Addition of the Proposed Diversions (2007_WB_Div_SP vs. 2007_WB_JB_MG_DR_B).....	126
Figure 6-39: Stage Comparison at Carrollton for the Closure of South Pass and the Addition of the Proposed Diversions (2007_WB_Div_SP vs. 2007_WB_JB_MG_DR_B) .....	127
Figure 6-40: Stage Comparison at Venice for the Closure of South Pass and the Addition of the Proposed Diversions (2007_WB_Div_SP vs. 2007_WB_JB_MG_DR_B).....	128
Figure 6-41: Stage Comparison at Baton Rouge for the Closure of Southwest Pass and the Addition of the Proposed Diversions (2007_WB_Div_SWP vs. 2007_WB_JB_MG_DR_B) .....	130
Figure 6-42: Stage Comparison at Carrollton for the Closure of Southwest Pass and the Addition of the Proposed Diversions (2007_WB_Div_SWP vs. 2007_WB_JB_MG_DR_B).....	131
Figure 6-43: Stage Comparison at Venice for the Closure of Southwest Pass and the Addition of the Proposed Diversions (2007_WB_Div_SWP vs. 2007_WB_JB_MG_DR_B) .....	132

Figure 6-44: Stage Comparison at Baton Rouge for the Closure of South and Southwest Pass, the Addition of the Proposed Diversions, and the Dredging of Pass a Loutr� to -50 ft (2007_WB_Div_SP_SWP_pal50 vs. 2007_WB_JB_MG_DR_B).....	134
Figure 6-45: Stage Comparison at Carrollton for the Closure of South and Southwest Pass, the Addition of the Proposed Diversions, and the Dredging of Pass a Loutr� to -50 ft (2007_WB_Div_SP_SWP_pal50 vs. 2007_WB_JB_MG_DR_B).....	135
Figure 6-46: Stage Comparison at Venice for the Closure of South and Southwest Pass, the Addition of the Proposed Diversions, and the Dredging of Pass a Loutr� to -50 ft (2007_WB_Div_SP_SWP_pal50 vs. 2007_WB_JB_MG_DR_B).....	136
Figure 6-47: Stage Comparison at Baton Rouge for the Closure of South and Southwest Pass, the Addition of the Proposed Diversions, and the Dredging of Pass a Loutr� to -40 ft (2007_WB_Div_SP_SWP_pal40 vs. 2007_WB_JB_MG_DR_B).....	137
Figure 6-48: Stage Comparison at Carrollton for the Closure of South and Southwest Pass, the Addition of the Proposed Diversions, and the Dredging of Pass a Loutr� to -40 ft (2007_WB_Div_SP_SWP_pal40 vs. 2007_WB_JB_MG_DR_B).....	138
Figure 6-49: Stage Comparison at Venice for the Closure of South and Southwest Pass, the Addition of the Proposed Diversions, and the Dredging of Pass a Loutr� to -40 ft (2007_WB_Div_SP_SWP_pal40 vs. 2007_WB_JB_MG_DR_B).....	139



## List of Tables

Table 2-1: MLODS Proposed Diversions with Design Discharge and Diversion Type for Planning Unit 1 .....	18
Table 2-2: MLODS Proposed Diversions with Design Discharge and Diversion Type for Planning Unit 2 .....	18
Table 4-1: Initial Boundary Conditions for Existing Diversions and Tributaries .....	67
Table 4-2: Original Flow Percentages of Venice for the Passes and West Bay .....	68
Table 4-3: Optimized Flow Percentages of Venice for the Passes and West Bay.....	68
Table 5-1: RMSE, Bias Error, and RMSE per Average Cross-section Depth for 2007 Calibration Simulation at the Comparison Gages.....	80
Table 5-2: RMSE, Bias Error, and RMSE per Average Cross-section Depth for 2003 Validation Simulation at the Comparison Gages.....	81
Table 5-3: RMSE, Bias Error, and RMSE per Average Cross-section Depth for 1999-2000 Validation Simulation at the Comparison Gages.....	82
Table 6-1: Model Simulations, Deviations from 2007 Calibration Simulation, and Target Flow Rates.....	86
Table 6-2: Average Percent Increase in Flow to the Passes, Fort St. Philip, Bayou Lamoque North, and Bayou Lamoque South due to the Closure of West Bay (2007_WB) .....	105
Table 6-3: Average Percent Increase in Flow to the Passes, Fort St. Philip, Bayou Lamoque North, and Bayou Lamoque South due to the Closure of South Pass and West Bay (2007_WB_SP) .....	107
Table 6-4: Average Percent Increase in Flow to the Passes, Fort St. Philip, Bayou Lamoque North, and Bayou Lamoque South due to the Closure of Southwest Pass and West Bay (2007_WB_SWP) .....	108
Table 6-5: Average Percent Increase in Flow to the Passes, Fort St. Philip, Bayou Lamoque North, and Bayou Lamoque South due to the Closure of South Pass, Southwest Pass, and West Bay and the Dredging of Pass a Loutr� to -50 ft (2007_WB_SP_SWP_pal50) .....	108
Table 6-6: Average Percent Increase in Flow to the Passes, Fort St. Philip, Bayou Lamoque North, and Bayou Lamoque South due to the Closure of South Pass, Southwest Pass, and West Bay and the Dredging of Pass a Loutr� to -40 ft (2007_WB_SP_SWP_pal40) .....	108

Table 6-7: Mean and Max Difference in Stage for the Addition of the Buras Diversion at the Comparison Gages (2007_WB_B vs. 2007_WB) .....	113
Table 6-8: Mean and Max Difference in Stage for the Addition of the Jesuit Bend Diversion at the Comparison Gages (2007_WB_JB_B vs. 2007_WB_B) .....	117
Table 6-9: Mean and Max Difference in Stage for the Addition of the Myrtle Grove Diversion at the Comparison Gages (2007_WB_JB_MG_B vs. 2007_WB_JB_B) .....	121
Table 6-10: Mean and Max Difference in Stage for the Addition of the Deer Range Diversion at the Comparison Gages (2007_WB_JB_MG_DR_B vs. 2007_WB_JB_MG_B) .....	125
Table 6-11: Mean and Max Difference in Stage for the Closure of South Pass and the Addition of the Proposed Diversions at the Comparison Gages (2007_WB_Div_SP) .....	128
Table 6-12: Average Percent Increase in Flow to the Passes, Fort St. Philip, Bayou Lamoque North, and Bayou Lamoque South due to the Closure of South Pass and the Addition of the Proposed Diversions (2007_WB_Div_SP) .....	129
Table 6-13: Mean and Max Difference in Stage for the Closure of Southwest Pass and the Addition of the Proposed Diversions at the Comparison Gages (2007_WB_Div_SWP) .....	132
Table 6-14: Average Percent Increase in Flow to the Passes, Fort St. Philip, Bayou Lamoque North, and Bayou Lamoque South due to the Closure of Southwest Pass and the Addition of the Proposed Diversions (2007_WB_Div_SWP) .....	133
Table 6-15: Average Percent Increase in Flow to the Passes, Fort St. Philip, Bayou Lamoque North, and Bayou Lamoque South due to the Addition of the Proposed Diversions, the Closure of South Pass, Southwest Pass, and West Bay and the Dredging of Pass a Loutr�� to -50 ft (2007_WB_SP_SWP_pal50) .....	139
Table 6-16: Average Percent Increase in Flow to the Passes, Fort St. Philip, Bayou Lamoque North, and Bayou Lamoque South due to the Addition of the Proposed Diversions, the Closure of South Pass, Southwest Pass, and West Bay and the Dredging of Pass a Loutr�� to -40 ft (2007_WB_SP_SWP_pal40) .....	140

## **Abstract**

Alterations along the Mississippi River, such as dams and levees, have greatly reduced the amount of freshwater and sediment that reaches the Louisiana coastal area. Several freshwater and sediment diversions have been proposed to combat the associated land loss problem. To aid in this restoration effort a 1-D numerical model was calibrated, validated, and used to predict the response of the river to certain stimuli, such as proposed diversions, channel closures, channel modifications, and relative sea level rise. This study utilized HEC-RAS 4.0, a 1-D mobile-bed numerical model, which was calibrated using a discharge hydrograph at Tarbert Landing and a stage hydrograph at the Gulf of Mexico, to calculate the hydrodynamics of the river. The model showed that RSLR will decrease the capacity of the Lower Mississippi River to carry bed material. The stage at Carrollton Gage is not significantly impacted by large scale diversions.

**Keywords:** Lower Mississippi River, Unsteady Hydrodynamics, Fixed Bed, Diversions, HEC-RAS Model

## Chapter 1: Introduction

Coastal Louisiana is in danger of being washed away and inundated by the Gulf of Mexico (GOM). Decades of river modifications, powerful hurricanes, resource extraction, and relative sea level rise have caused major coastal land losses. Alone, it was estimated that Hurricanes Katrina and Rita transformed approximately 50,700 acres of wetlands into open water, which is equivalent to 79 square miles (LPBF, 2008). Without the protection of the coastal wetlands, southern Louisiana, including New Orleans, will be subjected to record high surges similar to or even greater than the surge from Hurricane Katrina. Neither the community nor the economy will be able to survive another storm surge like that of Katrina. Figure 1-1 shows the Mississippi River sediment plume captured by the Moderate Resolution Imaging Spectroradiometer (MODIS) on board NASA's Terra satellite in March of 2001 (Visible Earth, 2010).



**Figure 1-1: MODIS Satellite Image of Mississippi River Sediment Plume (Visible Earth, 2010).**

Dams, reservoirs, and bank protection structures along the upper Mississippi River (MR) and its tributaries have reduced the historic sediment load in the Lower MR by more than 50%, which is a major factor in the land loss in southeastern Louisiana (Meade, 1995). The hydraulic structures along the Lower MR, which include levees and bank protection, also play a vital role in the

deterioration of the coast. These structures remove and/or prevent valuable water and sediment from accumulating downriver to form the MR Delta. There needs to be enough flow in the river to carry nutrient-rich sediment to the delta, overtop the natural levees, and combat saltwater intrusion from the GOM, in order to create additional land mass. Other causes of sediment and water loss include the dredging of the river's cross-section for navigation works and the removal of water for irrigation and water supply systems. Some major outflows include the Bonnet Carré Spillway, which is used for flood control when the MR stage exceeds 17 ft (NAVD 88) and has a maximum design capacity of 250,000 cfs; and the natural levee near Bohemia at River Mile (RM) 38.6, which acts as an overflow weir during high flows.

One way to help surrounding areas maintain or create wetlands is to build a freshwater or sediment diversion. These diversions remove a pre-designed percentage of the river's sediment-laden flow and direct it to a specific area in need of replenishment. Currently there are several diversions in the MR extending from Tarbert Landing, MS (RM 306) to the Head of Passes (RM 0). These diversions include the Davis Pond Freshwater Diversion, Caernarvon Freshwater Diversion, White Ditch Siphon, Naomi Siphon, Violet Siphon, West Pointe a la Hache Siphon, West Bay Sediment Diversion, and Bayou Lamoque North and South Diversions. Some of these structures are inoperable and need to be repaired or replaced. Another way to increase wetlands production is to utilize the hydrodynamics of the passes. As the flow in the river heads toward the GOM, it is distributed into the passes, including Baptiste Collette, Cubit's Gap (mostly Main Pass), Grand Pass and Tiger Pass, Southwest Pass, South Pass, and Pass a Loutr . However, the amount of flow discharged into each pass is uncertain. Southwest Pass, being the deepest and most conveniently located, is primarily used for navigational purposes. As a result, Southwest Pass has a large cross-section, which is maintained by dredging. Since both South Pass and Pass a Loutr  are occasionally shoaling due to insufficient sediment transport, most of the flow at the Head of Passes (HOP) is diverted into Southwest Pass. This creates a problem because the outlet of Southwest Pass is very deep and most of the sediment in the water is lost to the GOM. A possible remediation for this problem is to close South and Southwest Passes and dredge Pass a Loutr  into a navigational channel, to reduce the amount of wasted sediment discharged from Southwest Pass and to redirect it into the delta (LPBF, 2008).

The Lake Pontchartrain Basin Foundation (LPBF) has put together a comprehensive report detailing its Multiple Lines of Defense Strategy (MLODS). The MLODS is a planning methodology for proposed projects that will help in coastal accretion while also providing flood protection. Figure 1-2 from the MLODS report shows the areas targeted for restoration. This study will only consider Planning Units 1 and 2. The diversions included in this study consist of sustaining diversions ( $Q < 40,000$  cfs), delta-building diversions ( $Q > 75,000$  cfs), and controlled-crevasse diversions (spillway-type structures) (LPBF, 2008). Figure 1-3 shows the proposed diversions for Planning Unit 1, as well as the passes' closures and modification of Pass a Loutr , mentioned earlier. Figure 1-4 shows the planned diversions for Planning Unit 2, which targets the Barataria Basin for restoration.



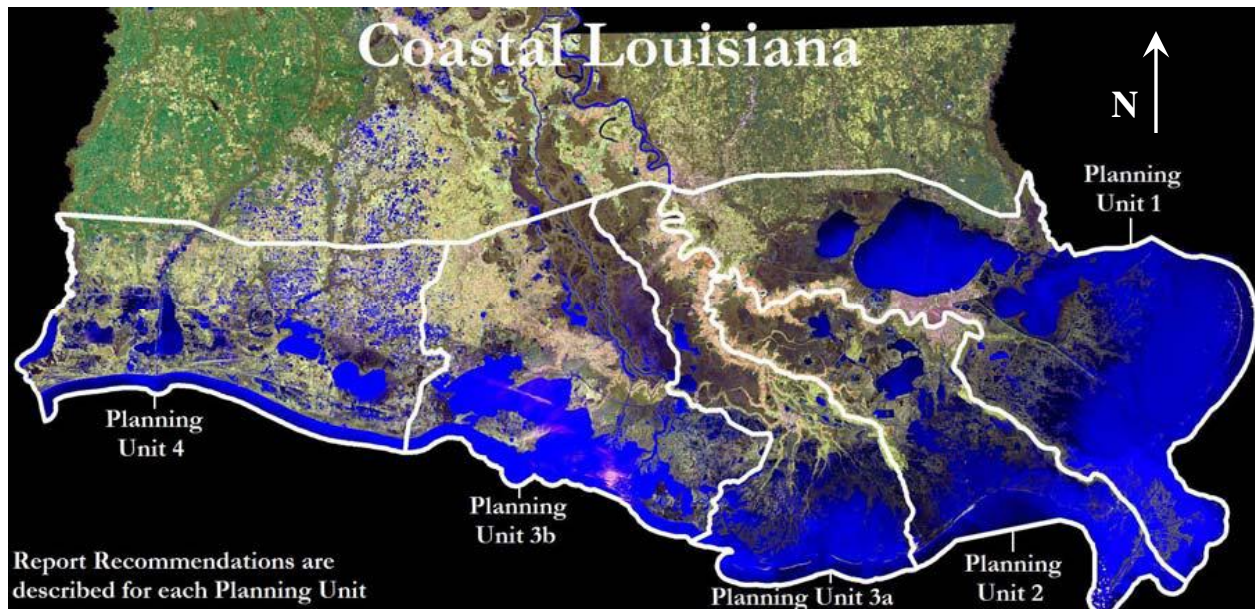


Figure 1-2: Planning Units for the Multiple Lines of Defense Strategy (LPBF, 2008).

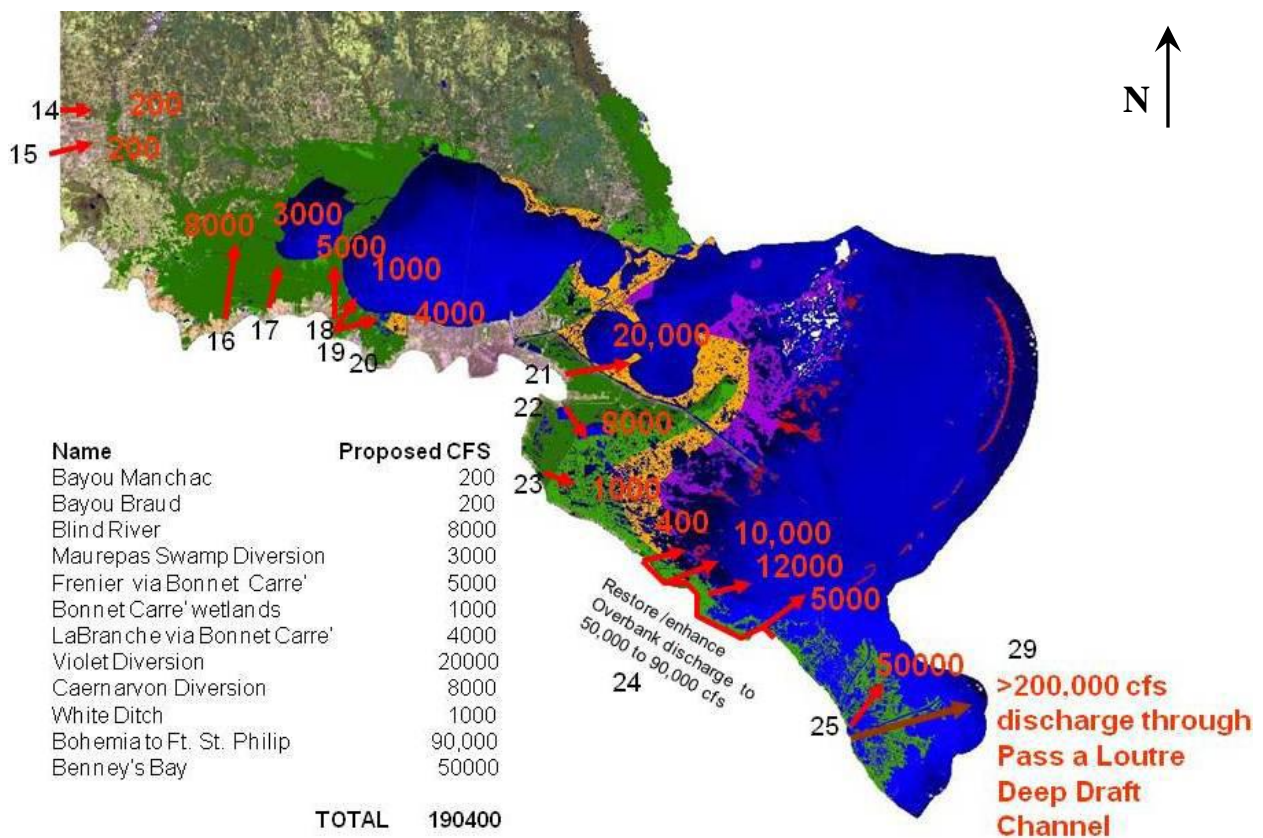
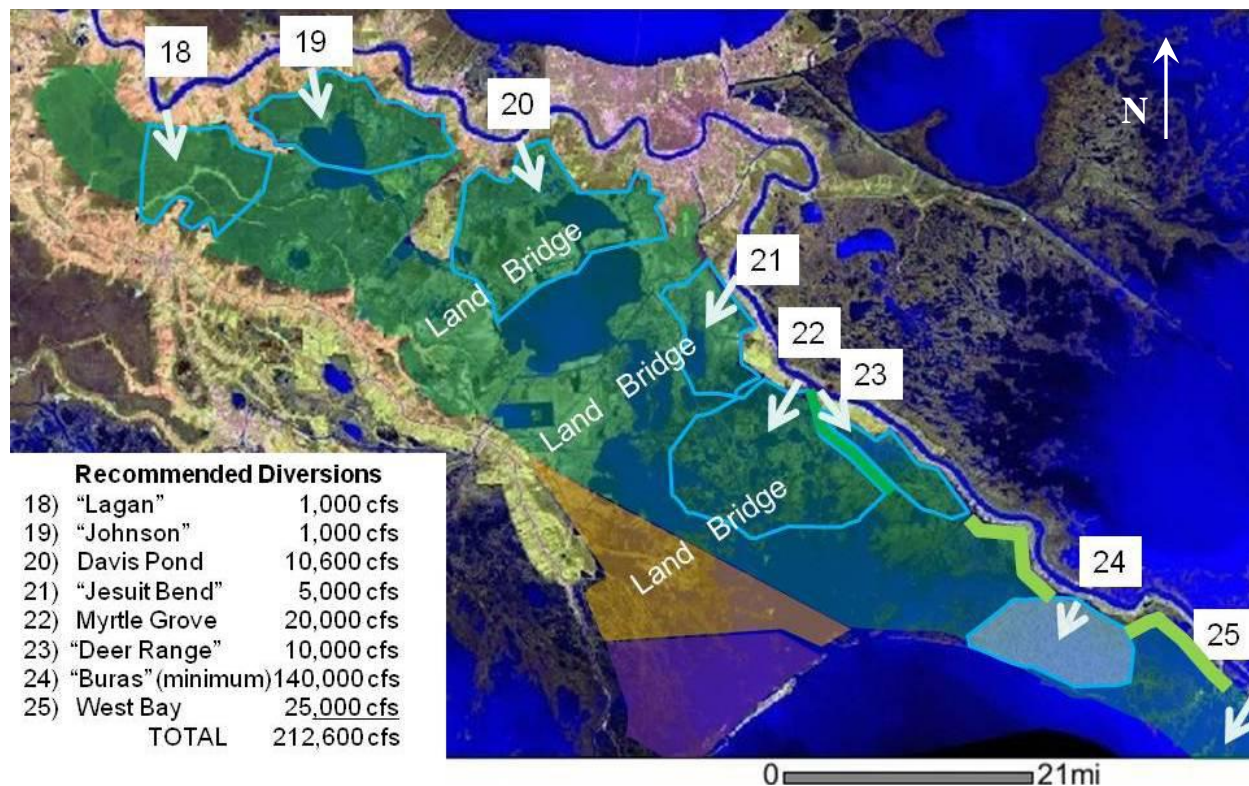


Figure 1-3: Proposed MR Diversions and Channel Modifications for Planning Unit 1 from the Multiple Lines of Defense Strategy (LPBF, 2008).



**Figure 1-4: Proposed MR Diversions for Planning Unit 2 from the Multiple Lines of Defense Strategy (LPBF, 2008).**

### ***1.1 Objectives***

The purpose of this study is to investigate the impacts of proposed freshwater diversions and distributary modifications on the discharge and stage along the Lower Mississippi River (MR). A one dimensional numerical model was needed to simulate the hydrodynamics of the river and its existing diversions and distributaries. Calibration and validation were needed to ensure accuracy of the model. After validation, the model was needed to investigate the effects of relative sea level rise on the potential for sediment transport in the MR. The model was then needed to simulate the effects of the West Bay closure on the flow distribution in the passes. The model was needed to simulate the closing of South and Southwest Passes and the dredging of Pass a Loutr . The model was also needed to estimate the impact of the future diversions, which are presented in Figures 1-3 and 1-4. Lastly, the model was needed to simulate the closing of South and Southwest Passes and the dredging of Pass a Loutr  in combination with the proposed diversions. The model could be used to simulate several scenarios of opening and closing diversions that may be required to identify the best operational practice to maximize wetland production.

### ***1.2 General Approach***

The 1-D numerical model chosen was HEC-RAS 4.0 (USACE HEC, 2008) because of its large spatial domain and long-term time predictions, among other reasons. Cross-sectional data from various sources, including the 2003-2004 Hydrographic Survey (USACE NOD, 2007), were used to replicate the channel geometry in the model. Equivalent channels were developed to



account for unknown survey data at several locations. Inline and lateral structures were inputted to imitate the existing diversion structures. Daily discharge and stage data were used as boundary conditions. Model parameters, such as discharge coefficients and flow roughness factors, were altered in order to calibrate the model based on recorded data. The model was run for several calendar years in order to validate the results. Stage data for the downstream boundary conditions were increased by 1.64, 3.28, and 4.92 ft (0.5, 1.0, and 1.5 m) to predict the effects of relative sea level rise. The West Bay reach was removed from the model to emulate the closing of that structure. Lateral structures were added to South and Southwest Passes to stop flow from the MR entering the channels. Cross-sectional data for Pass a Loutr  were altered to imitate the dredging of that channel. Channels and structures were added to replicate the proposed diversions. Several scenarios of opening and closing the existing and proposed diversions were simulated. Figure 1-5 shows the schematic of the HEC-RAS model overlaying a satellite view of southern Louisiana (Pereira *et al.* 2010).

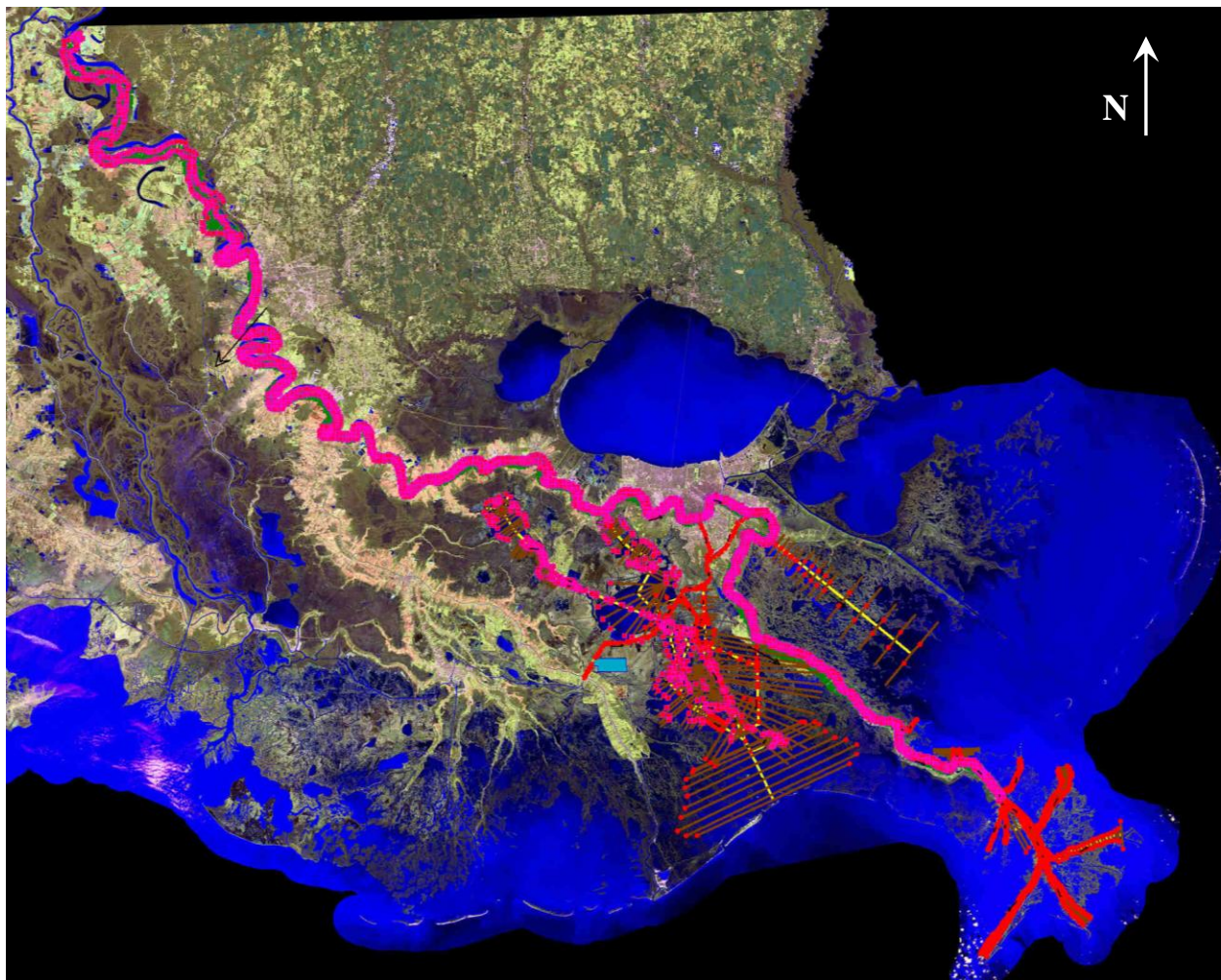


Figure 1-5: HEC-RAS Model Schematic Overlaying Satellite Imagery (Pereira *et al.* 2010).



### ***1.3 Background and Literature Review***

Numerical models are becoming the standard when it comes to analyzing problems in the hydraulics and coastal industries. Physical models are being abandoned due to geometry constraints and lack of applicability to alternate problems (Papanicolaou *et al.* 2008). In 2008, Louisiana State University's (LSU) Small Scale Physical Model (SSPM) of the Lower Mississippi River (MR) was tested to examine the possibility for freshwater and sediment diversions. One problem with the SSPM is that the scale for the vertical (1:500) is so much smaller than the length scale (1:12,000). This represents a distorted scale of 24, which is much too high to properly quantify mobile bed processes (Waldron, 2008). The necessary space required for a reliable SSPM could possibly take up an entire street block. Another problem with LSU's SSPM is the accuracy of the model. The gages used for measuring water surface elevation were showing un-realistic values. Therefore, they had to be resurveyed twice over the course of the study. It was suggested that the reason for the resurveys could be due to imprecise calibration of the benchmark elevations and/or possible settlement of the model since its installation. Waldron (2008) concluded the study saying that the SSPM was an adequate educational tool that can be effectively used to represent the qualitative responses of the river to proposed diversions.

#### ***1.3.1 Description of Numerical Models***

When it comes to numerical models, there are many options to choose from. Depending on the spatial-temporal capabilities necessary, there are many 1-, 2-, and 3-D models available for use. A 1-D numerical model has one spatial dimension either along a channel or a water column and can simulate both steady and unsteady state flows. A 2-D numerical model has two spatial dimensions, where one is along the channel and the other is along the water column. 2-D models can also simulate both steady and unsteady state flows, as well as solve steady and unsteady state mass equations. A 3-D numerical model has 3 spatial dimensions, where one is along the channel ( $x$ ), one is along the water column ( $z$ ), and the other is across the channel ( $y$ ). 3-D models are advanced mechanistic models that can simulate steady and unsteady state flows and can make steady and unsteady state mass computations. However, 3-D models are mostly used for the unsteady conditions (McCorquodale and Georgiou, 2006).

The term "steady state" refers to a time-independent situation. For example, a river with a constant flow rate is considered to have a steady state flow because at any point in time the flow is still the same as it was at the beginning. The term "unsteady state" refers to a time-dependent situation. For example, an uncontrolled diversion with a varying discharge is considered to have an unsteady state flow because as the time elapses the flow is constantly changing. The term "quasi-steady state" refers to a time-dependent situation, where the unsteady conditions are isolated in time and treated as steady state "events". For example, sediment transport into a distributary channel involves unsteady flow, but the shear stress of the bed material can only be calculated at individual instances in time. For this study, the Mississippi River's stage and discharge were the parameters being considered; therefore, a 1-D unsteady model was sufficient for the hydrodynamics calculations.

### ***1.3.2 Potential Numerical Models***

Numerical modeling is relatively new, but because of the modeling capabilities, such as predicting hydrodynamics, sediment transport, deposition/scour, and bank failure, they are becoming more and more popular (Papanicolaou *et al.* 2008). As a result, there are many 1-D numerical models to choose from; therefore, to simplify the selection process only the following models were researched for this study:

- CHARIMA
- HEC-6
- HEC-RAS
- MIKE 11

The selection process involves finding a model to best suit the project's needs and budget. McCorquodale and Georgiou (2006) put together a comprehensive list of model parameters to look for in each model, in order to make choosing a model easier. The model parameters necessary for this study included:

- Cost and Availability
- Time and Space Scales
- Data Requirements and Outputs
- Ease of Use and User's Manual Quality
- Source Code
- Interfaces
- Processes Included
- Precedence in Related Studies

CHARIMA is a general-purpose computer code developed by Holly in 1990 (Holly *et al.* 1990). The code is used to model hydrodynamics, sediment transport, and water quality under steady or unsteady flow conditions. The source code is written in FORTRAN and needs a user-supplied compiler. The data requirements include American Standard Code for Information Interchange (ASCII) files for the inputs and outputs. Also, any graphical outputs must be created by the user in a separate program. The program has a time scale on the order of years and a relatively small spatial domain. For hydrodynamics simulations, the program solves the de St. Venant equations of water-continuity and momentum. The model is under continuous development; therefore, it is not commonly released to outside users, and the source code is not available for altering. There is a user's manual as well as an addendum to provide the user with updated information. There have been several recent applications using CHARIMA. One such application modeled the sediment transport of the Mondego River in Portugal. The results of this study indicated a need for further development of the code because of the existence of trans-critical flow (Pereira *et al.* 2007).

HEC-6 is a mobile-bed numerical model developed by the U.S. Army Corps of Engineers Hydraulic Engineering Center (USACE HEC, 1993). The model is used to estimate hydrodynamics, sediment transport, and amount of deposition/scour. It is a public-domain model, which is available on the USACE website as a package of executable files. The source

code is written in FORTRAN and can be obtained and altered to fit the user's needs. The model requires a PC-DOS operating system with at least a 640K limit (HEC-6, 2008). Inputs are entered using a single input data file. The user has to specify what processes to simulate as well as the level of outputs desired. The user must also provide the software to store and illustrate the outputs. The program has a variable time scale, which is shorter for flood events and longer for low flow periods. The spatial domain is relatively small and only allows up to 500 cross-sections (extended memory version only) (HEC-6, 2008). The model is quasi-steady, which means it takes continuous flow data and breaks it up into individual instances. The model then calculates the water surface profile using the 1-D energy equation. Sediment transport and the amount of deposition and/or scour (Exner equation) are calculated. The model changes the channel geometry based on the new data. The next flow is then simulated and the procedure is repeated for each time step. The USACE HEC offers a user's manual with a systematic procedure for writing the input data files (USACE HEC, 1993). HEC-6 is one of the most utilized 1-D sediment models available.

HEC-RAS River Analysis System is another numerical model developed by the USACE HEC (2008). The model is used to predict hydrodynamics, sediment transport, and water quality. It is also a public domain model available on the USACE website; however, it is not an open source code. HEC-RAS provides a Windows-based graphical user interface where inputs are entered into tables. The program operates with Microsoft Windows 98, 2000, NT, or XP. The model offers many graphical and tabular outputs. It is capable of making long-term hydrodynamics predictions and allows a large spatial domain. The model simulates steady and unsteady flow regimes, as well as quasi-unsteady for the sediment transport module (source code from HEC-6). For unsteady hydrodynamics calculations, the model solves the equations of continuity and momentum. USACE HEC provides a comprehensive user's manual and reference manual. In 2009, Pereira *et al.* used HEC-RAS 4.0 to model the same section of the Mississippi River that is considered in this study.

MIKE-11 is a general river modeling system developed by the Danish Hydraulic Institute (DHI). The model is primarily used to simulate hydrodynamics. The software is proprietary (non-open source) and costs around \$3000. The program provides a Windows-based interactive graphical user interface and operates with Microsoft Windows 98, 2000, NT, or XP (DHI, 2003). Inputs can be of various data types including ASCII files and spreadsheet programs. The model also provides graphical and tabular outputs. It is capable of making long-term hydrodynamics predictions and allows a large spatial domain. The model simulates unsteady and quasi-steady flow regimes. For the unsteady hydrodynamics module, the model also solves the de St. Venant equations. A comprehensive user's guide and a reference manual are available for assistance with the purchase of the model. To get the complete experience of what MIKE-11 has to offer, the user is recommended to purchase the other module packages, which include hydrology, water quality, advection-dispersion, and cohesive and non-cohesive sediment transport (DHI, 2003). A recent application of MIKE-11 involved modeling the same study area considered here (Meselhe *et al.* 2005).

Two other numerical models were briefly considered for this study. The first model was FLUVIAL-11, which is a mathematical model used for water and sediment transport routing in channels (Chang, 1984). The model uses the continuity and momentum equations to calculate the

flow routing. For calibration of the model, Chang (1984) investigated the changes in the width and depth of a 2-mile reach of the San Dieguito River after several floods. The second model was MOBED, which is a mobile boundary flow model developed by Krishnappan (1985). The model uses a generalized expression for the energy slope to determine the unsteady flows. Validation of the model consisted of comparing laboratory and field data to model-predicted data.

For the purpose of this study, HEC-RAS Version 4.0 was chosen as the numerical model to simulate the 1-D unsteady hydrodynamics. Unlike CHARIMA and HEC-6, HEC-RAS and MIKE-11 offer a graphical user interface which is easier to work with because the user can see the inputs and spot errors in the data before running a simulation. For HEC-6 and CHARIMA, a simulation can blow up and it would be difficult to find where the error came from. Also, the user must provide additional software to view results when using HEC-6 or CHARIMA; whereas, HEC-RAS and MIKE-11 provide their own graphical and tabular outputs for each simulation. HEC-6, HEC-RAS, and MIKE-11 were used to model the same MR reach that was considered in this study. Although MIKE-11 has several advanced capabilities that HEC-RAS does not have, such as coupling the hydrodynamics module with the hydrology module and differentiating between sediment transport of cohesive and non-cohesive soils, the cost was too high for a graduate research study. In the end, HEC-RAS proved to be the best model for this study.

### ***1.3.3 Numerical Modeling of the Lower Mississippi River***

Previous 1-D modeling of the MR was conducted for the reach between Tarbert Landing (RM 306) and East Jetty (RM -20) using the Waterways Experiment Station's (WES) TABS-1 model (Copeland and Thomas, 1992). The study investigated the effects that diversions have on dredging the MR. The sediment transport module was used to predict the patterns of sand deposition downstream of a diversion by changing the concentration of sediment diverted from the river. Several diversion site alternatives were tested to compare the river's response to the location of a diversion. The results of the study indicated that the further upstream the diversion is located, the less dredging will be required because the flow would be high enough to re-suspend the recently deposited sediment just downstream of the diversion. The study also showed that the amount of sediment diverted plays an even bigger role in the resulting water surface and bed deposition because if no sediment were diverted there would not be enough flow to entrain the deposited sediment and dredging would be increased. In 2000, a supplemental study was developed using a HEC-6 model of the MR from Tarbert Landing to the Gulf of Mexico (GOM) via Southwest Pass (Barbé *et al.* 2000). Barbé *et al.* (2000) found that not only did the diversion's location and the amount of sediment diverted play important roles in the deposition and scouring of the river at Southwest Pass, but the sediment transport was also affected by the operation of the diversion structures themselves.

Another 1-D MR model developed in 2005 considered the reach between Tarbert Landing and (RM 10.7) using the MIKE-11 numerical model (Meselhe *et al.* 2005). This study investigated the hydrodynamics, salinity, water quality, and sediment transport of the river. The model was calibrated and validated by altering the Manning's roughness coefficient,  $n$ , with respect to depth (Meselhe *et al.* 2005). Meselhe *et al.* (2005) found that using stage data as both the upstream and

downstream boundary condition improved the calibration results. In 2009, Pereira *et al.* modeled the same reach using HEC-RAS 4.0. The model was first used to simulate the hydrodynamics of the river under unsteady flow conditions. The model was then used to simulate the sediment transport under quasi-unsteady conditions. Flow roughness factors as well as Manning's  $n$  values had to be adjusted for each calibration. This study also used the same datasets as Meselhe for the calibration procedure (Pereira *et al.* 2009).

In 2006, a morphodynamic model was presented which tried to capture the sediment transport processes of the Wax Lake Delta (Parker *et al.* 2006). The Wax Lake Outlet was a man-made channel that was overrun by an avulsion in the Atchafalaya River during the 1973 flood. Since then, the Wax Lake Delta has been growing because the freshwater has been supplying nutrients to the coastal marshes. The model was tested against field data in order to validate it. The purpose of Parker *et al.*'s (2009) study was to investigate the introduction of freshwater into a receiving body and quantify the resulting land formations. This study would provide insight for the design of possible diversions of the MR for similar land building. The results of the study supported this concept, but Parker *et al.* (2009) warned that other factors, such as costs and environmental impacts, have to be assessed before building any diversions in the MR.

## Chapter 2: Mississippi River

The Mississippi River (MR) is an invaluable resource for the United States, especially Louisiana, because of its economic and industrial contributions. One of the largest sources of revenue for the MR Basin is navigation. Louisiana is a major supplier of rice, sugar, salt, lime, sulphur, oil, and gas, as well as a bountiful area for fishing, fur trapping, cattle grazing, and hunting (LCWCRTF, 1997). As a result, the Port of New Orleans (PNO), located near River Mile (RM) 96, is a major contributor to the economy of southern Louisiana by exporting these locally produced goods. The PNO is responsible for approximately 160,500 jobs, \$8 billion in income, \$17 billion in expenses, and \$800 million in state taxes, according to a 2004 study (Port of New Orleans, 2009).

Navigation is also the primary cause of channel modifications in the river. For years, the river has accommodated barge traffic bringing goods from the north to the Gulf Coast. As a result, the MR channel bed has been dredged many times in order to maintain a safe travel course for ships. This repetitive dredging has removed the natural bed forms and has altered the natural thalweg, or meandering pattern, along the river, which modifies the roughness of the channel bed. Moreover, most of the dredge material has been disposed in the deep waters of the Gulf of Mexico (GOM), where it is wasted. Wing dikes have also been installed to hold the channel area steady and to prevent erosion of the banks, as well as to encourage scouring of the shipping channel. Along the upper MR, there are 29 lock-and-dam structures, which were mostly constructed for navigation purposes. The depth in the river would become too low to allow barge traffic to safely pass; therefore, the structures were built to sustain a minimum depth of 9 ft (Meade, 1995). This becomes a problem for the Lower MR because these dams retain the sediment-laden water, which would ordinarily flow to the coast. Also, this reduction in stage ultimately changes the flow characteristics of the river e.g. velocity, slope, and bed roughness. At New Orleans, the median stage was found to be 6.6 ft with the highest and lowest monthly stage at 12 ft and 3.25 ft, respectively, for the period from 1973 to 1996 (Ingenierie *et al.* 1997). Without the presence of these lock-and-dam structures in the upper MR, the stage at New Orleans could be significantly higher, which could increase the sediment transport potential of the river allowing more sediment to be distributed to the wetlands.

The river itself is a natural resource because it carries freshwater and sediment to the Louisiana coast, which uses the nutrient-rich sediment to sustain the wetlands. Artificial levees were built along almost the entire river in order to control the flow as well as to limit the amount of flooding to the surrounding communities. One major downfall of trying to control the river is that now sediment and nutrients are no longer entering the river from runoff because of these barriers. Similarly, the adjacent areas are no longer getting the sediments and nutrients freshwater provides during high stages and floods. This does not bode well for the Mississippi Delta, which relies on the sediment deposition for marsh cultivation. According to Meselhe (2005), the levees, dams, and navigation works have robbed the wetlands of about 220 million tons of sediment per year since their installation. Without this sediment, the wetlands cannot be sustained. It has been projected that in the year 2040 Louisiana will have lost around one million acres of wetlands and the GOM will have moved inland approximately 33 miles, which would leave many communities along the Lower MR without freshwater or sources of income (LCWCRTF, 1997). The addition of the artificial levees has also disrupted the natural course of



the channel, which if given the chance would probably divert towards the Atchafalaya River (Mississippi River, 2010). One major project that prevents the course of the MR from shifting to the Atchafalaya River is the Old River Control structure (RM 315), which was designed to artificially distribute 30% of the flow to the Atchafalaya River and 70% of the flow to the MR. According to Ingenierie *et al.* (1997), if the MR had been allowed to flow naturally into the Atchafalaya River, then the flow at New Orleans would have been dominated by tides and saltwater intrusion, which would ultimately deplete the availability of potable water for the neighboring communities. Therefore, the main objective of the project was to maintain the 1950 distributions of flow and sediment between the MR and Atchafalaya River (Ingenierie *et al.* 1997). The project consists of three structures: the Sidney A. Murray Hydroelectric Power Dam (HPD), the Low Sill Structure (LSS), and the Auxiliary Structure (AUX). Figure 2-1 shows the three Old River Control structures, along with the Overbank Structure (OVB) used for flood control, in Google Earth (2010).



**Figure 2-1: Google Earth Image of Old River Control Structures (2010).**

The dredging of the river is essential for the navigation industry, which helps sustain the economy of southern Louisiana, and the levees are needed to provide flood protection to the neighboring communities. However, the marshes are suffering from nutrient depletion because of these alterations. In order to save the Louisiana coastal wetlands, several diversions have been implemented and others have been proposed to direct the freshwater into areas of high need (LPBF, 2008). One such diversion is the Davis Pond Freshwater Diversion. This diversion directs much needed freshwater and some sediments to the Barataria Basin, which suffers from the effects of saltwater intrusion from the GOM (Park, 2002).

This study focuses on the proposed diversions specified by the MLODS (LPBF, 2008). The numerical model estimates the effects of the proposed diversions on the river's stage and discharge. The ultimate goal was to develop a model to determine the response of the river to the removal of sediment and freshwater. Based on this and other models, the negative impacts on the river will be evaluated and minimized.

### ***2.1 The Modeled Reach***

The current study incorporated Pereira *et al.*'s (2009) channel geometry of the MR from Tarbert Landing (RM 306) to Venice (RM 10.7), and extended the MR reach to include the HOP (RM 0). Also included in the model were Baptiste Collette (RM 11.5), Cubit's Gap (mostly Main Pass) (RM 3.6), Grand Pass (RM 10.4) and Tiger Pass, Southwest Pass (RM 0), South Pass (RM 0), and Pass a Loutr  (RM 0), which were added as distributaries near the end of the MR reach. In the past, the end of the Pass a Loutr  channel was bifurcated by North Pass. However, Google Earth Imagery (2010) shows that the North Pass channel and several hundred feet of the Pass a Loutr  channel have been washed out. As a result, North Pass and the extreme end of Pass a Loutr  were excluded from the model. Figure 2-2 shows the Google Earth image of the end of Pass a Loutr  in 2004 and Figure 2-3 shows the same image in 2007. The entire HEC-RAS schematic can be found in Figure 1-5, and the MR Bird's Foot Delta in HEC-RAS can be found in Figure 2-4.





**Figure 2-2: Google Earth Image of Pass a Loutr  and North Pass from 2004 (2010).**



**Figure 2-3: Google Earth Image of Pass a Loutr  and North Pass from 2007 (2010).**

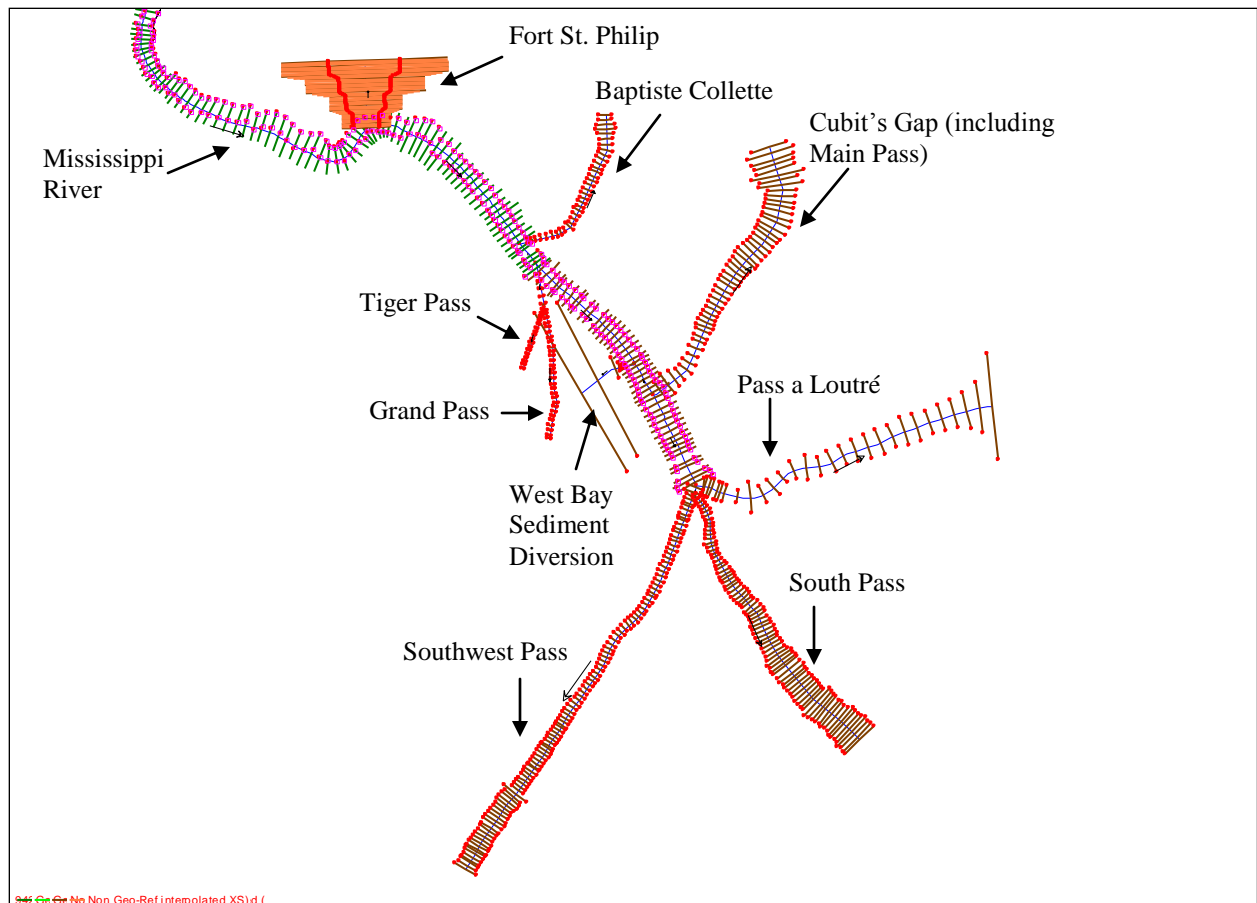


Figure 2-4: HEC-RAS Image of Mississippi River Bird's Foot Delta.

### 2.1.1 Existing Diversions

There are several existing freshwater and sediment diversions along the MR from Tarbert Landing to the GOM. These diversions were primarily designed for land building purposes. Other diversions along the MR include spillways, which are used for the dissipation of high floods. There are also several man-made channels along the river, which are primarily used for navigational purposes. For the purpose of this study, these channels are referred to as diversions because they too provide freshwater to a receiving basin. The following is a list of all the channels, diversions, and spillways that were included in the model:

- Davis Pond Freshwater Diversion
- Caernarvon Freshwater Diversion
- ICCW at Harvey
- ICCW at Chalmette
- Bayou Lamoque North
- Bayou Lamoque South
- Bonnet Carr  Spillway
- Bohemia Spillway
- Violet Siphon



- White Ditch Siphon
- West Bay Sediment Diversion
- Fort St. Philip

Also included in this list is Fort St. Philip, which is not an authorized diversion, a pass, nor a spillway. However, Figure 2-5 (Google Earth Imagery, 2010) shows several natural and man-made cuts in the river's east bank near Fort St. Philip, which are thought to remove a substantial amount of freshwater and sediment from the river (Meselhe *et al.* 2010). As a result, the cuts were modeled as an equivalent channel to account for these losses.



Figure 2-5: Google Earth Image of Cuts at Fort St. Philip (2010).

### 2.1.2 Future Diversions

The MLODS outlines several proposed diversions along the MR, which are intended to reintroduce freshwater and sediment into the Louisiana coastal area. The first type of diversion

mentioned in the MLODS is a “sustaining diversion”, which is typically a small diversion or siphon used to pass water over or through the levees into the neighboring marshes in order to encourage production and maintain salinity levels. The second type of diversion is a “delta-building diversion or uncontrolled-crevasse”, which is typically larger than a sustaining diversion and is used to build wetlands in areas that require flood protection. The third type of diversion is a “controlled-crevasse diversion”, which is a larger spillway-type diversion used to flood water and sediment into the estuary during high stage periods. The operation of these three diversion types can be varied in order to provide the maximum restoration possible. The diversions for each Planning Unit are designed to beneficially flood the entire basin during high flood years (LPBF, 2008). Table 2-1 below shows the diversion name, type, and design discharge for each of the proposed diversions that are considered in this study from Planning Unit 1. Table 2-2 lists the diversions considered in this study for Planning Unit 2. For both Tables, the number corresponds to the MLODS project number. Figures 1-3 and 1-4 show the locations of these project sites along the river.

**Table 2-1: MLODS Proposed Diversions with Design Discharge and Diversion Type for Planning Unit 1.**

Number	Name	Proposed Discharge (cfs)	Type
14	Bayou Manchac	200	Sustaining
15	Bayou Braud	200	Sustaining
16	Blind River	8000	Sustaining
17	Maurepas Swamp	3000	Sustaining
18	Frenier via Bonnet Carré	5000	Sustaining
20	LaBranche via Bonnet Carré	4000	Sustaining
21	Violet	20,000	Sustaining
23	White Ditch	1000	Sustaining
25	Benney’s Bay	50,000	Delta-Building
28	Channel Modifications and Pass Closures	200,000 (min)	Delta-Building

**Table 2-2: MLODS Proposed Diversions with Design Discharge and Diversion Type for Planning Unit 2.**

Number	Name	Proposed Discharge (cfs)	Type
18	Lagan	1000	Sustaining
19	Johnson	1000	Sustaining
21	Jesuit Bend	5000	Sustaining
22	Myrtle Grove	20,000	Sustaining
23	Deer Range	10,000	Sustaining
24	Buras	40,000	Delta-Building

### ***2.1.3 Miscellaneous***

There are several small bayous just downstream of Tarbert Landing (RM 306), which could support reverse flows and off-channel storage depending on the stage and limb of the MR hydrograph. In the same vicinity there is also an abandoned oxbow, called Raccourci Island, and several un-leveed areas, which could provide storage during high flows. As a result, these areas were measured and combined into an equivalent storage area, named Raccourci Island, to



account for this extra capacity. HEC-RAS requires a lateral structure to connect a storage area to a reach. Therefore, a small weir was designed on the west bank of the MR near RM 296.5 to route flow from the river during high stage. Figure 2-6 shows the Raccourci Island oxbow, the two small bayous, and some of the overland storage area from Google Earth (2010).



Figure 2-6: Google Earth Image of Raccourci Island, Small Bayous, and Overland Storage Areas (2010).

## 2.2 Barataria Basin

In order to ensure that the proposed diversions' discharges are not oversized, the Barataria Basin drainage network was included in the model. Freshwater from several tributaries flows into the Barataria Basin drainage network and is distributed, redistributed, and then reconnected at Barataria Bay, where the flow then heads into the GOM. The following is a list of major lakes, channels, and ponds that were included in the model:

- Lake Cataouatche

- Lake Salvador
- Bayou Rigolettes
- Bayou Perot
- Little Lake
- The Pen
- Barataria Bay Waterway
- Barataria Bay
- Tidal Passes between Barataria Bay and the GOM

The Barataria Basin has several conveyance systems and drainage basins, which include some existing diversions, channels, ponds, and lakes. The following is a list of these systems (some are repeated from the “Existing Diversions” section).

- Davis Pond Freshwater Diversion
- Lac Des Allemands
- Petit Lac Des Allemands
- Dixie Delta Canal
- ICCW at Larose
- ICCW at Chalmette
- ICCW at Harvey
- Wilkinson Canal

The Dixie Delta Canal is a pond located along the ICCW near Larose, LA and has an area of 6400 acres. Also included in this list was Wilkinson Canal, which is not a large contributor to the Barataria Basin flow. However, the proposed diversion at Myrtle Grove was designed to divert flow into the canal and subsequently into the basin. Therefore, the canal was included in order to assist in the addition of the Myrtle Grove diversion. Figure 2-7 shows the Google Earth (2010) image of the Barataria Basin. Figure 2-8 shows the Barataria Basin in the HEC-RAS model.



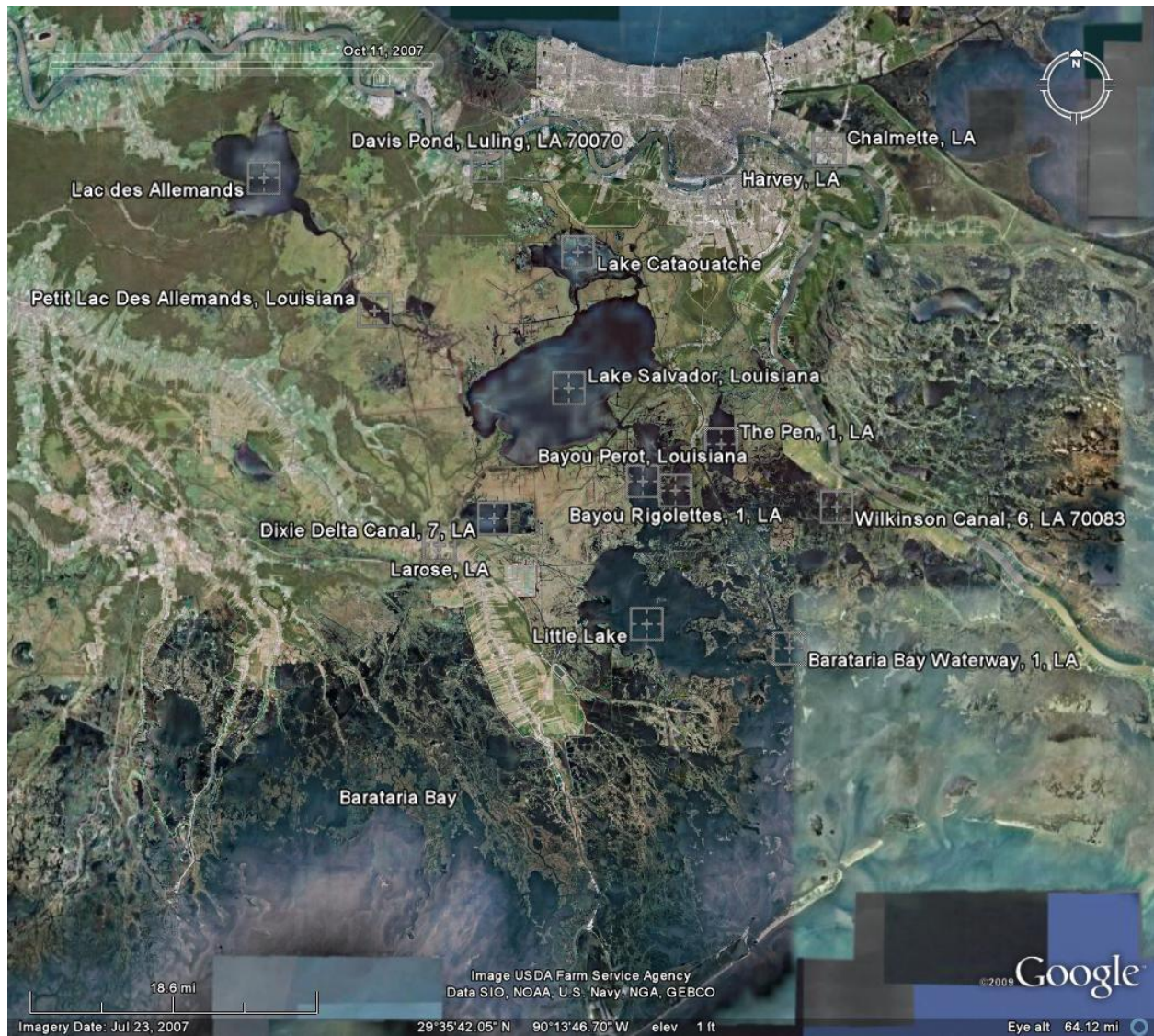


**Figure 2-7: Google Earth Image of Barataria Basin (2010).**



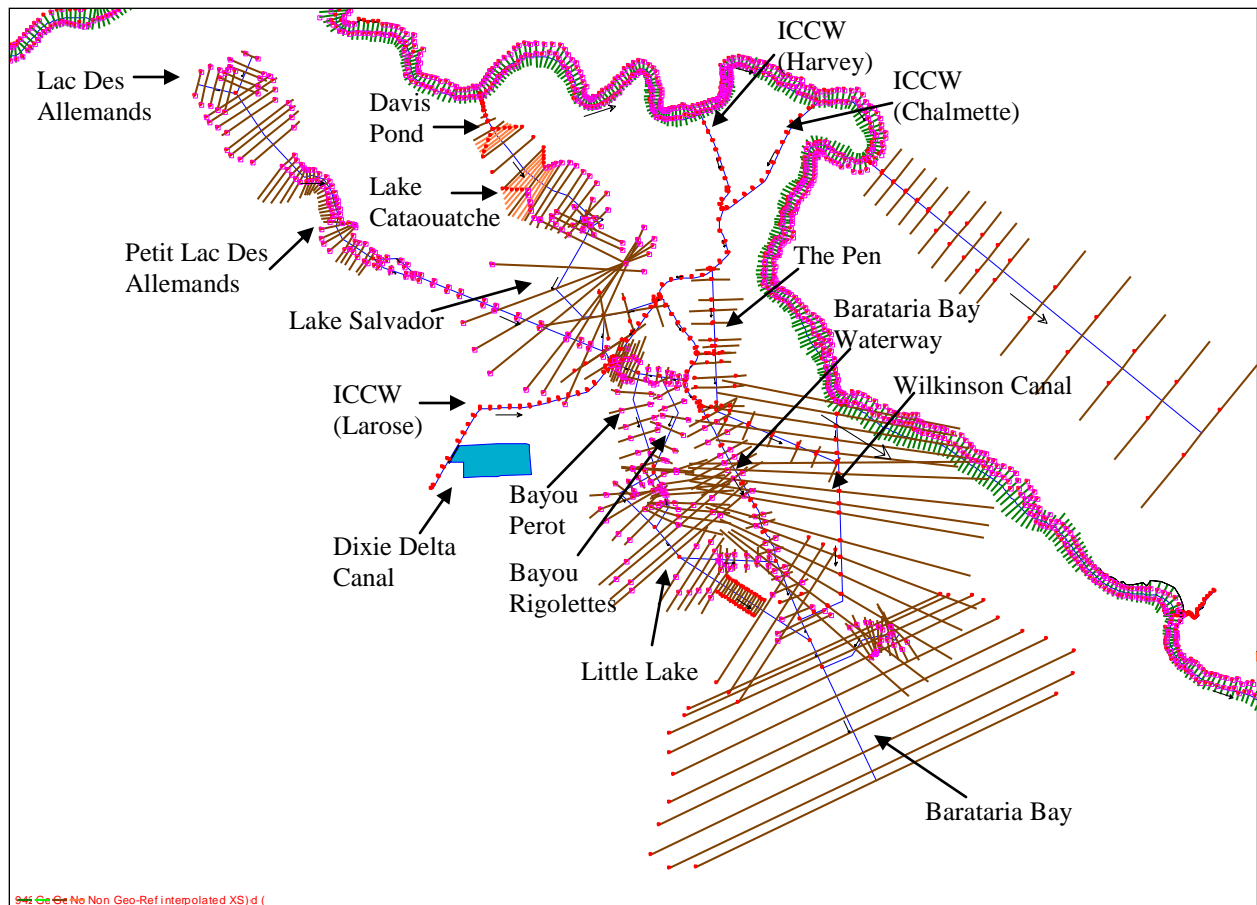


**Figure 2-8: HEC-RAS Image of Barataria Basin.**

## Chapter 3: Description of HEC-RAS Model

### 3.1 Overview

In this study, HEC-RAS 4.0, a 1-D numerical model, was used to simulate the hydrodynamics of the MR under unsteady flow and fixed-bed conditions (USACE HEC, 2008). HEC-RAS is a public domain model created by the Hydrologic Engineering Center (HEC) of the U.S. Army Corps of Engineers, and is an upgrade from its predecessors, HEC-2 and HEC-6, because it includes a user interface and graphical outputs. Some of these outputs include tables which show stages, discharges, velocities, water surface elevations, shear stresses, and many other hydrodynamic features for each cross-section at each user-specified time interval. Other outputs include stage and discharge hydrographs, longitudinal flow profiles, rating curves, and cross-sectional flow profiles. The graphical outputs can also be animated to show how the parameters change at every user-specified time step. The user interface includes buttons with colored icons, a drawing area for the river schematic, a color-coded legend for plots, zooming and panning options, identification labels for reaches, junctions, storage areas, and cross-sections, flow directionality arrows, and multiple windows for viewing purposes. HEC-RAS can make long-term predictions and can handle large scale project areas. Also, tributary and distributary systems can be modeled as a network, like that of the Barataria Basin. Unit options are U.S. Customary and System International (SI). The model can simulate steady and unsteady hydrodynamics. It can also simulate sediment transport under quasi-steady flow regimes.

#### 3.1.1 Geometric Data Editor

A *reach* herein is described as a river, lake, stream, channel, or a portion of these drawn in the geometry data window. A reach is comprised of at least two user-entered cross sections. Cross-sections can be depicted by a maximum of 500 station and elevation coordinates with the first station being zero. All stations should be entered from left to right looking downstream. Data such as Manning's  $n$  values, bank stations, reach lengths, and expansion/contraction coefficients are required for each cross-section. Manning's  $n$  values are used primarily for calibration purposes. They can be varied laterally or vertically. They can also be varied as a function of the channel flow rate by entering flow roughness factors that will be multiplied by the  $n$  values for individual flow rates.

A *junction* herein is described as a connection of two or three reaches for either split flows or flow confluences. The default value for the length across a junction is taken as the reach length of the last cross-section of the reach upstream of the junction. This length can be manually changed for each reach of a junction and a value of zero should replace the reach length of the last upstream cross-section.

The model is capable of estimating flow through, over, and/or around hydraulic structures. These structures include weirs, gates, spillways, storage areas, levees, pumps, culverts, and bridges. The structures are specified as inline structures, lateral structures, bridges/culverts, storage areas, and pumps. An inline structure can be modeled as a weir or a weir with gates (spillway). A lateral structure can be modeled as a weir, a spillway, a weir with culverts, a weir with gates and culverts, or a lateral diversion rating curve. Lateral structures also have the option to divert flow

out of the system, into a storage area, or into a cross-section or range of cross-sections. Lateral structures can be placed on the left or right bank or next to the left or right bank station. Stations, elevations, a weir coefficient, a weir width, a weir crest shape, and the distance to the upstream cross-section are needed for all lateral and inline structures. For gates, the data required are width, height, invert, centerline stations, type, submerged orifice coefficient, overflow weir shape and coefficient. Storage areas in the model are considered to be offline storage and require a lateral structure to connect to a reach. Multiple storage areas can be connected to each other via storage area connections. Inputting a storage area requires a representative area and a minimum elevation or an elevation versus volume curve.

### ***3.1.2 Unsteady Flow Data Editor***

To simulate unsteady flows, both boundary conditions and initial conditions are required. Upstream and downstream boundary conditions are required for all reaches with the following exceptions: If the upstream boundary of a reach is a junction, then only a downstream boundary is necessary; If both boundaries are junctions, then no boundary condition is required. For reaches, the boundary conditions consist of stage hydrographs, flow hydrographs, stage/flow hydrographs, rating curves, and normal depths. For lateral structures with gates, the possible boundary conditions are elevation controlled gates, time series gate openings, and rules. Inline structures have the same boundary conditions as lateral structures except they can also have navigation dams. There is also an option to add an internal boundary condition. Internal boundary conditions consist of lateral inflow hydrographs, uniform lateral flow, groundwater interflow, and internal boundary stage/flow hydrographs. There is also an option to add a lateral inflow hydrograph as a boundary condition for storage areas. Initial conditions consist of the initial flow distribution for the upstream cross-section of each reach and the initial elevation of water in each storage area. There is an option to add a flow change location for any cross-section (except the first of the reach) or any lateral or inline structure of any reach. If any flows are entered with a negative sign, they will be considered outflows.

### ***3.1.3 Unsteady Flow Analysis Editor***

A *plan* herein is described as a simulation setup file with a specific geometry file, a specific unsteady flow data file, a specific starting date and time, and a specific ending date and time. The user must specify which plan to simulate, otherwise the program will run the most recent plan. The model offers the option of selecting which programs to run. These include the geometry preprocessor, the unsteady flow simulation, or the post processor. The user must select a computation time interval, a hydrograph output interval, and a detailed output interval. Some other simulation options available include mixed flow options, initial backwater flow optimizations, calculation options and tolerances, and runtime computational options. Before running a simulation, the program checks that all boundary and initial conditions were entered, that geometry requirements were satisfied, and that all necessary data was provided. If there are any errors or missing input data, the program will stop running and will provide a detailed error message indicating the problem in a separate window. During a simulation, an additional window opens and displays the status of the simulation. After the program stops running, all graphical and tabular outputs are available to check the results.

### 3.2 Governing Equations

Flow in the Mississippi River (MR) is considered unsteady because the velocity in the channel changes with time. Since there are no hydraulic drops or jumps in the considered reach, the flow can be assumed to be gradually varied unsteady flow. The two unsteady equations that HEC-RAS solves for the hydrodynamics are the conservation of mass (continuity) and the conservation of momentum. These two equations were first introduced in their partial differential forms by de St. Venant in 1871 (Mahmood and Yevjevich, 1975). Because of the complexity of the equations, exact integration is not possible unless step methods or simplifying assumptions are used (Chow, 1959). As a result, many mathematicians and engineers have developed their own derivations. HEC-RAS's unsteady flow routing is based on Liggett's derivations of the de St. Venant unsteady flow equations (USACE HEC, 2008). The coordinate system used herein designates  $x$  as the horizontal (longitudinal) direction of primary flow,  $y$  as the horizontal (lateral) direction normal to the primary flow, and  $z$  as the vertical direction.

#### 3.2.1 Conservation of Mass (Continuity)

The conservation of mass dictates that any mass flowing into a control volume (CV) has to come out. Therefore, the net rate of inflow should equal the rate of change in storage in the CV. Consider the CV shown below (Figure 3-1).

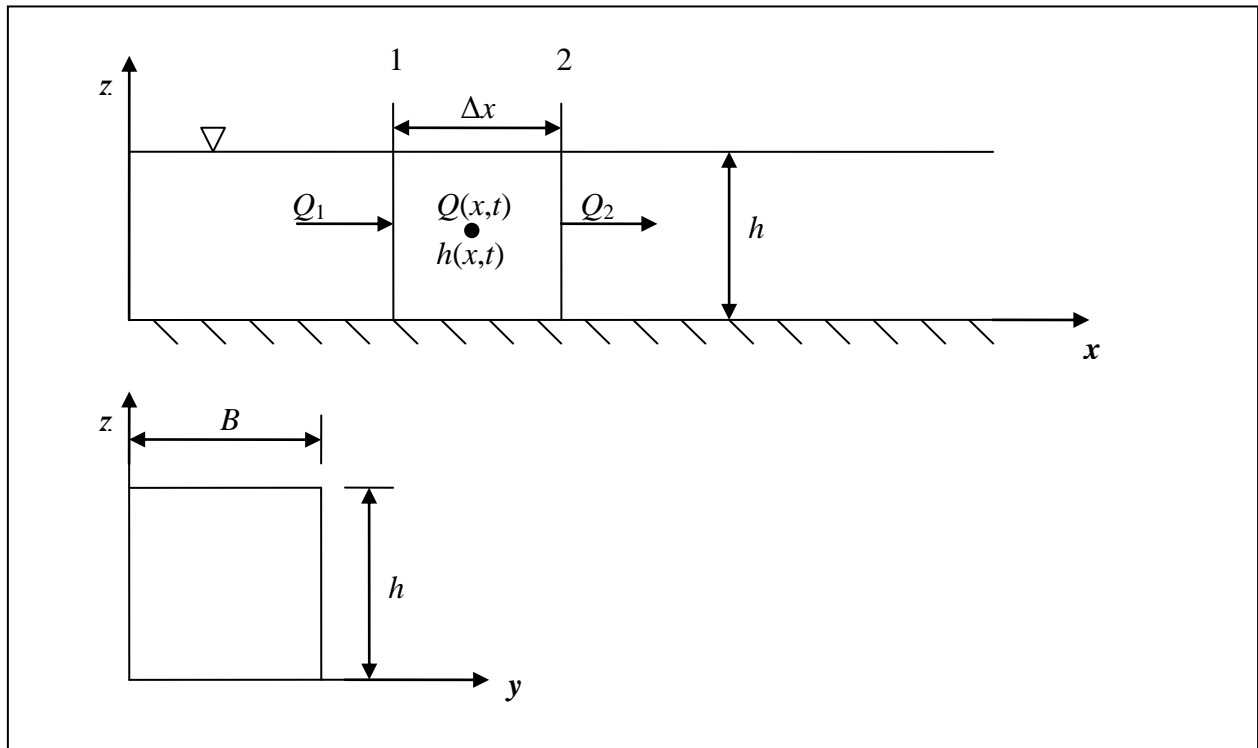


Figure 3-1: Representative Control Volume for Conservation of Mass (Continuity).

In this study, the dependent variables are the velocity,  $v$ , and the channel depth,  $h$ . The independent variables are the longitudinal distance,  $x$ , and the time,  $t$ . This means that the velocity and depth are functions of the distance and time, which are kept constant.

The flow rate,  $Q$ , is a function of the channel area and fluid velocity. As the flow travels from one cross-section to another, across a distance,  $\Delta x$ , the area is considered to be changing with respect to the  $x$ -axis. As a result, the flow rate is also changing over the distance,  $\Delta x$ . This change in flow over distance is represented as  $\partial Q / \partial x$ . The net rate of inflow,  $Q_1$ , equals the flow at the centroid of the CV minus the change in flow at the centroid with respect to the distance between face 1 and the centroid. The net rate of inflow is represented as:

$$Q_1 = Q - \frac{\partial Q}{\partial x} \frac{\Delta x}{2} \quad (3-1)$$

Similarly, the net rate of outflow,  $Q_2$ , equals the flow at the centroid plus the change in flow at the centroid with respect to the distance between face 2 and the centroid. The net rate of outflow is represented as:

$$Q_2 = Q + \frac{\partial Q}{\partial x} \frac{\Delta x}{2} \quad (3-2)$$

The rate of change in storage,  $V^*$ , is equal to the change in volume over time. Since  $x$  is an independent variable, the change in storage becomes  $\partial A \Delta x$ . The rate of change in storage is written as:

$$V^* = \frac{\partial A}{\partial t} \Delta x \quad (3-3)$$

So the conservation of mass can be written as:

$$\rho \frac{\partial A}{\partial t} \Delta x = \rho \left[ \left( Q - \frac{\partial Q}{\partial x} \frac{\Delta x}{2} \right) - \left( Q + \frac{\partial Q}{\partial x} \frac{\Delta x}{2} \right) \right] \quad (3-4)$$

This is simplified into:

$$\rho \frac{\partial A}{\partial t} \Delta x = \rho \left[ -\frac{\partial Q}{\partial x} \Delta x \right] \quad (3-5)$$

Dividing through by  $\rho \Delta x$  yields:

$$\frac{\partial A}{\partial t} = -\frac{\partial Q}{\partial x}$$

or:

$$\frac{\partial Q}{\partial x} + \frac{\partial A}{\partial t} = 0 \quad (3-6)$$

For most natural and man-made channels, additional flow enters the channel due to runoff, precipitation, or by other means. As a result, these lateral flows must be accounted for when considering continuity. Therefore, another term is added to the above equations to consider this extra mass entering the CV. Equation (3-4) becomes:

$$\rho \frac{\partial A}{\partial t} \Delta x = \rho \left[ \left( Q - \frac{\partial Q}{\partial x} \frac{\Delta x}{2} \right) - \left( Q + \frac{\partial Q}{\partial x} \frac{\Delta x}{2} \right) + Q_L \right] \quad (3-7)$$

This is simplified into:

$$\rho \frac{\partial A}{\partial t} \Delta x = \rho \left[ Q_L - \frac{\partial Q}{\partial x} \Delta x \right] \quad (3-8)$$

Assuming the fluid is incompressible, the density,  $\rho$ , is considered constant. Dividing (3-8) by  $\rho \Delta x$  yields:

$$\frac{\partial A}{\partial t} = \frac{Q_L}{\Delta x} - \frac{\partial Q}{\partial x}$$

or:

$$\frac{\partial Q}{\partial x} + \frac{\partial A}{\partial t} - q_L = 0 \quad (3-9)$$

Equation (3-9) is the simplified version of the conservation of mass equation. where:

$Q_1$  = net rate of inflow

$Q_2$  = net rate of outflow

$Q$  = flow rate at the centroid of the CV

$\Delta x$  = differential longitudinal width of the CV

$V^*$  = rate of change of storage ( $= \partial V / \partial t = \partial A \Delta x / \partial t$ )

$A$  = cross-sectional area of the CV ( $= Bh$ )

$B$  = top width of the CV

$h$  = depth of the CV

$t$  = time

$\rho$  = density of the water

$Q_L$  = lateral inflow into the CV

$q_L$  = lateral inflow per unit length of the CV ( $= Q_L / \Delta x$ )

$\partial$  = partial derivative function

### 3.2.2 Conservation of Momentum

From Newton's second law, the conservation of momentum states that the rate of change of momentum of a fluid in a control volume (CV) equals the sum of all the external forces acting on that CV. HEC-RAS only solves the momentum equation in the  $x$ -direction, and the external forces acting on the CV are pressure, gravity, and friction. Figure 3-2 shows a representative CV and the external forces acting on it.

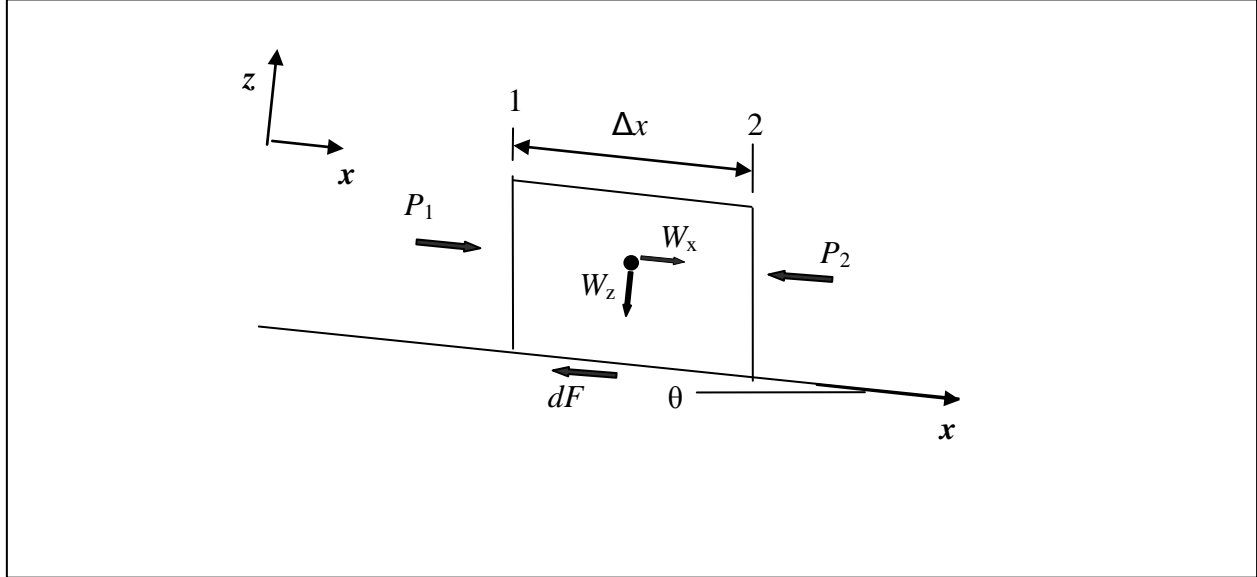


Figure 3-2: Representative Control Volume for Conservation of Momentum.

The conservation of momentum is expressed as:

$$\sum F_x = \frac{dm}{dt} a \quad (3-10)$$

Taking into account the external forces from Figure 3-2 and taking the positive  $x$ -direction to be the right, Equation (3-10) can be written as:

$$P_1 - P_2 + W_x - dF = \frac{dm}{dt} a \quad (3-11)$$

where:

$P_1$  = pressure force along face 1 of the CV

$P_2$  = pressure force along face 2 of the CV

$W_x$  = weight of the water in the CV along the  $x$ -axis ( $= W \sin \theta$ )

$W_z$  = weight of the water in the CV along the  $z$ -axis ( $= W \cos \theta$ )

$dF$  = friction force along the bed of the CV ( $= -\gamma A S_f \Delta x$ )

$dm$  = change in mass in the CV ( $= \rho A \Delta x$ )

$a$  = acceleration of the control volume

$\rho$  = density of the water

$A$  = cross-sectional area of the CV

$\Delta x$  = differential longitudinal width of the CV

$W$  = weight of the water in the CV ( $= \gamma V$ )

$\gamma$  = specific weight of water  
 $V$  = volume of water in the CV ( $= A\Delta x$ )

From Equation (3-11), the acceleration term,  $a$ , has two components. The first is the temporal component,  $a_T$ , which represents the change in velocity in time at the centroid of the CV. The second is the spatial component,  $a_S$ , which represents the change in velocity with respect to the distance between the face and the centroid of the CV. These two components can be represented by:

$$a_T = \frac{\partial v}{\partial t} \quad (3-12)$$

$$a_S = v \frac{\partial v}{\partial x} \quad (3-13)$$

where:

$$a = a_T + a_S$$

or:

$$a = \frac{\partial v}{\partial t} + v \frac{\partial v}{\partial x} \quad (3-14)$$

where:

$v$  = velocity in the CV  
 $t$  = time

Now Equation (3-11) looks like the following:

$$P_1 - P_2 + W_x - dF = dm \left( \frac{\partial v}{\partial t} + v \frac{\partial v}{\partial x} \right) \quad (3-15)$$

The mass in the CV,  $dm$ , is a function of the density and volume of the water.

$$dm = \rho V \quad (3-16)$$

Volume is defined as the product of the length, width, and height of a CV. For this study, the length is designated as  $\Delta x$ , the width is designated as  $B$ , and the height is designated as  $h$ . The cross-sectional area,  $A$ , is defined as the width times the height or  $Bh$ . Therefore, the mass in the CV can be written as the following:

$$dm = \rho A \Delta x \quad (3-17)$$



Equation (3-15) can be written as follows:

$$P_1 - P_2 + W_x - dF = \rho A \Delta x \left( \frac{\partial v}{\partial t} + v \frac{\partial v}{\partial x} \right) \quad (3-18)$$

The pressure,  $p$ , acting on the face of the CV is defined as the force caused by the surrounding water per unit area of the face. According to Liggett, shallow water theory assumes that the pressure is hydrostatic, and it therefore has a linear distribution along the depth (Mahmood and Yevjevich, 1975). The hydrostatic pressure equation is as follows:

$$p = \rho g (h - z) \quad (3-19)$$

where:

- $p$  = pressure
- $\rho$  = density of the water
- $g$  = acceleration due to gravity
- $h$  = water depth
- $z$  = vertical coordinate

Multiplying by the cross-sectional area of the CV to represent a pressure force,  $P$ , Equation (3-19) becomes:

$$P = \rho g A (h - z) \quad (3-20)$$

If the pressure at the centroid of the CV is designated as  $P$ , then the pressure at face 1,  $P_1$ , would be the pressure  $P$  minus the change in pressure  $P$  from face 1 to the centroid, times the distance between face 1 and the centroid. The same applies to the pressure at face 2,  $P_2$ , except the change in pressure is added to the pressure  $P$  at the centroid. See Equations (3-21) and (3-22) below:

$$P_1 = P - \frac{\partial P}{\partial x} \frac{\Delta x}{2} \quad (3-21)$$

$$P_2 = P + \frac{\partial P}{\partial x} \frac{\Delta x}{2} \quad (3-22)$$

Subtracting the pressures at the faces of the CV yields:

$$P_1 - P_2 = \left( P - \frac{\partial P}{\partial x} \frac{\Delta x}{2} \right) - \left( P + \frac{\partial P}{\partial x} \frac{\Delta x}{2} \right)$$

or:

$$P_1 - P_2 = - \frac{\partial P}{\partial x} \Delta x \quad (3-23)$$

Integrating Equation (3-20) between  $h$  and  $z$  with respect to the  $x$ -axis and setting  $\rho$ ,  $g$ , and  $A$  as constants, Equation (3-23) becomes:

$$P_1 - P_2 = -\rho g A \Delta x \frac{\partial z}{\partial x}$$

or:

$$P_1 - P_2 = -\gamma A \Delta x \frac{\partial z}{\partial x} \quad (3-24)$$

Substituting Equation (3-24) into Equation (3-18) yields:

$$-\gamma A \Delta x \frac{\partial z}{\partial x} + W_x - dF = \rho A \Delta x \left( \frac{\partial v}{\partial t} + v \frac{\partial v}{\partial x} \right) \quad (3-25)$$

The weight of the CV,  $W$ , is defined as the mass,  $dm$ , times the acceleration due to gravity,  $g$ . Using Equation (3-16), the weight can be written as:

$$W = \rho g A \Delta x \quad (3-26)$$

For this study, the weight is separated into two components: the  $x$  component,  $W_x$ , and the  $z$  component,  $W_z$ . Where, the  $x$  component is parallel to the channel bed and the  $z$  component is perpendicular to the channel bed. If  $\theta$  is the angle of the channel bed with respect to the horizontal, and taking into account only the  $x$  component, then:

$$W_x = W \sin \theta$$

or:

$$W_x = \rho g A \Delta x \sin \theta$$

or:

$$W_x = \gamma A \Delta x \sin \theta \quad (3-27)$$

In natural channels, the angle  $\theta$  is quite small. Therefore,  $\sin \theta$  can be written as  $\tan \theta$ , which is the slope of the channel bed,  $S_0$ . Equation (3-25) becomes:

$$-\gamma A \Delta x \frac{\partial z}{\partial x} + \gamma A \Delta x S_0 - dF = \rho A \Delta x \left( \frac{\partial v}{\partial t} + v \frac{\partial v}{\partial x} \right) \quad (3-28)$$

The friction force acting on the CV,  $dF$ , is defined as the product of the boundary shear stress,  $\tau_0$ , the wetted perimeter,  $P_w$ , and the length,  $\Delta x$ , of the CV or:

$$dF = \tau_0 P_w \Delta x \quad (3-29)$$

The boundary shear stress can be written as:

$$\tau_0 = \rho C_D v^2 \quad (3-30)$$

where  $C_D$  is the drag coefficient, which can be defined as:

$$C_D = \frac{g}{C^2} \quad (3-31)$$

The denominator,  $C$ , is the Chezy coefficient, which helps define the velocity in the Chezy equation:

$$v = C \sqrt{RS_f} \quad (3-32)$$

where:

$R$  = hydraulic radius ( $= A/P_w$ )

$S_f$  = friction slope

Combining Equations (3-29) and (3-30) yields:

$$dF = \rho C_D v^2 P_w \Delta x \quad (3-33)$$

Plugging Equation (3-31) into Equation (3-33) shows:

$$dF = \rho \frac{g}{C^2} v^2 P_w \Delta x \quad (3-34)$$

Plugging Equation (3-32) into Equation (3-34) yields:

$$dF = \rho \frac{g}{C^2} \left( \sqrt{RS_f} \right)^2 P_w \Delta x$$

or:

$$dF = \rho \frac{g}{C^2} C^2 S_f R P_w \Delta x \quad (3-35)$$

Using the expressions for  $\gamma$  and  $A$ , Equation (3-35) can be simplified to:

$$dF = \gamma A \Delta x S_f \quad (3-36)$$

Equation (3-35) can be plugged into Equation (3-28) to:

$$-\gamma A \Delta x \frac{\partial z}{\partial x} + \gamma A \Delta x S_0 - \gamma A \Delta x S_f = \rho A \Delta x \left( \frac{\partial v}{\partial t} + v \frac{\partial v}{\partial x} \right) \quad (3-37)$$

Dividing Equation (3-37) through by  $\rho A \Delta x$  and combining like terms, yields the simplified equation of the conservation of momentum:

$$\frac{\partial v}{\partial t} + v \frac{\partial v}{\partial x} + g \left( \frac{\partial z}{\partial x} - S_0 + S_f \right) = 0 \quad (3-38)$$

### **3.3 Finite Difference Method**

Due to the presence of non-linear terms in the above conservation equations, a numerical method is required to solve the equations. Several methods, such as the method of characteristics and finite-difference methods are used more often than others (Roberson *et al.* 1988). The HEC-RAS program uses a finite difference method, which takes a channel and divides it into  $N$  reaches each with a length of  $\Delta x$ . Each reach is defined by two nodes: an upstream node and a downstream node. If the first node of the channel is labeled 1, then the last node would be labeled  $N+1$ . The equations are solved at distinct instances in time, where the difference in two times is called a computational time step,  $\Delta t$  (Roberson *et al.* 1988). In HEC-RAS, the computational time step is inputted by the user. A computational grid is then created using the independent variables  $x$  and  $t$ . HEC-RAS uses the four-point implicit scheme, or box scheme, to solve the equations of continuity and momentum. Figure 3-3 shows the computational grid for the box scheme.

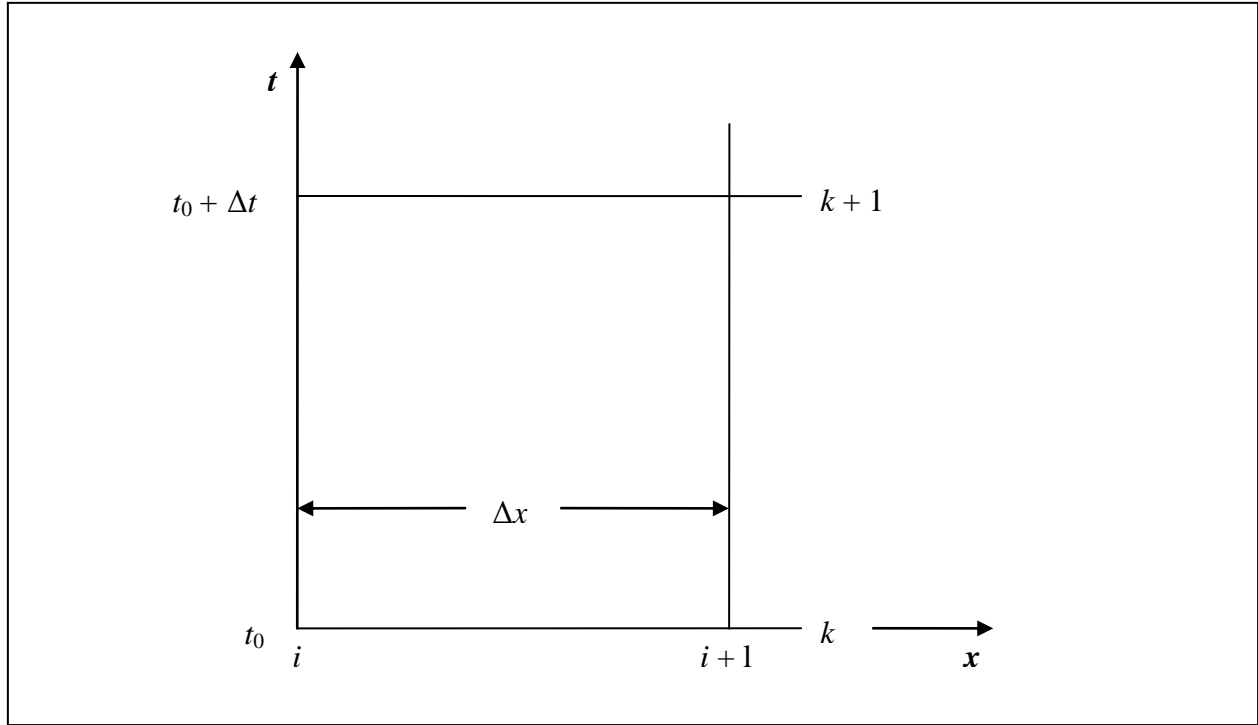


**Figure 3-3: Computational Grid for the Box Scheme.**

The partial derivatives of the governing equations (3-9) and (3-38) are substituted by finite-difference approximations, which become algebraic equations that are easier to solve. If the known variables at  $t_0$  represent the initial conditions, then the unknown variables correspond to  $t_0 + \Delta t$ . For the implicit scheme, the algebraic equations are in terms of the unknown variables and are computed at each node, simultaneously.

### ***3.4 Hydraulic Structures Equations***

In this study, several hydraulic structures were inputted, including sluice gates and overflow weirs. The following procedure shows how HEC-RAS computes flow through or over these structures (USACE HEC, 2008).

A sluice gate is a structure where the gate moves up and allows water to flow underneath. Figure 3-4 shows an example of a sluice gate with a broad crested spillway.

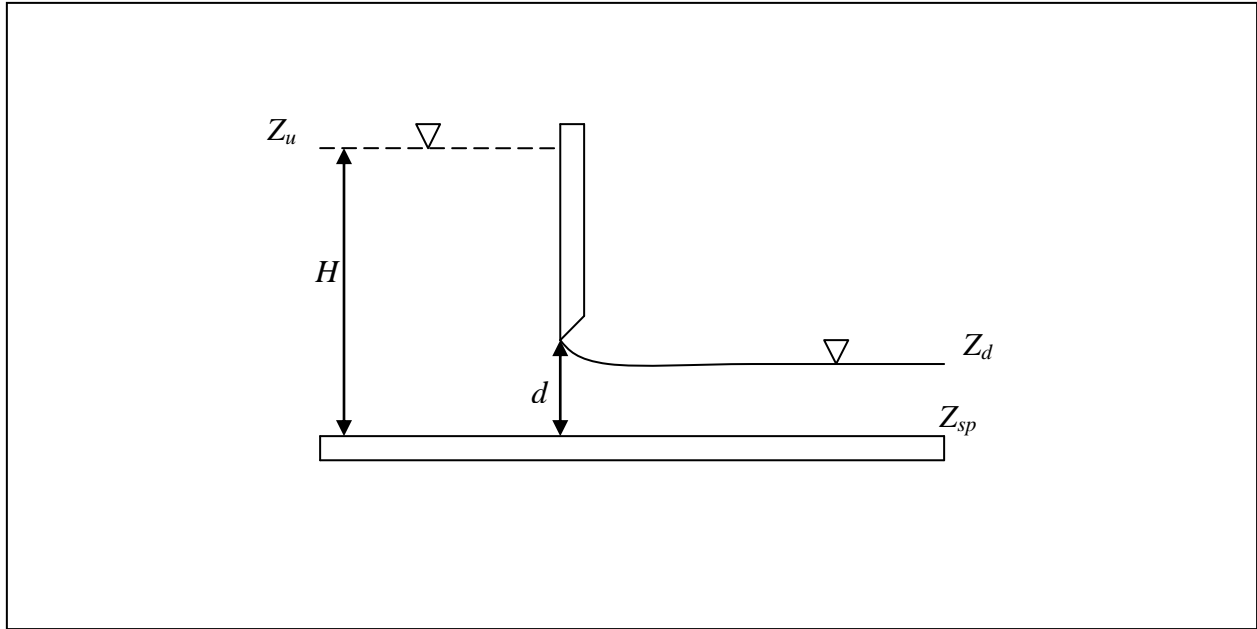


**Figure 3-4: Sluice Gate with Broad Crested Spillway.**

The free-flowing sluice gate equation is as follows:

$$Q = Cwd \sqrt{2gH} \quad (3-39)$$

where:

- $Q$  = flow rate under the gate
- $C$  = coefficient of discharge (typically 0.5 to 0.7)
- $w$  = width of the gated spillway
- $d$  = opening height of the gate
- $g$  = acceleration due to gravity
- $H$  = upstream energy head ( $= Z_u - Z_{sp}$ )
- $Z_u$  = upstream water surface elevation
- $Z_d$  = downstream water surface elevation
- $Z_{sp}$  = spillway elevation

If the downstream tailwater increases to the point where the tailwater depth divided by the upstream energy head equals 0.67, then submergence has taken place and the program uses the following equation:

$$Q = Cwd \sqrt{2gkH} \quad (3-40)$$

where:

- $H = Z_u - Z_d$
- $k$  = submergence factor

When the submergence reaches 0.8, the program switches to the fully submerged orifice flow equation as shown below:

$$Q = CA\sqrt{2gH} \quad (3-41)$$

where:

$A$  = gate opening area

$H = Z_u - Z_d$

$C$  = discharge coefficient (typically 0.8)

If the upstream water surface becomes less than or equal to the height of the gate opening, then the program switches to the standard weir equation shown below:

$$Q = CLH^{3/2} \quad (3-42)$$

where:

$C$  = weir flow coefficient (typically 2.6 to 4)

$L$  = length of spillway crest

$H$  = upstream energy head ( $= Z_u - Z_{sp}$ )

For lateral structures with weirs, the standard weir equation is applied unless specified by the user to use the Hager's Equation. The Hager's Equation is the standard weir equation except there is a change in how the discharge coefficient is found. The equation for the discharge coefficient is as follows:

$$C = \frac{3}{5} C_0 \sqrt{g} \left[ \frac{1-W}{3-2y-W} \right]^{0.5} \left\{ 1 - \beta + S_0 \left[ \frac{3(-y)}{y-W} \right]^{0.5} \right\} \quad (3-43)$$

$$W = \frac{h_w}{H_t + h_w} \quad (3-44)$$

$$y = \frac{H + h_w}{H_t + h_w} \quad (3-45)$$

where:

$H$  = height of the water surface above the weir

$h_w$  = height of the weir above the ground

$H_t$  = height of the energy grade line above the weir

$S_0$  = average main channel bed slope

$\beta$  = main channel contraction angle [= radians] (0 if weir is parallel to the main channel)

$C_0$  = base discharge coefficient (function of weir shape)

and:

$C_0 = 1.0$  for sharp crested weirs

$C_0 = 8/7$  for zero height weirs

For broad crested weirs ( $b$  = weir width):

$$C_0 = 1 - \frac{2}{9 \left[ 1 + \left( \frac{H_t}{b} \right)^4 \right]} \quad (3-46)$$

For round or ogee weirs ( $r$  = weir radius)

$$C_0 = \frac{\sqrt{3}}{2} \left[ 1 + \frac{\frac{22}{81} \left( \frac{H_t}{r} \right)^2}{1 + \frac{1}{2} \left( \frac{H_t}{r} \right)^2} \right] \quad (3-47)$$



## Chapter 4: Model Development

### 4.1 Geometry Data<sup>1</sup>

As stated previously, the cross-sections of the Mississippi River (MR) reach from Tarbert Landing to Venice were taken from the 2009 HEC-RAS study (Pereira *et al.* 2009). The additional cross-sections of the MR from Venice to the HOP, as well as Baptiste Collette, Cubits' Gap (Main Pass), Grand Pass and Tiger Pass, Southwest Pass, South Pass, and Pass a Loutr , were taken from the 2003-2004 Hydrographic Survey (USACE NOD, 2007). Design cross-sectional data for the Intracoastal Waterway (ICCW) at Harvey, Chalmette, and Larose and for the Barataria Bay Waterway were obtained from the 1985 New Orleans Area Map (USACE MRC, 1985). Google Earth Imagery was used to measure the top widths of several representative sections along each of these channels. For the Davis Pond channel, the design parameters, such as bottom width, bottom elevation (NGVD 29), and length, were taken from the project fact sheet (Project Fact Sheet, 2003), and the top widths of the cross-sections were taken from Google Earth Imagery. Figure 4-1 shows the Davis Pond channel in Google Earth (2010). Data for the rest of the Barataria Basin, including Lake Cataouatche, Lake Salvador, Bayou Rigolettes, Bayou Perot, Little Lake, The Pen, Barataria Bay Waterway, Barataria Bay, Lac Des Allemands, Petit Lac Des Allemands, and Wilkinson Canal, were extracted from the 2003 LIDAR/bathymetry dataset<sup>2</sup> in Tecplot 10. According to Georgiou *et al.* (2010), this dataset was a composite of LIDAR topography data from the Louisiana State University Atlas website and bathymetry data from various sources.

---

<sup>1</sup> A table of all the junctions and their upstream and downstream reaches is presented in Appendix A.

<sup>2</sup> Appendix B shows the 2003 LIDAR/bathymetry image for the entire Barataria Basin in Tecplot.



**Figure 4-1: Google Earth Image of Davis Pond Freshwater Diversion Channel (2010).**

#### ***4.1.1 Geometry Issues in HEC-RAS***

The 2003 LIDAR/bathymetry dataset from Georgiou *et al.* (2010) was used to obtain the stations and elevations of the lakes, ponds, and channels in the Barataria Basin. In order to extract the required information from the LIDAR/bathymetry file, a number of polylines or transects were needed through each water body. Each polyline represents a user-specified number of data points consisting of  $x$ ,  $y$ , and  $z$  coordinates. The number of transects drawn for each channel depended on the shape of the water body. If a lake, for example, has an odd shape where the cross-section rapidly expands or contracts, then several transects would be needed in order to capture the unique shape of the lake. A normal transect would slice perpendicular to the flow from right to left. The direction of the slice is important because the USACE has adopted a method of determining the left and right banks depending on the perspective of the viewer. This method concludes that the left bank is always the bank that would be on a viewer's left side if the viewer were looking downstream of the water body. Some channels in the LIDAR/bathymetry file are

discontinuous due to mesh constraints. This can be seen in Figure 4-2 for Lac Des Allemands. For this case, the portion of the channel near Lake Salvador looks choppy, but in reality, it is not. Therefore, transects were only drawn through the light green sections, which represent the channel. The same procedure was repeated for other channels with similar discontinuities.

The upstream section of Lac Des Allemands has an irregular shape, as shown in Figure 4-2. From the legend, the darker blue color represents a negative depth or positive elevation. Therefore, a transect across the two upstream “tips” of the lake shows a raised portion (darker blue) in the center. This higher elevation acts as an island in between two channels and causes a split flow in the HEC-RAS program. To fix this problem, two reaches were created at the inlet. The transects for each reach extended from right to left and met at the center of the “island.” These two reaches were labeled Des Allemands Reach 1 and Des Allemands Reach 2, and connected to form a third reach called Des Allemands Reach 3. Farther down the lake, near Petit Lac Des Allemands, the flow splits into two separate channels. As a result, Des Allemands Reach 4 and Reach 5 were created to account for this separation. These two reaches were combined to form Des Allemands Reach 6, which connected to Davis Pond Reach Lake Salvador Left at junction Des Allemands 4. Figure 4-3 shows the Des Allemands reaches in HEC-RAS.

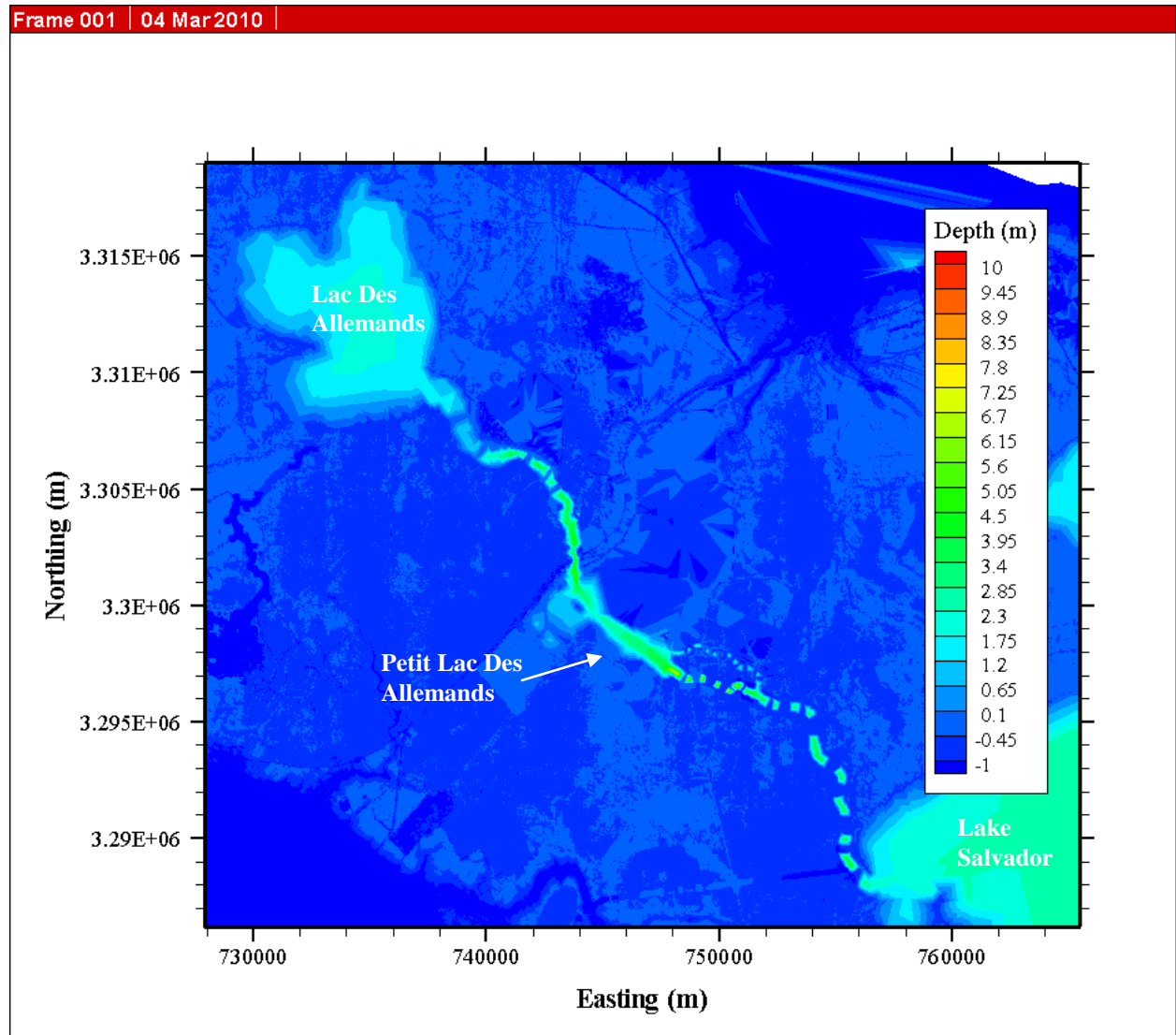
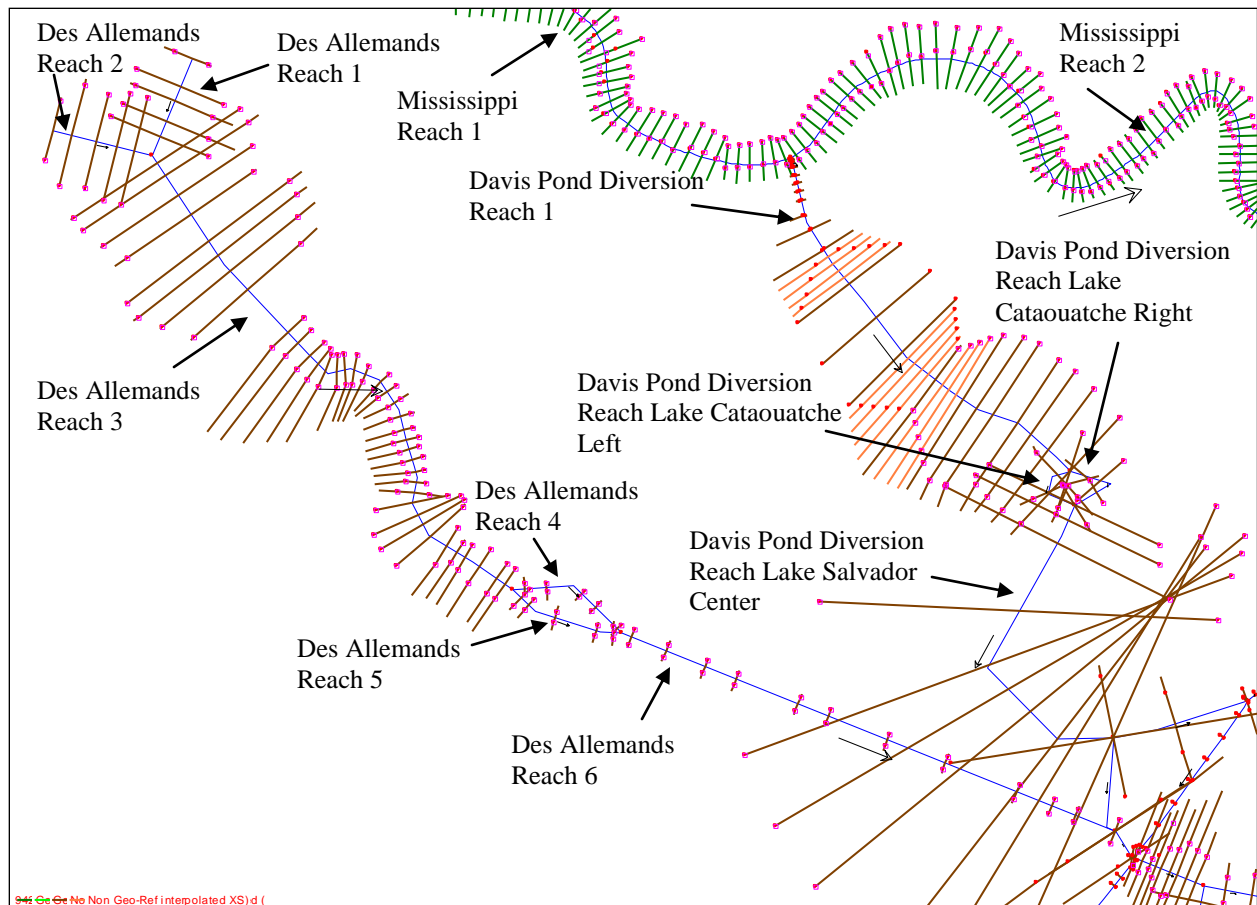


Figure 4-2: Tecplot Image of Lac Des Allemands from 2003 LIDAR/bathymetry.



**Figure 4-3: HEC-RAS Image of Des Allemands Channels and Others.**

The Pen is a small lake on the east side of the Barataria Bay Waterway, and connects to the ICCW near Crown Point via several small canals, as shown in Figure 4-4 (Google Earth Imagery, 2010). The Pen also connects to the Barataria Bay Waterway at two separate locations. These two connections resemble small channels. As a result, transects were drawn across each of them in Tecplot to create two small reaches, which were labeled The Pen Reach 1.5 (top) and The Pen Reach 2.5 (bottom). The outlet of The Pen, labeled The Pen Reach 3, leads to a marsh area that connects to Wilkinson Canal (to be discussed later).





**Figure 4-4: Google Earth Image of The Pen (2010).**

Figure 4-5 shows the LIDAR/bathymetry for Lake Cataouatche (top) and Lake Salvador (center). From the figure, the downstream section of Lake Cataouatche shows two separate limbs that lead to Lake Salvador. A single transect across these limbs illustrates an island with a channel on either side. Therefore, each limb was given its own set of transects to create two distinct channels. These were labeled Davis Pond Reach Lake Cataouatche Left and Davis Pond Reach Lake Cataouatche Right, and were combined to form Davis Pond Reach Lake Salvador Center. The figure also shows that Lake Salvador is split into two separate limbs on the right. Therefore, Lake Salvador Center was split to form two reaches labeled Davis Pond Reach Lake Salvador Right and Davis Pond Reach Lake Salvador Left. From the figure, Davis Pond Reach Lake Salvador Right combines with three other channels at one location<sup>3</sup>. Two of these three channels

<sup>3</sup> For the purpose of this study, the small channel on the immediate right of Lake Salvador (Bayou Segnette Waterway) was not included because it is not directly connected to the MR and does not contribute a large amount of flow to the Barataria Basin.

are the ICCW, and the third channel is the Barataria Bay Waterway. HEC-RAS can only simulate channel splits from one channel into two channels, or channel combinations of two channels into one channel. As a result, the combination of the four channels was replaced by a combination of two reaches leading to an intermediate channel which was split into the other two reaches. The intermediate channel was comprised of two cross-sections from the ICCW. The upstream junction was labeled Barataria Bay Waterway 1 and connected ICCW Reach 2 and Barataria Bay Waterway Reach 1. The intermediate reach was labeled ICCW Reach 3 and connected to a junction labeled Lake Salvador 2. This junction connected ICCW Reach 4 with Davis Pond Reach Lake Salvador Right. From Figure 4-5, a similar situation occurs at the second limb of Lake Salvador, which connects with the ICCW and Bayou Perot. Therefore, Davis Pond Reach 4 was combined with ICCW Reach 4 to form junction ICCW 1. The intermediate reach, Davis Pond Reach 5, consisted of cross-sections from Lake Salvador, and combined with ICCW Reach 5 to create Bayou Perot Reach 1 at junction ICCW 2.

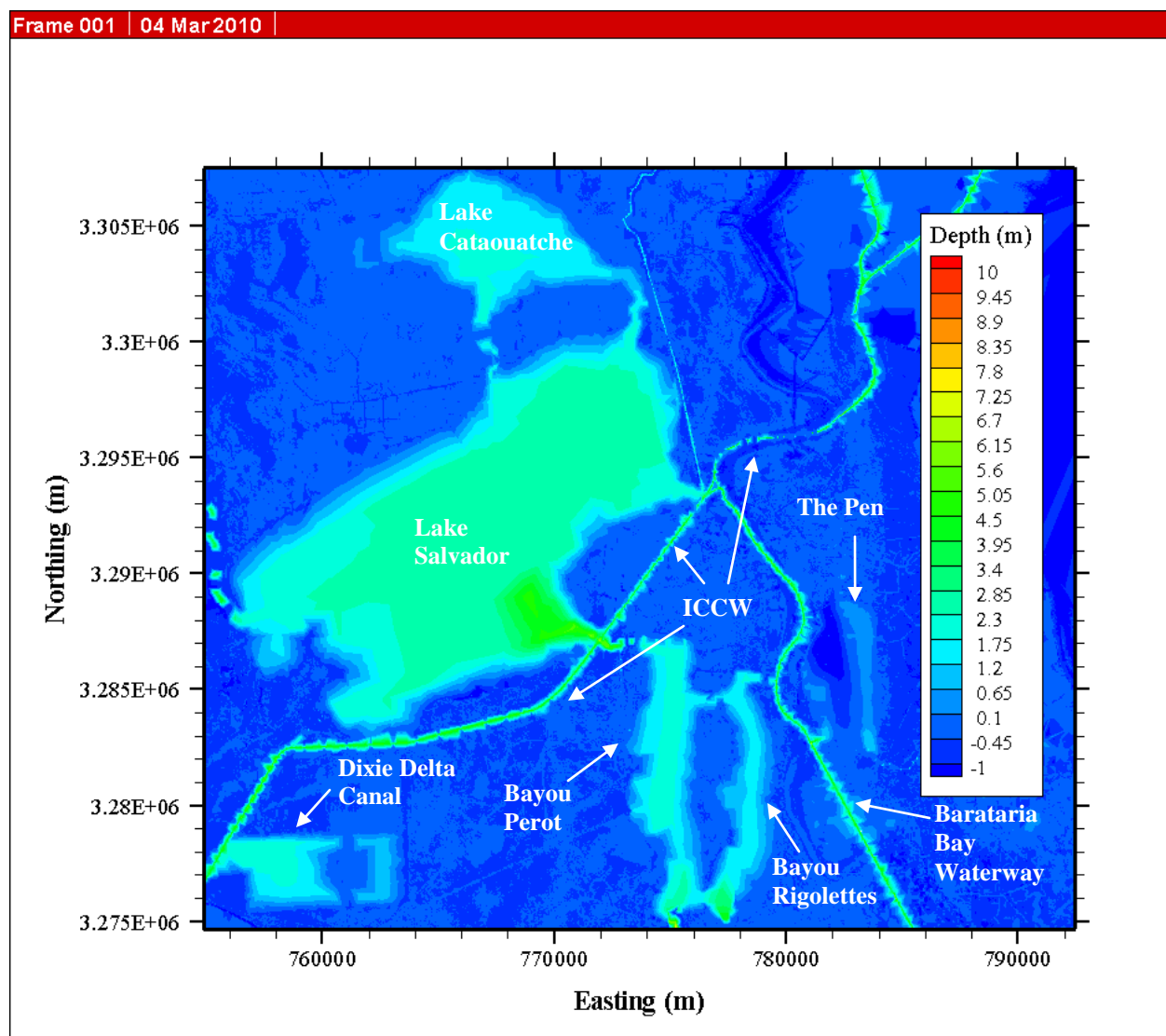


Figure 4-5: Tecplot Image of Lake Cataouatche, Lake Salvador, Bayou Rigolettes, Bayou Perot, The Pen, Barataria Bay Waterway, ICCW, and Dixie Delta Canal from 2003 LIDAR/bathymetry.

Figure 4-5 shows a wide section of the Barataria Bay Waterway just downstream of The Pen (Barataria Bay Waterway Reach 4). As a result, transects along this section were collected and were inserted between the design cross-sections mentioned previously.

As seen in Figure 4-5, Bayous Perot and Rigolettes connect at two places (bottom center). Initially, transects were taken across both bayous to create a single reach. However, the island in between the bayous caused a split flow in the HEC-RAS program. As a result, several reaches were created to account for this setup. The top connection between the bayous was designed as its own channel with transects from Tecplot and was labeled Bayou Rigolettes Reach 1. Bayou Perot Reach 1, mentioned previously, was connected to Bayou Perot Reach 2 and Bayou Rigolettes Reach 1 at junction Bayous P&R 1. The connection from Bayou Rigolettes to the Barataria Bay Waterway was labeled Bayou Rigolettes Reach 2 and was connected to Bayou Rigolettes Reach 3 at junction Bayou Rigolettes. The bottom connection between the bayous was designed as a junction, labeled Bayous P&R 2, which combined Bayou Rigolettes Reach 3 with Bayou Perot Reach 2. A transect was also taken at the connection and copied to create a small channel, which was called Bayous P&R Reach 1.

From Figure 4-6, both Bayou Rigolettes and Bayou Perot connect to Little Lake via individual channels. As a result, two reaches were designed to split from Bayous P&R Reach 1 at junction Little Lake 1. These channels were labeled Little Lake Reach 1 and Little Lake Reach 2. Due to the presence of an island in the middle of Little Lake, these two reaches were extended to a junction, Little Lake 2, by drawing transects through Little Lake up to the island. Downstream of the island, transects were drawn to create a single reach, Little Lake Reach 3. The lake then splits into two reaches, where the upper reach, Little Lake Reach 4, is well defined and connects to Barataria Bay Waterway Reach 4 at the junction Barataria Bay 1. The lower reach, Little Lake Reach 5, connects to Barataria Bay Reach 2 at junction Barataria Bay 3, but it is not well defined. Therefore, an equivalent channel was created by taking many transects through that area and obtaining an average depth and average width. This equivalent channel was added to the transects of the well-formed portions of the channel to create Little Lake Reach 5.

Also in Figure 4-6, Wilkinson Canal is shown as the small light blue line running north to south on the immediate left of the legend. The figure also shows shallow water bodies surrounding the canal, which act as storage areas. An equivalent channel was designed to represent a modified Wilkinson Canal and was given inline storage to account for this naturally occurring storage capacity. This equivalent channel was given a depth of 15 ft and a width of 172 ft, and the inline storage was given a depth of 2 ft and variable width ranging from 80,000 – 90,000 ft (to capture the surrounding areas). This channel was labeled Wilkinson Canal Reach 1 and was connected to The Pen Reach 3 at the junction Wilkinson Canal 1. This combination forms the channel Wilkinson Canal Reach 2, which connects to Barataria Bay Reach 1 at junction Barataria Bay 2.

Figure 4-7 shows the LIDAR/bathymetry image of Barataria Bay, which does not have well-defined boundaries. As a result, long transects were drawn to capture the full width of the Bay and extended to the outlets or passes that lead into the GOM. Due to the irregular shape of the Bay, a small reach was created to account for a small limb extending from the right of the Bay that could not be accurately represented with the standard transects. This small reach was labeled Barataria Bay Reach 4 and connected to Barataria Bay Reach 3 at junction Barataria Bay 4.



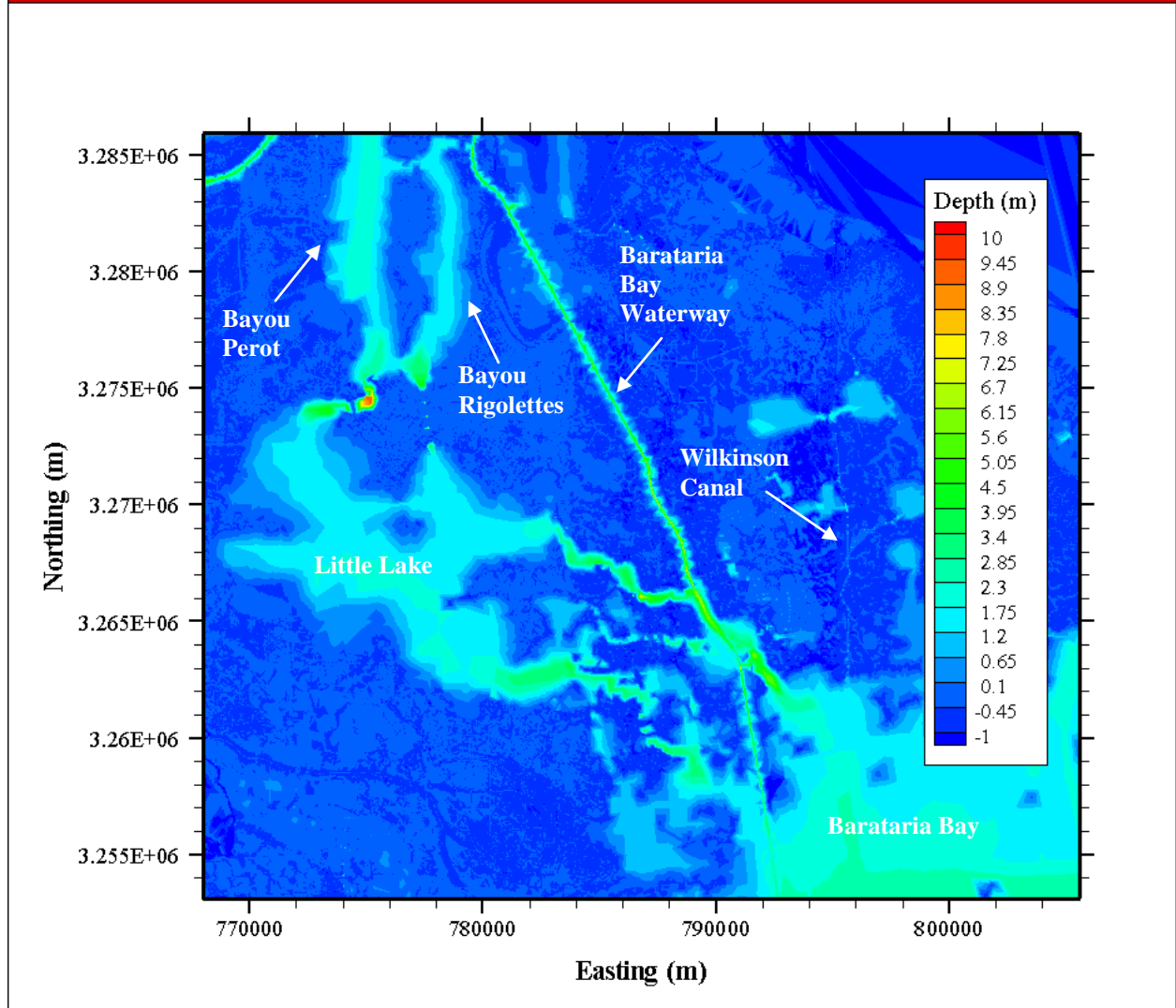


Figure 4-6: Tecplot Image of Bayou Perot, Bayou Rigolettes, Little Lake, Barataria Bay Waterway, Barataria Bay, and Wilkinson Canal from 2003 LIDAR/bathymetry.

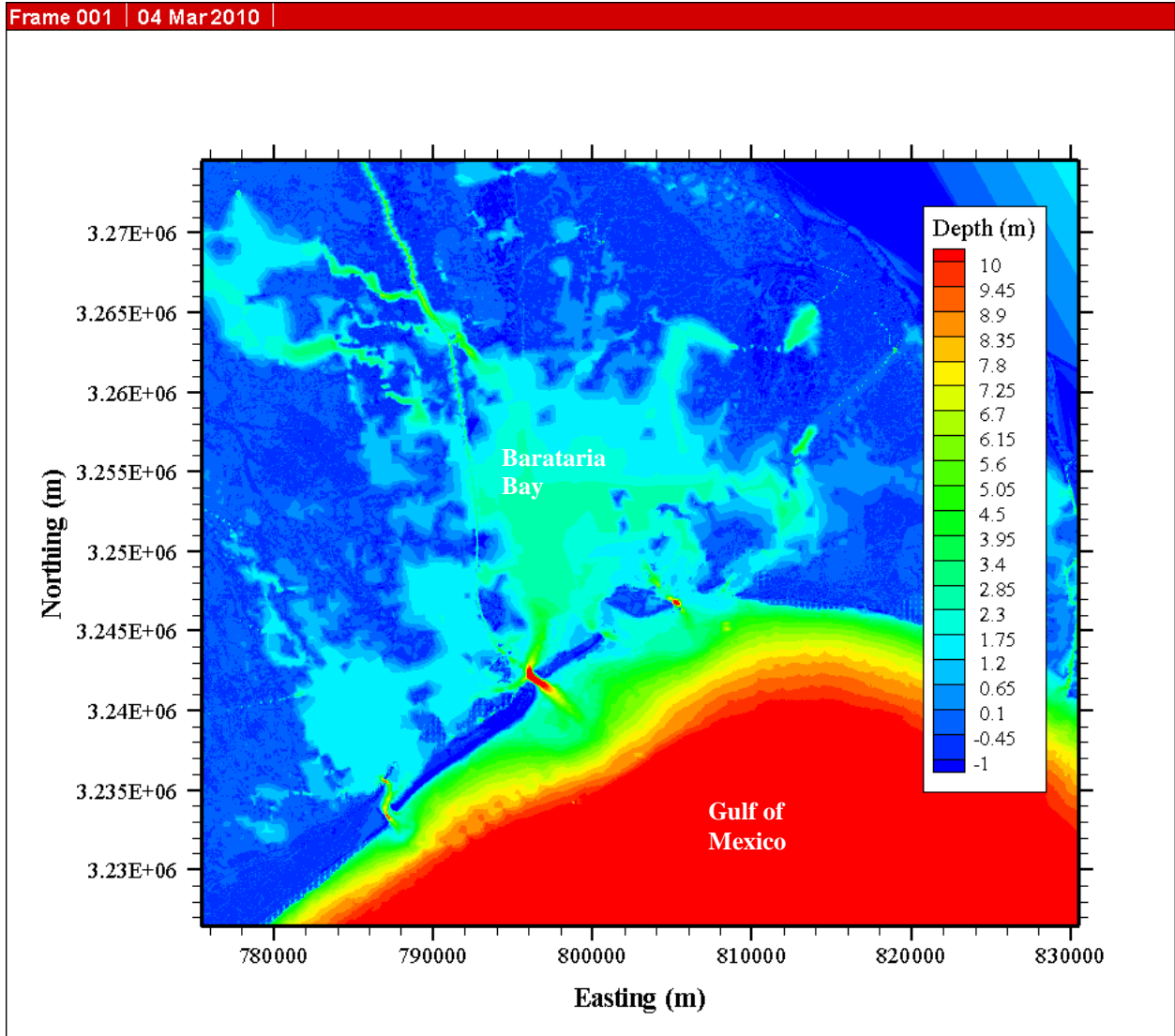


Figure 4-7: Tecplot Image of Barataria Bay from 2003 LIDAR/bathymetry.

#### 4.1.2 Geometry Issues with Available Data

Geometry data for several of the channels was not readily available for this study. Also, closer investigation of the channels identified areas of additional flow capacity. Therefore, alternative methods for inputting the necessary geometry data were explored and utilized. The method chosen was creating equivalent channels, which uses Google Earth Imagery and/or the Lacey Regime Equations<sup>4</sup>. An equivalent channel is a representative channel that attempts to capture the flow capacity. The depths of the equivalent channels were either based on the hydraulic radius of the original channel, where possible, or were estimated using known relative depths in the area, where original channel data were not available.

Due to insufficient survey data of the Bayou Lamoque channels, equivalent channels were used. The Lacey Regime Equations, along with top widths obtained from Google Earth, were used to

<sup>4</sup> The Lacey Regime Equations are presented in Appendix C.

create these equivalent channels for Bayou Lamoque North, Bayou Lamoque South, and Bayou Lamoque. Since HEC-RAS is a 1-D model, the shape of the channels does not matter as long as the full capacity of the channel is accounted for, including ineffective storage areas. Therefore, the cross-sections were assumed to be rectangular. The heights of the banks were estimated using the Google Earth elevation feature, which gives an approximate value. Figure 4-8 shows the equivalent channels in HEC-RAS. Bayou Lamoque North Reach 1 (top) combines with Bayou Lamoque South Reach 1 (bottom) to create Bayou Lamoque Reach 1.

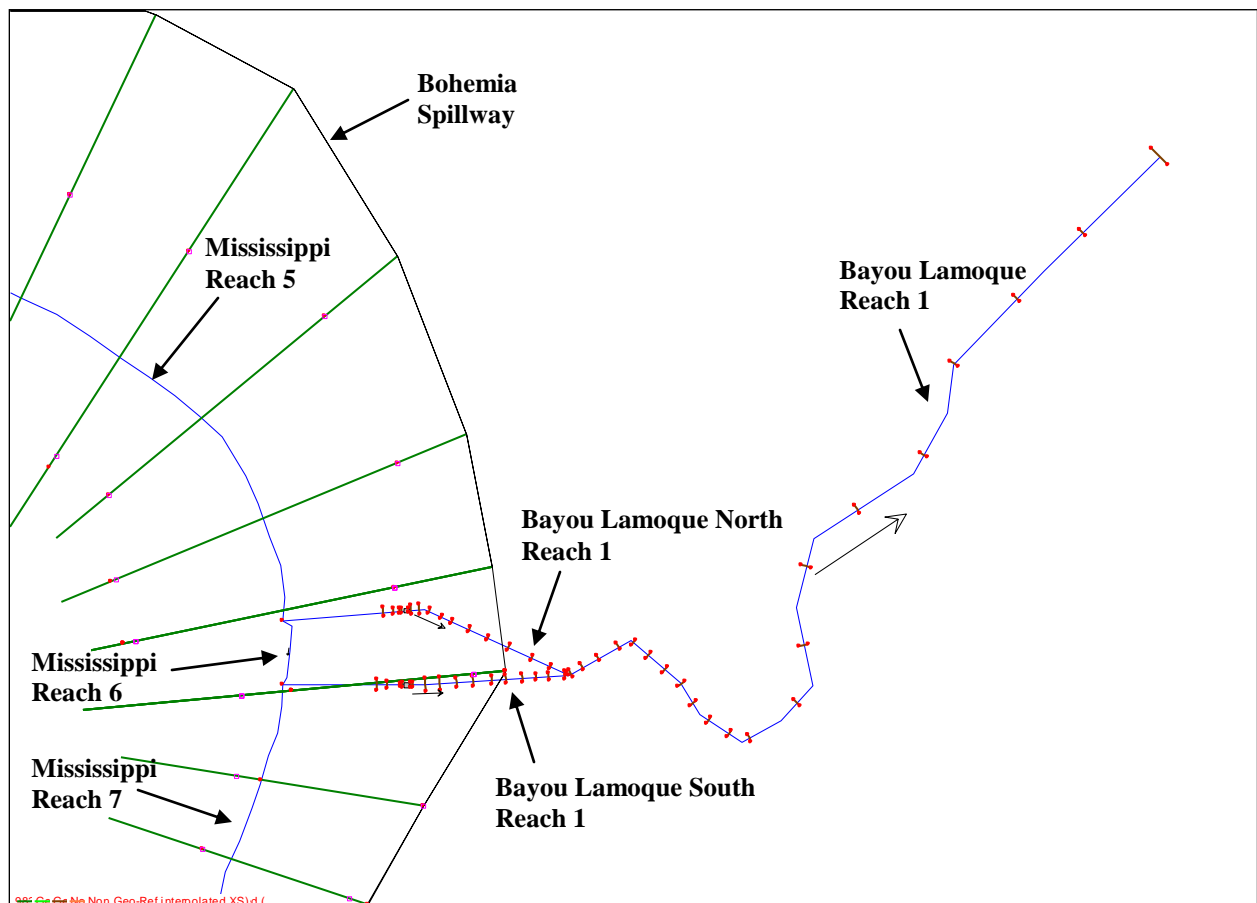


**Figure 4-8: HEC-RAS Image of Bayou Lamoque North, Bayou Lamoque South, and Bayou Lamoque Channels.**

For the Fort St. Philip reach (RM 19.4), an equivalent channel was created using the top widths of the cuts from Google Earth Imagery (2010). The cuts extend along the MR from the Ostrica Lock (RM 25.2) to Baptiste Collette (RM 11.5) and collectively equal 5455 ft wide (Meselhe *et al.* 2010). The travel distance from the inlet to the outlet was estimated as 30,000 ft, using the Google Earth ruler function. The channel depth was varied from 5 ft at the inlet to 3.5 ft at the outlet. Inline storage was created to account for extra capacity flowing through the marsh during high flows. Representative widths were measured using Google Earth to define the widths for the inline areas. The channel width, including inline storage, was expanded from the inlet at 10,379 ft to the outlet at 35,000 ft. Intermediate cross-sections (orange) were calculated using HEC-RAS RS interpolation. Figure 2-2 shows some of the cuts near Fort St. Philip. Figure 4-9 shows the equivalent Fort St. Philip channel in HEC-RAS.

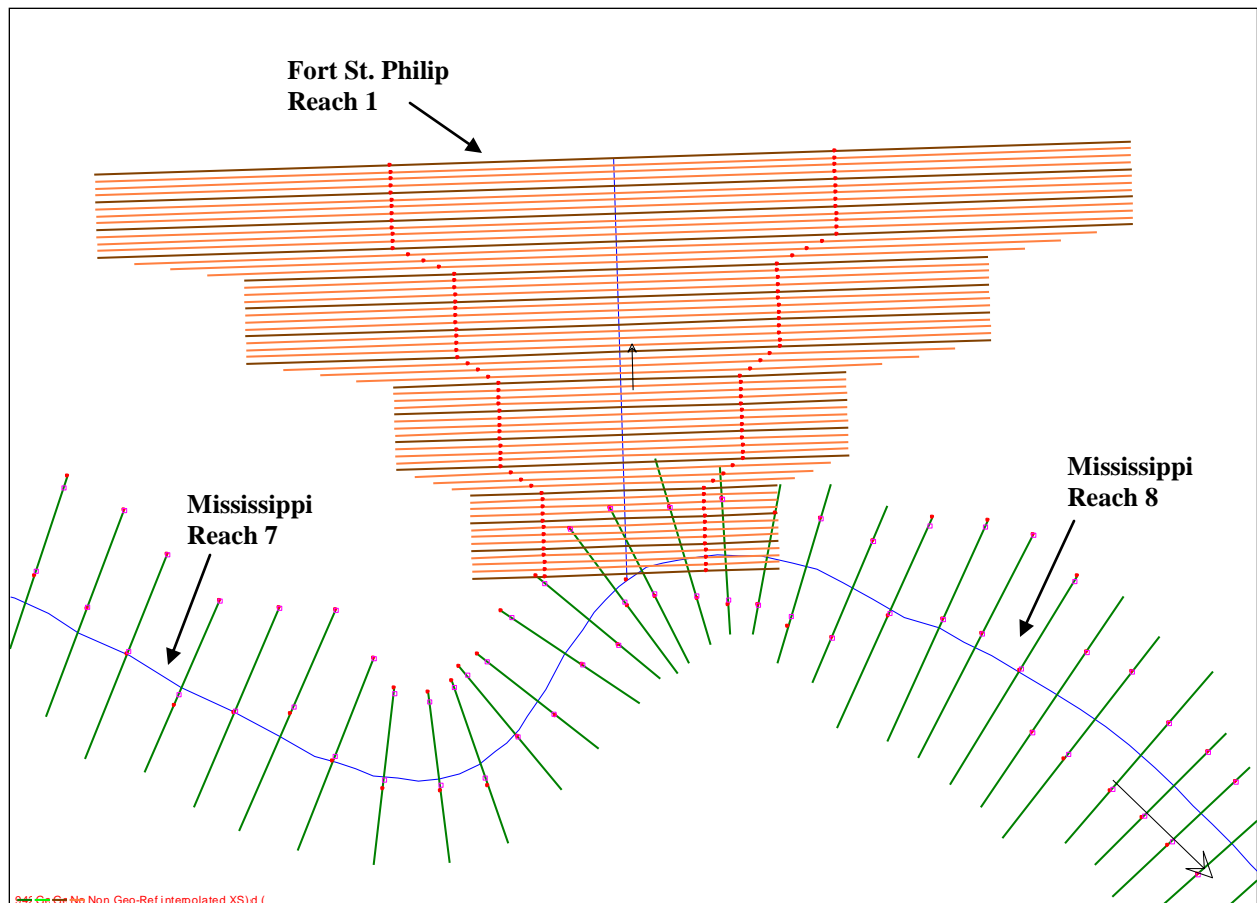


**Figure 4-9: HEC-RAS Image of Fort St. Philip Equivalent Channel.**

Google Earth Imagery was also used to create an equivalent channel for the Caernarvon Diversion by measuring the top widths near the diversion structure as well as representative widths at locations downstream of the diversion up to Breton Sound. A representative length of 142,414 ft was also measured from the inlet at the MR to Breton Sound. The channel depth was varied from 15 ft at the inlet to 3 ft at the outlet. Inline storage was created for extra capacity, similar to the Fort St. Philip channel. The channel width, including inline storage, was expanded from downstream of the diversion structure at 20,548 ft to the Breton Sound outlet at 65,255 ft. Figure 4-10 shows the equivalent Caernarvon reach in HEC-RAS.

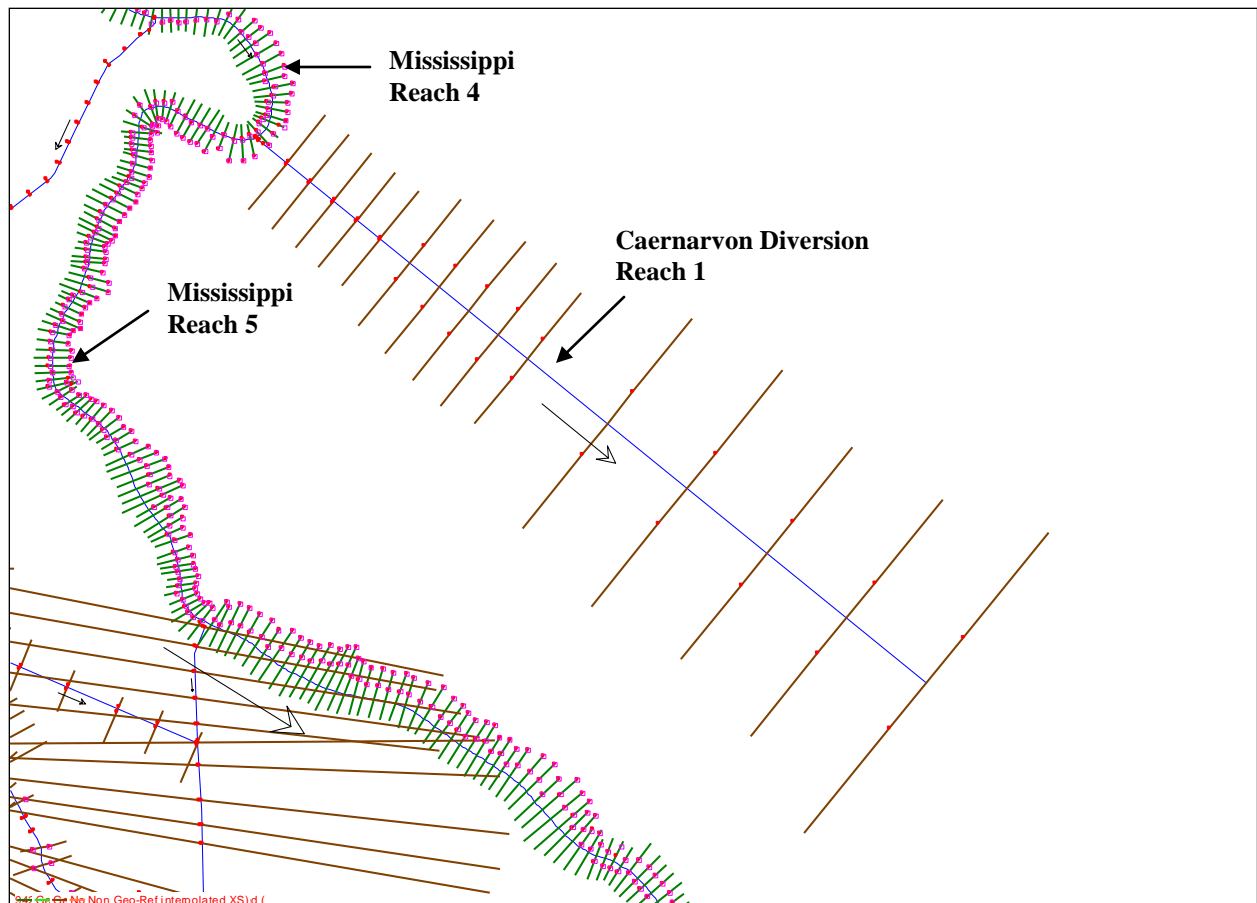


**Figure 4-10: HEC-RAS Image of Caernarvon Channel.**

Looking closely at the Passes on Google Earth, several avulsions were found, which were assumed to convey additional capacities that were not originally considered. As a result, the widths of the avulsions were measured using Google Earth's ruler function and extra storage was created using the Lacey Regime Equations. Equivalent channels were created for Baptiste Collette, Cubit's Gap (including Main Pass), Pass a Loutr , South Pass, and Southwest Pass. Figure 4-11 shows a close up of Cubit's Gap, including Main Pass and its many avulsions, Octave Pass, Brant Bayou, and Raphael Pass (Google Earth Imagery, 2010). In HEC-RAS, Cubit's Gap was originally designated as a single channel labeled Main Pass, which only took into account that pass. The updated channel of Main Pass took into account the avulsions along the pass as well as the other smaller passes. Figure 4-12 shows the original Main Pass channel in HEC-RAS and Figure 4-13 shows the altered channel. As seen in Figure 4-13, the widths of the cross-sections increase from the junction at the Mississippi to the end of the channel. This was done to account for the previous avulsions' capacities up to that point along the channel plus the capacity of the immediate avulsion. Grand Pass was not given an equivalent channel because only a few small avulsions were visible and they did not appear to be significant relative to the pass as a whole. Tiger Pass was not given an equivalent channel because the avulsions were so large that the pass was considered open water after the first 16,000 ft of channel. Figure 4-14 shows the Google Earth image of Grand Pass and Tiger Pass.



**Figure 4-11: Google Earth Image of Cubit's Gap with Main Pass, Avulsions, and Smaller Passes (2010).**

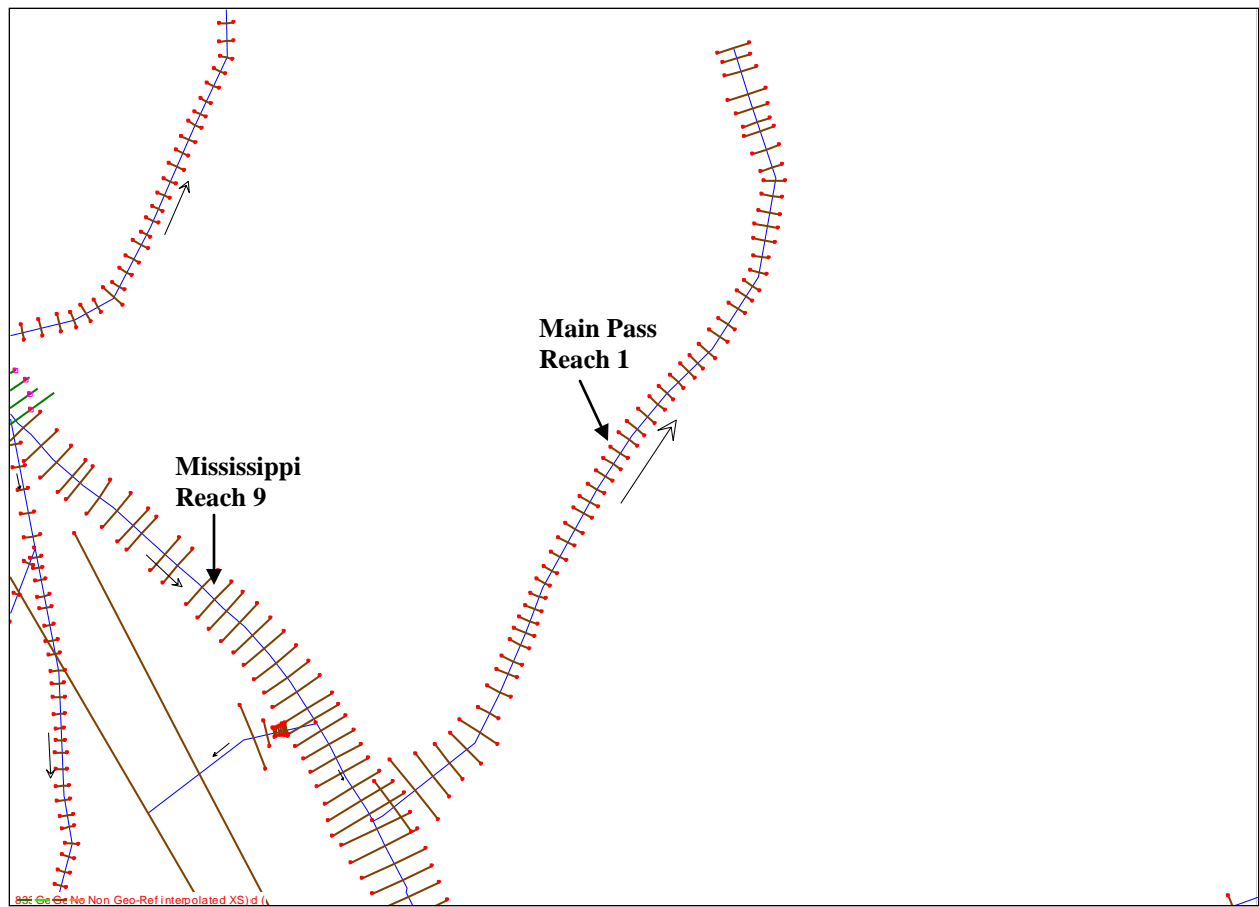


**Figure 4-12: HEC-RAS Image of Original Main Pass Channel.**

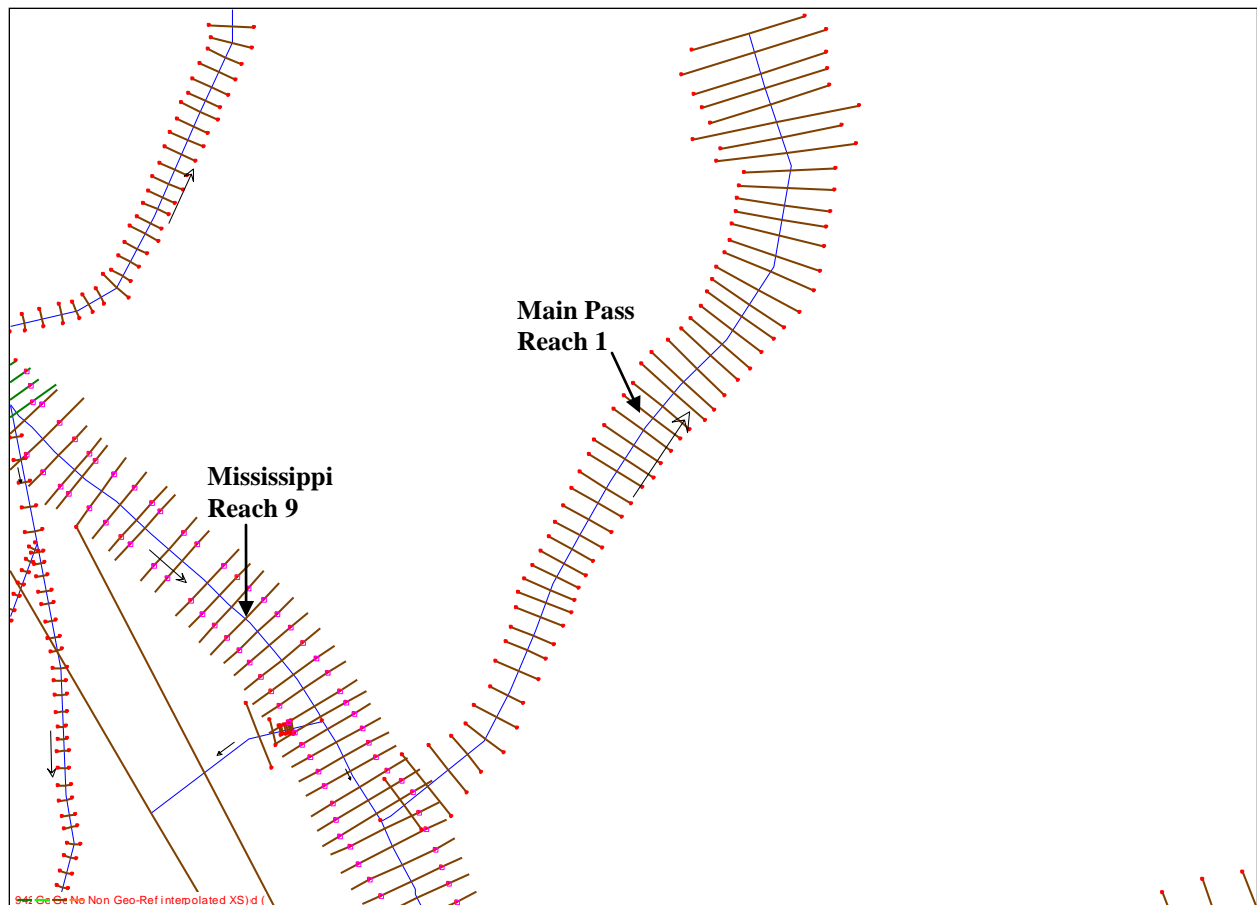


**Figure 4-13: HEC-RAS Image of Altered Main Pass Channel.**





**Figure 4-14: Google Earth Image of Grand Pass and Tiger Pass (2010).**

The West Bay Sediment Diversion (RM 4.9) was drawn as a reach connecting the MR to West Bay. The actual diversion consists of a deep crevasse extending from the center of the MR channel to 2600 ft into West Bay (Miller, 2008). Cross-sectional data for the diversion channel were obtained from USACE NOD (2009) survey data. The diversion channel was cut at an angle of diversion of  $120^\circ$  in order to create a separation between high-velocity water and low-velocity water. The purpose was to divert the low-velocity water containing high concentrations of sediment, which can be found near the bed, into the receiving bay; and to retain the high-velocity water, which can be found near the surface and near the thalweg, in the river (Andrus, 2007). In HEC-RAS, West Bay Reach 1 was extended beyond the design length, using wide equivalent cross-sections, to help the flow transition into open water. The equivalent cross-sections were created using widths of the Bay from Google Earth and a set depth of -30 ft. Figure 4-15 shows an image of the West Bay reach in HEC-RAS.

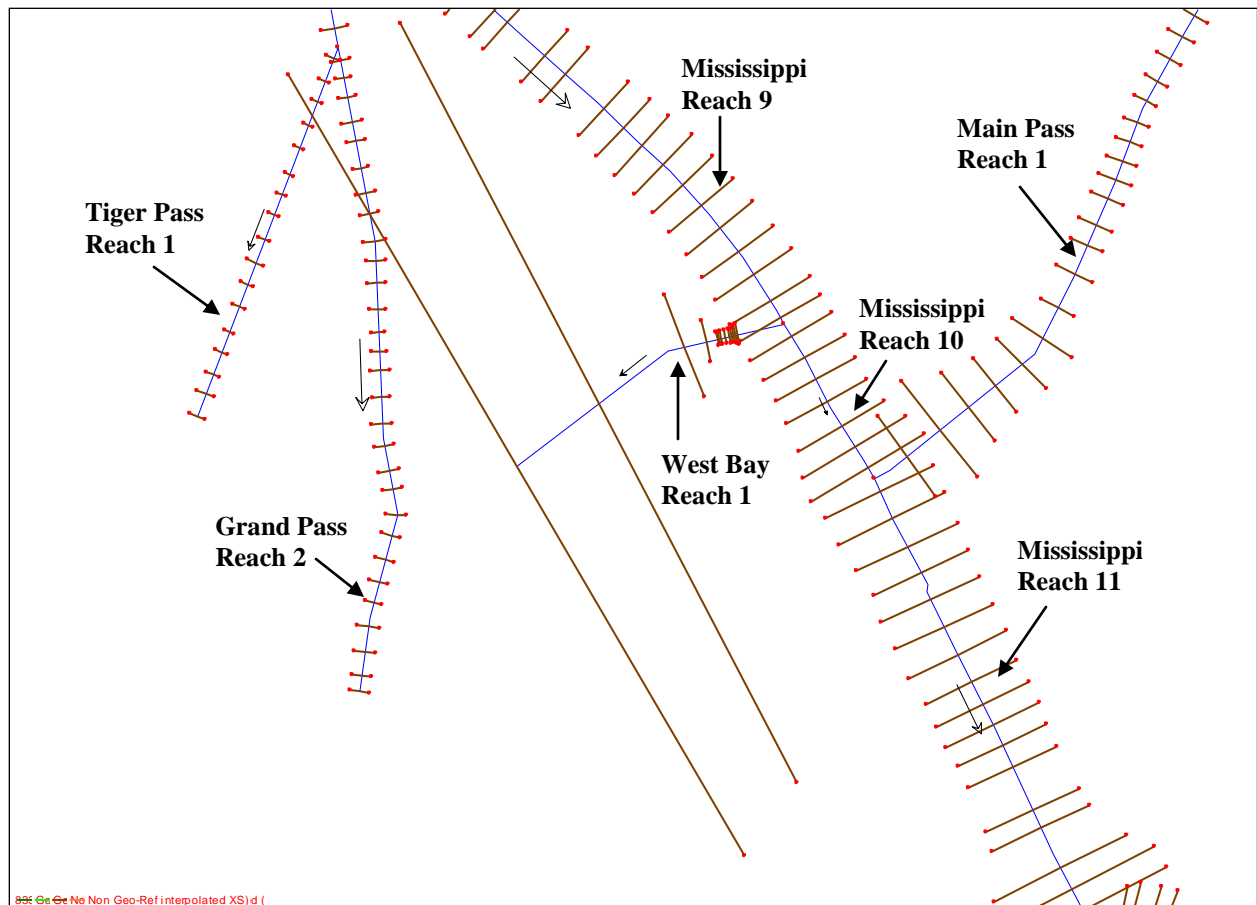


Figure 4-15: HEC-RAS Image of the West Bay Sediment Diversion Channel.

#### 4.1.3 Hydraulic Structures

Several hydraulic structures were added to the HEC-RAS model to take into account the effects of the actual hydraulic structures. Lateral structures were added to route flow out of the system or into storage areas. Inline structures were added to control the amount of flow entering the diversions and channels. These hydraulic structures include weirs, gates, and gated spillways.

Lateral structures were added to the model to represent the Bonnet Carré and Bohemia Spillways (RM 128.6 and RM 38.6, respectively). The Bonnet Carré Spillway structure has 350 gates with 20 ft wide bays. There are 176 bays at a sill elevation of 17 ft and 174 bays with a sill elevation of 15 ft (McCorquodale *et al.* 2008). The structure was inputted as sixteen gate groups. A gate group consists of a maximum of 25 gates. Fourteen of these gate groups contained 348 gates. The two remaining gate groups were used for leakage purposes (#8 and #16). To stay consistent with the actual structure, 176 of the gates were inputted with a sill elevation of 17 ft and a gate height of 10 ft. These gate groups included #1 through #8. The other 174 gates were given a sill elevation of 15 ft and a gate height of 12 ft. These gate groups included #9 through #16. Gate group #15 was given only 23 gates to account for the leakage gate in gate group #16. All of the gates were given a width of 20 ft except for gate groups #8 and #16, which were given widths of 50 ft and 40 ft, respectively. To account for the actual spillway piers, a width of 2 ft was added between each gate. The weir was designed with an elevation of 30 ft (NAVD 88) to prevent

overflow and a length of 7728 ft. Figure 4-16 shows an image of the Bonnet Carré structure in the HEC-RAS model. The grey area represents the weir and the black and white stripes represent the gates.

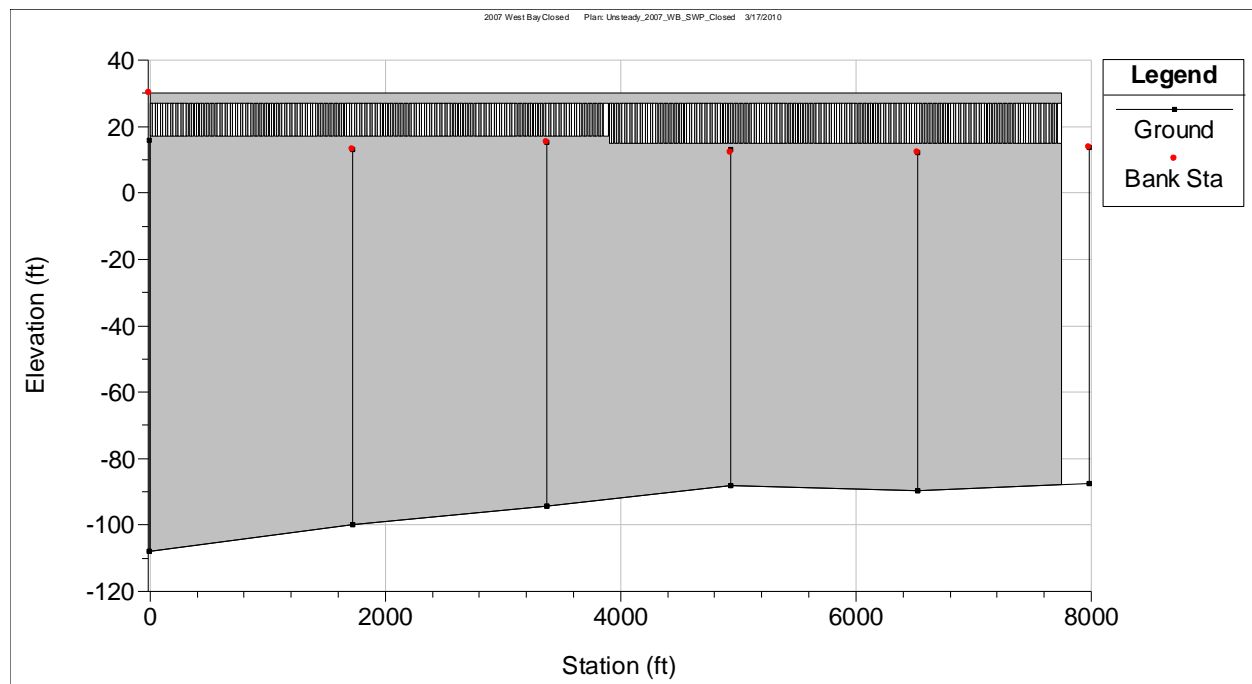


**Figure 4-16: HEC-RAS Image of the Bonnet Carré Spillway.**

The gates of the Bonnet Carré Spillway were defined as sluice gates and were given a sluice discharge coefficient of 0.55, which is reasonable (USACE HEC, 2008). The model requires a weir shape and a weir discharge coefficient. As a result, the ogee weir shape was chosen because it was most similar to the actual spillway shape, and a weir coefficient of 4.2 was used because it was near the recommended range (USACE HEC, 2008).

The actual Bohemia structure consists of an elevated road built on a natural levee along the east bank of the MR from Bohemia at RM 38.6 to the Ostrica Lock at RM 25.2 (LPBF, 2008). In 2005, Hurricane Katrina damaged several sections of the road and breached several culverts, which allowed excess water to pass through during high flows (LPBF, 2008). Figure 4-17 shows a breach in the road and metal culverts due to high flows in 2008.





**Figure 4-17: 2008 Bohemia Spillway Roadway and Culvert Breach (LPBF, 2008).**

In the model, the Bohemia structure was depicted by an overflow weir with a constant elevation of 4 ft. The structure was inputted as a broad crested weir with a weir coefficient of 1.8. Bayou Lamoque North and South intersect the Bohemia structure at RM 32.7 and 32.4, respectively. However, HEC-RAS does not allow a lateral structure to cross a junction. As a result, three separate lateral structures were developed to operate on either side of the two Bayous. Because the distance between the Bayous was small, there were no MR cross-sections to define a reach. As a result, the two cross-sections immediately upstream and downstream of the Bayous were copied to create a small reach for the lateral structure. A 600 ft long and 4 ft deep breach was removed from the section of weir in this small reach between the Bayous to account for losses from the culverts and roadway breaches. Figure 4-18 shows the image of the upstream Bohemia weir in HEC-RAS. Figure 4-19 shows the image of the middle Bohemia weir with the missing section in HEC-RAS. Figure 4-20 shows the image of the downstream Bohemia weir in HEC-RAS.

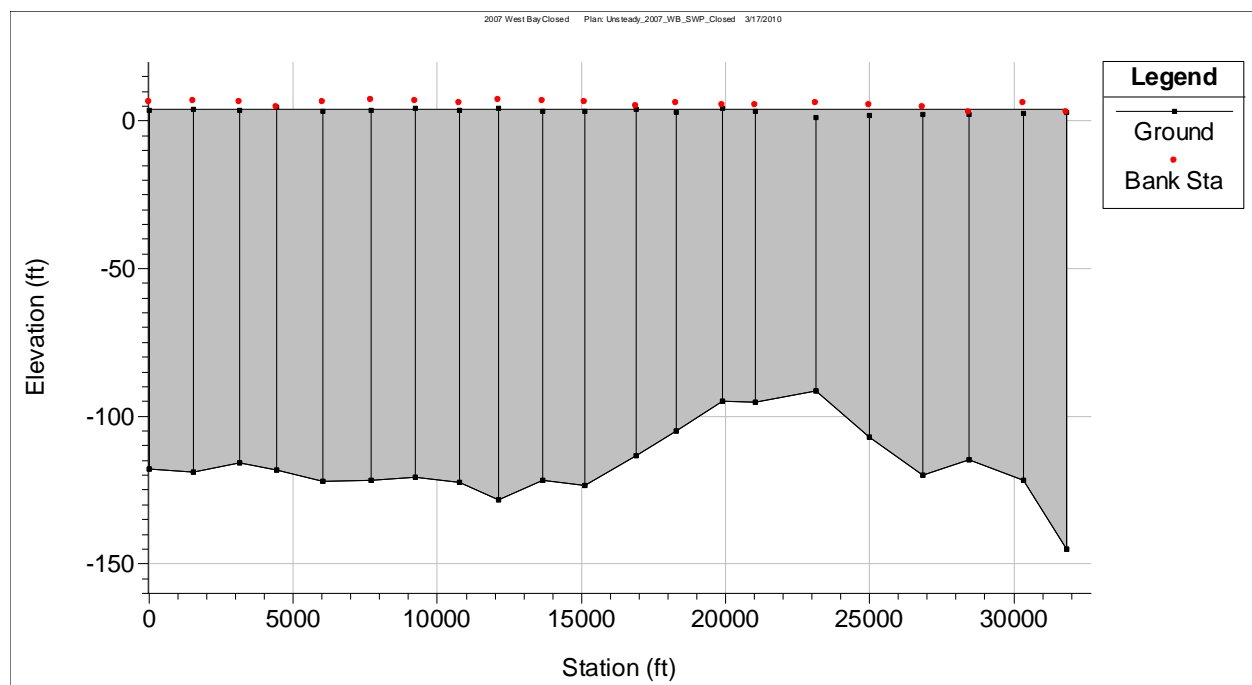


**Figure 4-18: HEC-RAS Image of Upstream Section of Bohemia Spillway.**

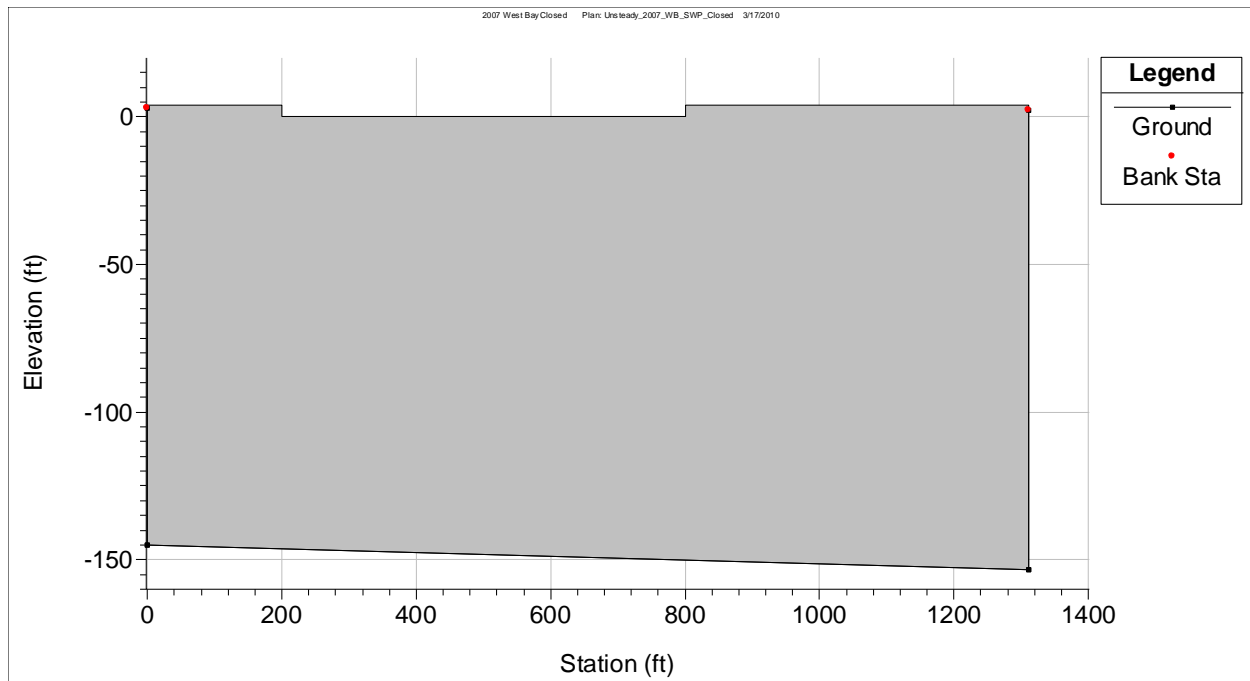


**Figure 4-19: HEC-RAS Image of Middle Section of Bohemia Spillway.**

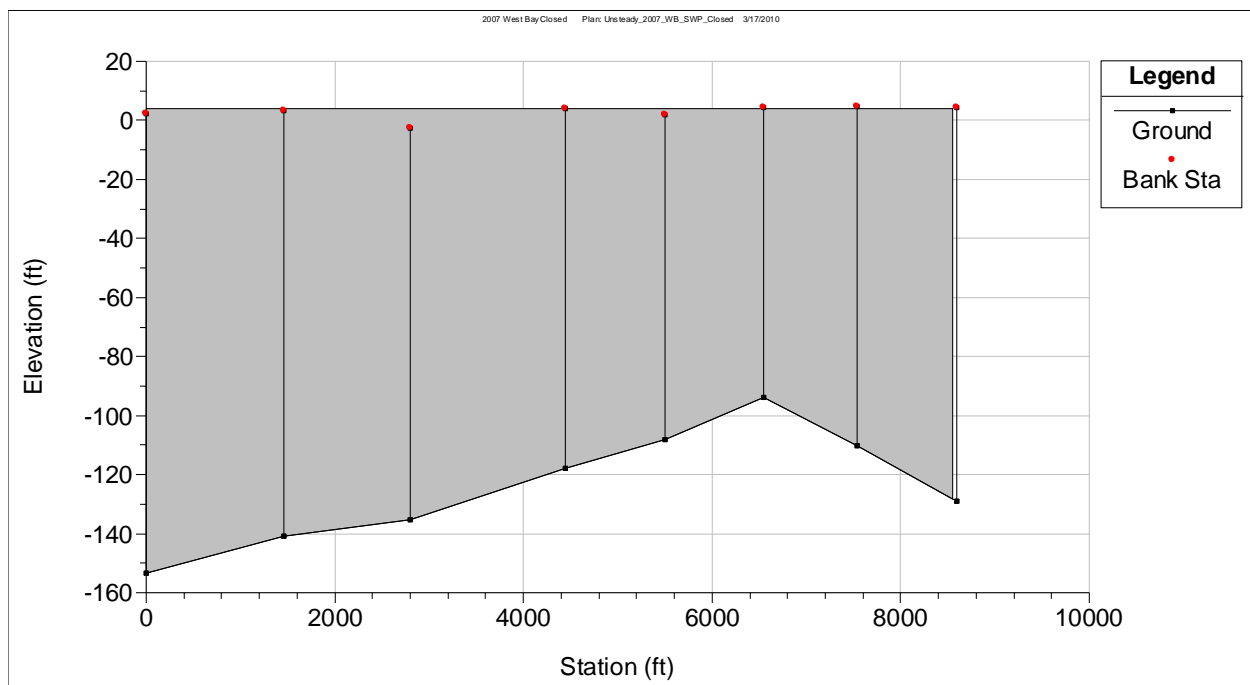


**Figure 4-20: HEC-RAS Image of Downstream Section of Bohemia Spillway.**

Bayou Lamoque North and South each have their own reach and corresponding gated structure. For Bayou Lamoque North (RM 32.7), an inline structure was inputted as four gate groups each with a 10 ft x 10 ft sluice gate at a sill elevation of -10 ft (NAVD 88). A distance of 2 ft was inputted for the width of the structure's piers. The sluice discharge coefficient was taken as 0.5 for sluice gate flow. The orifice coefficient for submerged orifice flow was set as 0.8, which is typical (USACE HEC, 2008). For weir flow, the broad crested weir shape was chosen with a

weir coefficient of 3. The deck of the structure was inputted as a broad crested weir with a length of 85 ft, an elevation of 8 ft, a width of 73.2 ft, and a weir coefficient of 2.6. For Bayou Lamoque South (RM 32.4), an inline structure was inputted as four gate groups with a single 12 ft x 12 ft sluice gate for each having a sill elevation of -12 ft (NAVD 88). A distance of 2 ft was also inputted for the width of the structure's piers. The sluice discharge coefficient, orifice coefficient, weir shape, and weir coefficient for the gates were the same as Bayou Lamoque North. The deck of the Bayou Lamoque South structure was given a length of 85 ft, an elevation of 7 ft, a width of 93.5 ft, and a weir coefficient of 2.6. Figures 4-21 and 4-22 show the Bayou Lamoque North and South structures in HEC-RAS, respectively.

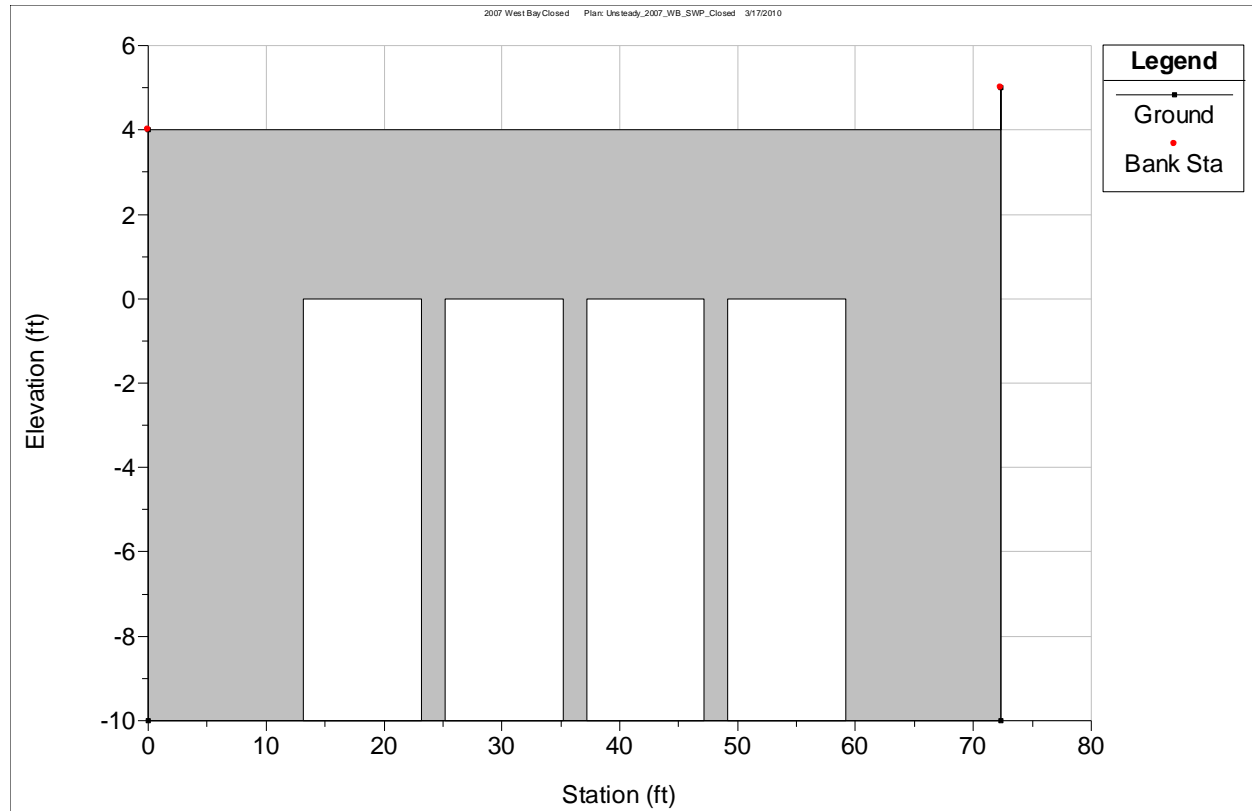


**Figure 4-21: HEC-RAS Image of Bayou Lamoque North Gates.**

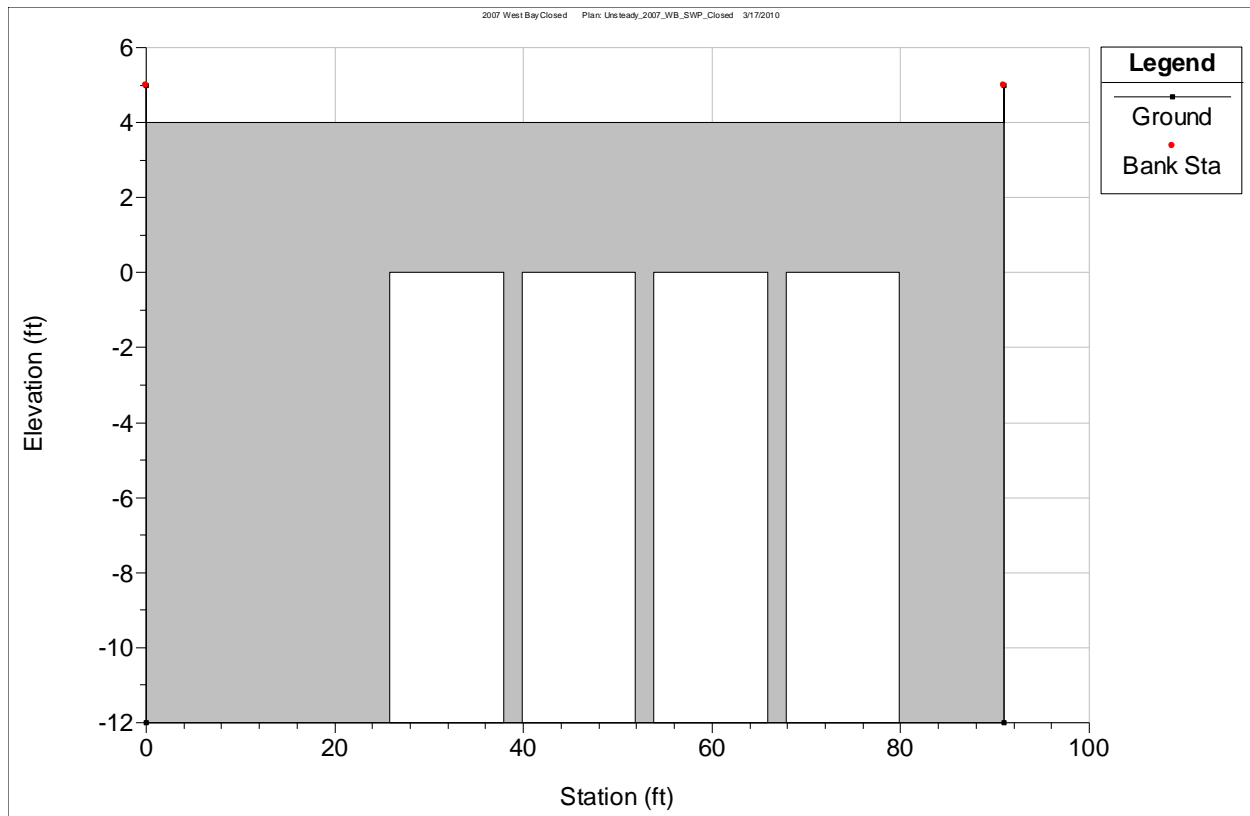


**Figure 4-22: HEC-RAS Image of Bayou Lamoque South Gates.**

For the Davis Pond Freshwater Diversion, an inline structure was entered to represent the actual gated structure, which consists of four gate groups each with a 14 ft x 14 ft sluice gate at a sill elevation of -12.69 ft (NAVD 88). A distance of 3 ft was designated for the width of the piers between each gate. The inline structure consisted of four gate groups each with one gate for operational variability. The sluice discharge coefficient and orifice coefficient were chosen as 0.55 and 0.8, respectively. For weir flow, a broad crested weir shape with a weir coefficient of 3 was chosen. The deck of the actual structure was modeled as a broad crested weir and was given a length of 356 ft, an elevation of 22 ft, a width of 830 ft, and a weir coefficient of 2.6. The Davis Pond reach connected to the GOM via Lake Salvador, Lake Cataouatche, Bayou Perot, Bayou Rigolettes, Little Lake, and Barataria Bay. Figure 4-23 shows the image of the Davis Pond gated structure in HEC-RAS.



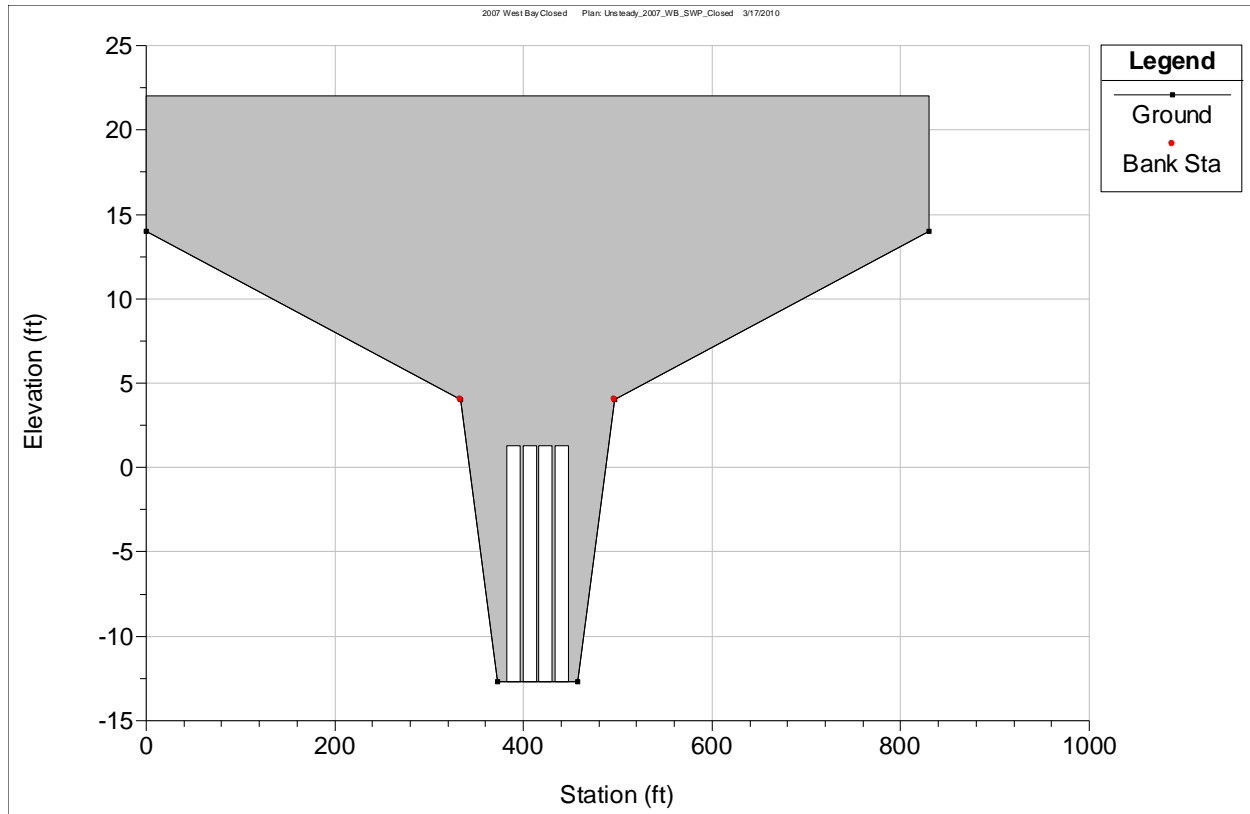


**Figure 4-23: HEC-RAS Image of the Davis Pond Freshwater Diversion.**

Another inline structure was added to represent the Caernarvon Freshwater Diversion. The structure included five gate groups each consisting of a single 15 ft x 15 ft sluice gate at a sill elevation of -15 ft (NAVD 88). A distance of 2 ft was designated for the width of the piers between each gate. The sluice discharge coefficient and orifice coefficient were set as 0.5 and 0.8, respectively. For weir flow through the gates, a broad crested weir shape with a weir coefficient of 3 was chosen. The deck of the actual structure was modeled as a broad crested weir and was given a length of 375 ft, an elevation of 17 ft, a width of 87 ft, and a weir coefficient of 2.6. Figure 4-24 shows the Caernarvon Diversion in HEC-RAS.

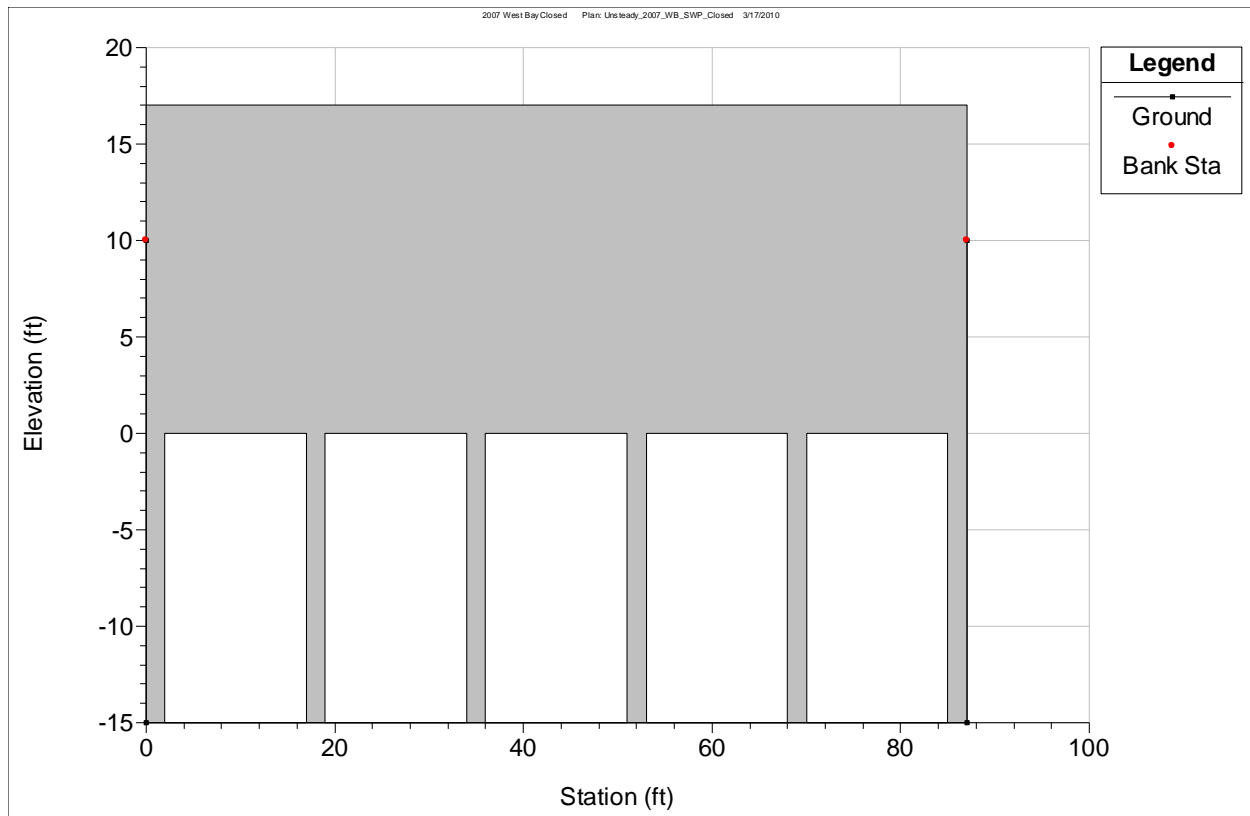


**Figure 4-24: HEC-RAS Image of the Caernarvon Freshwater Diversion.**

As mentioned previously, a storage area was added near RM 296.5 to account for additional storage capacity from the abandoned oxbow at Raccourci Island and from several small bayous and overland storage areas in the vicinity. The Google Earth Imagery ruler function was used to measure the top widths of the small bayous connecting to the MR and to measure the surface areas of the overland storage areas, including the oxbow at Raccourci Island. A cumulative storage area of 31,050 acres was calculated using the capacities of the bayous found with the Lacey Regime Equations and the surface areas of the oxbow and overland areas. The HEC-RAS storage area was given a minimum depth of 0 ft (NAVD 88) to allow it to fill up without overtopping during high flows. A lateral structure was added to direct the flow from the MR into the storage area. The structure was inputted as a broad crested weir with an overflow weir coefficient of 3.1. The weir dimensions were specified as a length of 800 ft, a width of 10 ft, and an elevation of 47 ft. Figure 4-25 shows the plan view of the storage area and weir for Raccourci Island in HEC-RAS. Figure 4-26 shows the cross-sectional view of the weir for Raccourci Island in HEC-RAS.

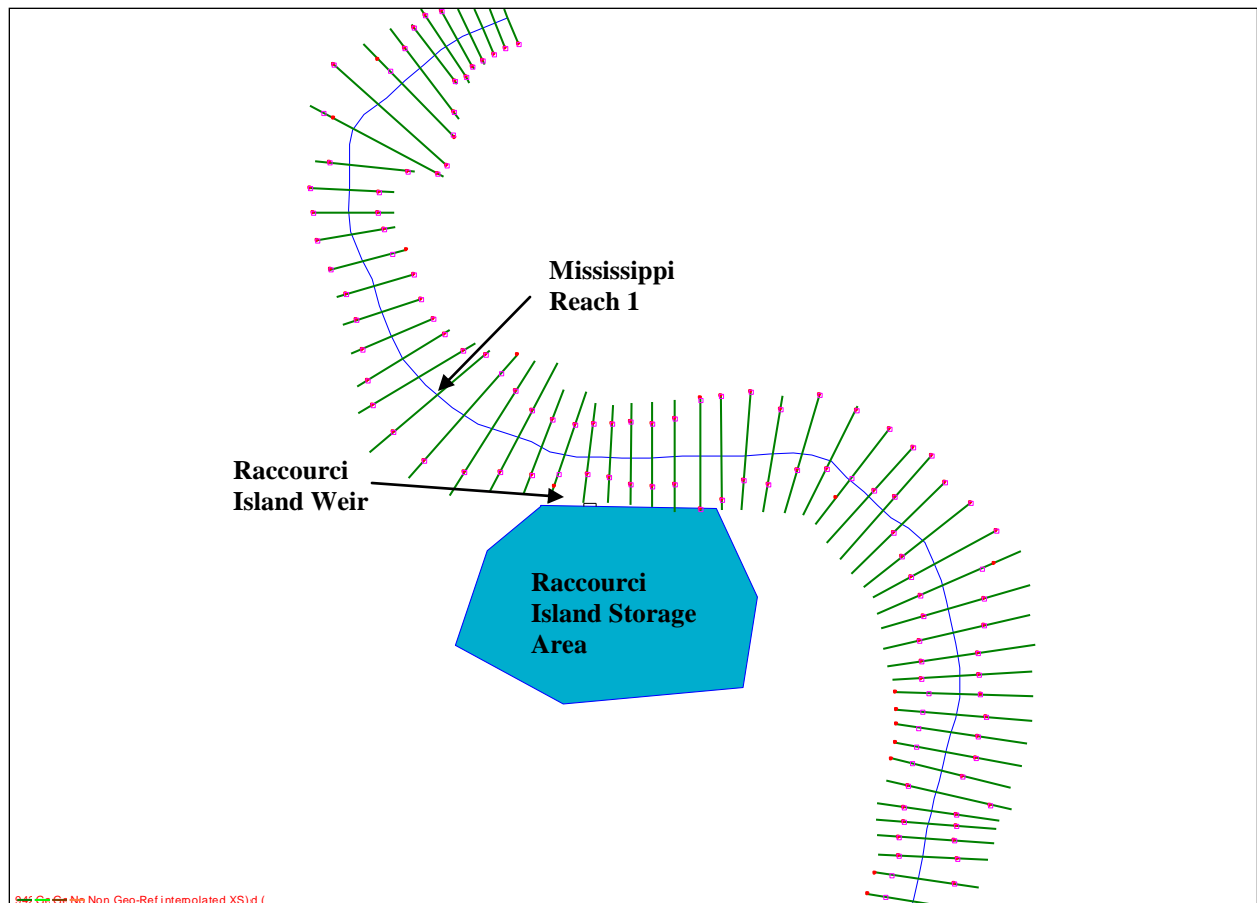


Figure 4-25: HEC-RAS Image of Raccourci Island Storage Area and Weir (Plan View).

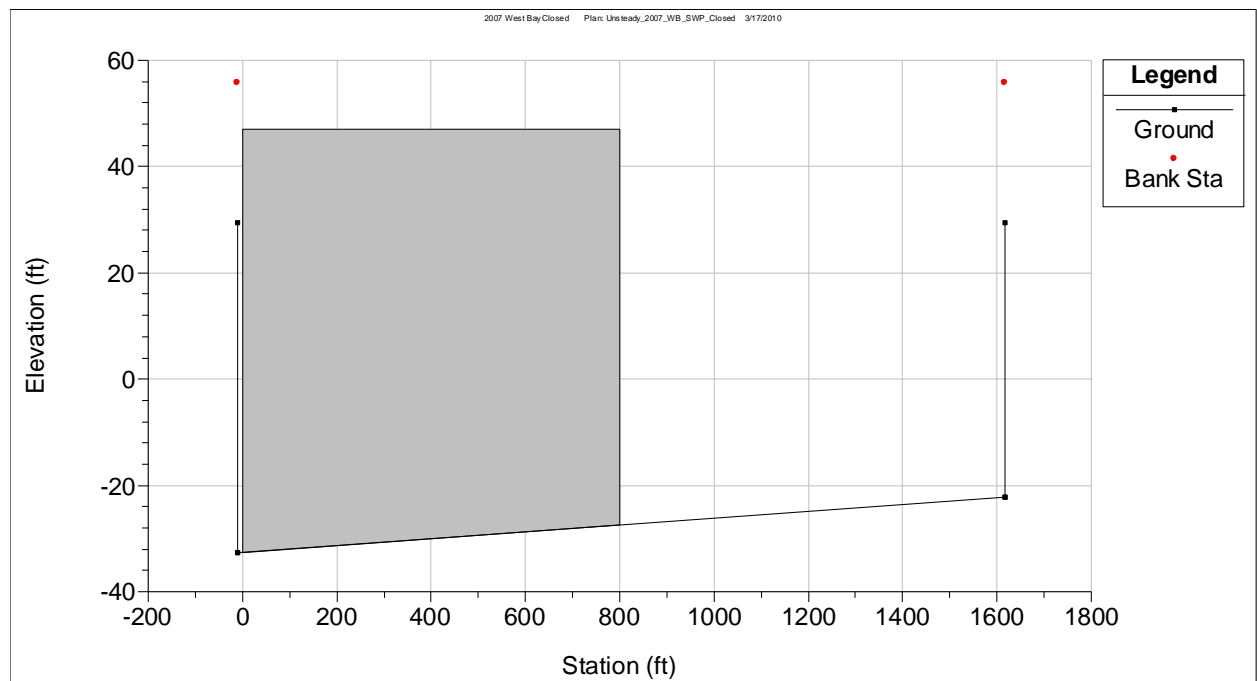


Figure 4-26: HEC-RAS Image of Raccourci Island Weir (Cross-section View).

#### 4.1.4 Channel Roughness

According to Manning's Equation (4-1), the flow in a channel is dependent on the roughness of the channel. Manning defined this roughness with a coefficient,  $n$ . The Manning's Equation is written as:

$$Q = \frac{c'}{n} A R^{2/3} S^{1/2} \quad (4-1)$$

where:

$Q$  = discharge [cfs or cms]

$c'$  = conversion factor (= 1.486 for U.S.; = 1.0 for S.I.)

$A$  = cross-sectional area [ $\text{ft}^2$  or  $\text{m}^2$ ]

$R$  = hydraulic radius ( $= A/P$ ) [ft or m]

$P_w$  = wetted perimeter [ft or m]

$S$  = bed slope

$n$  = roughness coefficient

It has been established that the roughness is a function of many factors relating to the channel at hand (Chow, 1959). Chow described the following factors:

- Surface Roughness
- Vegetation
- Channel Irregularities
- Channel Alignment
- Silting and Scouring
- Obstructions
- Size and Shape of Channel
- Stage and Discharge
- Seasonal Change
- Suspended Material and Bed Load

According to Chow (1959), the channel surface roughness depends on the grain material of the wetted perimeter, or the part of the channel under water. It was determined that fine grains result in a lower  $n$  value, and coarse grains result in a higher  $n$  value. The contribution of the bed material grain size to  $n$  is proportional to  $D_{50}^{1/6}$ , where  $D_{50}$  is the median grain size. The presence of vegetation in a channel retards the flow through the channel by varying degrees, depending on height, density, distribution, and type of vegetation. Smaller water depths give higher  $n$  values because the main flow is distributed through the vegetation. High flow depths tend to bend and submerge the vegetation, which reduces the  $n$  value. A lower flow rate produces a high  $n$  value because it requires more energy to pass through or over the vegetation. The steeper the channel side slopes, the faster the velocity becomes, which in turn compresses the vegetation and lowers the  $n$  value. Other irregularities in the channel bed, such as sand bars and/or deep holes, cause additional resistance to the flow. Severe meandering also causes additional resistance. Silting or depositing can fix the channel irregularities and reduce the  $n$  value, but scouring does the

opposite and can increase the  $n$  value. The type of bed material also determines how the bed will scour. Finer material, like clay, scours non-uniformly and can cause pits or holes, which increases the  $n$  value. Coarser material, like sand or gravel, scours uniformly, which reduces the  $n$  value. Obstructions, such as bridge piers and debris, can increase the value of  $n$ , depending on their nature, size, shape, number, and distribution. Chow (1959) indicated that the size and shape of the channel were minor factors affecting the channel roughness. As the stage increases during high flows, inundation of the floodplains takes place, which increases the composite  $n$  value because floodplains typically have a higher  $n$  value than the channel. The  $n$  value can also change depending on the season because of the seasonal growth of the vegetation. Lastly, sediment transport of the suspended material and bed load requires additional energy, which increases the value of  $n$ . Chow (1959) also presented a comprehensive table of Manning's  $n$  values for several man-made conduit and channel materials, natural channel materials, vegetation requirements, and meandering patterns.

The lower MR channel has many meanders, several bridges and groins, bars, deep holes, and islands, as well as some vegetation (at high flow); in addition, it transports a range of sediment from coarse sand to fine clays, which altogether causes additional resistance to the flow. However, it also becomes narrower as it nears the GOM; is for the most part controlled by the flood protection levees on both sides; has relatively cohesive banks; and has a large depth in most places, which altogether reduces the amount of resistance to the flow. The  $n$  in the MR is also complicated by the presence of bed forms or sand dunes that vary in height and wave length as the bed shear in the channel changes. The distribution of bed forms in the channel is both spatial and temporal. Altogether, these bed forms tend to increase the effective roughness. As a result, the value of Manning's  $n$  cannot be accurately measured for the MR. For this study, values of Manning's  $n$  ranging from 0.026 to 0.019 were determined by calibration based on measured flows and stage data.

## **4.2 Unsteady Flow Data**

### **4.2.1 Initial Conditions<sup>5</sup>**

The initial boundary condition for Mississippi River Reach 1 was a single recorded discharge at Tarbert Landing for the simulation period of interest. Initial boundary conditions for the existing diversions in the MR and existing tributaries for the Barataria Basin were estimated based on recorded discharge data and design discharge capacities. Table 4-1 shows the estimated initial boundary conditions for these channels for the 2007 calibration period. The flow rates in the subsequent MR reaches were calculated by subtracting the existing diversions' capacities from the upstream MR reach discharge. HEC-RAS can use the initial flow to compute a steady state initial stage along the entire river.

---

<sup>5</sup> The initial boundary conditions of all the channels in HEC-RAS for every simulation are presented in Appendix D.

**Table 4-1: Initial Boundary Conditions for Existing Diversions and Tributaries.**

<b>Reach</b>	<b>Initial Flow (cfs)</b>
Davis Pond Diversion Reach 1	4,000
Des Allemands Reach 1	250
Des Allemands Reach 2	250
ICCW Harvey Reach 1	100
ICCW Chalmette Reach 1	100
ICCW Reach 5	200
Bayou Lamoque N Reach 1	4,000
Bayou Lamoque S Reach 1	8,000
Wilkinson Canal Reach 1	0 (20,000) <sup>6</sup>
Barataria Bay Reach 4	100
Caernarvon Diversion Reach 1	3,000
White Ditch Siphon <sup>7</sup>	500
Violet Diversion <sup>8</sup>	100

The discharges for Des Allemands Reaches 1 and 2 were determined by the hydrology of the area. The discharges for the ICCW at Harvey and Chalmette were determined based on the lock operations. For the ICCW at Larose (Reach 5), the discharge was determined based on lock operations and the flow from Terrebonne via the Gulf Intracoastal Waterway (GIWW). The discharges for the diversions, including Davis Pond, Caernarvon, White Ditch, and Violet, were determined based on their nominal flow. Distribution of flow through the Barataria Basin network was estimated using the ratio of the cross-sectional areas of the two receiving reaches of a junction. Flow distribution to the passes and West Bay was originally estimated using Acoustic Doppler Current Profiler (ADCP) values, which were recorded as percentages of the flow at Venice (Pratt, 2009)<sup>9</sup>. These values were then altered using flow optimization in the model. The original flow distribution for the 2007 calibration is shown in Table 4-2.

<sup>6</sup> Wilkinson Canal was originally given an initial boundary discharge of 0 cfs because it was not connected to the MR; however, the value was changed to 20,000 cfs for the simulations where it was connected to the MR via the Myrtle Grove Diversion.

<sup>7</sup> The White Ditch Siphon was modeled as a lateral inflow hydrograph with a constant daily discharge of 500 cfs leaving the MR.

<sup>8</sup> The Violet Diversion was modeled as a lateral inflow hydrograph with a constant daily discharge of 100 cfs leaving the MR.

<sup>9</sup> The ADCP charts from Pratt (2009) are shown in Appendix E.

**Table 4-2: Original Flow Percentages of Venice for the Passes and West Bay.**

<b>Reach</b>	<b>Flow Percentage of Venice<sup>10</sup></b>
Baptiste Collette	12%
Grand Pass	11%
Main Pass	13%
Pass a Loutr�	10%
South Pass	10%
Southwest Pass	38%
West Bay	6%
Fort St. Philip <sup>11</sup>	2%

The flow optimization option in HEC-RAS is an iterative process that attempts to adjust the user-specified flow for each junction and hydraulic structure (USACE HEC, 2008) in order to satisfy the need for a unique energy head on the upstream side of the junction. With the optimization turned on, the discharges calculated in the passes and in the MR (Reaches 7 and 8) were copied to an external spreadsheet and were compared to the assumed values, which were based on the initial flow distribution. Based on the percent of MR flow from the HEC-RAS simulation, an average percentage was retrieved and was used as the new initial flow percentage. Table 4-3 shows the optimized flow percentages for the passes, Fort St. Philip, and West Bay during the 2007 calibration period.

**Table 4-3: Optimized Flow Percentages of Venice for the Passes and West Bay.**

<b>Reach</b>	<b>Flow Percentage of Venice<sup>10</sup></b>
Baptiste Collette	15.45%
Grand Pass	10.98%
Main Pass	11.01%
Pass a Loutr�	7.78%
South Pass	15.12%
Southwest Pass	34.56%
West Bay	5.10%
Fort St. Philip <sup>11</sup>	1.39%

#### **4.2.2 Boundary Conditions<sup>12</sup>**

Daily discharges measured at Tarbert Landing were used as the upstream boundary condition for the MR reach for each of the periods simulated. A single daily stage hydrograph, which included the 2007 stage and influence of the salinity wedge profile at the GOM, was used as the downstream boundary condition for Barataria Bay, the passes, the Caernarvon Freshwater Diversion, Bayou Lamoque, Fort St. Philip, and the West Bay Sediment Diversion for all simulations except for the relative sea level rise study and the 2007-2008 simulation. For the

<sup>10</sup> The station for Venice is located in Mississippi Reach 8, which is used to determine the flow for the passes and West Bay only.

<sup>11</sup> The Fort St. Philip channel was added to Table 4-2 because the amount of flow entering the channel is unknown and is therefore set as a function of the flow in the MR, specifically in Mississippi Reach 7.

<sup>12</sup> The boundary conditions of all the channels and structures in HEC-RAS for every simulation are presented in Appendix F



relative sea level rise study, the stage hydrograph was altered by adding a constant 1.64, 3.28, and 4.92 ft (0.5, 1.0, and 1.5 m, respectively) for three separate simulations. For the 2007-2008 simulation, the stage hydrograph included the end of the 2007 stage and salinity wedge profile for the GOM as well as the 2008 stage and salinity profile.

An estimated constant discharge of 500 cfs was assigned to Lac Des Allemands, with 250 cfs for Lac Des Allemands Reach 1 and 250 cfs for Lac Des Allemands Reach 2. The boundary condition for the ICCW at Larose (Reach 5) was set as a constant inflow of 200 cfs. The Raccourci Island storage area was given a constant lateral inflow of 100 cfs to account for inflow into the river from the neighboring bayous during low stage. Based on operational data for the White Ditch Siphon and the Violet Diversion, constant lateral outflows of 500 cfs and 100 cfs were set along the MR at RM 64.5 and 83.9, respectively. The boundary condition for Wilkinson Canal Reach 1 was set as a constant flow hydrograph of 0 cfs because it was not connected to the MR. For Barataria Bay Reach 4, the boundary condition was set as a constant flow hydrograph of 0 cfs because it resembles a still pond.

The Bonnet Carré Spillway gated structure was given a time-series of gate openings boundary condition. For the simulation periods where the spillway was closed (1999-2000, 2003, and 2007), all of the gate groups were given a height of 0 ft (closed) except for gate group numbers 8 and 16, which were given gate heights of 10 ft and 12 ft (open), respectively, for leakage. For the 2008 opening of the spillway (2007-2008 simulation), gate group numbers 1, 3, 5, 7, 10, 12, 13, and 14 were opened and closed based on recorded operational data (USACE NOD, 2010). Gate group #8 was left open for the entire simulation to account for leakage of the unopened gates during high flows, and gate group #16 was left open for the entire simulation, except during the actual opening of the spillway, to account for leakage of the opened gates before and after they were opened.

The elevation controlled gates option was chosen as the boundary condition for both the Davis Pond Freshwater Diversion and the Caernarvon Freshwater Diversion structures. For the Davis Pond structure, gate group #2 was left closed for all simulations, based on observed field operations of the diversion. Gate group numbers 1, 3, and 4 were operated based on trial and error (see Calibration). For the Caernarvon Diversion, the gate operations were designed by trial and error (see Calibration) to maintain a discharge in the channel below 8000 cfs, which is the maximum discharge that is normally allowed.

Both the Bayou Lamoque North and South gated structures were given a time-series of gate openings boundary condition. For all simulations, the Bayou Lamoque North structure was given the following operations: gate group #1 was left completely open at 10 ft, gate group #2 was kept partially open at 6 ft, and gate group numbers 3 and 4 were left fully closed, which coincided with observed gate operations. Similarly, for Bayou Lamoque South the following gate operations were inputted for all simulations: gate group #1 was left partially open at 8 ft, and gate group numbers 2, 3, and 4 were left fully closed, which was based on field observations.

### ***4.3 Specific Model Limitations***

The model requires an initial discharge for each reach, but for the passes, West Bay, and Fort St. Philip, the amount of flow diverted by each is unknown. Several studies give approximate percentages of flow based on upstream known flow data such as, Venice or Tarbert Landing. Due to the constraints with surveying equipment, it is next to impossible to measure the flow in each reach at one specific time. Even if all the flows in the passes are measured in a single day, the change in tide or upstream flow throughout the day could have a large affect on the subsequent discharges in the passes (Meselhe *et al.* 2010). As a result, approximate values are used and the optimization in the model is used to correct these estimates (see Initial Conditions).

For the 2008 opening of the Bonnet Carré Spillway, the model estimates a peak in the river stage just before the first gates open, followed by a dip during which all the gates are opened, and then another peak after the gates are closed. The observed data, however, show a smooth curve with no peaks or dips for the period when the gates are opened and closed. This discrepancy in the stage can be seen at locations just upstream of the spillway, and it is carried throughout the river downstream of the structure. As a result, the actual operation of the structure was disregarded and the gates were operated to obtain a total discharge leaving the structure equal to the actual discharge.

## Chapter 5: Hydrodynamics Simulations

In order to utilize any results from the model simulations, the model had to be calibrated using a known dataset for one period, and it had to be validated using a dataset from a different period. After validation and calibration, the model was considered to be serviceable for other applications. Channel geometry is constantly changing due to natural and man-made factors, including channel maintenance, sediment transport, floods, and relative sea level rise (Raphelt *et al.* 2008). Therefore, the volume or capacity of the channels changes on a seasonal and annual basis. To minimize the effect of these changes on the calibration and validation, all simulations were performed for single year events. More than 1000 cross-sections were included in the model; the available survey data were limited to certain years; therefore, the channel geometry was kept constant for all simulations and the channel roughness was altered to match the model output with the recorded data.

### 5.1 Calibration<sup>13</sup>

For the calibration procedure, the model was given boundary conditions for the calendar year of 2007, which was a median flow year. The model included the existing diversions at Bonnet Carré, Bohemia, Davis Pond, Caernarvon, Bayou Lamoque North and South, White Ditch, Violet, and West Bay. Also included were the passes and the Barataria Basin drainage network. The boundary condition for the channels leading to the GOM was set at mean sea level (MSL) (NAVD 88). The Bonnet Carré gates were left closed except for gate group numbers 8 & 16, which were designed for leakage during high stages.

For the ICCW at Harvey and Chalmette, the flow entering the channel from the MR is small because of the navigation locks at each. HEC-RAS, however, does not have a lock structure feature, and therefore, removes more water than it should from the MR at Harvey and Chalmette. The following procedure was developed to compensate for this: (i) the first three cross-sections of each were designed as rectangular sections with a depth of 10 ft and a width of 20 ft to contract the flow entering the channel; (ii) the friction of the channels had to be exaggerated in order to reduce the amount of flow entering the channels. The first three rectangular cross-sections of each channel were given an exaggerated Manning's  $n$  of 0.7, and the rest of the cross-sections were designated with a Manning's  $n$  of 0.03, which is typical (USACE HEC, 2008). Figures 5-1 and 5-2 show the navigation locks at Harvey and Chalmette, respectively.

---

<sup>13</sup> The Manning's  $n$  value for every reach and cross-section are presented in Appendix G.



**Figure 5-1: Google Earth Image of the ICCW Lock at Harvey (2010).**





**Figure 5-2: Google Earth Image of the ICCW Lock at Chalmette (2010).**

Similarly, the modeled flow diverted from the MR was too high compared to the measured flow at the Davis Pond Freshwater Diversion and the West Bay Sediment Diversion. To match the measured flows at these diversions, the Manning's  $n$  value for Davis Pond was set to an exaggerated 0.2 for the inflow channel, which included the cross-sections upstream of the gated structure, and for the first two cross-sections of the guide channel immediately downstream of the gated structure. This increased friction corrected for the energy loss in the hydraulic jump downstream of the structure. Figure 4-1 shows the Davis Pond Freshwater Diversion in Google Earth (2010). For West Bay, the original channel cross-sections were assigned a Manning's  $n$  of 0.2 to account for the loss due to the angle of diversion which retarded the incoming flow. The wide equivalent cross-sections were given  $n$  values of 0.021 for the banks and 0.023 for the main channel to account for the deep channel invert. Figure 5-3 shows the West Bay Sediment Diversion in Google Earth (2010).

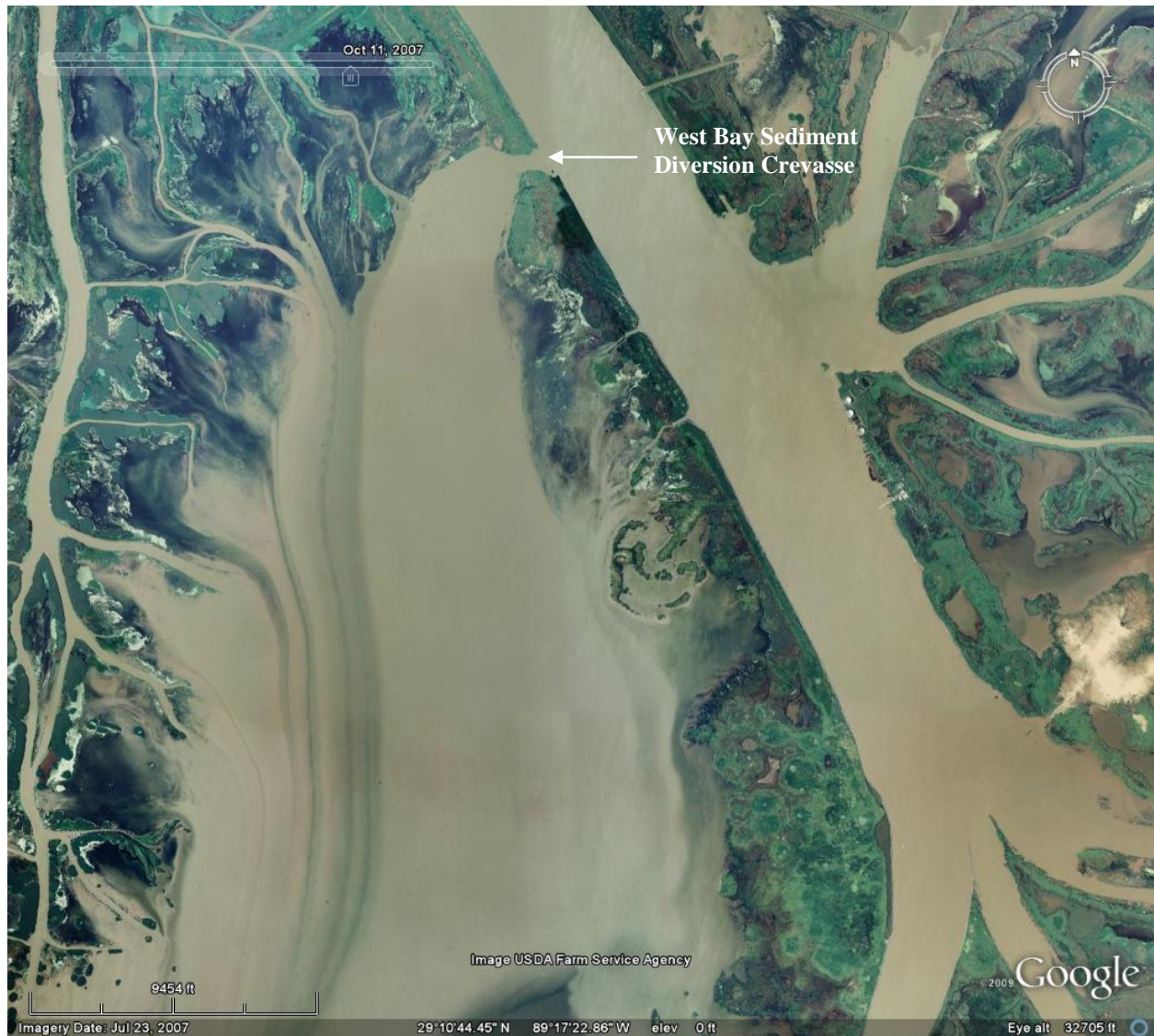


**Figure 5-3: Google Earth Image of the West Bay Sediment Diversion (2010).**

The cross-sections of the equivalent channel at Fort St. Philip are representative of the accumulated individual cuts. As a result, a Manning's  $n$  of 0.2 was applied to the entire reach to maintain a low flow throughout the channel, which would be seen in the field. Discharge records<sup>14</sup> from the major passes indicate that up to 30% of the flow in the MR is lost between Bohemia and Baptiste Collette. According to Meselhe *et al.* (2010), the amount of flow leaving the MR at Fort St. Philip is unknown. Therefore, for this model, it was originally estimated that an average of 2% of this deficit is removed by the cuts at Fort St. Philip on a daily basis. Figure 2-4 shows the cuts at Fort St. Philip in Google Earth (2010).

The Caernarvon Diversion structure was modeled by the “elevation controlled gates” option, which means the gate opening height depends on the difference in stage of two user specified cross-sections. Mississippi Reach 4 (RS 81.5) and Caernarvon Reach 1 (RS 20) were chosen as

<sup>14</sup> The passes discharge records are presented in Appendix H.

the two cross-sections to dictate the gate operations. The program requires a stage difference to open the gates and a stage difference to close the gates. For the calibration procedure, these stage difference values were altered to keep the channel from drying up or overflowing. For the Caernarvon Diversion, the stage difference values were set at 2 ft to open the gates and 4 ft to close the gates. Both the gate opening and gate closing speeds were set at 0.1 ft/min. The actual value of the opening and closing speeds did not matter because the output interval specified was 1 day; therefore, the gates would have opened or closed before the next day. All five gate groups were given an initial and maximum height of 5 ft to keep the discharge in the channel below 8000 cfs, and the gates were given a minimum gate opening of 2 ft to keep the channel from drying up. Similarly, the gate operations for gate group numbers 2, 3, and 4 for the Davis Pond structure were determined based on keeping the peak discharge in the channel below 10,000 cfs, which is close to the design maximum of 10,650 cfs.

Stage results in the MR were compared to known data from the USACE River Gages website (Mississippi River & Passes, 2010) at the following locations: Baton Rouge (RM 228.4), Donaldsonville (RM 175.4), North of Bonnet Carré (RM 129.2), Bonnet Carré Spillway (RM 127.1), Carrollton (RM 102.8), West Pointe a la Hache (RM 48.7), and Venice (RM 10.7). The computed discharge hydrographs for the passes, Fort St. Philip, and West Bay were collected and divided by the flow in the MR at Venice to obtain a daily flow percentage. These daily values were then averaged to find an average flow percentage for each channel. The new average was multiplied to the initial flow at Venice to obtain the new initial flow at each. These initial flows were then set as the initial boundary conditions. The amount of flow leaving the MR at the three Bohemia Spillway structures was collected and summed to get a total flow leaving curve. Also included on this curve were the total upstream and downstream flow rates in the MR. Figure 5-4 shows the original stage comparison for Carrollton.



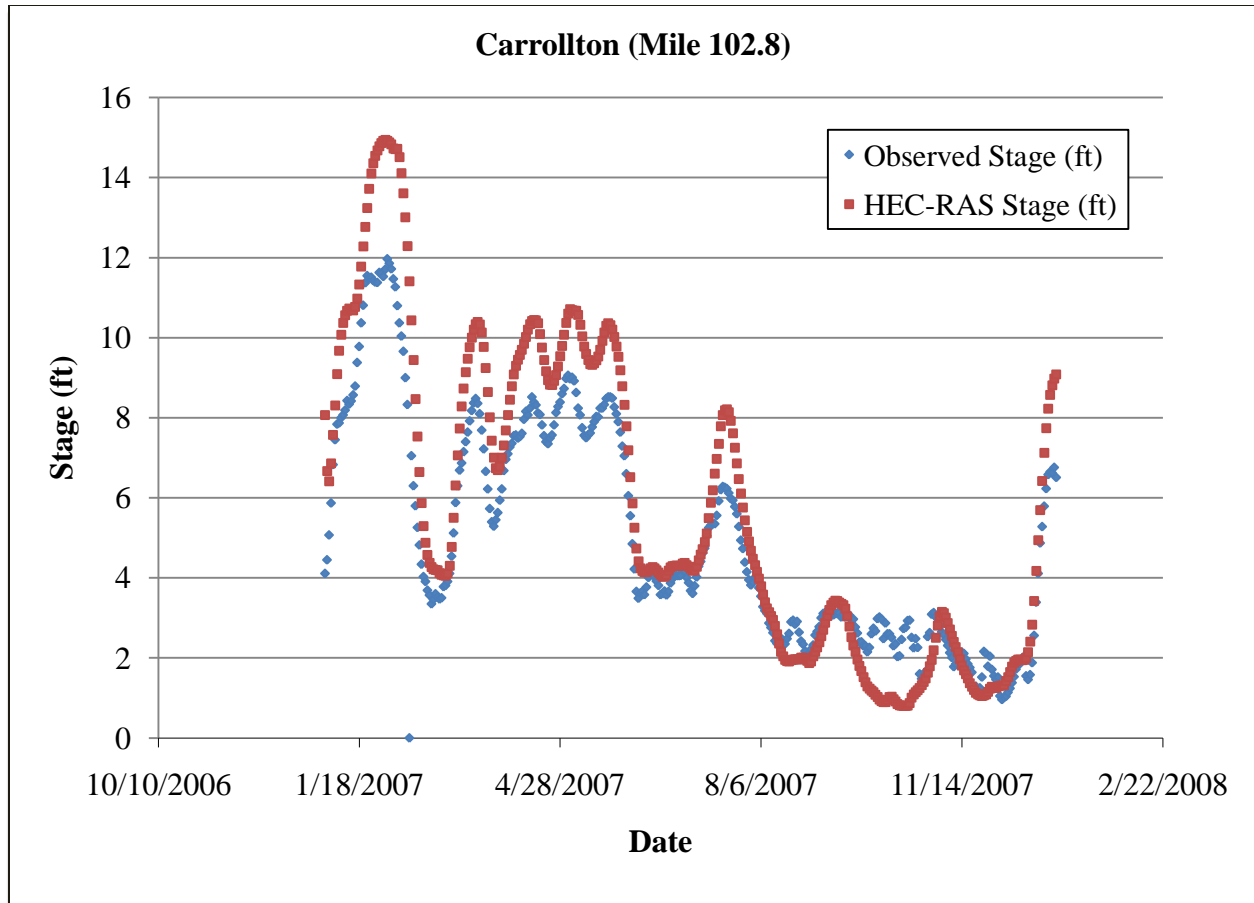


**Figure 5-4: Carrollton Stage Comparison for 2007 Calibration (Original).**

The Manning's  $n$  value was altered along several reaches of the MR to achieve better agreement between the calculated and the known data. After changing the  $n$  values for a particular reach, the model was run and the results were analyzed. For reaches with a calculated stage (HEC-RAS) less than the observed stage, the  $n$  values were reduced; and for reaches with a calculated stage above the observed stage, the  $n$  values were increased. The range of  $n$  values used for the MR was from 0.026 to 0.019. Appendix G shows the  $n$  values for all of the Mississippi reaches, as well as for the other reaches in the model. Figure 5-5 shows the stage calibration at Carrollton using the adjusted  $n$  values.

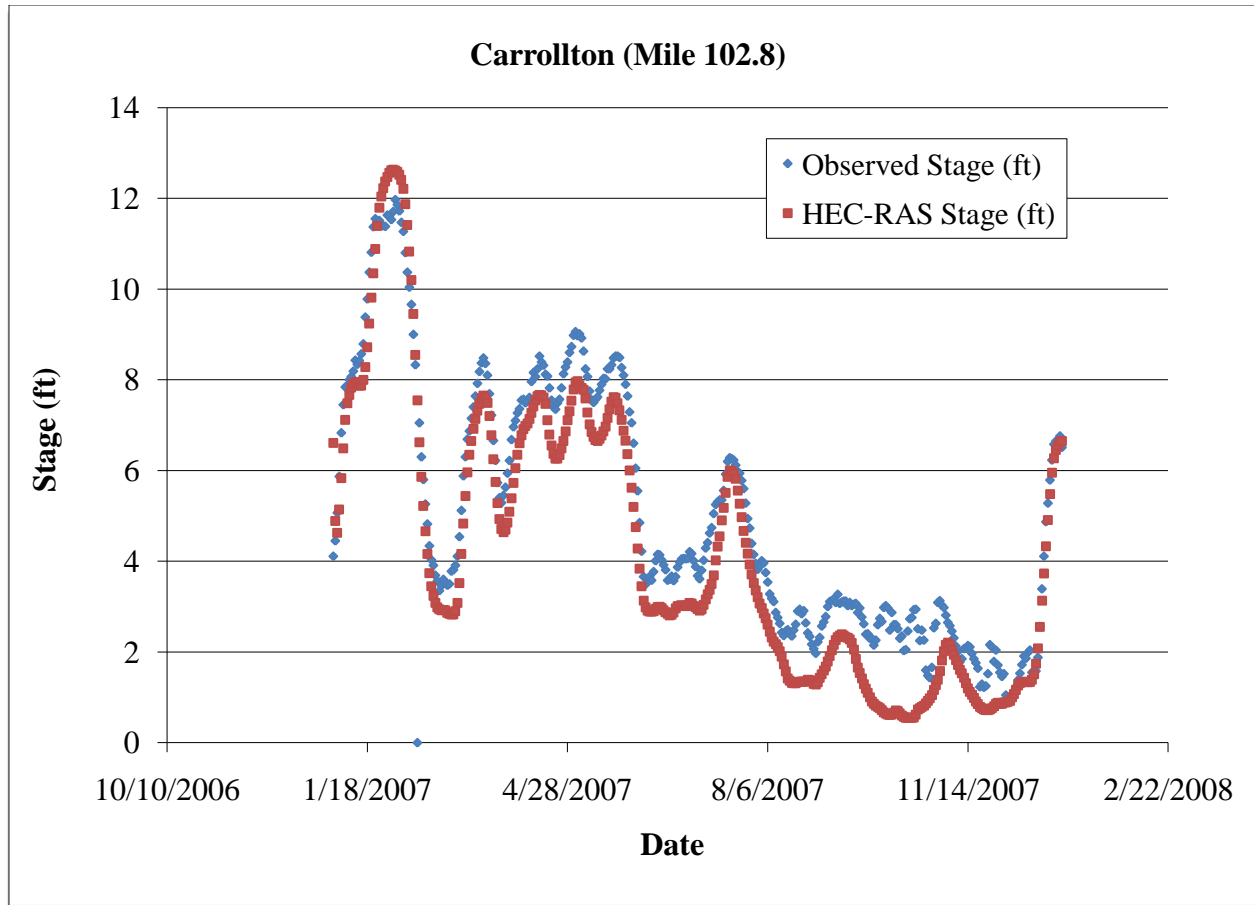


**Figure 5-5: Carrollton Stage Comparison for 2007 Calibration (Manning's  $n$  Adjusted).**

As previously stated, the roughness of the channels changes with respect to the velocity in the channel; therefore, the roughness was also altered using flow rated roughness factors<sup>15</sup>, which are multiplied to the Manning's  $n$  for a specific range of flow values. After analyzing the stage values, a higher flow roughness factor was applied to reduce the stage values and a lower factor was applied to increase the stage values. Figure 5-6 shows the stage comparison for Carrollton, based on the flow roughness factors that were applied throughout the MR.

<sup>15</sup> The flow roughness factors are presented in Appendix I.

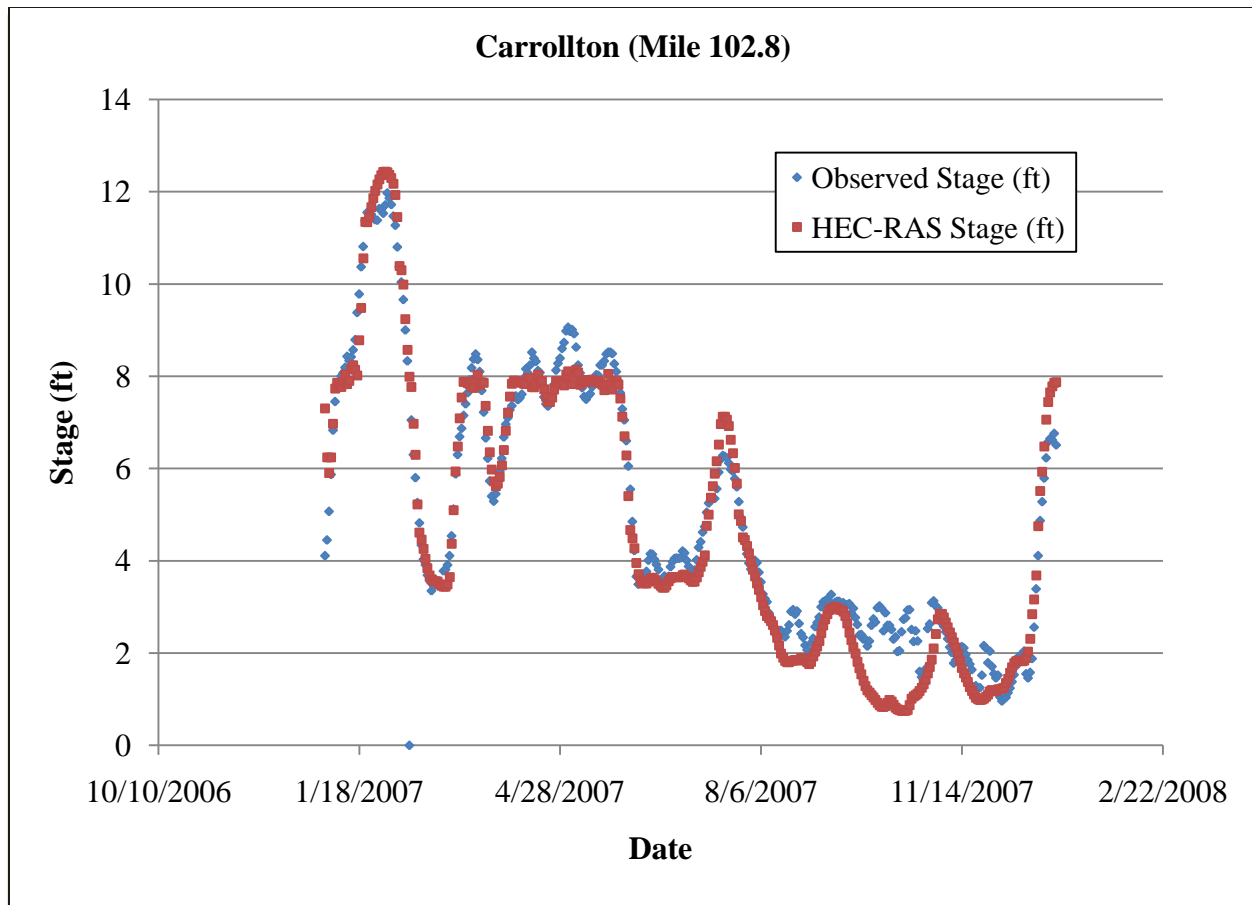


**Figure 5-6: Carrollton Stage Comparison for 2007 Calibration (Flow Roughness Factors Included).**

This new figure (Figure 5-6) shows a closer agreement to the observed values, but there is a slight disparity for median to low flows. This difference was assumed to be an effect of the downstream boundary condition set for the channels leading to the GOM. The initial downstream boundary condition for these reaches did not account for tides or saltwater intrusion from the GOM. During high flows, the stage in the Delta is high enough to dampen the effects of the GOM tides. However, during low flows, the stage in the Delta drops, which causes a more pronounced tidal affect from the GOM because there is insufficient momentum to counteract the tide. Also, during high flows, the salt water wedge is forced downstream due to shear stress of the water heading downstream. However, during low flows, the salt water wedge advances upstream and ultimately increases the stage in the river due to the differential density effect. For example, a minimum of 300,000 cfs passing New Orleans is required to keep the saltwater wedge from infiltrating the water supply intakes (LPBF, 2008). In order to account for these effects, three steps were taken: (i) three-hour stage data measurements from the GOM for the calendar year of 2007 were collected and averaged to obtain daily average stage values to account for the tidal contribution; (ii) hourly surface salinity data from Southwest Pass for the calendar year of 2007 were obtained and averaged to get a daily surface salinity value. This value was then depth-averaged based on a diffusive coefficient of 3; (iii) the following equation was used to calculate the total stage, considering both tidal and salinity influences:

$$S_T = S_{tide} + d_{ref} \left( \frac{\bar{C}_s}{1000} \right) \quad (5-1)$$

where:

$S_T$  = total stage [ft]

$S_{tide}$  = stage due to tidal influences [ft]

$d_{ref}$  = reference depth (= 40 ft)

$\bar{C}_s$  = depth-averaged salinity [ppt]

These new stage values were then entered as the downstream boundary condition for all channels leading to the GOM. Figure 5-7 shows the new stage comparison at Carrollton, using the new total daily stage values as the GOM boundary condition.

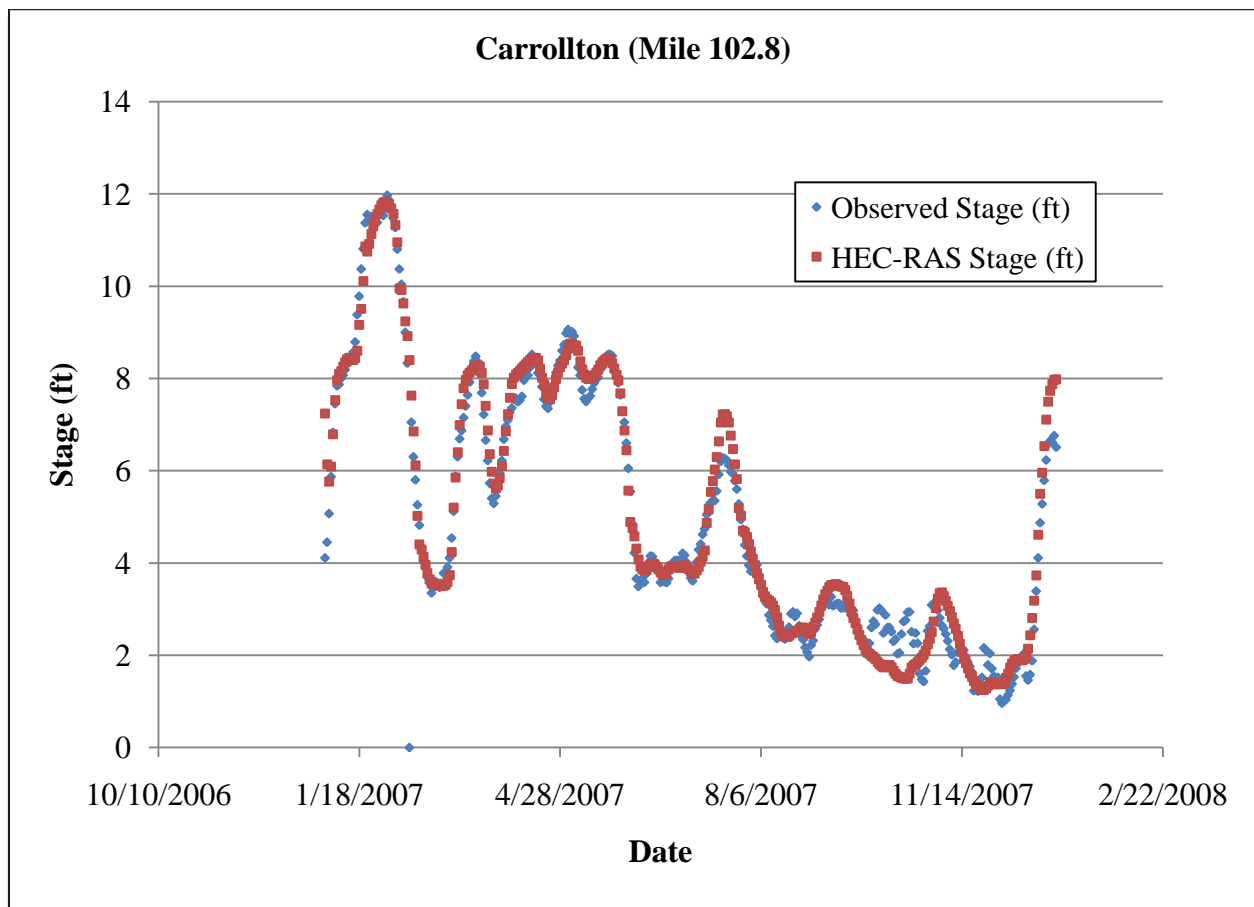


**Figure 5-7: Carrollton Stage Comparison for 2007 Calibration (Tides and Salinity Included).**

Figure 5-7 shows a better agreement throughout, especially during March through May. During those periods on the previous graphs (Figures 5-4, 5-5, and 5-6), the measured stage did not capture the peaks and troughs. As a result, the new stage values were set as the downstream boundary condition for all simulations for the calendar year of 2007. The new stage hydrograph is presented in Appendix F with the boundary conditions.

To determine the accuracy or validity of the model, the root mean square error (RMSE) and bias error between the calculated and observed data were measured. The equations for the RMSE and the bias error are as follows:

$$RMSE = \sqrt{\frac{\sum (z_{model} - z_{obs'd})^2}{N}} \quad (5-2)$$

$$BiasError = \frac{\sum (z_{model} - z_{obs'd})}{N} \quad (5-3)$$

where:

$z_{model}$  = stage value calculated by the model  
 $z_{obs'd}$  = stage value observed in the field  
 $N$  = number of observations

The RMSE, bias error, and RMSE per average cross-section depth were calculated for the 2007 calibration. Table 5-1 shows these errors for each comparison gage.

**Table 5-1: RMSE, Bias Error, and RMSE per Average Cross-section Depth for 2007 Calibration Simulation at the Comparison Gages.**

Parameter / Gage	Baton Rouge	Donaldsonville	North of Bonnet Carré	Bonnet Carré	Carrollton	West Pointe a la Hache	Venice
RMSE (ft)	1.19	0.81	0.70	0.75	0.46	0.46	1.00
Bias Error (ft)	-0.80	0.36	0.49	0.42	0.08	0.13	-0.89
RMSE/Avg Depth	2.73%	1.74%	0.92%	1.34%	0.73%	0.71%	2.03%

## 5.2 Validation

For the validation procedure, the model was given boundary conditions for the calendar years of 2003, which was a high flow year, and 1999-2000, which had both high and low flows. The 2003 validation included all the major passes, the Barataria Basin drainage network, and the existing diversions similar to the calibration procedure except for the White Ditch Siphon, which was inoperable at the time (BS-12, n.d.). Also, the West Bay Sediment Diversion was given an inline structure to prevent flow from being diverted from the MR until November of 2003, which was when the construction was completed and the diversion was officially opened (Guilbeau, n.d.). The boundary condition for the channels leading to the GOM was set as the 2007 calibration GOM stage, including the tidal and salinity effects, because GOM stage and salinity data were not readily available for the calendar year of 2003. Figure 5-8 shows the stage comparison at Carrollton for the 2003 validation. Table 5-2 shows the RMSE, bias error, and RMSE per average cross-section depth for the 2003 validation.

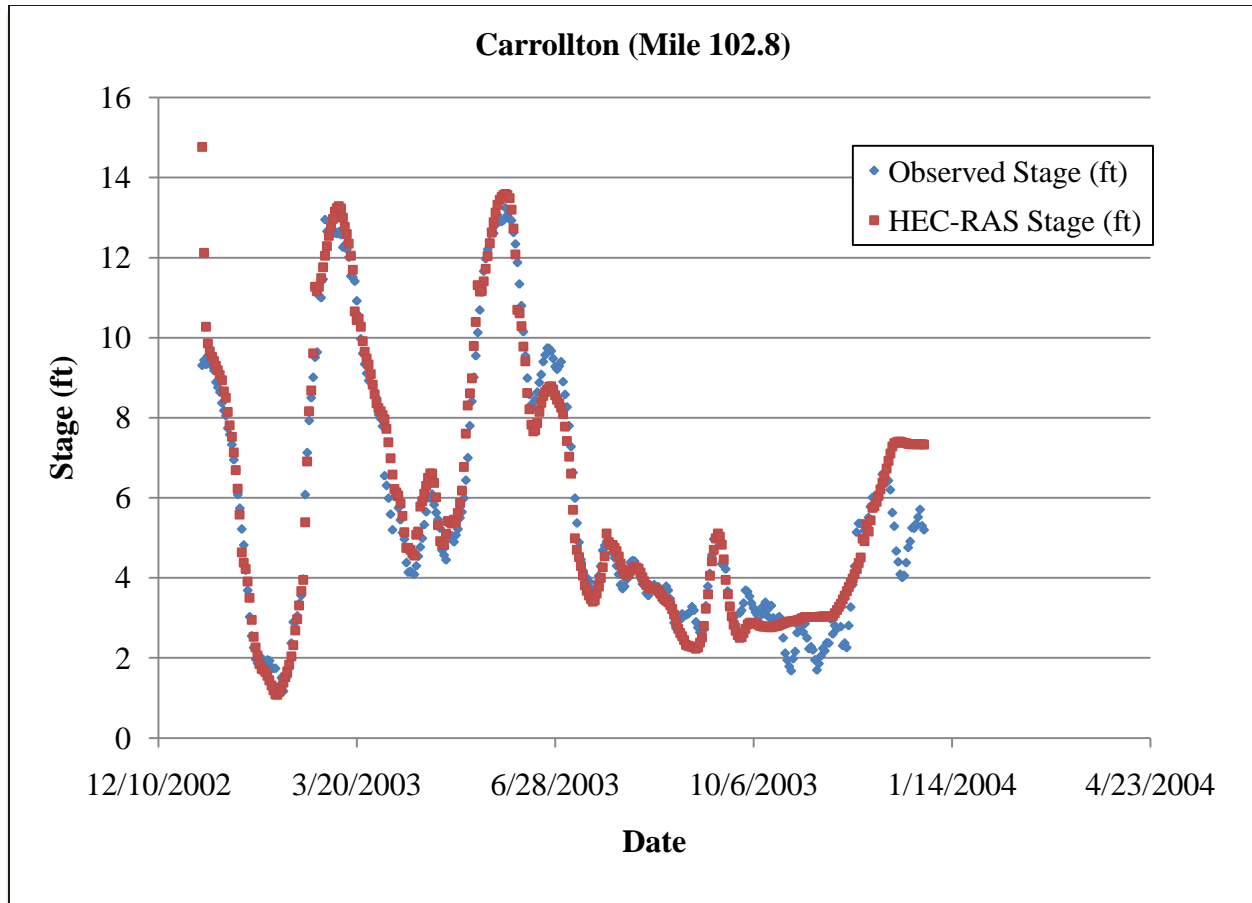


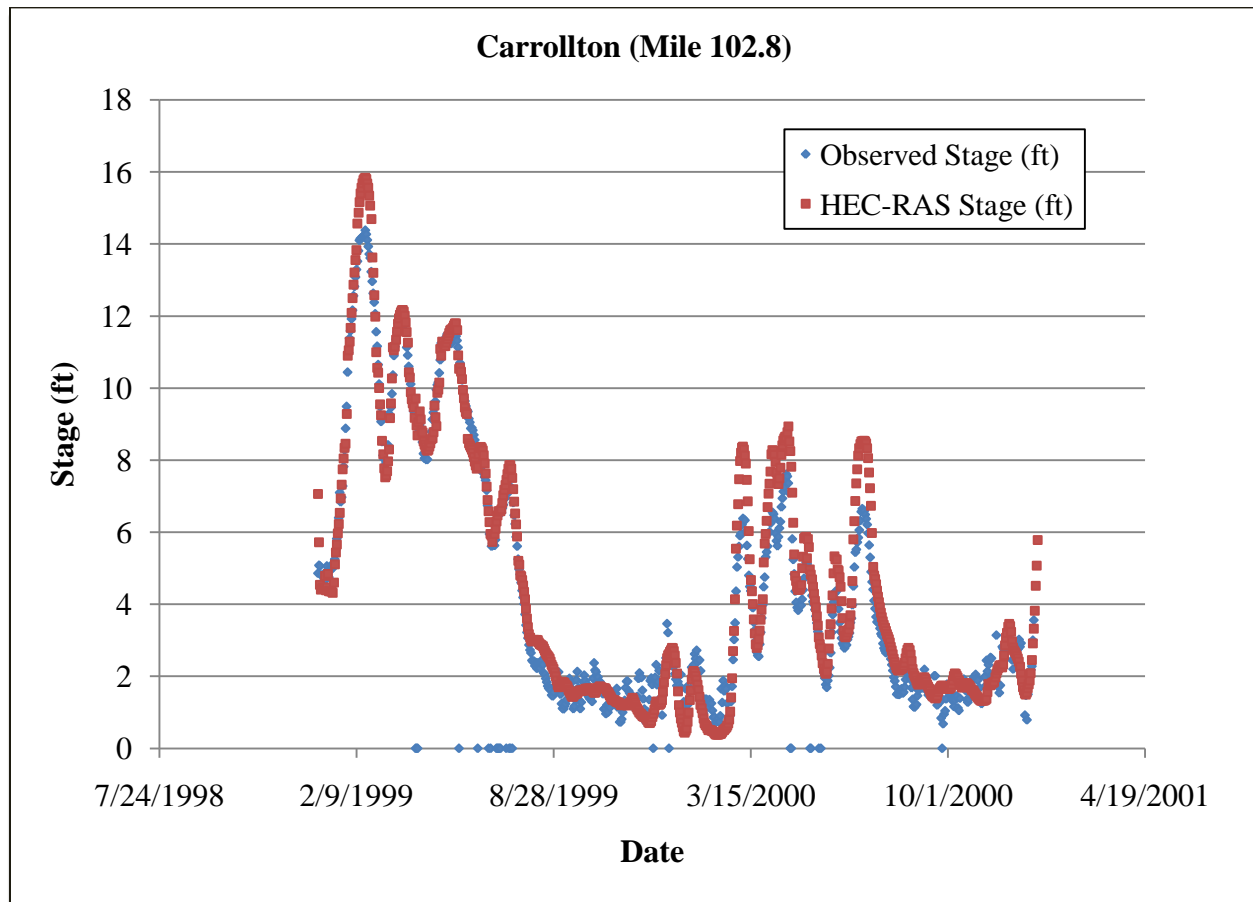
Figure 5-8: Carrollton Stage Comparison for 2003 Validation.

Table 5-2: RMSE, Bias Error, and RMSE per Average Cross-section Depth for 2003 Validation Simulation at the Comparison Gages.

Parameter / Gage	Baton Rouge	Donaldsonville	North of Bonnet Carré	Bonnet Carré	Carrollton	West Pointe a la Hache	Venice
RMSE (ft)	1.76	1.36	N/A	0.98	0.78	0.52	1.06
Bias Error (ft)	-0.25	0.31	N/A	0.46	0.19	-0.12	-0.97
RMSE/Avg Depth	4.02%	2.88%	N/A	1.77%	1.22%	0.81%	2.16%

The 1999-2000 validation included all the major passes, the Barataria Basin drainage network, and the existing diversions except for the following: (i) the West Bay Sediment Diversion was not constructed yet (Guilbeau, n.d.); (ii) the Davis Pond Freshwater Diversion was not constructed yet (DPFDP, 2002); (iii) the White Ditch Siphon was inoperable (BS-12, n.d.). Since the Davis Pond Diversion was not open, the cross-sections for the inflow and guide channels and the ponding area were removed up to Lake Cataouatche, and a local runoff daily flow hydrograph of 150 cfs was set as the upstream boundary condition. The West Bay Diversion channel was completely removed from the model. The inflow hydrograph at White Ditch was

also removed from the boundary conditions. Figure 5-9 show the stage comparison at Carrollton for the 1999-2000 validation.



**Figure 5-9: Carrollton Stage Comparison for 1999-2000 Validation.**

Figures 5-8 and 5-9 show good agreement between the observed and calculated stage; therefore, the Manning's  $n$  values and flow roughness factors did not have to be re-evaluated. Table 5-3 shows the RMSE, bias error, and RMSE per average cross-section depth for the 1999-2000 validation.

**Table 5-3: RMSE, Bias Error, and RMSE per Average Cross-section Depth for 1999-2000 Validation Simulation at the Comparison Gages.**

Parameter / Gage	Baton Rouge	Donaldsonville	North of Bonnet Carré	Bonnet Carré	Carrollton	West Pointe a la Hache	Venice
RMSE (ft)	0.93	0.90	N/A	0.94	0.71	0.53	0.72
Bias Error (ft)	-0.09	0.44	N/A	0.58	0.25	0.26	-0.52
RMSE/Avg Depth	2.29%	2.05%	N/A	1.67%	1.16%	0.80%	1.46%



### 5.3 Model Limitations

The original calibration simulation was set up for the 2007-2008 high flood year. The daily stage hydrograph at Tarbert Landing (RM 306) was used as the upstream boundary condition for the MR. The GOM daily salinity stage hydrograph for the period of December 19, 2007 to June 27, 2008 was used as the downstream boundary condition. All other boundary conditions were the same as the 2007 calibration. In 2008, 160 of the bays of the Bonnet Carré Spillway were opened due to high stage in the river (USACE NOD, 2010). The gates in the model were given a time-series gate opening boundary condition, and the actual daily operations were replicated in the model for the period from April 11, 2008 to May 8, 2008. Figure 5-10 shows the stage comparison at Carrollton for the observed spillway opening and the calculated spillway opening.

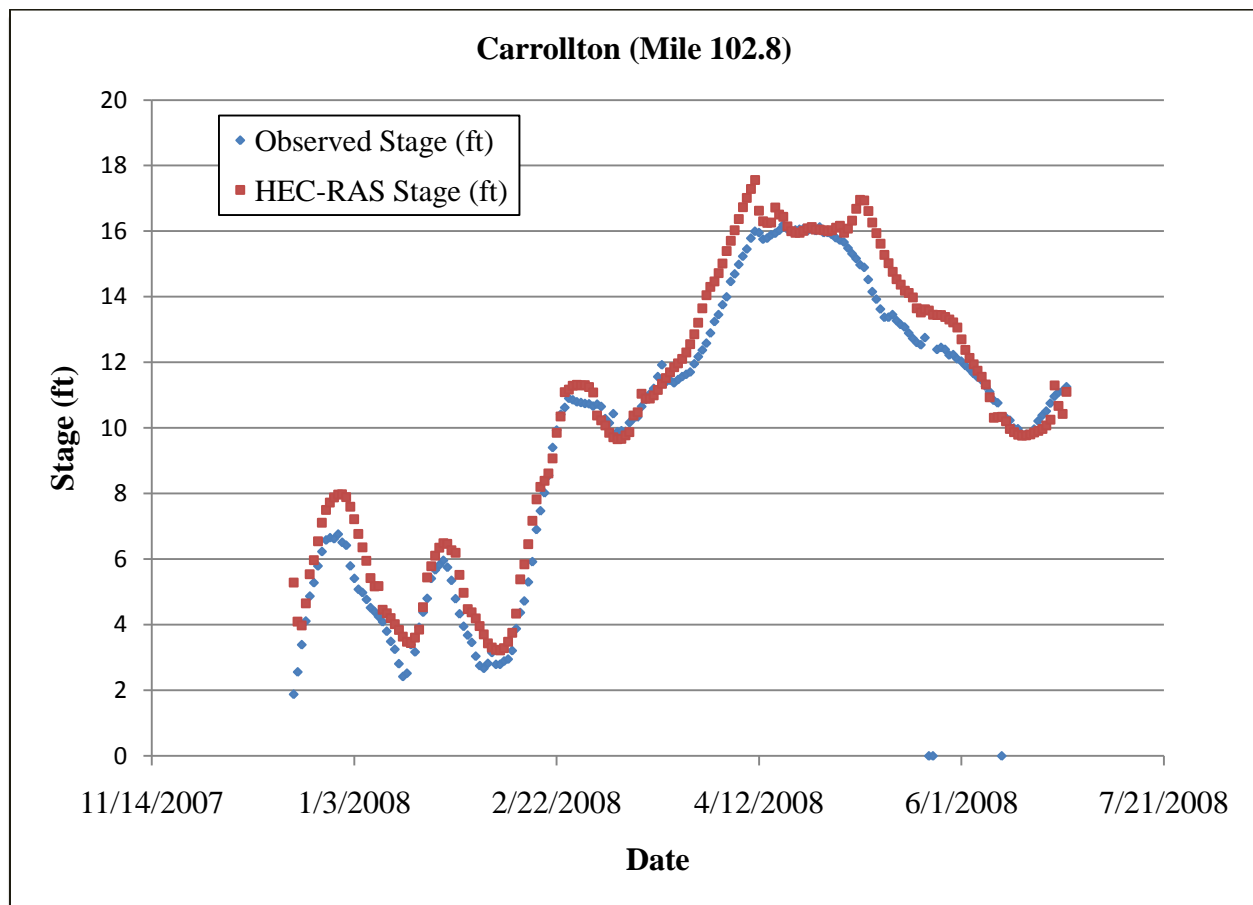


**Figure 5-10: Carrollton Stage Comparison for 2007-2008 Simulation.**

The disparity at peak flow was consistently observed throughout the MR starting at the gage at North of Bonnet Carré (RM 129.2) and continuing to the gage at Venice (10.7). Also, the original operation of the gates in HEC-RAS involved increasing the gate height from 0 ft at day zero to the recommended gate height at day 1. Gate heights were calculated based on the number of gates actually opened per day. For days where twenty five or more gates were opened, an entire gate group, which consists of twenty five gates, was given its respective gate height (10 or 12 ft). To account for days with less than or more than twenty five gates opened, the gate height

for one gate group was proportioned to allow the same cross-sectional area that was provided by the actual gates. The following equation was used to calculate the recommended gate heights.

$$H_P = \left( \frac{N_{AG} H}{N_{GG}} \right) \quad (5-4)$$

where:

$H_P$  = proportioned gate height [ft]

$N_{AG}$  = number of gates actually opened

$H$  = height of gate group gates (10 or 12 ft)

$N_{GG}$  = number of gates per gate group

From the discharge hydrograph, the closing of the actual gates began on April 26, 2008 and ended on May 8, 2008. Therefore, the gates in the model were closed using a linear series in Microsoft Excel for those dates. The discharge hydrograph comparison for the flow leaving the gates was not agreeable using these gate operations. Therefore, the model gates were operated by trial and error to achieve a total discharge leaving the river during the opening similar to that of the actual discharge leaving. The trial and error process consisted of increasing the proportioned gate heights to allow more flow to leave the system. Also, the closing of the model gates was altered to have several gate groups fully closed before May 8. Figure 5-11 shows the daily discharge hydrograph comparison for the 2008 gate opening using the new gate operations.

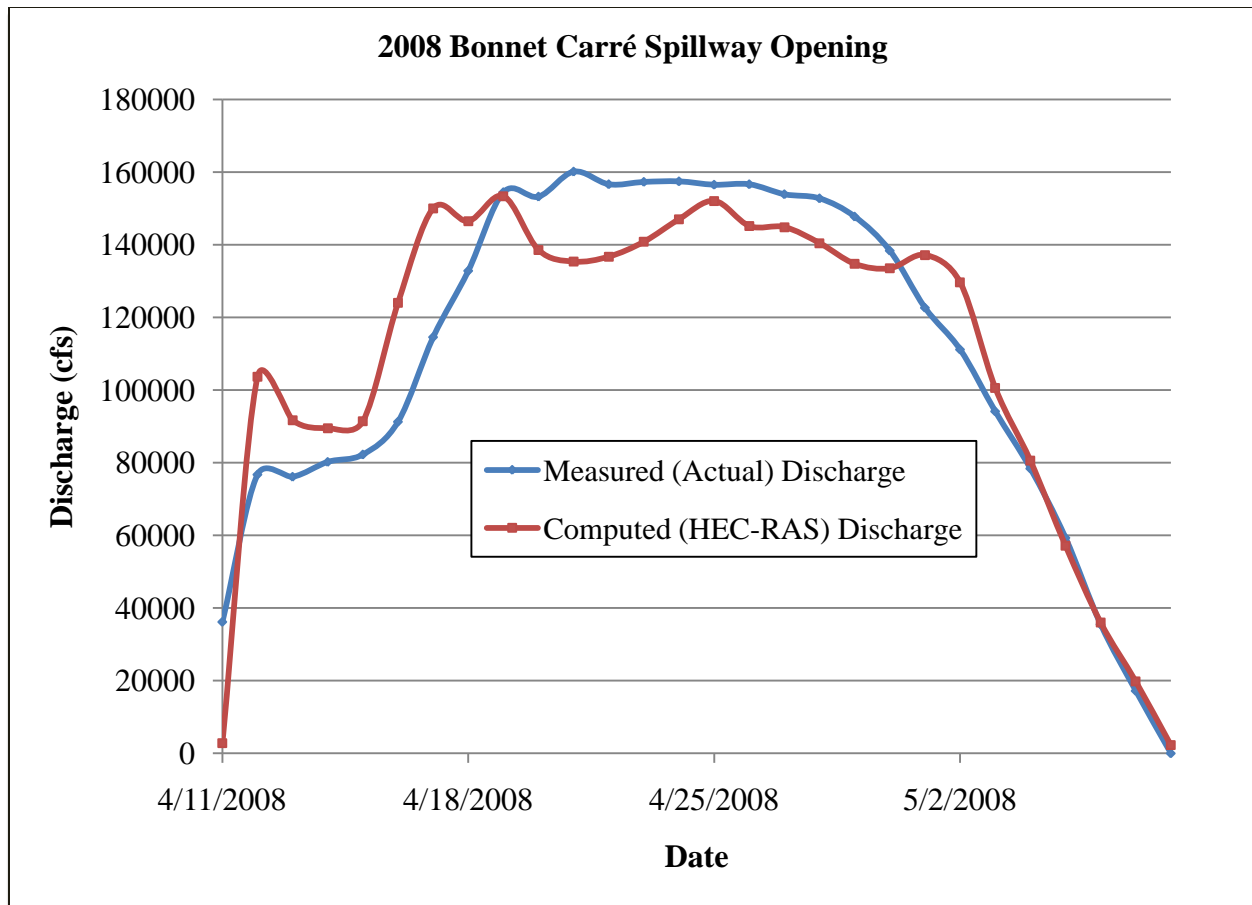


**Figure 5-11: Discharge Comparison for the 2008 Bonnet Carré Spillway Opening.**

As seen, the computed curve does not fit the actual curve, but the difference in total flow leaving the system was found to be 6200 cfs, which is roughly 0.2% of the total observed discharge leaving. Therefore, the new gate operations were accepted. Due to the disparities and inconsistencies in the stage and discharge hydrographs, the 2007-2008 simulation was no longer used for the calibration procedure and the calendar year of 2007 was chosen instead.

## Chapter 6: Applications

### 6.1 Modeling Schemes

The purpose of this study was to create a river response model that would estimate the impacts that coastal restoration and management efforts would have on the lower Mississippi River (MR). Therefore, several cases were simulated using the existing diversions, proposed reach closures, possible channel modifications, and proposed diversions. Table 6-1 is a list of the modeled studies along with any deviations from the 2007 calibration and the target flow rates for the proposed diversions.

**Table 6-1: Model Simulations, Deviations from 2007 Calibration Simulation, and Target Flow Rates.**

Simulation	Deviations from 2007 Calibration Simulation	Target Flow Rate, cfs
2007_RSLR_0.5	GOM stage boundary condition raised by 1.64 ft (0.5 m)	-
2007_RSLR_1.0	GOM stage boundary condition raised by 3.28 ft (1.0 m)	-
2007_RSLR_1.5	GOM stage boundary condition raised by 4.92 ft (1.5 m)	-
2007_WB	West Bay channel removed	-
2007_WB_SP	Same as 2007_WB with South Pass channel closed	-
2007_WB_SWP	Same as 2007_WB with Southwest Pass channel closed	-
2007_WB_SP_SWP_pal50	Same as 2007_WB with South and Southwest Passes closed and Pass a Loutr� dredged to -50 ft	-
2007_WB_SP_SWP_pal40	Same as 2007_WB_SP_SWP_pal50 with Pass a Loutr� dredged to -40 ft	-
2007_WB_B	Same as 2007_WB with Buras channel included	59,900
2007_WB_JB_B	Same as 2007_WB_B with Jesuit Bend channel and gated structure included	5000
2007_WB_JB_MG_B	Same as 2007_WB_JB_B with Myrtle Grove channel and gated structure included	20,000
2007_WB_JB_MG_DR_B	Same as 2007_WB_JB_MG_B with Deer Range channel and gated structure included	10,000
2007_WB_Div_SP	Same as 2007_WB_JB_MG_DR_B with South Pass closed	-
2007_WB_Div_SWP	Same as 2007_WB_JB_MG_DR_B with Southwest Pass closed	-
2007_WB_Div_SP_SWP_pal50	Same as 2007_WB_JB_MG_DR_B with South and Southwest Passes closed and Pass a Loutr� dredged to -50 ft	-
2007_WB_Div_SP_SWP_pal40	Same as 2007_WB_Div_SP_SWP_pal50 with Pass a Loutr� dredged to -40 ft	-

## 6.2 Results

### 6.2.1 Relative Sea Level Rise Study

This study was performed to predict the effects of relative sea level rise from the Gulf of Mexico (GOM) on the Mississippi River (MR). The 2007 GOM boundary condition was raised by 1.64, 3.28, and 4.92 ft (0.5, 1.0, and 1.5 m). The parameters under consideration were shear stress, to determine the sediment transport potential, and the discharge and water surface elevation, to create a rating curve. These parameters were checked at the following locations along the MR: Violet (RM 83.9), Belle Chasse (RM 76), Myrtle Grove (RM 59.3), and West Pointe a la Hache (RM 48.7). Figures 6-1, 6-2, 6-3, and 6-4 show the shear stress results for each of these locations.

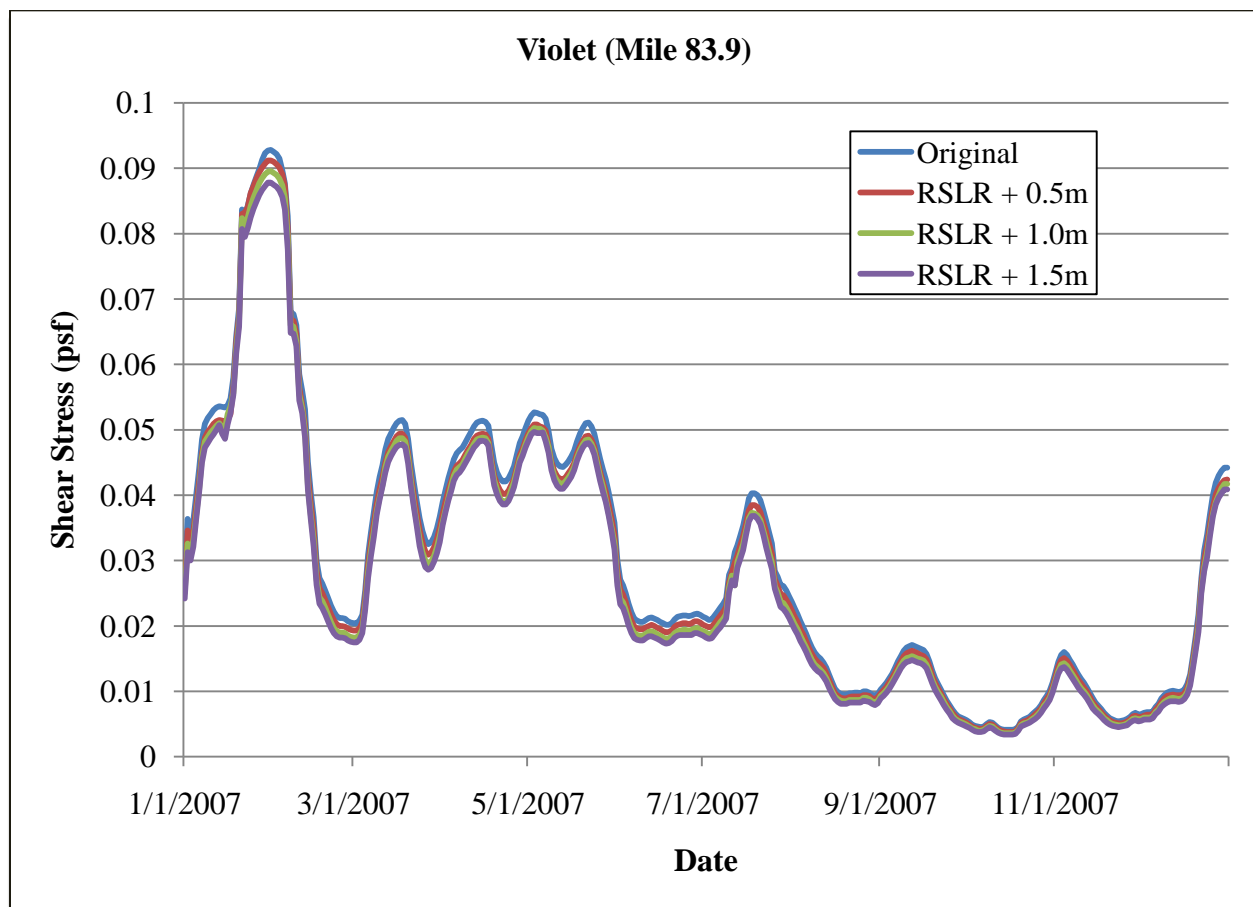
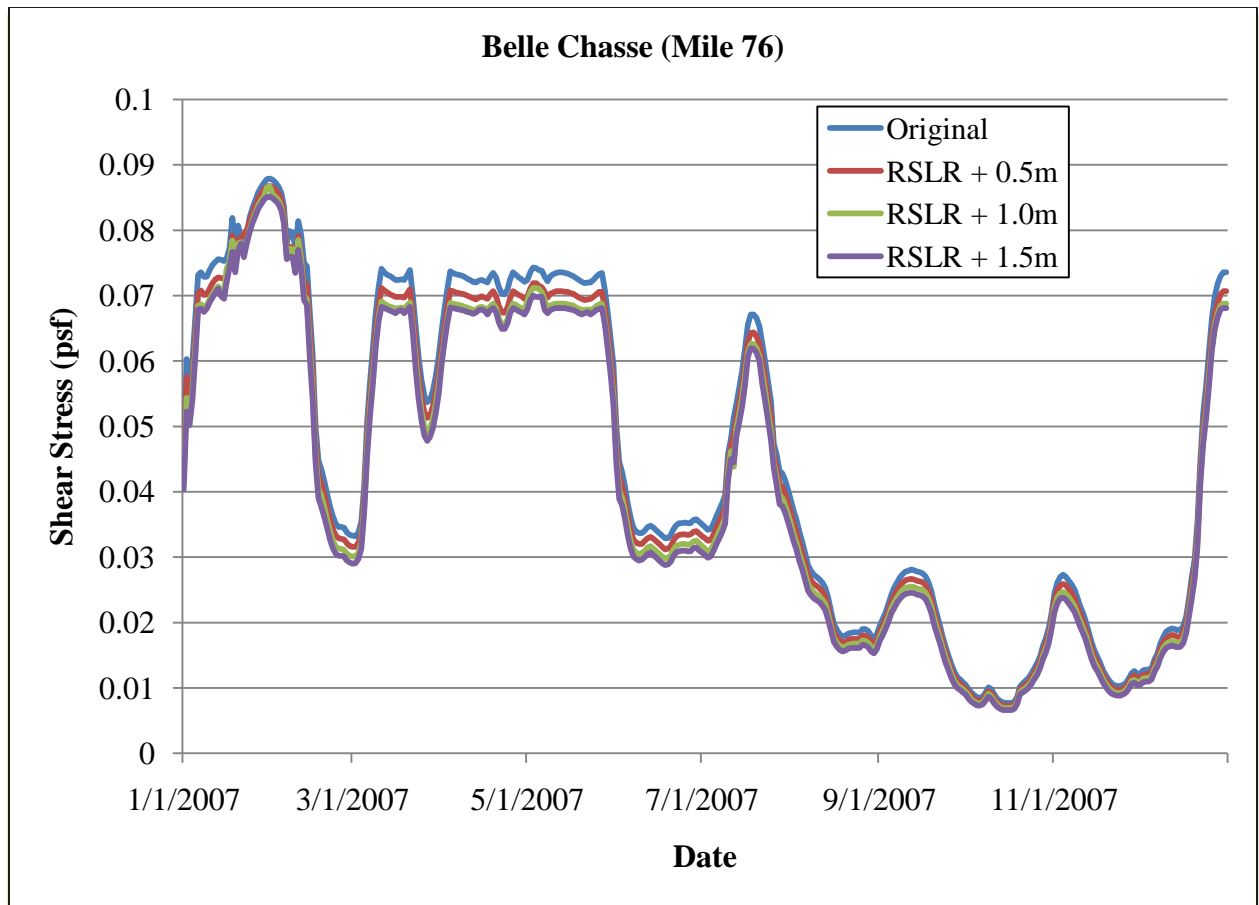
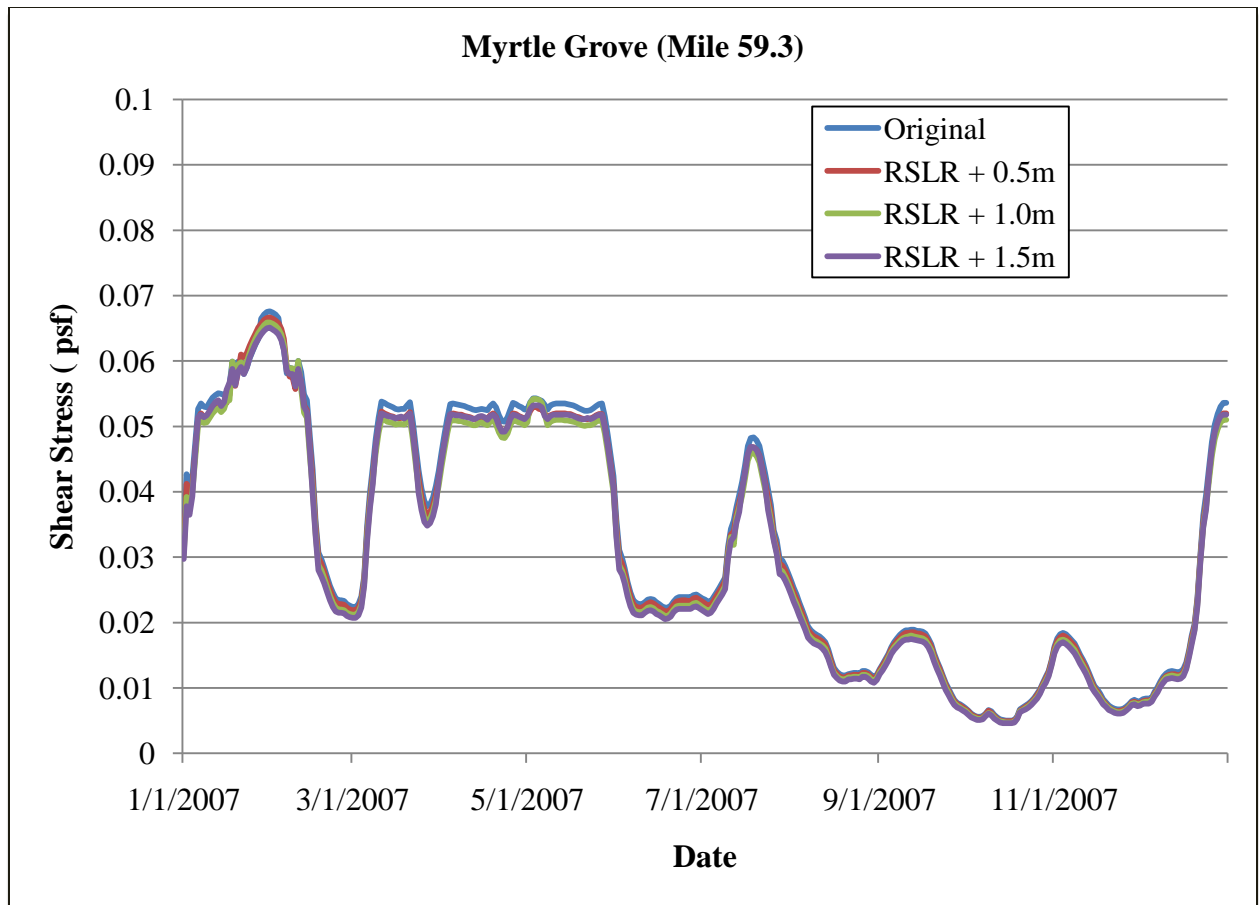


Figure 6-1: Shear Stress Comparison for Violet (2007).



**Figure 6-2: Shear Stress Comparison for Belle Chasse (2007).**



**Figure 6-3: Shear Stress Comparison for Myrtle Grove (2007).**



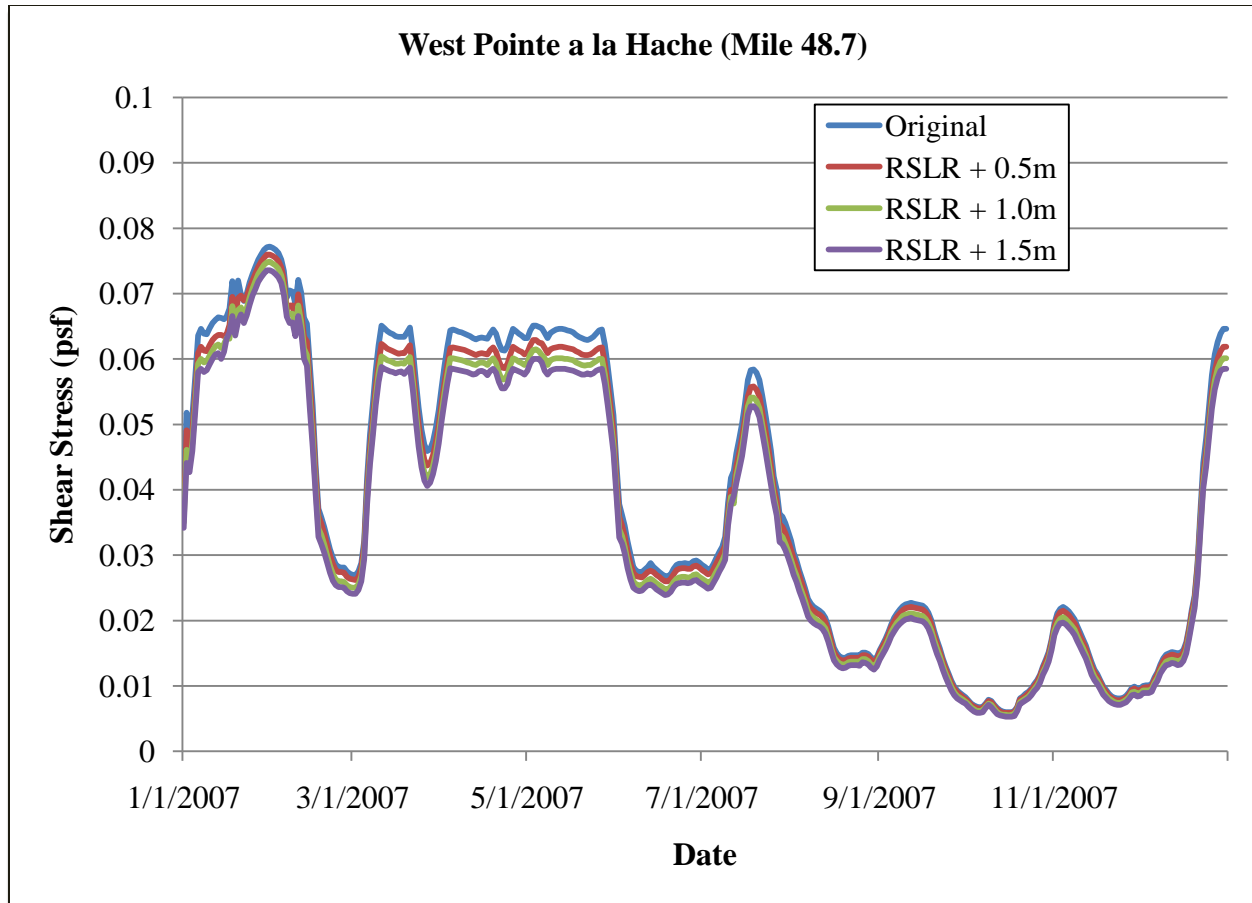


Figure 6-4: Shear Stress Comparison for West Pointe a la Hache (2007).

Using the shear stress results, the bed material transport was then calculated using the DuBoys-Straub Equation<sup>16</sup> below:

$$q_s = C_s \tau_o \left( \tau_o - \tau_c \right) \quad (6-1)$$

where:

$q_s$  = bed material transport per unit length [= ft<sup>3</sup>/sec/ft]

$C_s$  = Straub coefficient

$\tau_o$  = bed shear stress [= lb/ft<sup>2</sup>]

$\tau_c$  = critical shear stress [= lb/ft<sup>2</sup>]

For a median grain size in the MR of 0.25 mm (typical), the Straub table yields a Straub coefficient of 0.48 and a critical shear stress of 0.017 psf. Figures 6-5, 6-6, 6-7, and 6-8 show the bed material transport comparison of the same four locations for the different cases of relative sea level rise.

<sup>16</sup> Equation 6-1 has not been calibrated and is intended to present the relative effects of RSLR on bed material transport rates.

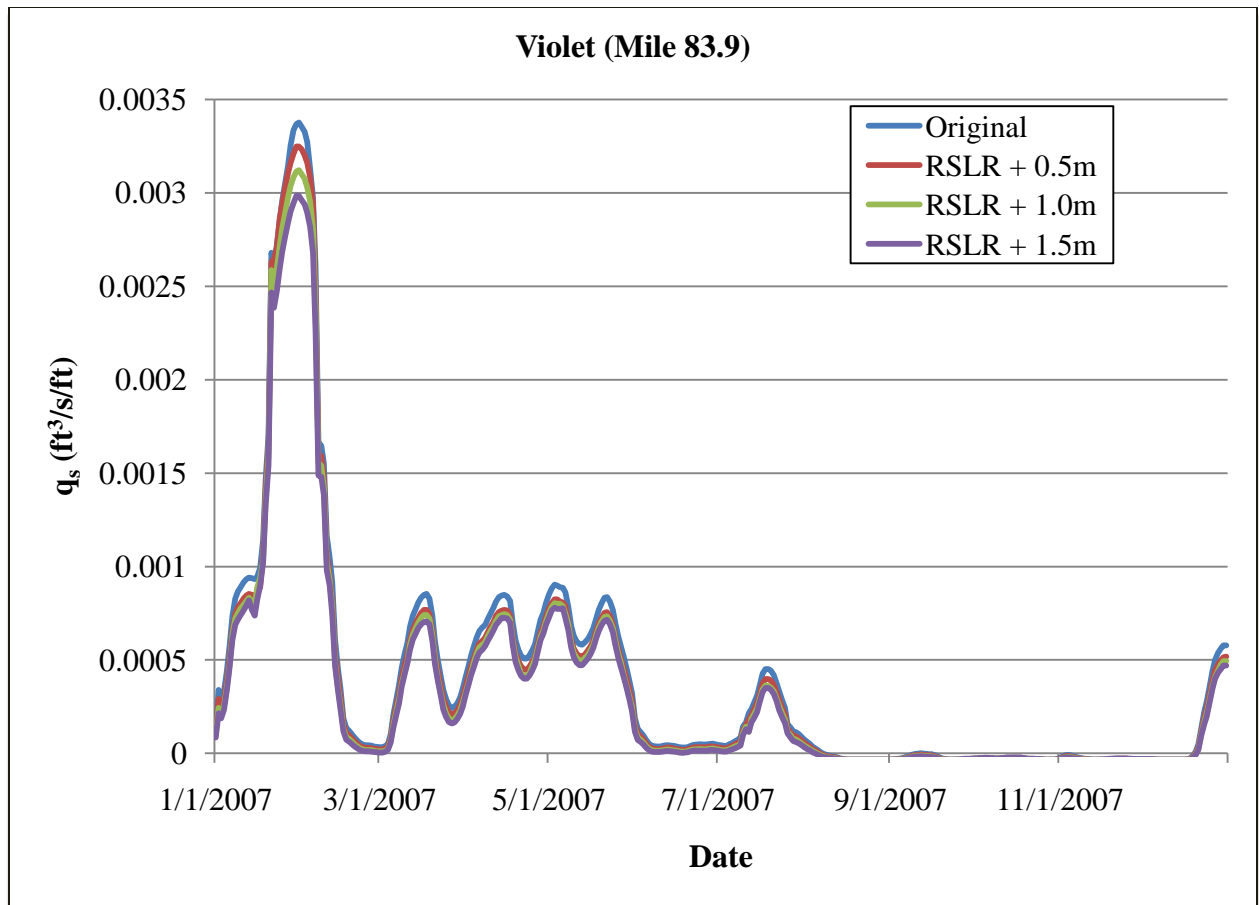


**Figure 6-5: Bed Material Transport ( $q_s$ ) Comparison for Violet (2007).**

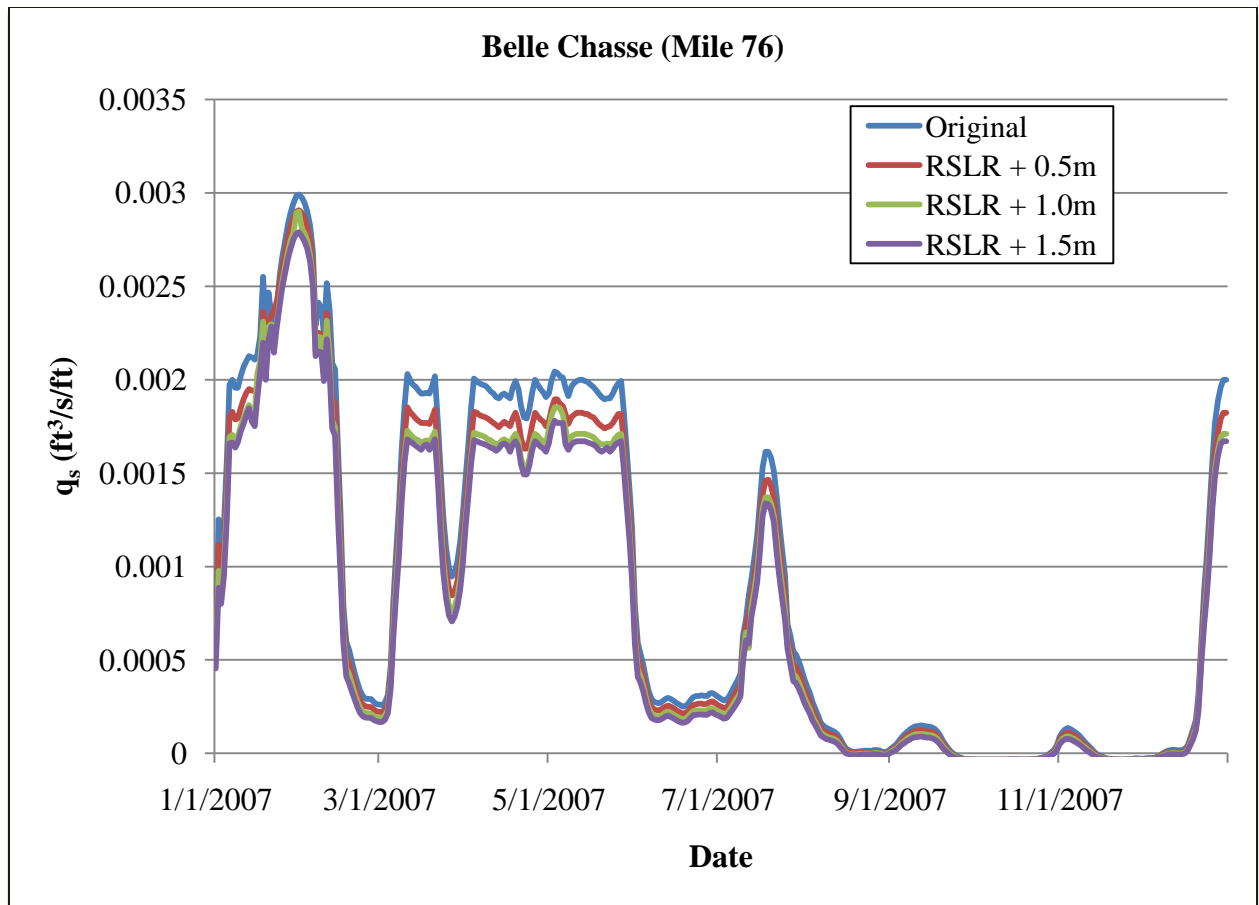


**Figure 6-6: Bed Material Transport ( $q_s$ ) Comparison for Belle Chasse (2007).**

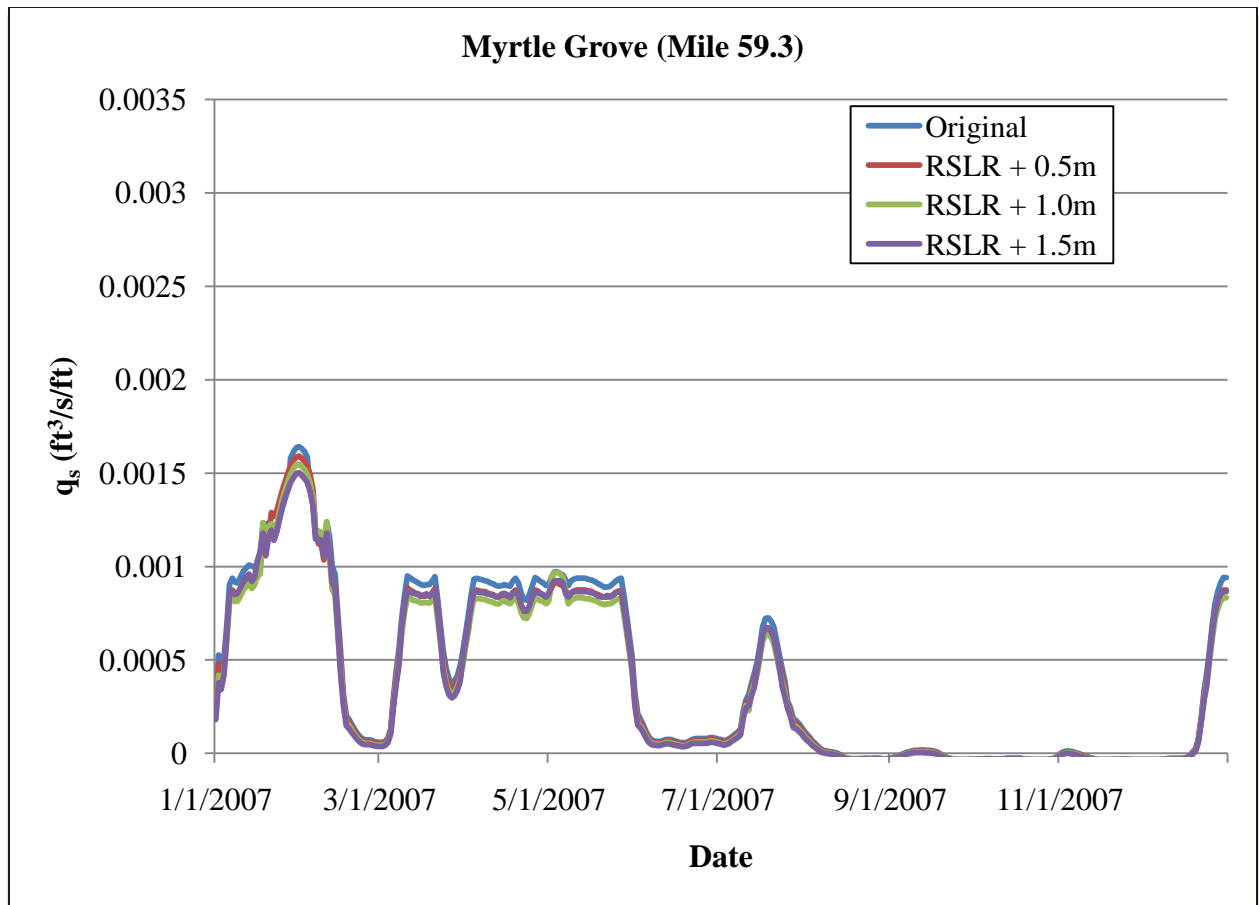


**Figure 6-7: Bed Material Transport ( $q_s$ ) Comparison for Myrtle Grove (2007).**

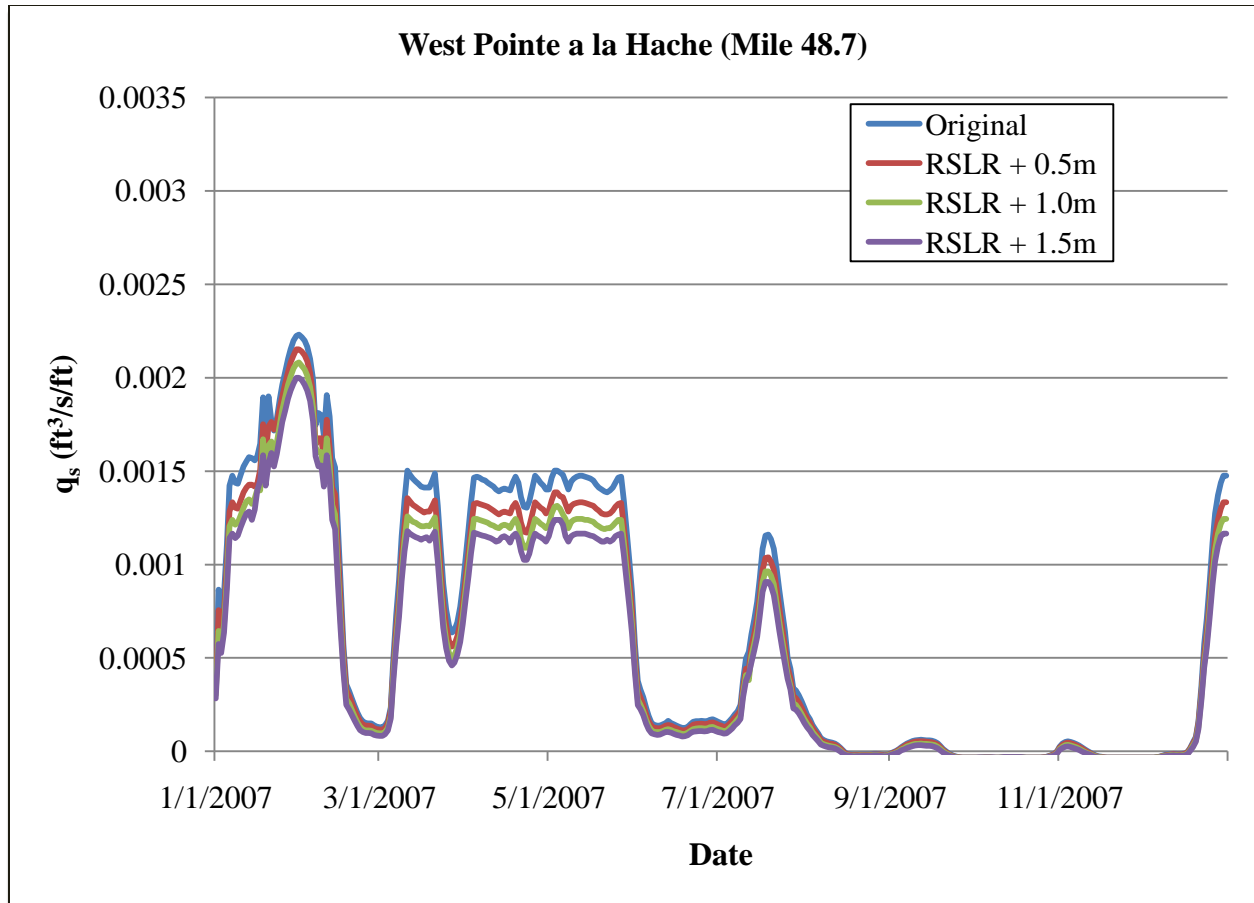


**Figure 6-8: Bed Material Transport ( $q_s$ ) Comparison for West Pointe a la Hache (2007).**

From Figures 6-5, 6-6, 6-7, and 6-8, the bed material transport reduces as the stage in the river increases. Figures 6-9, 6-10, 6-11, and 6-12 show the alternative rating curves for the four cases at the four locations.

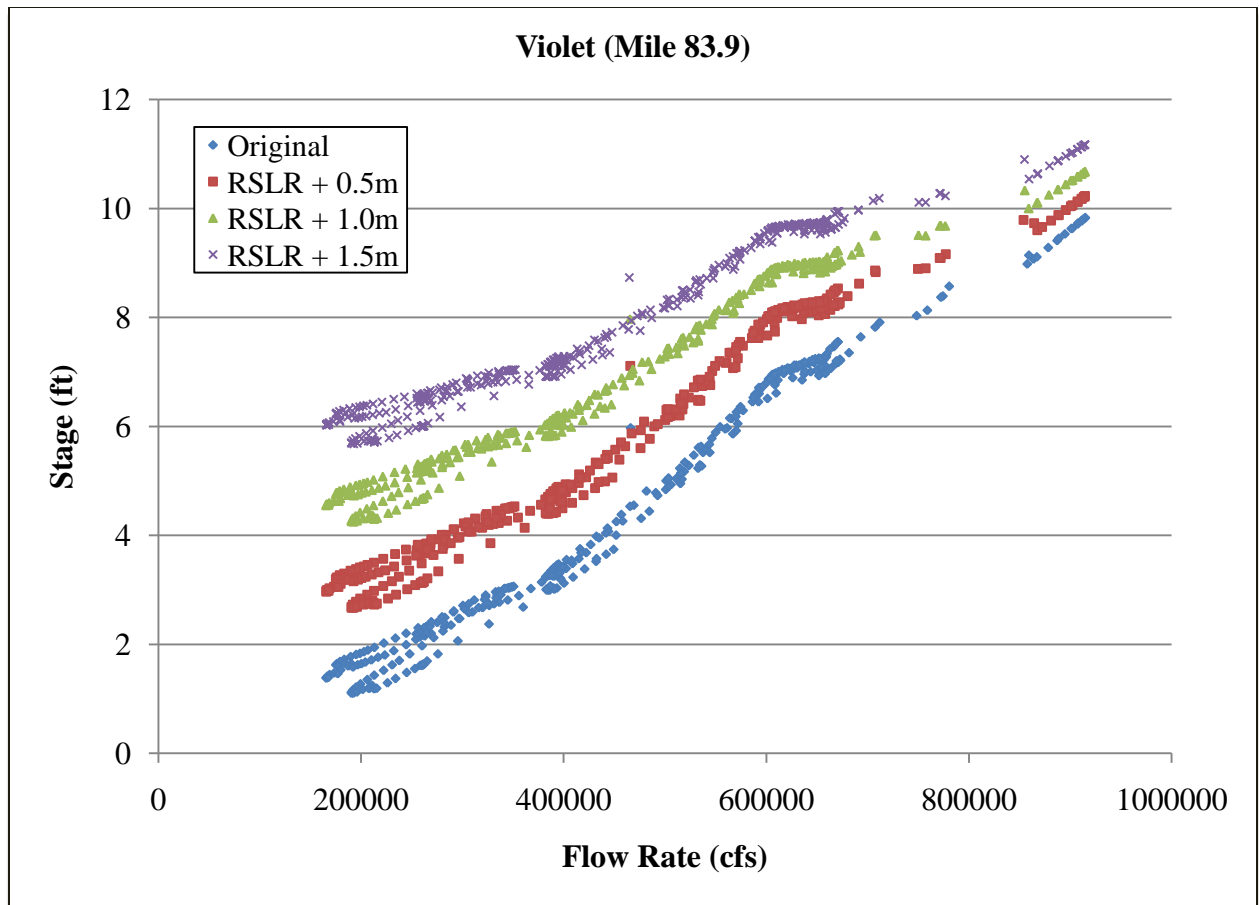


**Figure 6-9: Rating Curve Comparison for Violet (2007).**

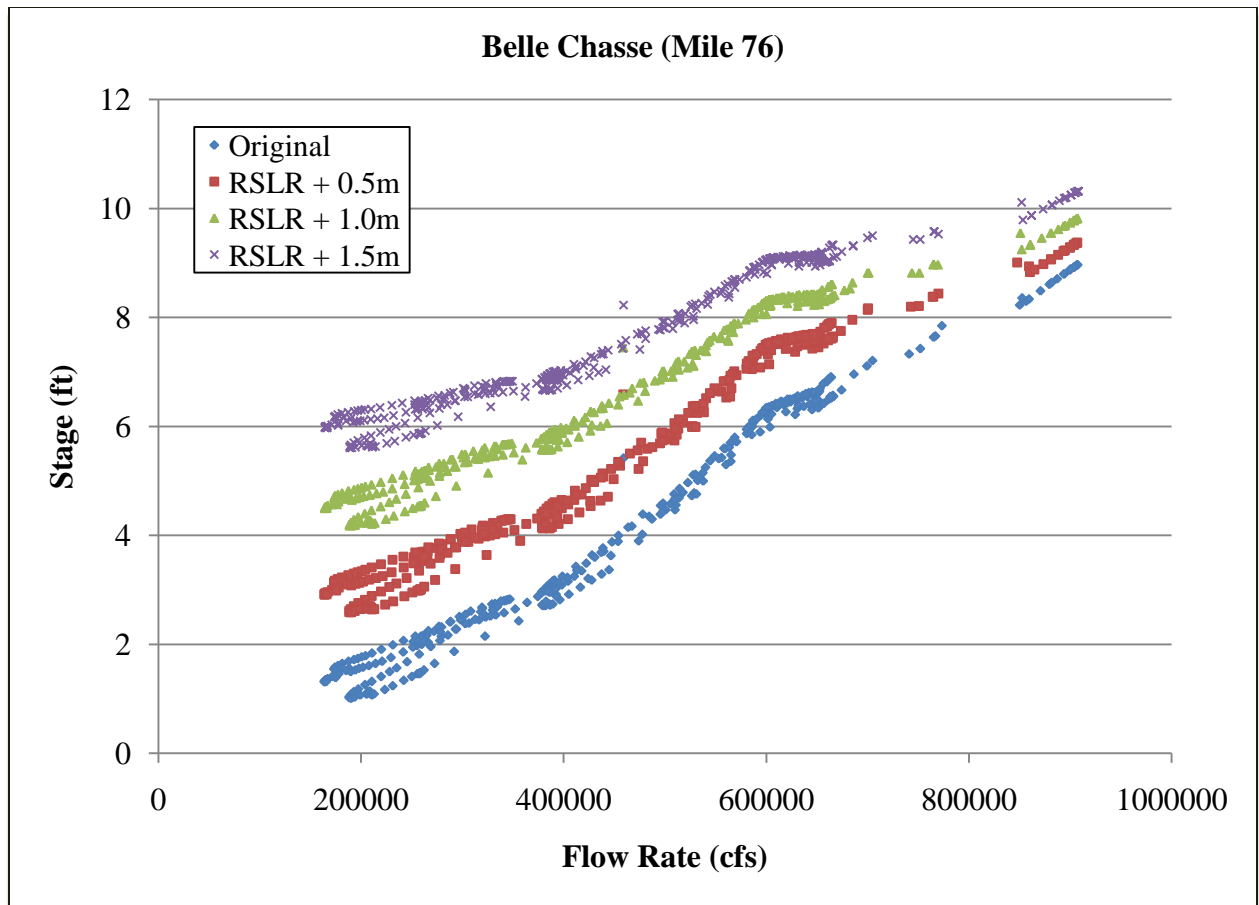


**Figure 6-10: Rating Curve Comparison for Belle Chasse (2007).**



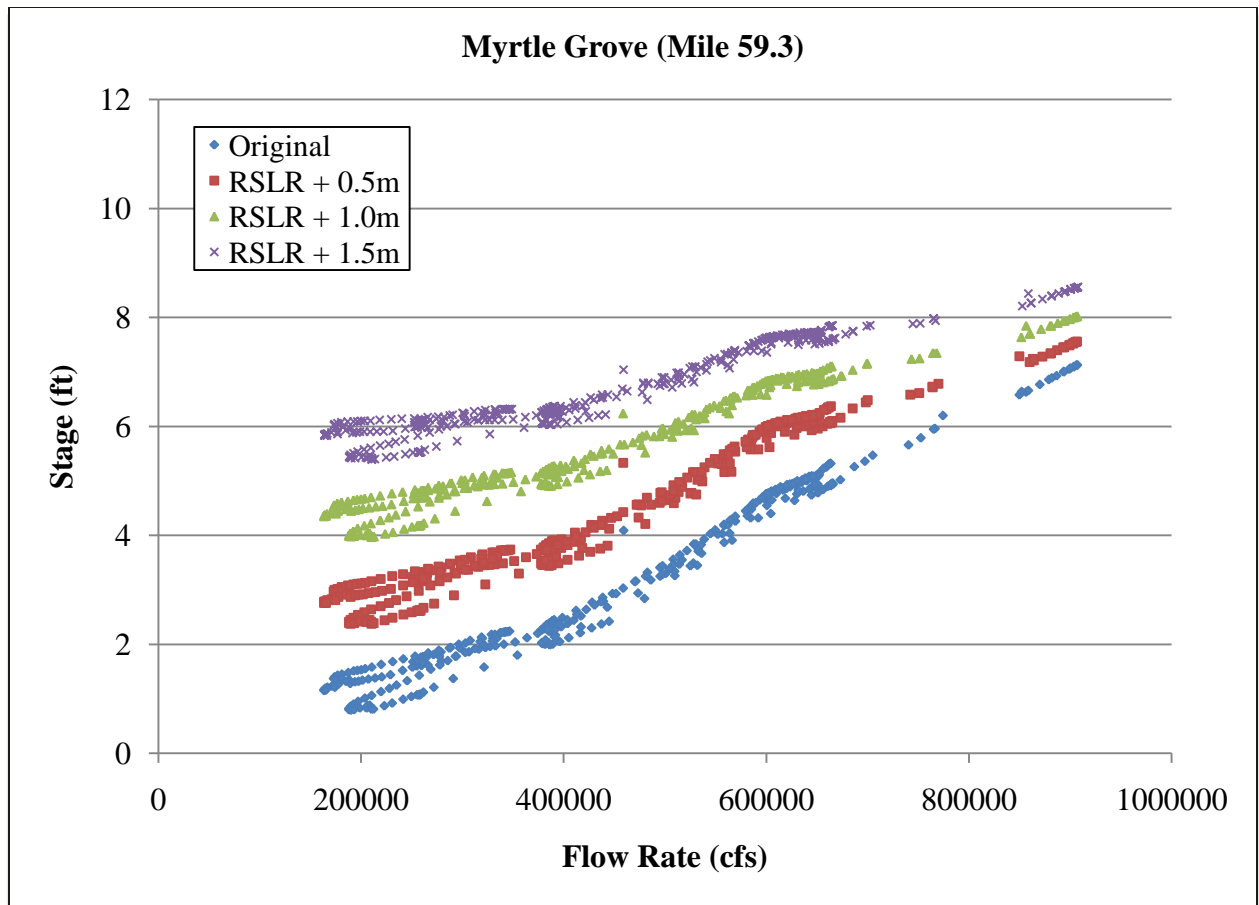


**Figure 6-11: Rating Curve Comparison for Myrtle Grove (2007).**

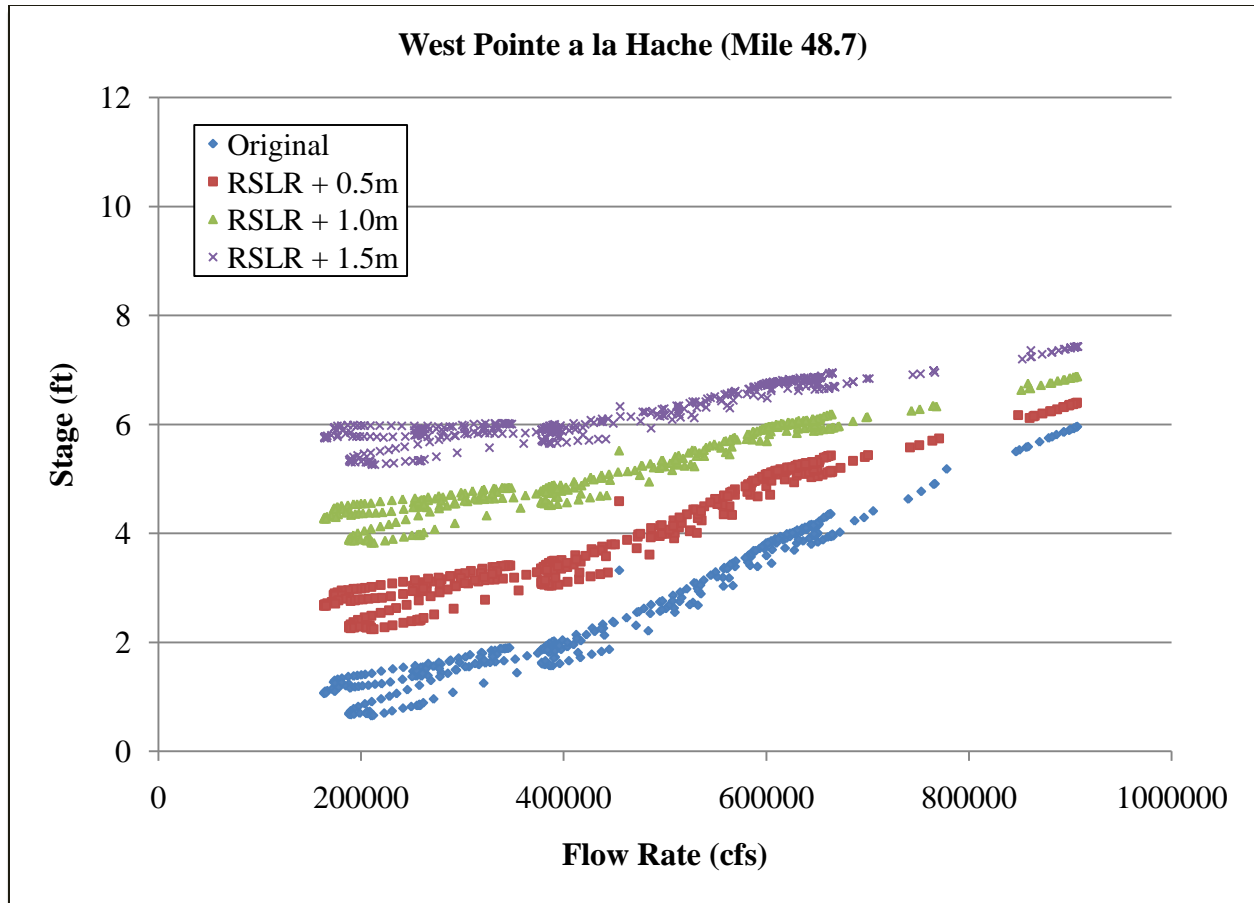


Figure 6-12: Rating Curve Comparison for West Pointe a la Hache (2007).

From Figures 6-9, 6-10, 6-11, and 6-12, the effects of relative sea level rise on the stage and flow become less prominent the further upstream they are. For example, the rating curves for Violet (Figure 6-9) are relatively close together and are converging at peak flows. However, the rating curves for West Pointe a la Hache (Figure 6-12) are more widely spread out and do not converge at peak flows.

### 6.2.2 West Bay Closure Study

This study was performed to estimate the effects of closing the West Bay Sediment Diversion. The West Bay channel in the model was completely removed and the flow distribution to the passes was assumed. Figures 6-13, 6-14, 6-15, 6-16, 6-17, 6-18, and 6-19 show the change in flow rate from the original 2007 calibration and the 2007\_WB simulation for Baptiste Collette, Fort St. Philip, Grand Pass, Main Pass, Pass a Loutr , South Pass, and Southwest Pass, respectively.

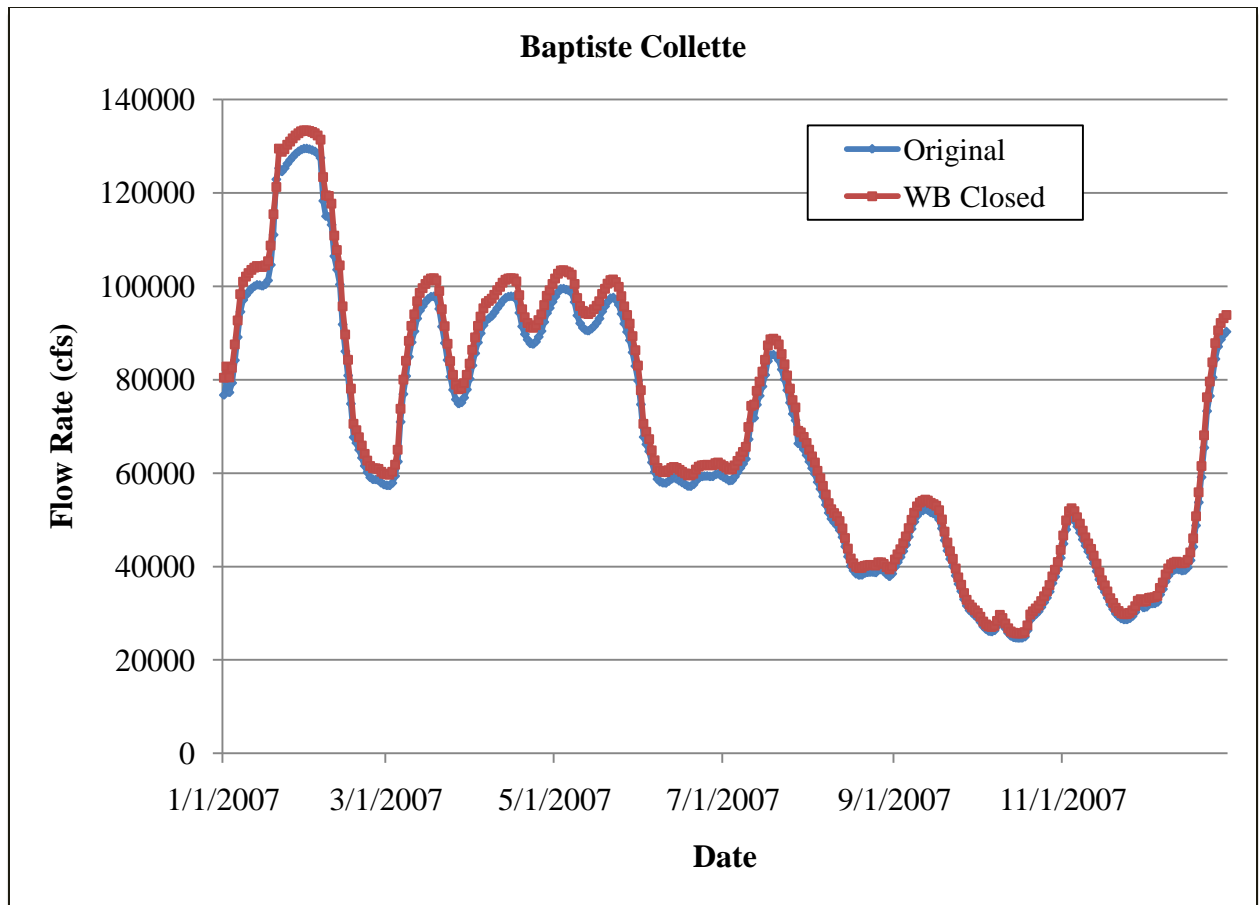


Figure 6-13: Flow Comparison for Baptiste Collette with West Bay Closed (2007\_WB).

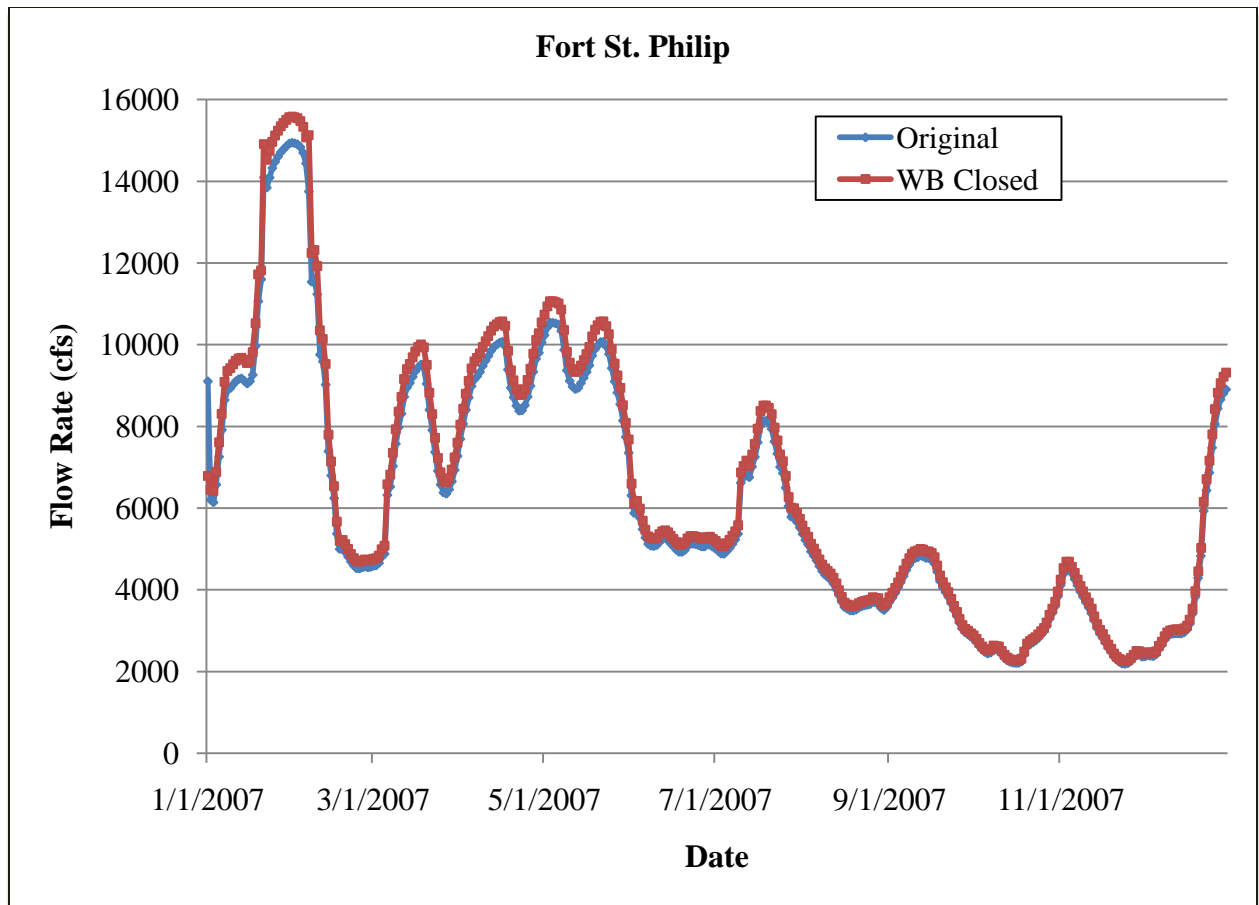


Figure 6-14: Flow Comparison for Fort St. Philip with West Bay Closed (2007\_WB).

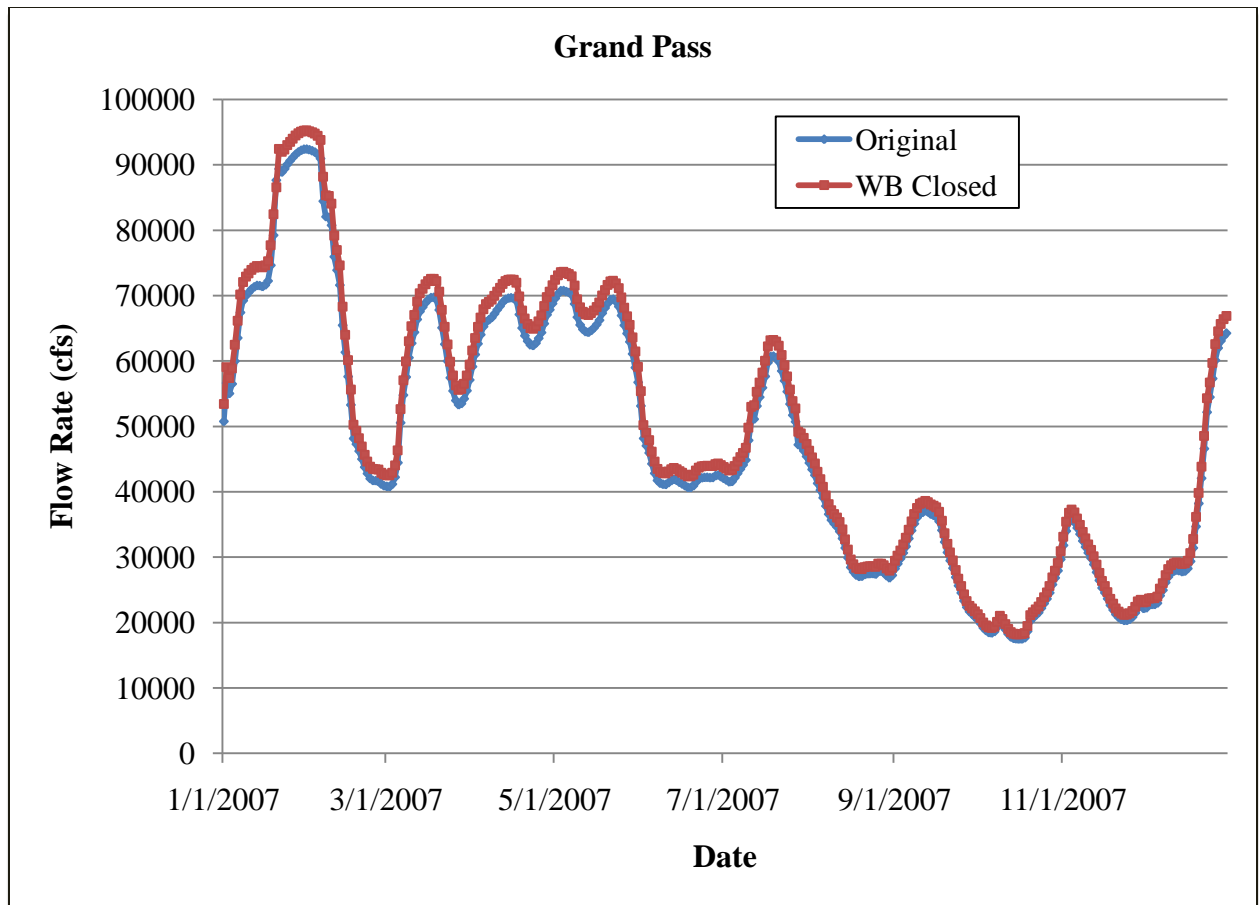


Figure 6-15: Flow Comparison for Grand Pass with West Bay Closed (2007\_WB).

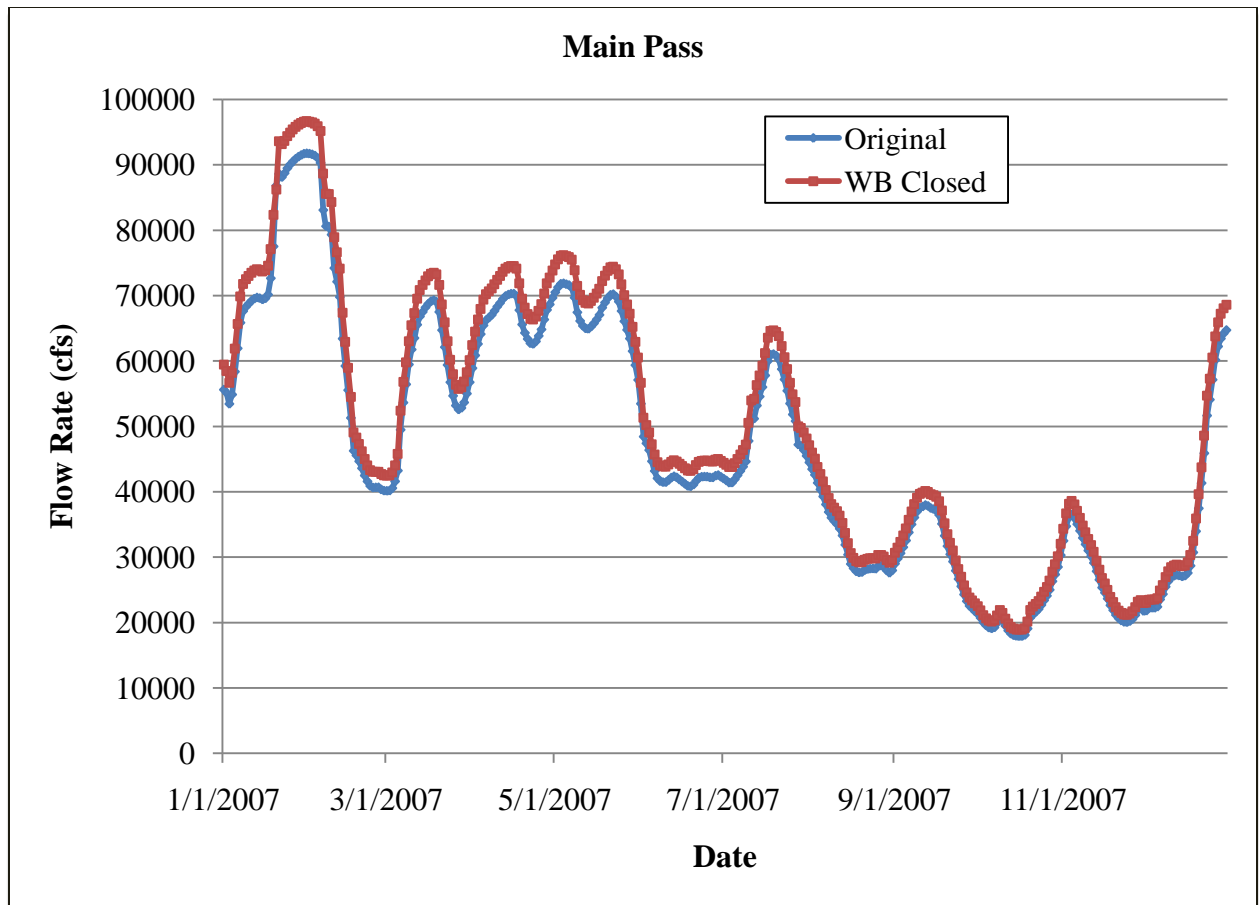


Figure 6-16: Flow Comparison for Main Pass with West Bay Closed (2007\_WB).

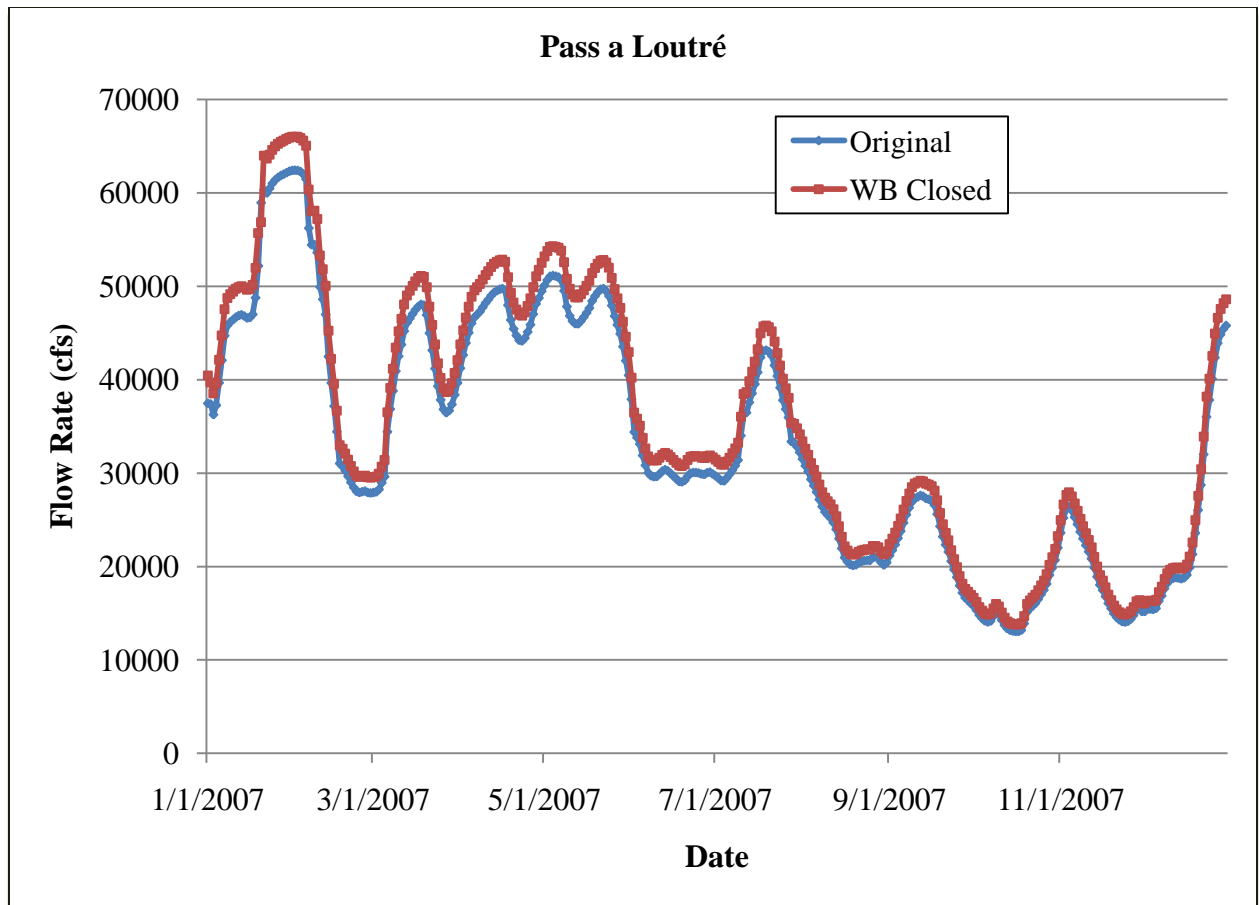


Figure 6-17: Flow Comparison for Pass a Loutr  with West Bay Closed (2007\_WB).

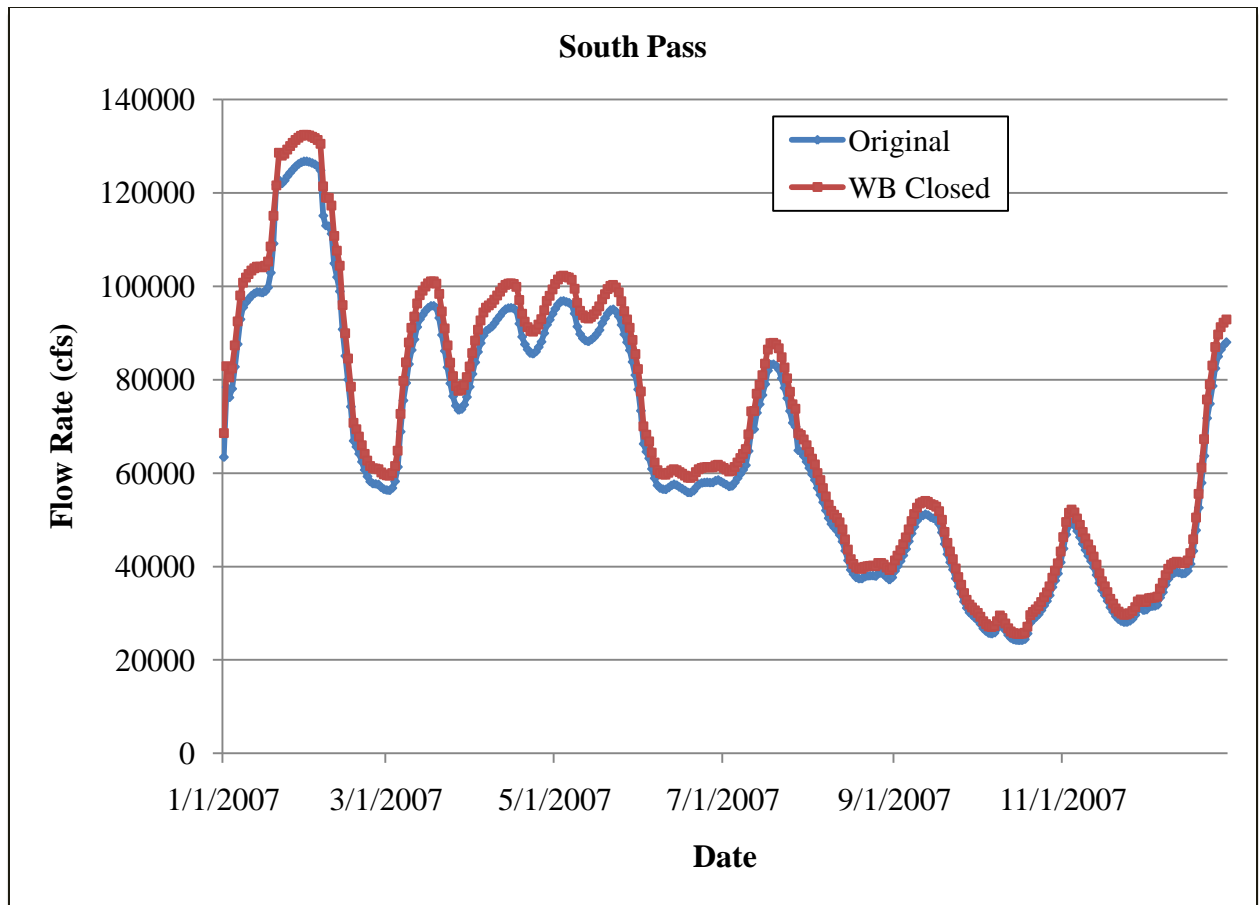
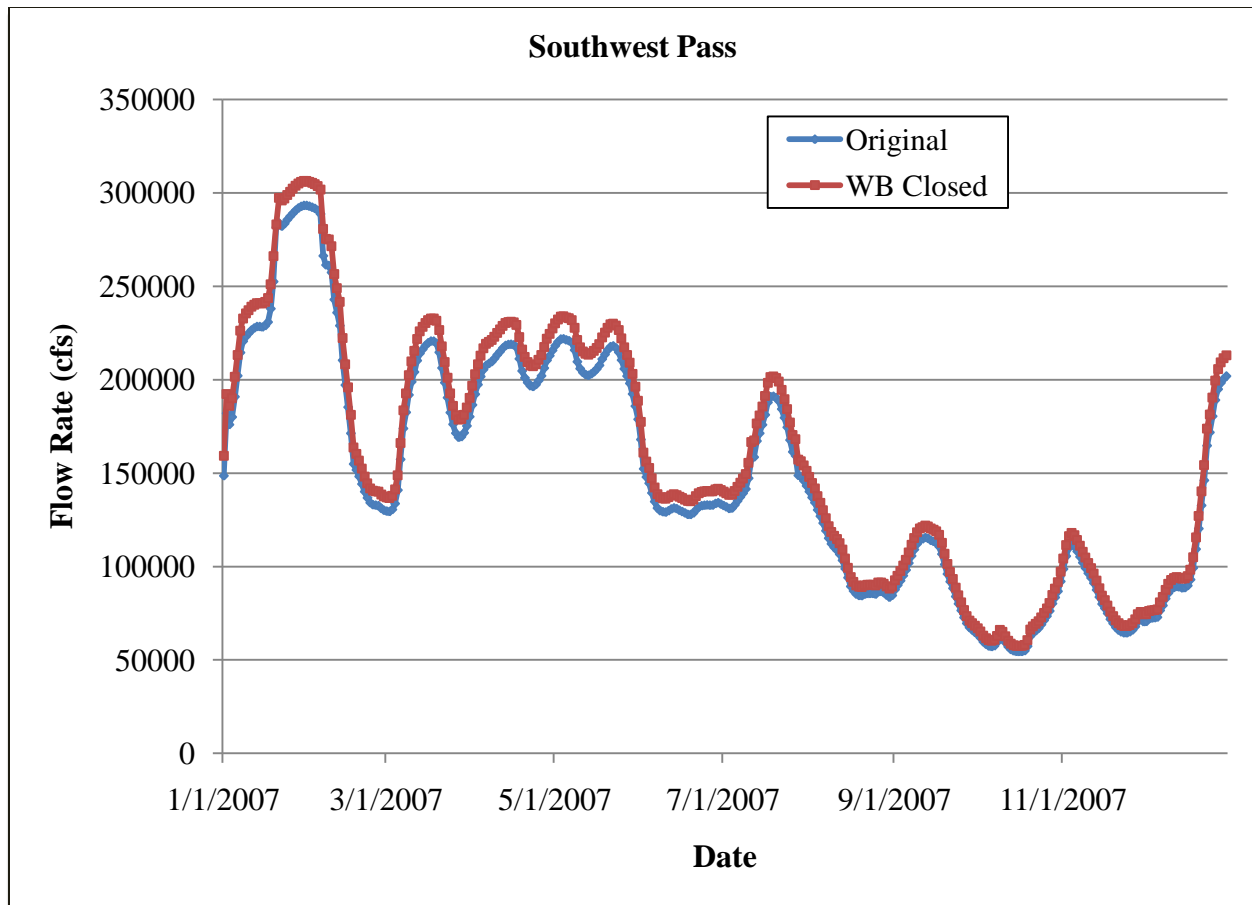


Figure 6-18: Flow Comparison for South Pass with West Bay Closed (2007\_WB).





**Figure 6-19: Flow Comparison for Southwest Pass with West Bay Closed (2007\_WB).**

The closure of West Bay caused the water that would ordinarily flow through West Bay to disperse amongst the passes, Fort St. Philip, and Bayou Lamoque North and South. Table 6-2 shows the average percent increase in flow that each channel received and the respective standard deviation.

**Table 6-2: Average Percent Increase in Flow to the Passes, Fort St. Philip, Bayou Lamoque North, and Bayou Lamoque South due to the Closure of West Bay (2007\_WB).**

Pass/Channel	Average Percent Increase	Standard Deviation
Baptiste Collette	4.00%	0.35%
Fort St. Philip	4.03%	0.86%
Grand Pass	4.12%	0.35%
Main Pass	5.85%	0.39%
Pass a Loutr�	5.98%	0.56%
South Pass	5.57%	1.16%
Southwest Pass	5.55%	0.35%
Bayou Lamoque North	1.97%	0.36%
Bayou Lamoque South	2.21%	0.30%

### 6.2.3 Changes to the Delta Distributaries Study

The Multiple Lines of Defense Strategy (MLODS) identifies several channel modifications to the passes. The three alternatives simulated were the closing of South Pass, the closing of Southwest Pass, and the closing of South and Southwest Passes and the dredging of Pass a Loutr . The West Bay channel was also removed for each of these simulations. For the closing of South Pass, a weir was added to the channel to prevent flow from entering. The weir was 50 ft long, 1500 ft wide, and was given an elevation of 1 ft (NAVD 88) and a weir coefficient of 2.6. Figure 6-20 shows the weir in South Pass. Table 6-3 shows the average percent increase in flow that each of the other passes and local channels received and the respective standard deviation of the closure of South Pass.

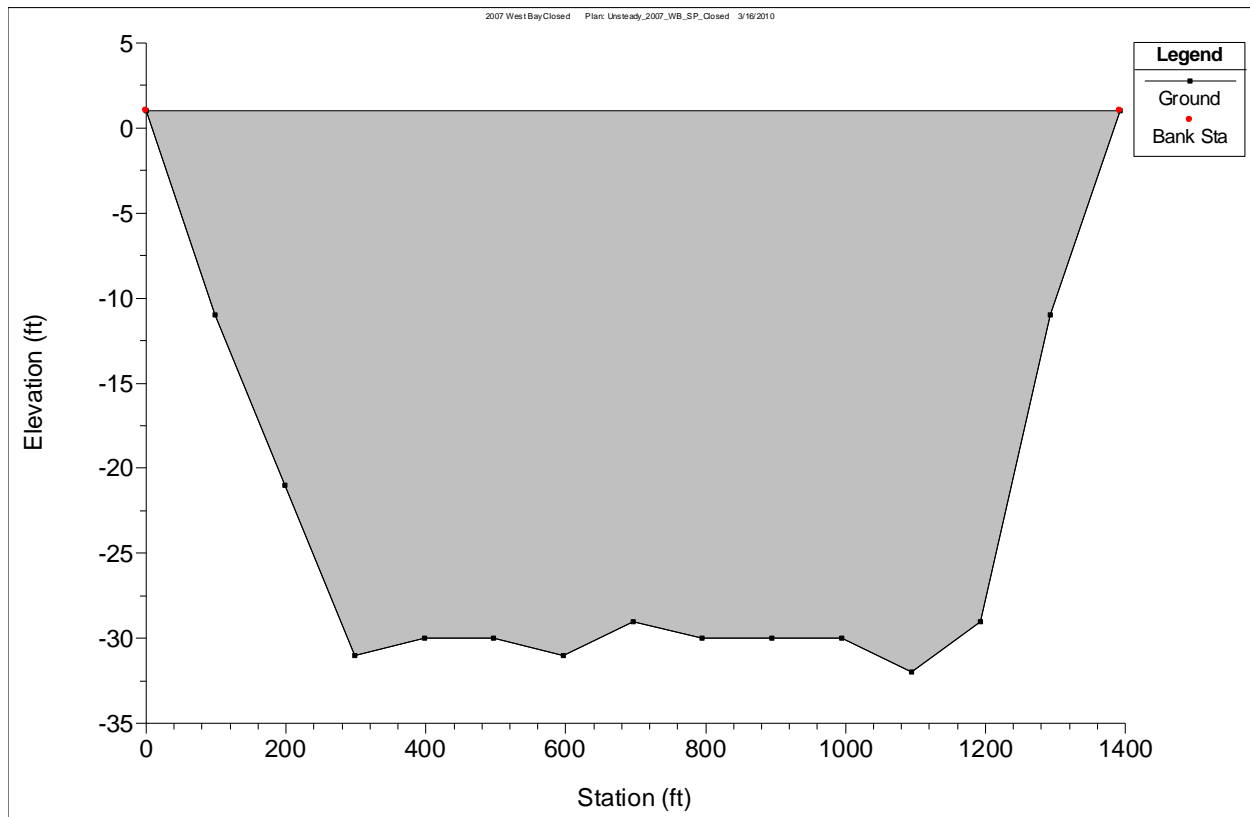
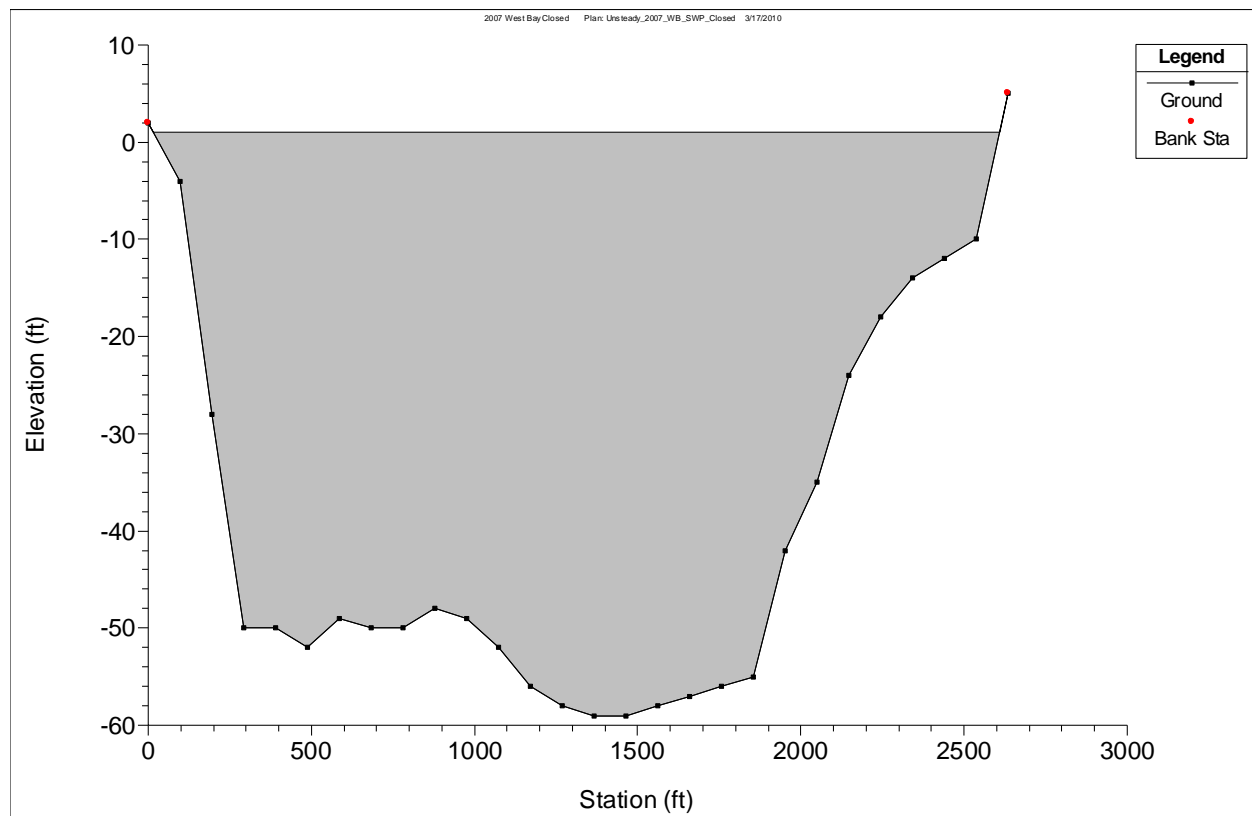


Figure 6-20: HEC-RAS Image of South Pass Closure Weir (2007\_WB\_SP).

**Table 6-3: Average Percent Increase in Flow to the Passes, Fort St. Philip, Bayou Lamoque North, and Bayou Lamoque South due to the Closure of South Pass and West Bay (2007\_WB\_SP).**

Pass	Average Percent Increase	Standard Deviation
Baptiste Collette	11.76%	0.84%
Fort St. Philip	12.61%	3.07%
Grand Pass	12.05%	0.86%
Main Pass	19.52%	0.74%
Pass a Loutr�	24.08%	1.26%
South Pass	-	-
Southwest Pass	21.79%	1.13%
Bayou Lamoque North	6.17%	1.00%
Bayou Lamoque South	7.19%	1.83%

Similar to the South Pass closure simulation, a weir was added to the Southwest Pass channel to prevent flow from entering. The weir was 20 ft long, 3000 ft wide, and was given an elevation of 1 ft (NAVD 88) and a weir coefficient of 2.6. Figure 6-21 shows the weir in Southwest Pass. Table 6-4 shows the average percent increase in flow that each of the other passes and local channels received and the respective standard deviation for the closure of Southwest Pass.



**Figure 6-21: HEC-RAS Image of Southwest Pass Closure Weir (2007\_WB\_SWP).**

**Table 6-4: Average Percent Increase in Flow to the Passes, Fort St. Philip, Bayou Lamoque North, and Bayou Lamoque South due to the Closure of Southwest Pass and West Bay (2007\_WB\_SWP).**

Pass	Average Percent Increase	Standard Deviation
Baptiste Collette	38.24%	3.85%
Fort St. Philip	45.17%	9.53%
Grand Pass	39.08%	3.91%
Main Pass	61.45%	3.19%
Pass a Loutr�	74.65%	4.20%
South Pass	65.85%	4.87%
Southwest Pass	-	-
Bayou Lamoque North	20.69%	2.27%
Bayou Lamoque South	24.03%	3.17%

For the last two simulations with South and Southwest Passes closed, the Pass a Loutr  channel was dredged to -50 ft and -40 ft (NAVD 88). Tables 6-5 and 6-6 show the average percent increase in flow that each of the other passes and local channels received and the respective standard deviation for the closure of South and Southwest Passes and the dredging of Pass a Loutr  to -50 ft and -40 ft, respectively.

**Table 6-5: Average Percent Increase in Flow to the Passes, Fort St. Philip, Bayou Lamoque North, and Bayou Lamoque South due to the Closure of South Pass, Southwest Pass, and West Bay and the Dredging of Pass a Loutr  to -50 ft (2007\_WB\_SP\_SWP\_pal50).**

Pass	Average Percent Increase	Standard Deviation
Baptiste Collette	-15.59%	0.62%
Fort St. Philip	-14.24%	2.72%
Grand Pass	-16.10%	0.64%
Main Pass	-31.10%	0.71%
Pass a Loutr� (dredged to -50 ft)	810.19%	42.31%
South Pass	-	-
Southwest Pass	-	-
Bayou Lamoque North	-7.31%	1.03%
Bayou Lamoque South	-8.38%	0.92%

**Table 6-6: Average Percent Increase in Flow to the Passes, Fort St. Philip, Bayou Lamoque North, and Bayou Lamoque South due to the Closure of South Pass, Southwest Pass, and West Bay and the Dredging of Pass a Loutr  to -40 ft (2007\_WB\_SP\_SWP\_pal40).**

Pass	Average Percent Increase	Standard Deviation
Baptiste Collette	-6.61%	0.37%
Fort St. Philip	-6.29%	1.36%
Grand Pass	-6.82%	0.38%
Main Pass	-13.27%	0.49%
Pass a Loutr� (dredged to -40 ft)	750.30%	38.57%
South Pass	-	-
Southwest Pass	-	-
Bayou Lamoque North	-3.13%	0.63%
Bayou Lamoque South	-3.46%	0.89%

#### ***6.2.4 Proposed Diversions Study***

The first simulation for the MLODS proposed diversions was 2007\_WB\_B, which includes a channel at Buras (RM 24.9). The proposed diversion is an uncontrolled crevasse-type diversion similar to the West Bay Sediment Diversion. Therefore, the West Bay channel cross-sections were copied and widened to a width of 2000 cfs because the target discharge of 59,900 cfs is over twice the amount of the West Bay Sediment Diversion design discharge of 25,000 cfs. Also, a wide cross-section with inline storage was designed and copied to capture and transmit the target flow along a length of 45,000 ft, which is the distance from Buras to Barataria Bay. Figure 6-22 shows the wide cross-section for the Buras channel. The diversion was kept open for the entire calendar year of 2007. Figures 6-23, 6-24, and 6-25 compare the stage at Baton Rouge (RM 228.4), Carrollton (RM 102.8), and Venice (RM 10.7), respectively, for 2007\_WB\_B and 2007\_WB. Table 6-7 shows the mean and max difference in stage from the previous simulation (2007\_WB) at the comparison gages for the addition of the Buras Diversion.

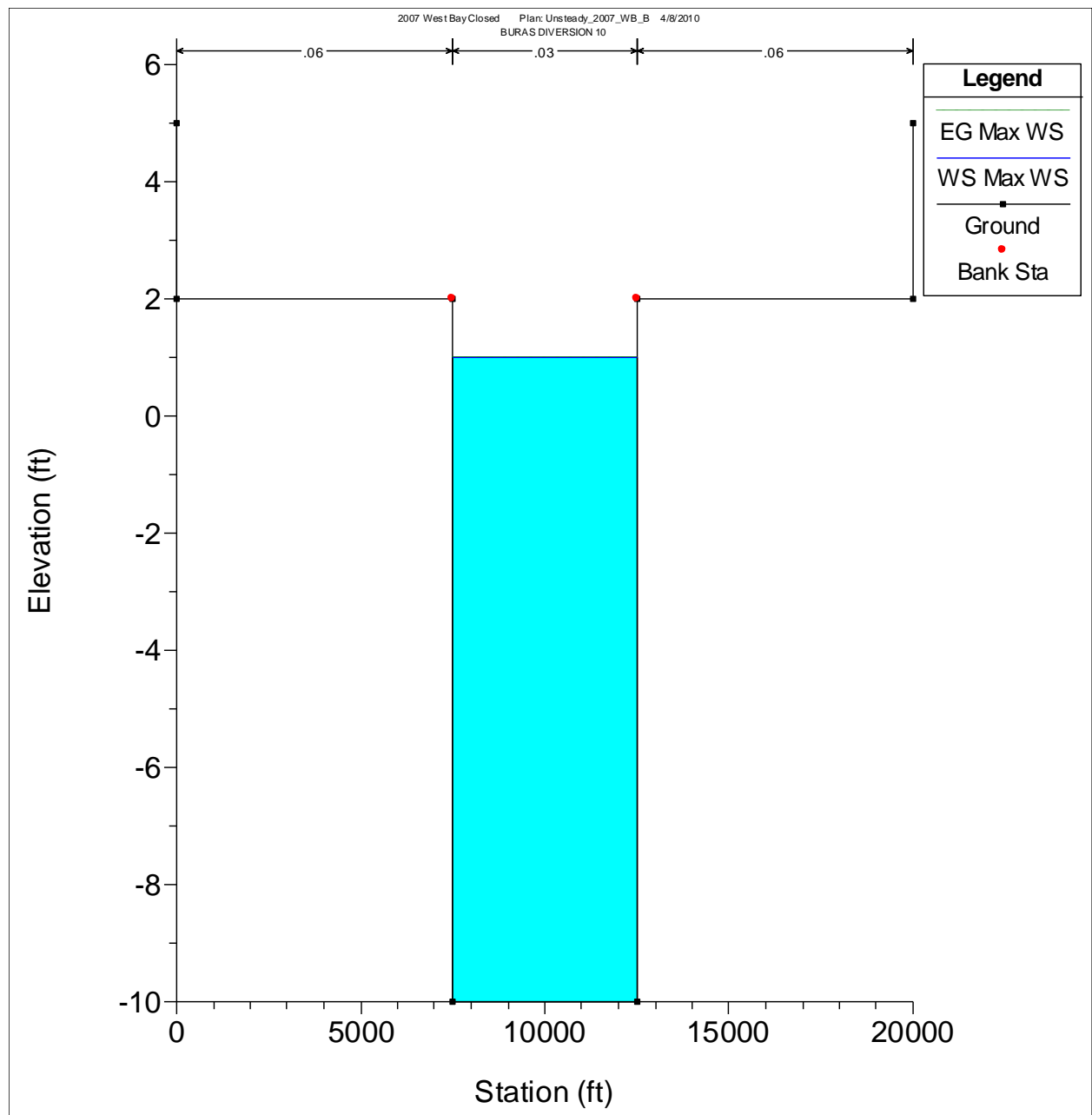
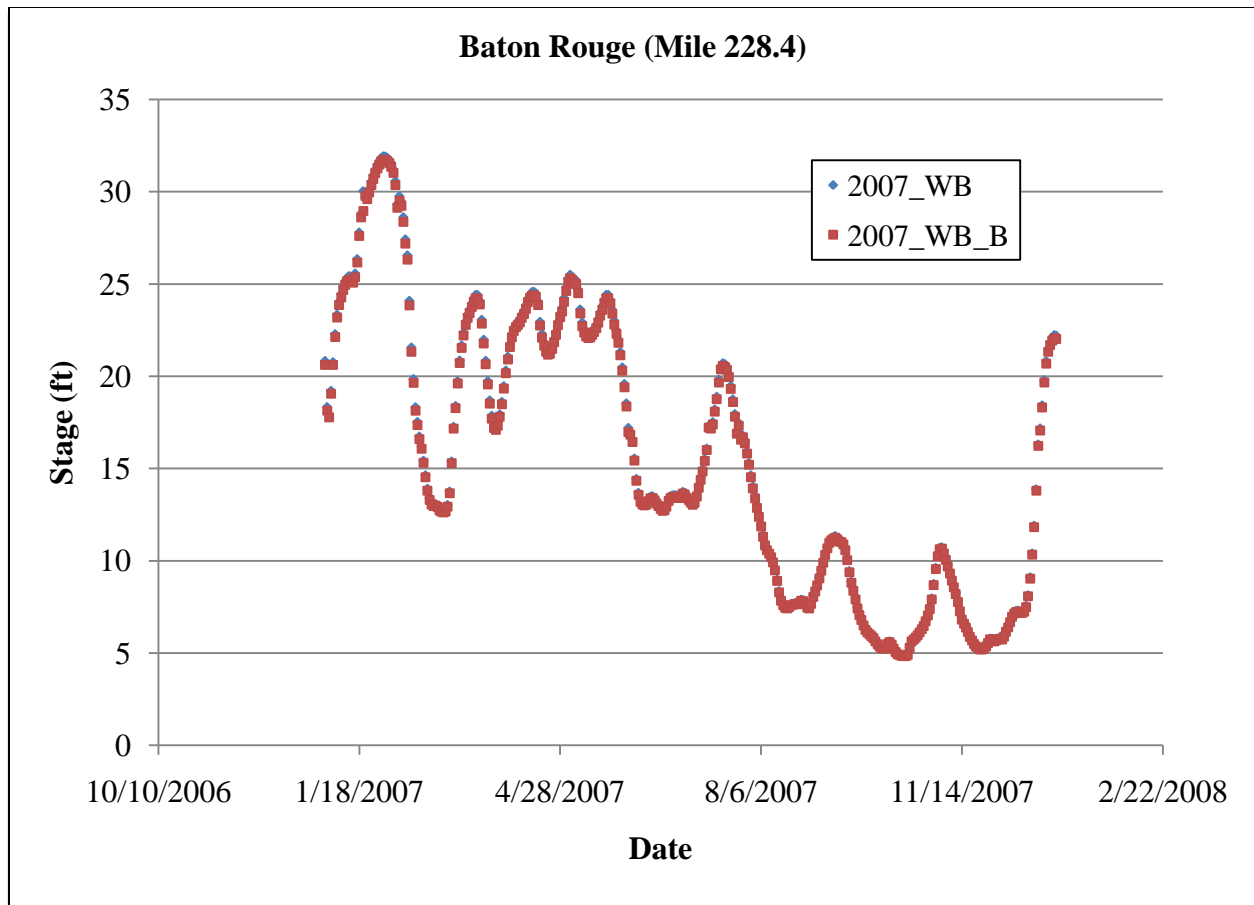
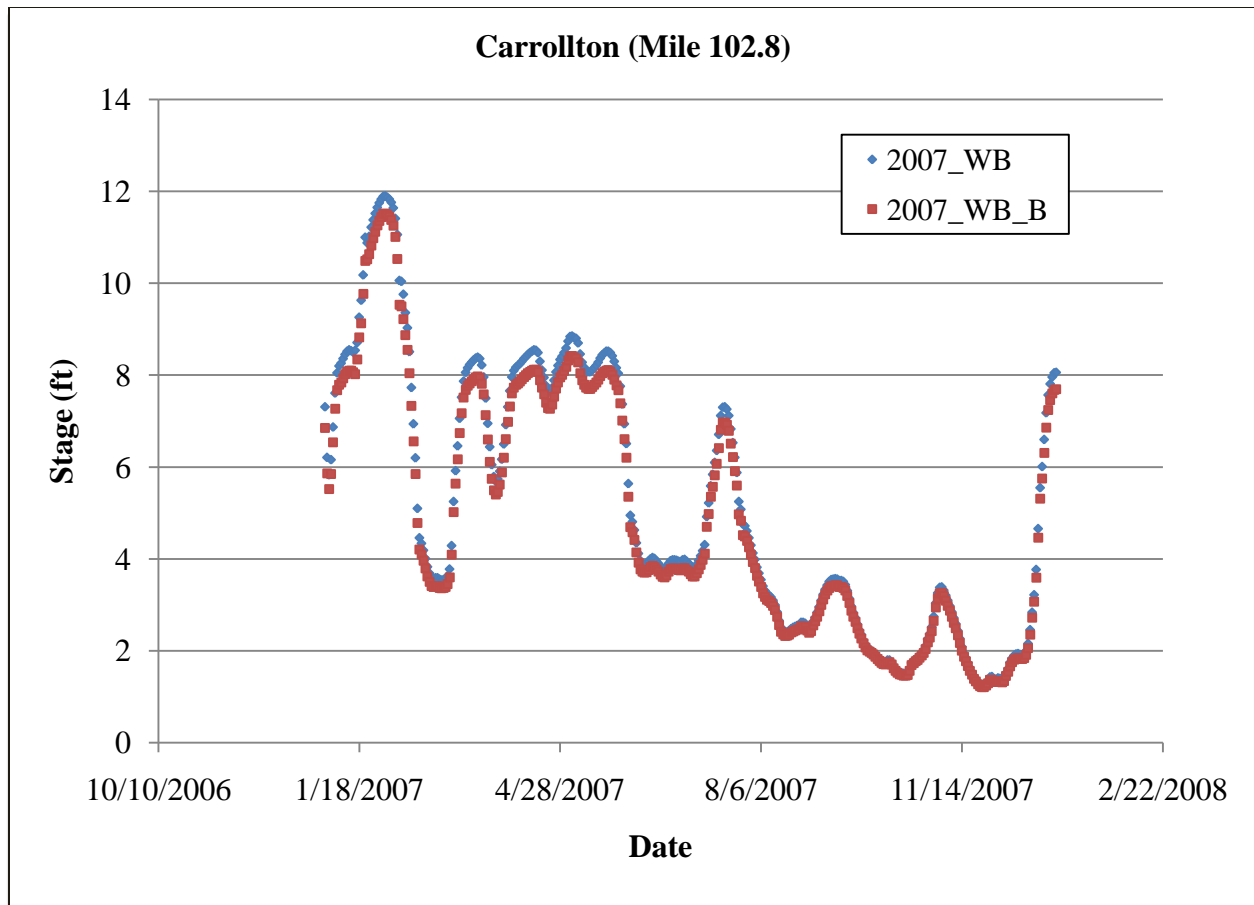


Figure 6-22: HEC-RAS Image of Wide Cross-section for Buras Channel (RS 1).



**Figure 6-23: Stage Comparison at Baton Rouge for the Addition of the Buras Diversion (2007\_WB\_B).**



**Figure 6-24: Stage Comparison at Carrollton for the Addition of the Buras Diversion (2007\_WB\_B).**



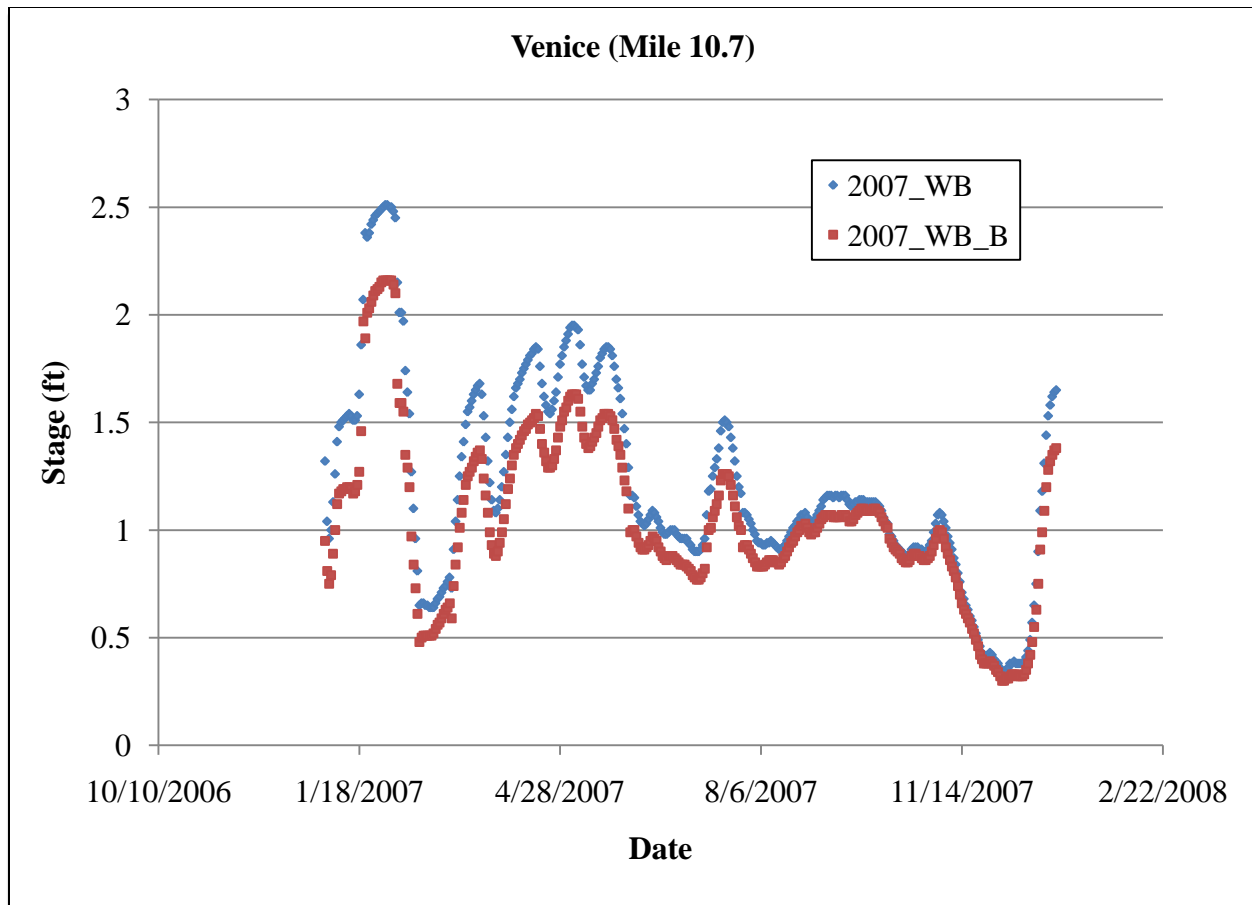


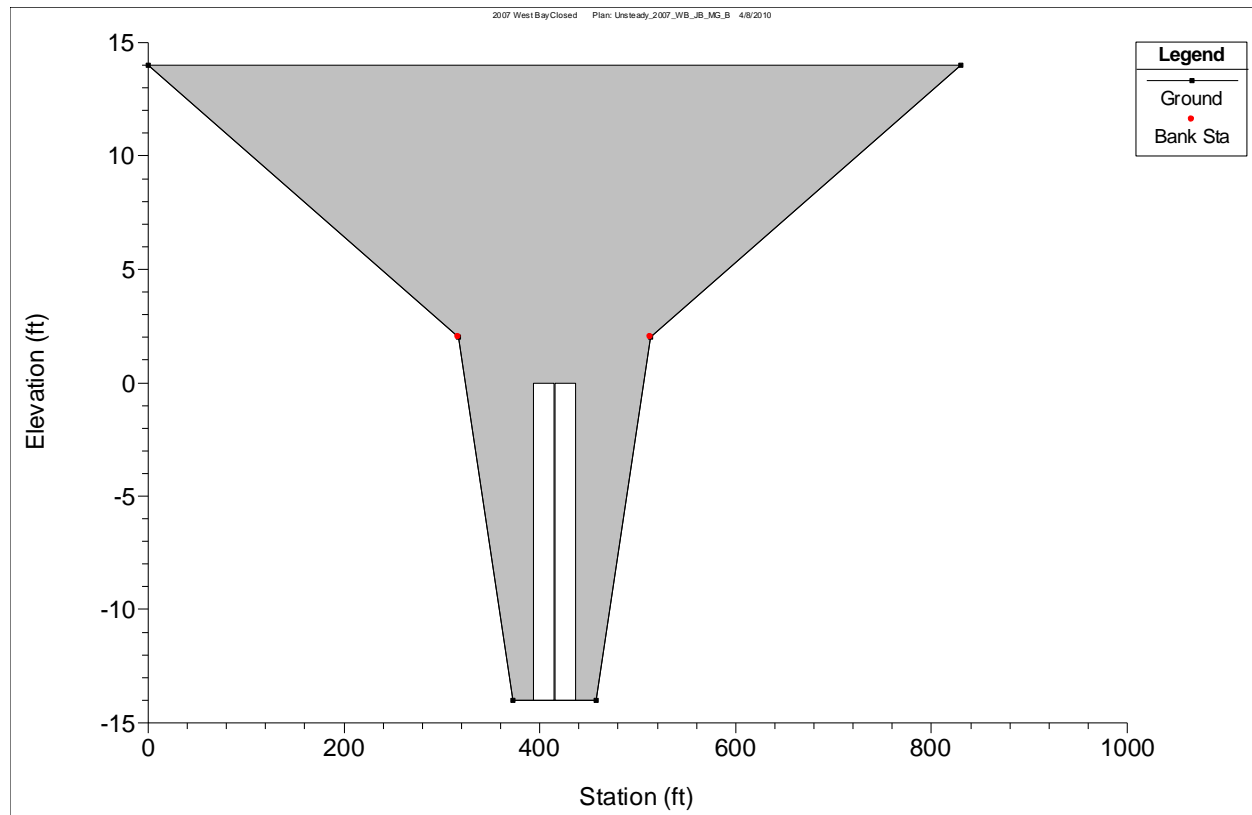
Figure 6-25: Stage Comparison at Venice for the Addition of the Buras Diversion (2007\_WB\_B).

Table 6-7: Mean and Max Difference in Stage for the Addition of the Buras Diversion at the Comparison Gages (2007\_WB\_B vs. 2007\_WB).

Parameter / Gage	Baton Rouge	Donaldsonville	North of Bonnet Carré	Bonnet Carré	Carrollton	West Pointe a la Hache	Venice
Mean Stage Difference (ft)	-0.12	-0.18	-0.21	-0.21	-0.23	-0.26	-0.17
Max Stage Difference (ft)	-1.08	-1.13	-0.48	-0.49	-0.54	-0.63	-0.49

The second simulation for the MLODS proposed diversions was 2007\_WB\_JB\_B, which includes a channel at Buras (RM 24.9), and a channel and gated structure at Jesuit Bend (RM 68). The proposed diversion at Jesuit Bend is a gated spillway similar to the diversion at Davis Pond. Therefore, the Davis Pond channel cross-sections were copied. Also, a weir was designed with a width of 830 ft, an elevation of 14 ft (NAVD 88), a length of 50 ft, and a weir coefficient of 2.6. Two gates with a width of 20 ft, a height of 14 ft, an invert of -14 ft (NAVD 88), a sluice discharge coefficient of 0.5, a submerged orifice coefficient of 0.8 (typical), and an overflow weir coefficient of 3 were entered to capture the target discharge of 5,000 cfs. The pier width

between the gates was set at 2 ft. Figure 6-26 shows the gated structure for the Jesuit Bend Diversion. The gates were given an opening height of 14 ft (open) from January 2007 to July 2007 and a gate height of 0 ft (closed) from July 2007 to January 2008, according to design specifications. Figures 6-27, 6-28, and 6-29 compare the stage at Baton Rouge, Carrollton, and Venice, respectively, for 2007\_WB\_JB\_B, 2007\_WB\_B, and 2007\_WB. Table 6-8 shows the mean and max difference in stage from the previous simulation (2007\_WB\_B) at the comparison gages for the addition of the Jesuit Bend Diversion.



**Figure 6-26: HEC-RAS Image of Jesuit Bend Diversion Structure.**

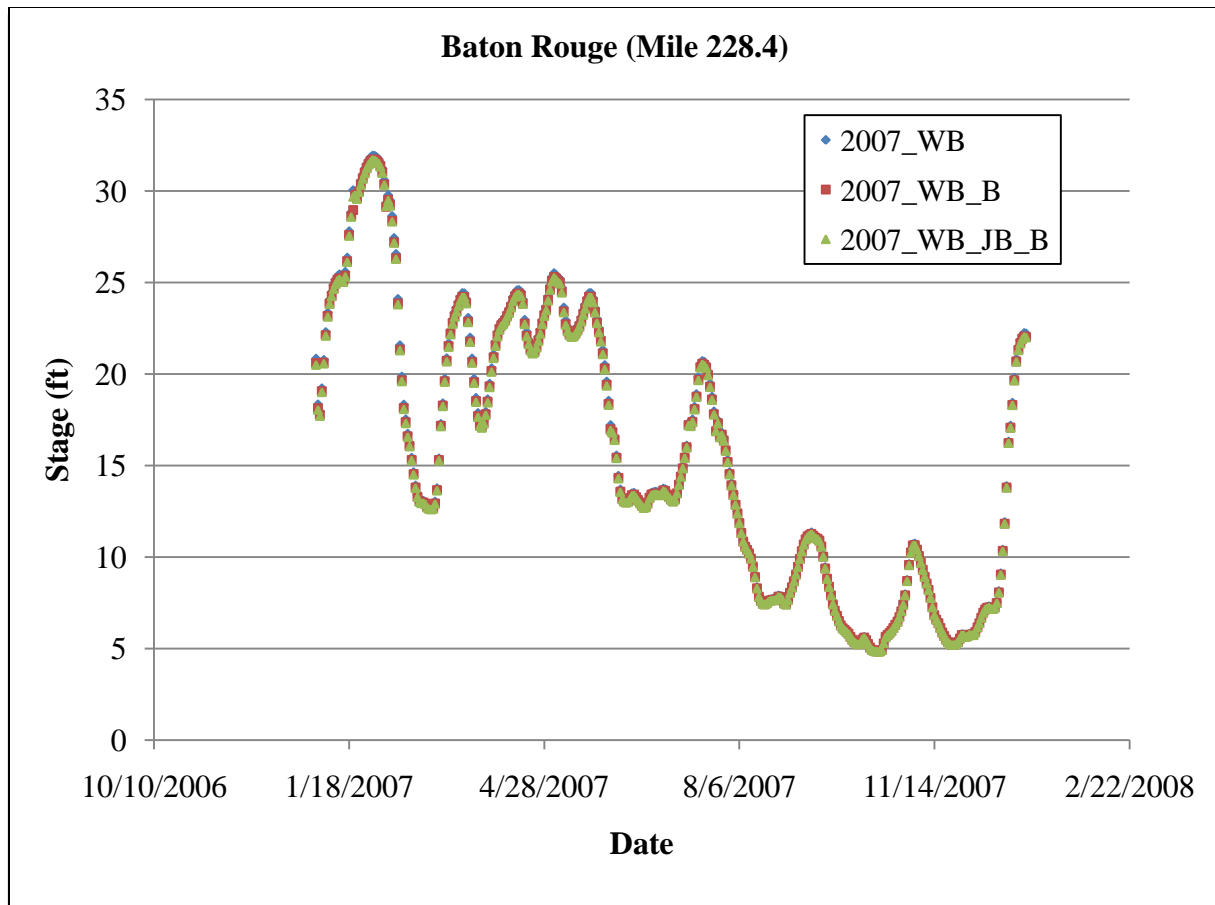


**Figure 6-27: Stage Comparison at Baton Rouge for the Addition of the Jesuit Bend Diversion (2007\_WB\_JB\_B).**

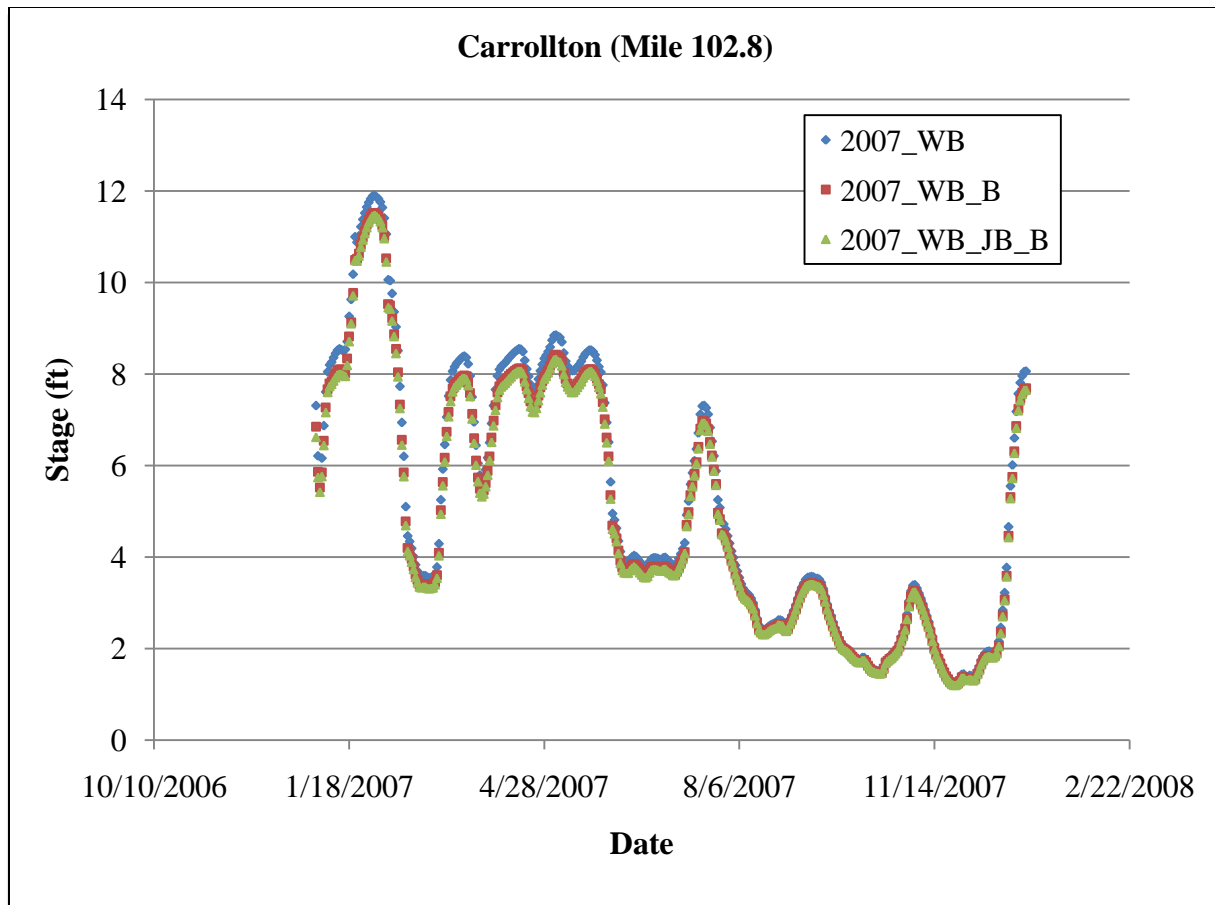


**Figure 6-28: Stage Comparison at Carrollton for the Addition of the Jesuit Bend Diversion (2007\_WB\_JB\_B).**

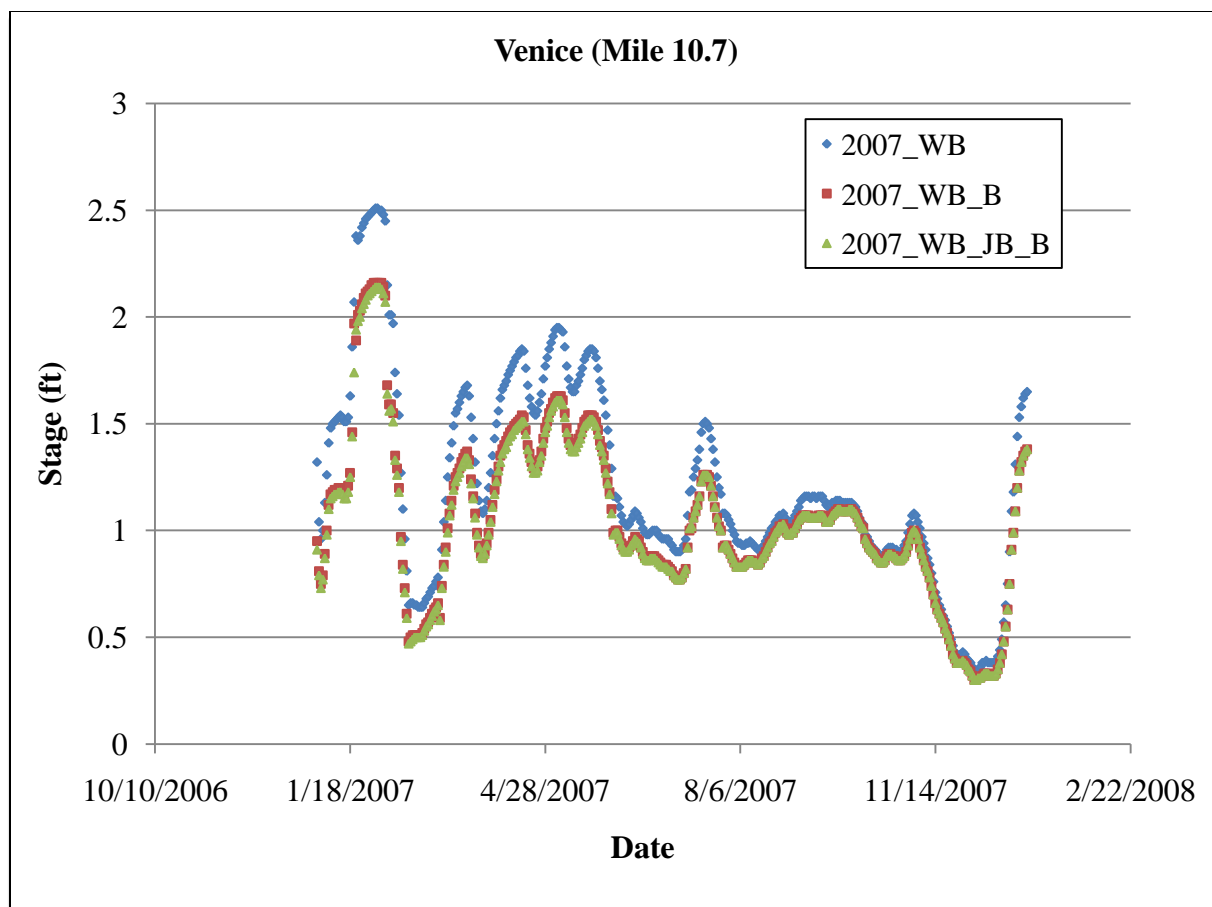


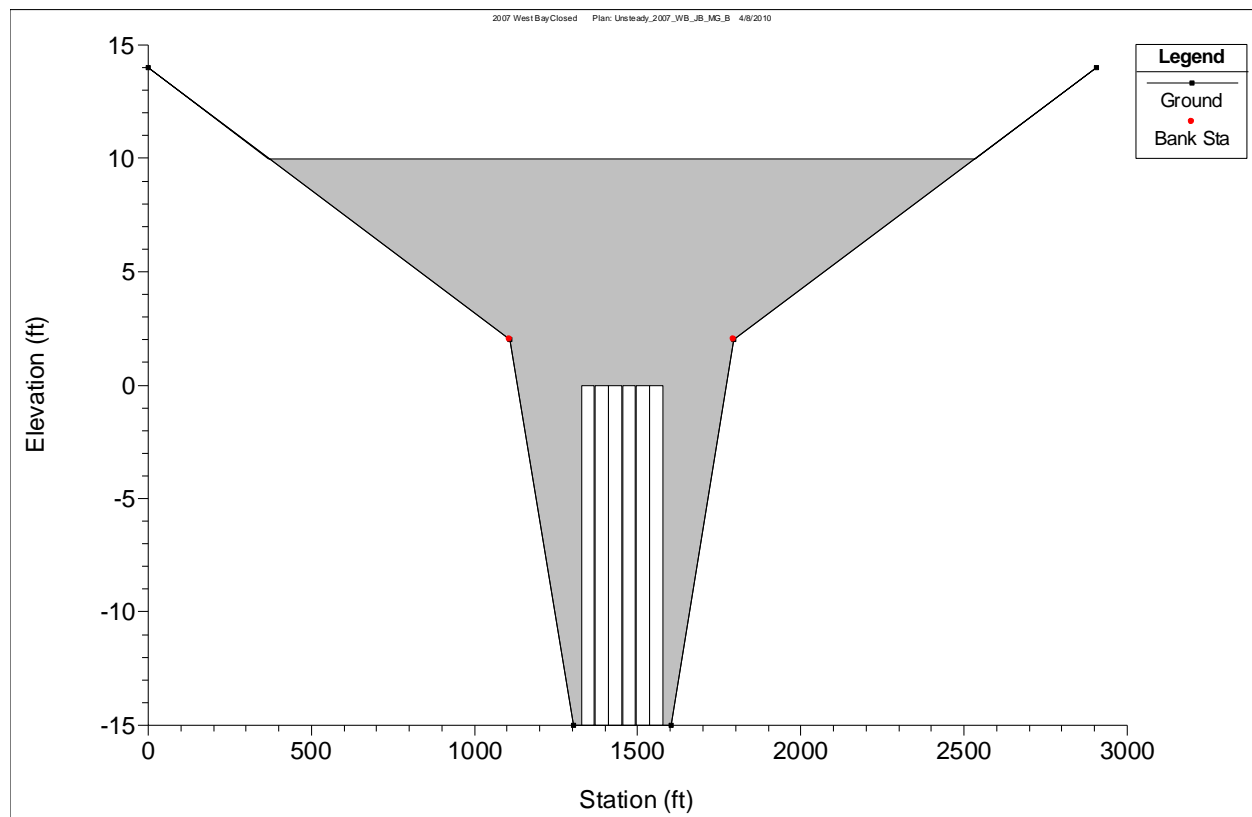
Figure 6-29: Stage Comparison at Venice for the Addition of the Jesuit Bend Diversion (2007\_WB\_JB\_B).

Table 6-8: Mean and Max Difference in Stage for the Addition of the Jesuit Bend Diversion at the Comparison Gages (2007\_WB\_JB\_B vs. 2007\_WB\_B).

Parameter / Gage	Baton Rouge	Donaldsonville	North of Bonnet Carré	Bonnet Carré	Carrollton	West Pointe a la Hache	Venice
Mean Stage Difference (ft)	-0.02	-0.03	-0.04	-0.04	-0.05	-0.02	-0.01
Max Stage Difference (ft)	-0.73	-0.14	-0.11	-0.11	-0.15	-0.37	-0.23

The third simulation for the MLODS proposed diversions was 2007\_WB\_JB\_MG\_B, which includes a channel at Buras (RM 24.9), and channels and gated structures at Jesuit Bend (RM 68) and Myrtle Grove (RM 59.3). The proposed diversion at Myrtle Grove is a gated spillway which is also similar to the diversion at Davis Pond. Therefore, the Davis Pond channel cross-sections were copied and multiplied by a factor of 3.5 to increase the channel capacity. These cross-sections replaced the original cross-sections of Wilkinson Canal Reaches 1 and 2. Also, a weir was designed with a width of 2905 ft, an elevation of 12 ft (NAVD 88), a length of 50 ft, and a weir coefficient of 2.6. Six gates with a width of 40 ft, a height of 15 ft, an invert of -15 ft

(NAVD 88), a sluice discharge coefficient of 0.5, a submerged orifice coefficient of 0.8 (typical), and an overflow weir coefficient of 3 were entered to capture the target discharge of 20,000 cfs. The pier width between the gates was set at 2 ft. Figure 6-30 shows the gated structure for the Myrtle Grove Diversion. The gates were given an opening height of 15 ft (open) from January 2007 to July 2007 and a gate height of 0 ft (closed) from July 2007 to January 2008, according to design specifications. Figures 6-31, 6-32, and 6-33 compare the stage at Baton Rouge, Carrollton, and Venice, respectively, for 2007\_WB\_JB\_MG\_B, 2007\_WB\_JB\_B, 2007\_WB\_B, and 2007\_WB. Table 6-9 shows the mean and max difference in stage from the previous simulation (2007\_WB\_JB\_B) at the comparison gages for the addition of the Myrtle Grove Diversion.



**Figure 6-30: HEC-RAS Image of Myrtle Grove Diversion Structure.**

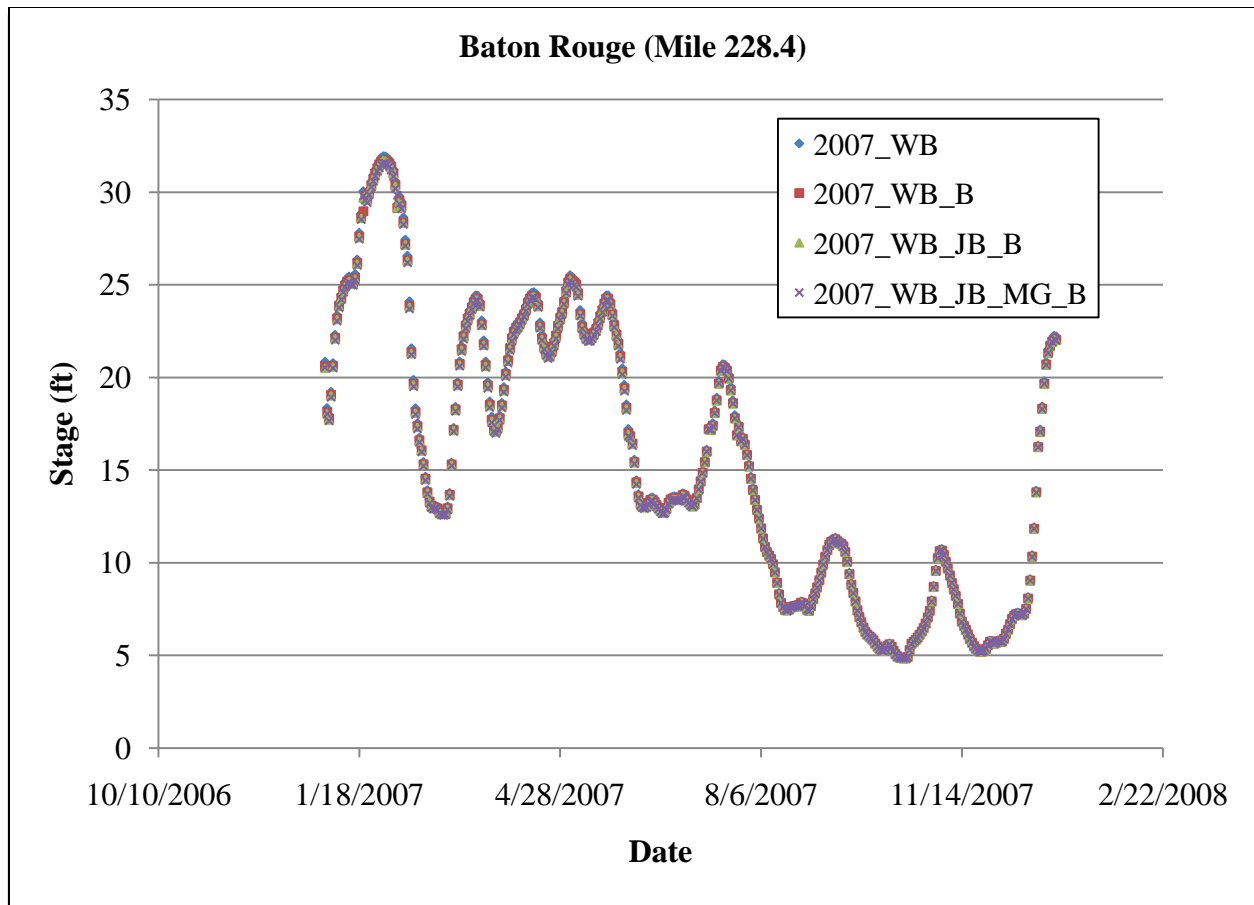


**Figure 6-31: Stage Comparison at Baton Rouge for the Addition of the Myrtle Grove Diversion (2007\_WB\_JB\_MG\_B).**

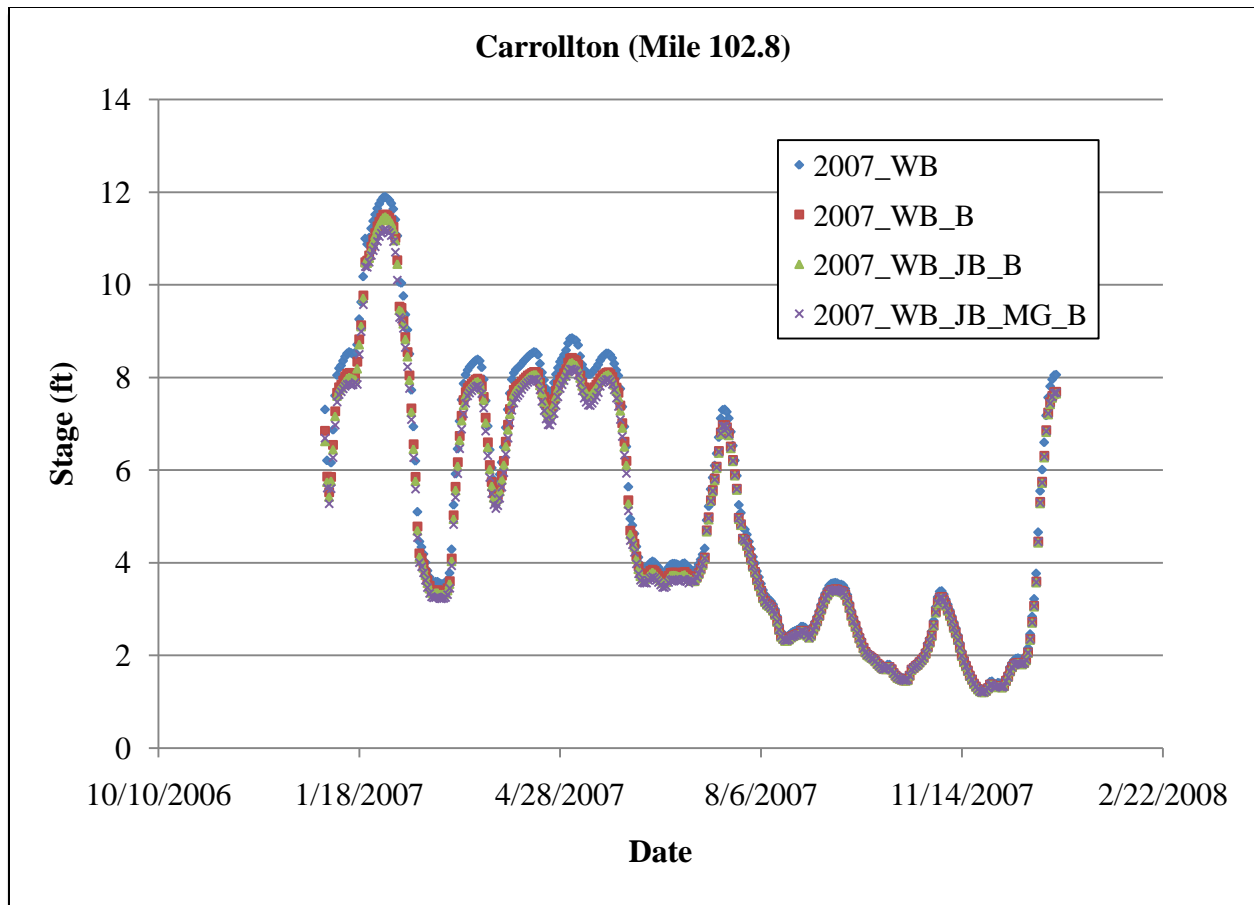


**Figure 6-32: Stage Comparison at Carrollton for the Addition of the Myrtle Grove Diversion (2007\_WB\_JB\_MG\_B).**



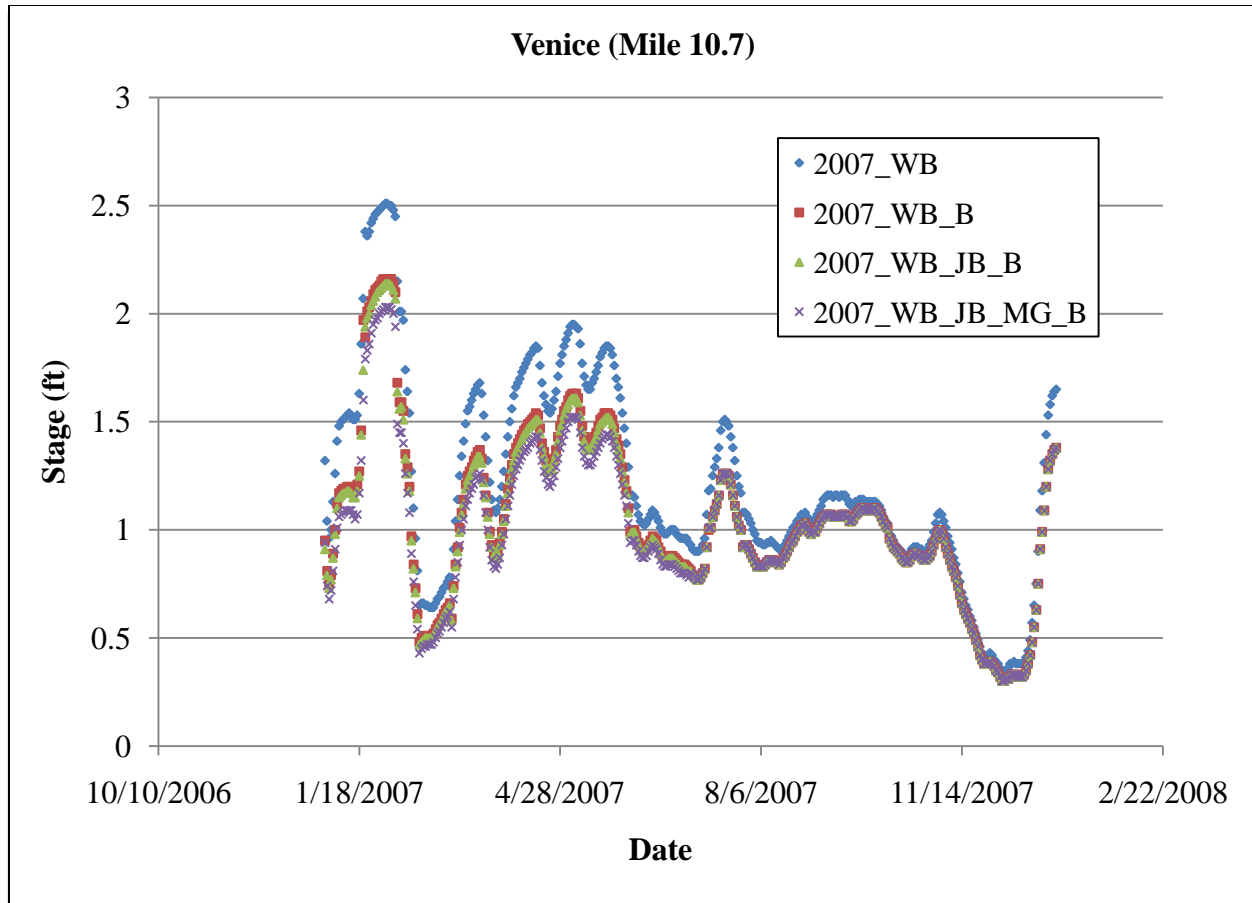


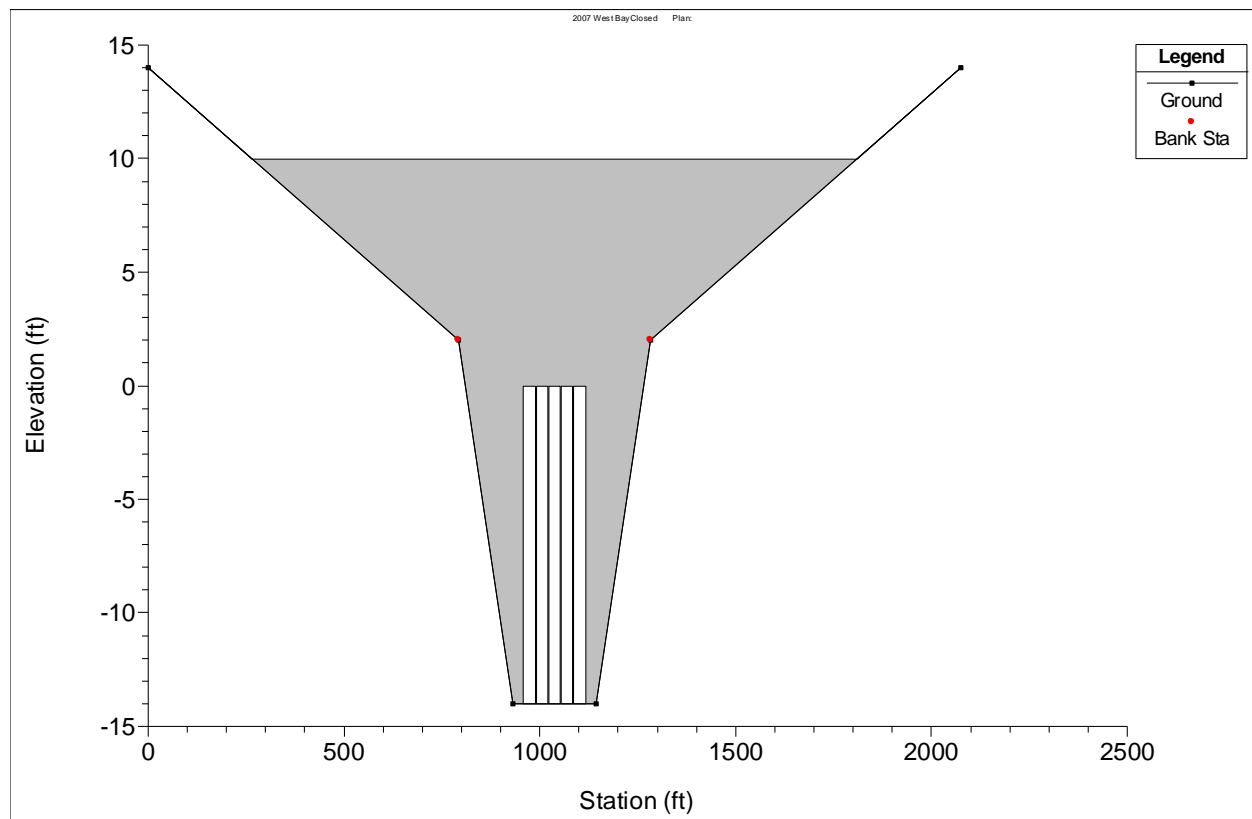
Figure 6-33: Stage Comparison at Venice for the Addition of the Myrtle Grove Diversion (2007\_WB\_JB\_MG\_B).

Table 6-9: Mean and Max Difference in Stage for the Addition of the Myrtle Grove Diversion at the Comparison Gages (2007\_WB\_JB\_MG\_B vs. 2007\_WB\_JB\_B).

Parameter / Gage	Baton Rouge	Donaldsonville	North of Bonnet Carré	Bonnet Carré	Carrollton	West Pointe a la Hache	Venice
Mean Stage Difference (ft)	-0.03	-0.05	-0.06	-0.06	-0.07	-0.08	-0.03
Max Stage Difference (ft)	-0.66	-0.27	-0.26	-0.27	-0.35	-0.58	-0.15

The fourth simulation for the MLODS proposed diversions was 2007\_WB\_JB\_MG\_DR\_B, which includes a channel at Buras (RM 24.9), and channels and gated structures at Jesuit Bend (RM 68), Myrtle Grove (RM 59.3), and Deer Range (RM 53.9). The proposed diversion at Deer Range is a gated spillway similar to the diversion at Davis Pond. Therefore, the Davis Pond channel cross-sections were copied and multiplied by a factor of 2.5 to increase the channel capacity. Also, a weir was designed with a width of 2075 ft, an elevation of 10 ft (NAVD 88), a length of 50 ft, and a weir coefficient of 2.6. Five gates with a width of 30 ft, a height of 14 ft, an

invert of -14 ft (NAVD 88), a sluice discharge coefficient of 0.5, a submerged orifice coefficient of 0.8 (typical), and an overflow weir coefficient of 3 were entered to capture the target discharge of 10,000 cfs. The pier width between the gates was set at 2 ft. Figure 6-34 shows the gated structure for the Deer Range Diversion. The gates were given an opening height of 14 ft (open) from January 2007 to July 2007 and a gate height of 0 ft (closed) from July 2007 to January 2008, according to design specifications. Figures 6-35, 6-36, and 6-37 compare the stage at Baton Rouge, Carrollton, and Venice, respectively, for 2007\_WB\_JB\_MG\_DR\_B, 2007\_WB\_JB\_MG\_B, 2007\_WB\_JB\_B, 2007\_WB\_B, and 2007\_WB. Table 6-10 shows the mean and max difference in stage from the previous simulation (2007\_WB\_JB\_MG\_B) at the comparison gages for the addition of the Deer Range Diversion.



**Figure 6-34: HEC-RAS Image of Deer Range Diversion Structure.**

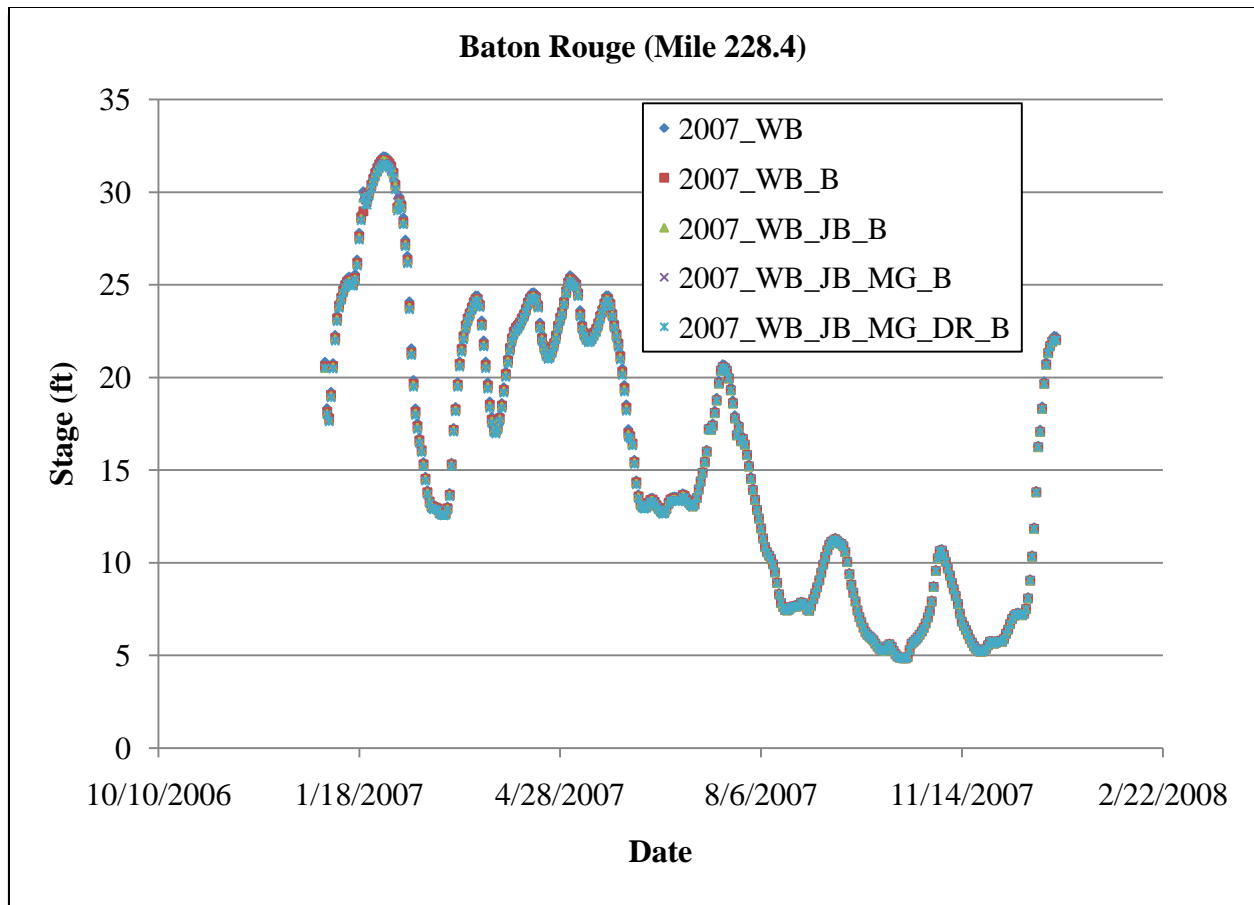


**Figure 6-35: Stage Comparison at Baton Rouge for the Addition of the Deer Range Diversion (2007\_WB\_JB\_MG\_DR\_B).**

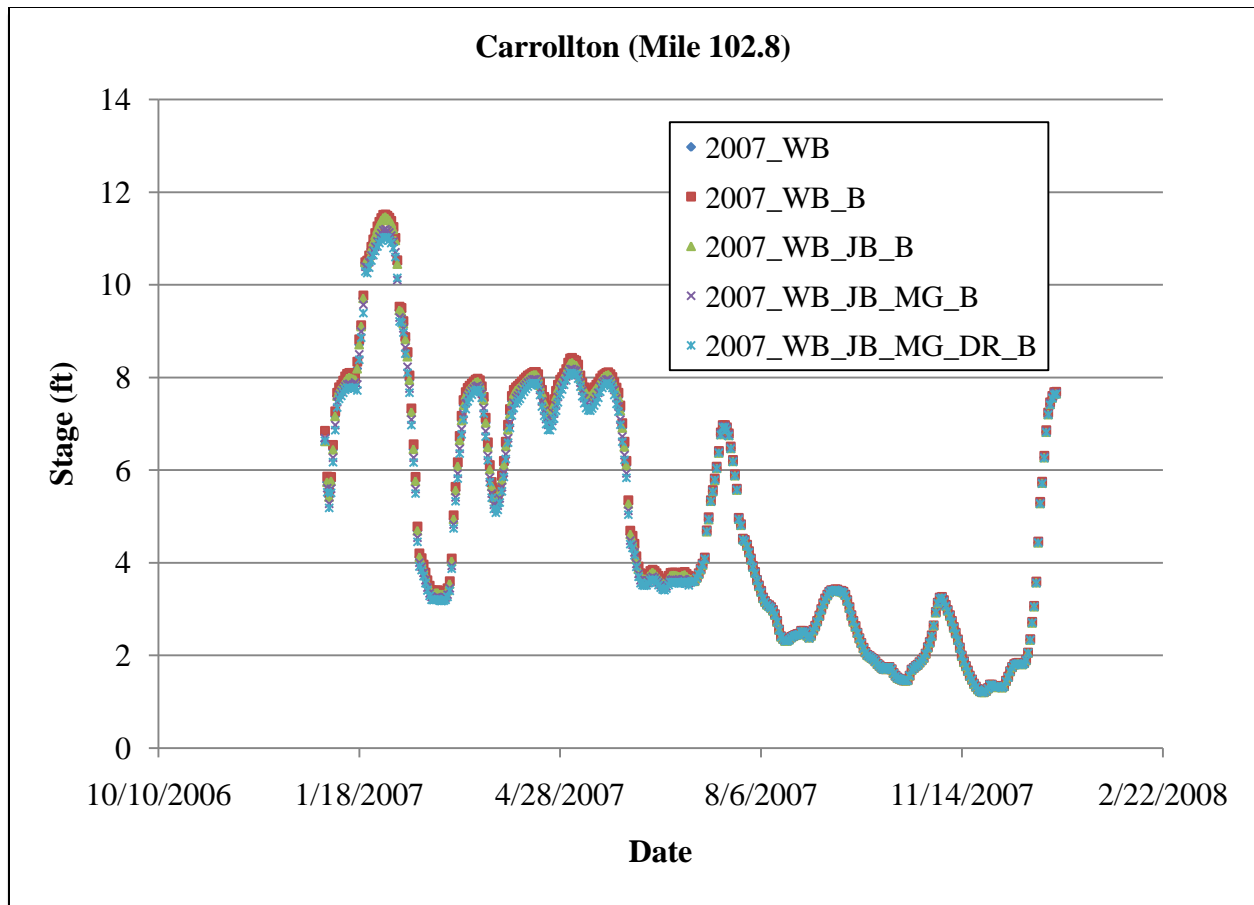


**Figure 6-36: Stage Comparison at Carrollton for the Addition of the Deer Range Diversion (2007\_WB\_JB\_MG\_DR\_B).**

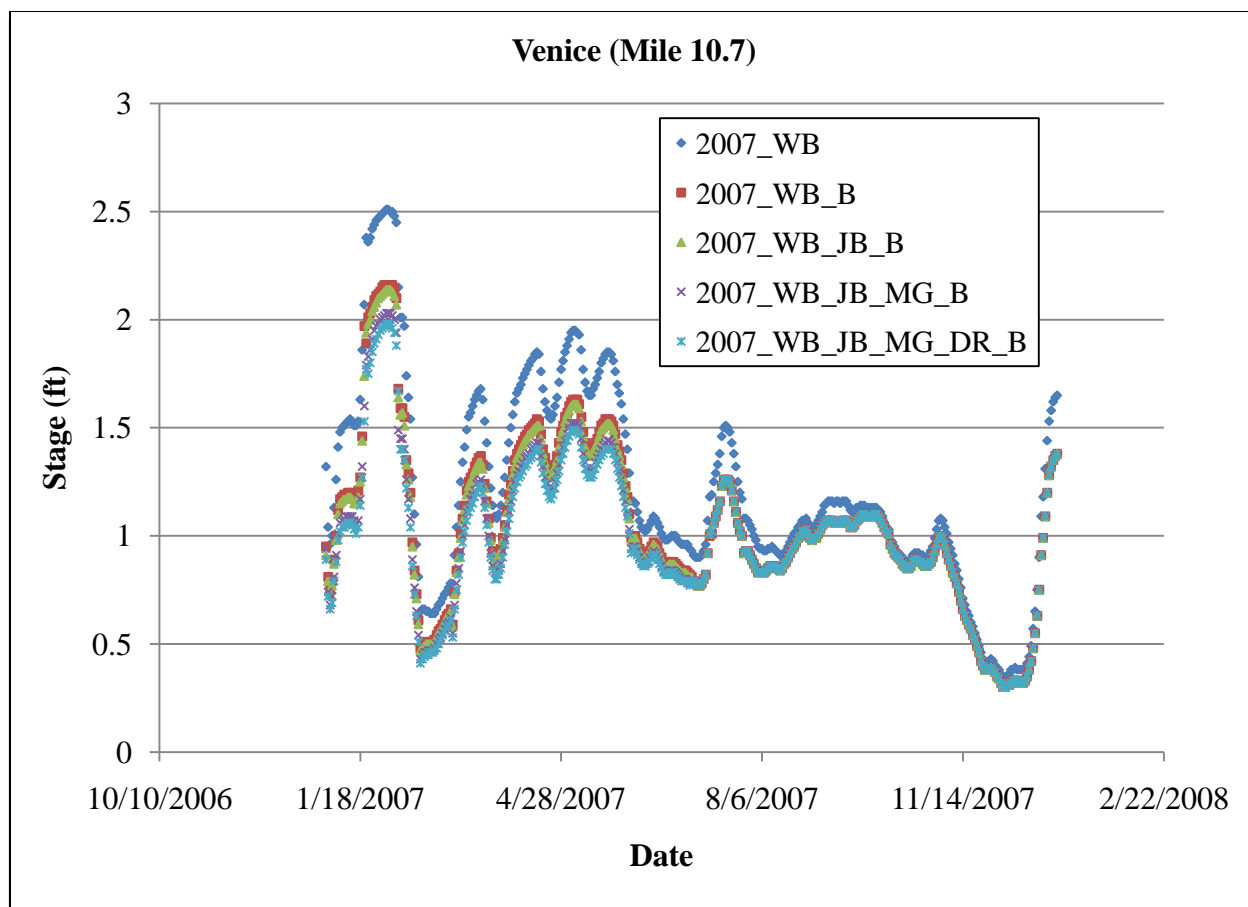


Figure 6-37: Stage Comparison at Venice for the Addition of the Deer Range Diversion (2007\_WB\_JB\_MG\_DR\_B).

Table 6-10: Mean and Max Difference in Stage for the Addition of the Deer Range Diversion at the Comparison Gages (2007\_WB\_JB\_MG\_DR\_B vs. 2007\_WB\_JB\_MG\_B).

Parameter / Gage	Baton Rouge	Donaldsonville	North of Bonnet Carré	Bonnet Carré	Carrollton	West Pointe a la Hache	Venice
Mean Stage Difference (ft)	-0.03	-0.04	-0.05	-0.05	-0.05	-0.03	-0.01
Max Stage Difference (ft)	-0.84	-1.07	-0.15	-0.16	-0.18	-0.45	-0.18

### 6.2.5 Proposed Diversions Combined with Changes to the Delta Distributaries Study

The first simulation with the MLODS proposed diversions and channel modifications was 2007\_Div\_SP, which includes the diversions at Buras, Jesuit Bend, Myrtle Grove, and Deer Range, and the weir in South Pass to close off the flow to that channel. Figures 6-38, 6-39, and 6-40 compare the stage at Baton Rouge, Carrollton, and Venice, respectively, for 2007\_WB\_JB\_MG\_DR\_B vs. 2007\_WB\_Div\_SP. Table 6-11 shows the mean and max

difference in stage at the comparison gages for the closure of South Pass and the addition of the proposed diversions. Table 6-12 shows the average percent increase in flow to the passes, Fort St. Philip, Bayou Lamoque North, and Bayou Lamoque South at the comparison gages.

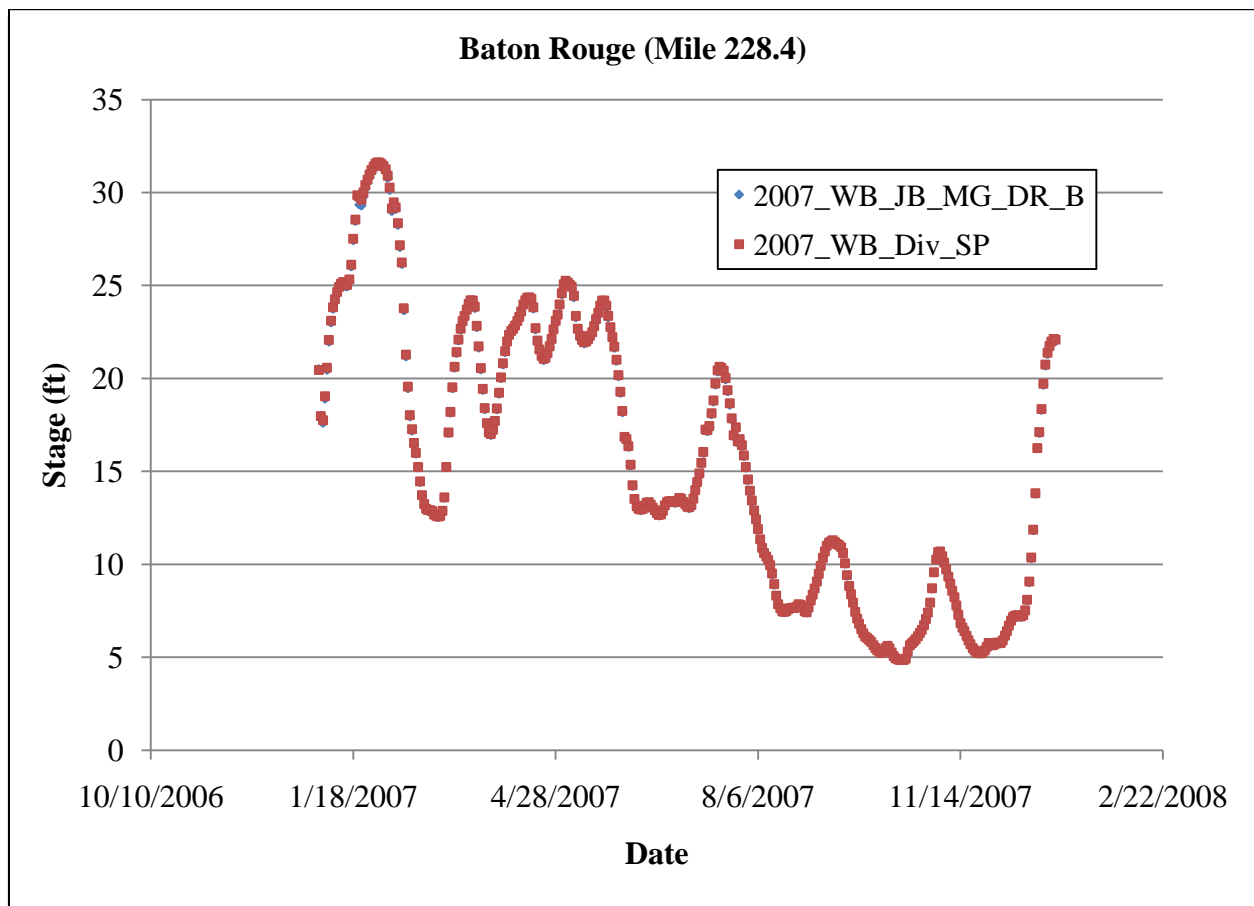


**Figure 6-38: Stage Comparison at Baton Rouge for the Closure of South Pass and the Addition of the Proposed Diversions (2007\_WB\_Div\_SP vs. 2007\_WB\_JB\_MG\_DR\_B).**

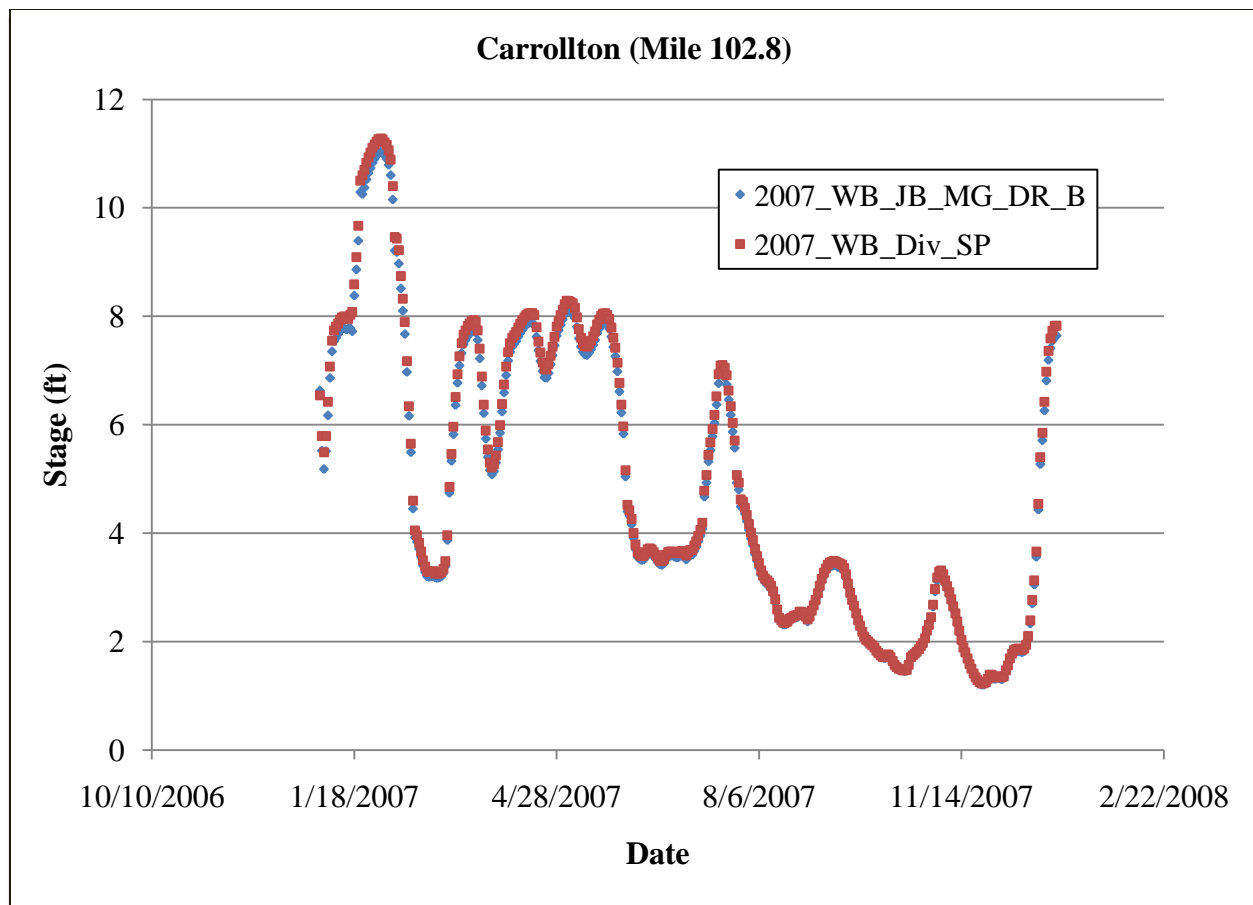


**Figure 6-39: Stage Comparison at Carrollton for the Closure of South Pass and the Addition of the Proposed Diversions (2007\_WB\_Div\_SP vs. 2007\_WB\_JB\_MG\_DR\_B).**

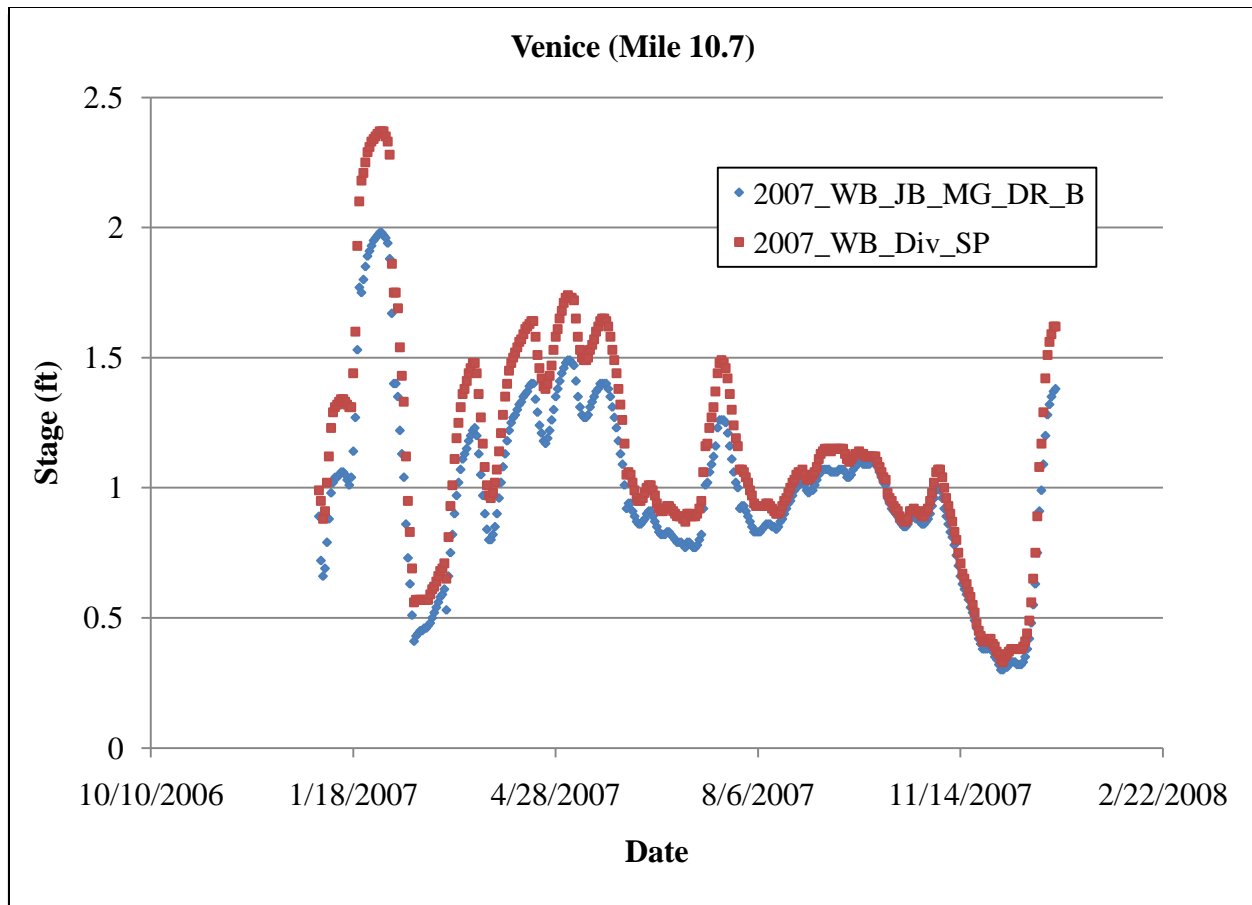


**Figure 6-40: Stage Comparison at Venice for the Closure of South Pass and the Addition of the Proposed Diversions (2007\_WB\_Div\_SP vs. 2007\_WB\_JB\_MG\_DR\_B).**

**Table 6-11: Mean and Max Difference in Stage for the Closure of South Pass and the Addition of the Proposed Diversions at the Comparison Gages (2007\_WB\_Div\_SP).**

Parameter / Gage	Baton Rouge	Donaldsonville	North of Bonnet Carré	Bonnet Carré	Carrollton	West Pointe a la Hache	Venice
Mean Stage Difference (ft)	0.06	0.09	0.11	0.11	0.12	0.13	0.15
Max Stage Difference (ft)	0.45	1.31	0.35	0.35	0.36	0.37	0.43



**Table 6-12: Average Percent Increase in Flow to the Passes, Fort St. Philip, Bayou Lamoque North, and Bayou Lamoque South due to the Closure of South Pass and the Addition of the Proposed Diversions (2007\_WB\_Div\_SP).**

Pass	Average Percent Increase	Standard Deviation
Baptiste Collette	10.88%	0.59%
Fort St. Philip	10.50%	2.00%
Grand Pass	11.18%	0.60%
Main Pass	18.29%	0.52%
Pass a Loutr�	22.59%	0.95%
South Pass	-	-
Southwest Pass	20.91%	0.83%
Bayou Lamoque North	4.96%	0.95%
Bayou Lamoque South	6.06%	0.59%

The second simulation with the MLODS proposed diversions and channel modifications was similar to the first except Southwest Pass included the closure weir instead of South Pass (2007\_WB\_Div\_SWP). Figures 6-41, 6-42, and 6-43 compare the stage at Baton Rouge, Carrollton, and Venice, respectively, for 2007\_WB\_JB\_MG\_DR\_B vs. 2007\_WB\_Div\_SWP. Table 6-13 shows the mean and max difference at the comparison gages for the closure of Southwest Pass and the addition of the proposed diversions. Table 6-14 shows the average percent increase in flow to the passes, Fort St. Philip, Bayou Lamoque North, and Bayou Lamoque South at the comparison gages.

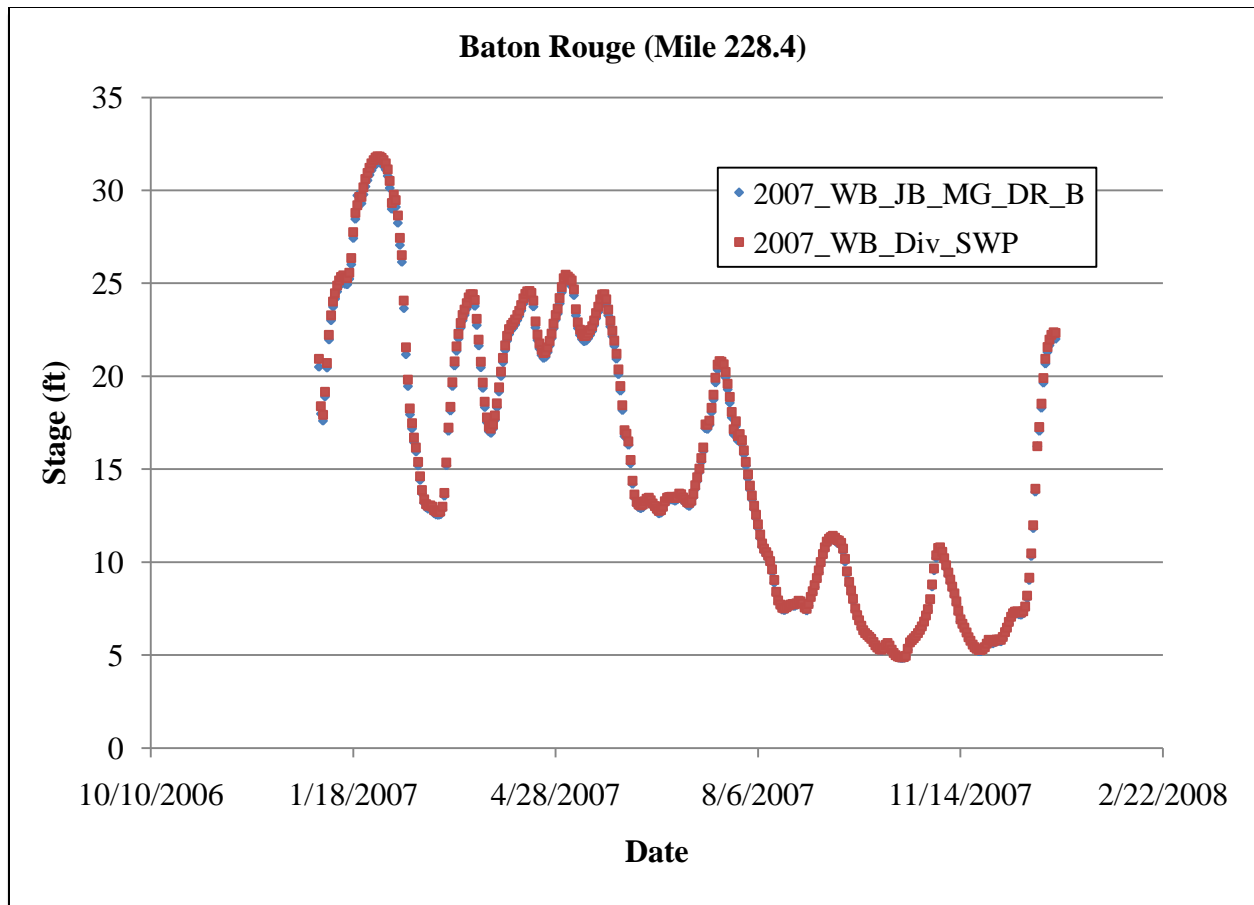


**Figure 6-41: Stage Comparison at Baton Rouge for the Closure of Southwest Pass and the Addition of the Proposed Diversions (2007\_WB\_Div\_SWP vs. 2007\_WB\_JB\_MG\_DR\_B).**

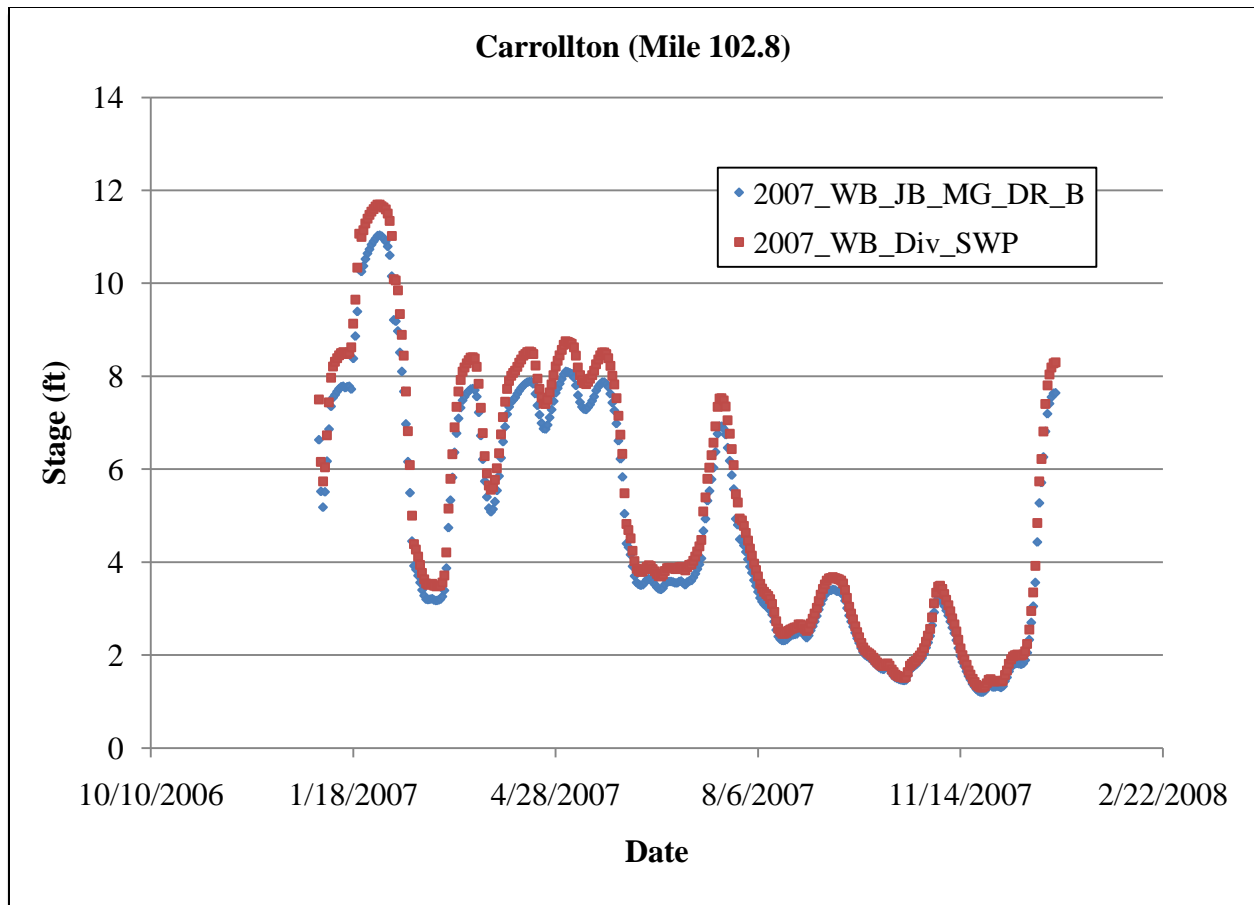


**Figure 6-42: Stage Comparison at Carrollton for the Closure of Southwest Pass and the Addition of the Proposed Diversions (2007\_WB\_Div\_SWP vs. 2007\_WB\_JB\_MG\_DR\_B).**

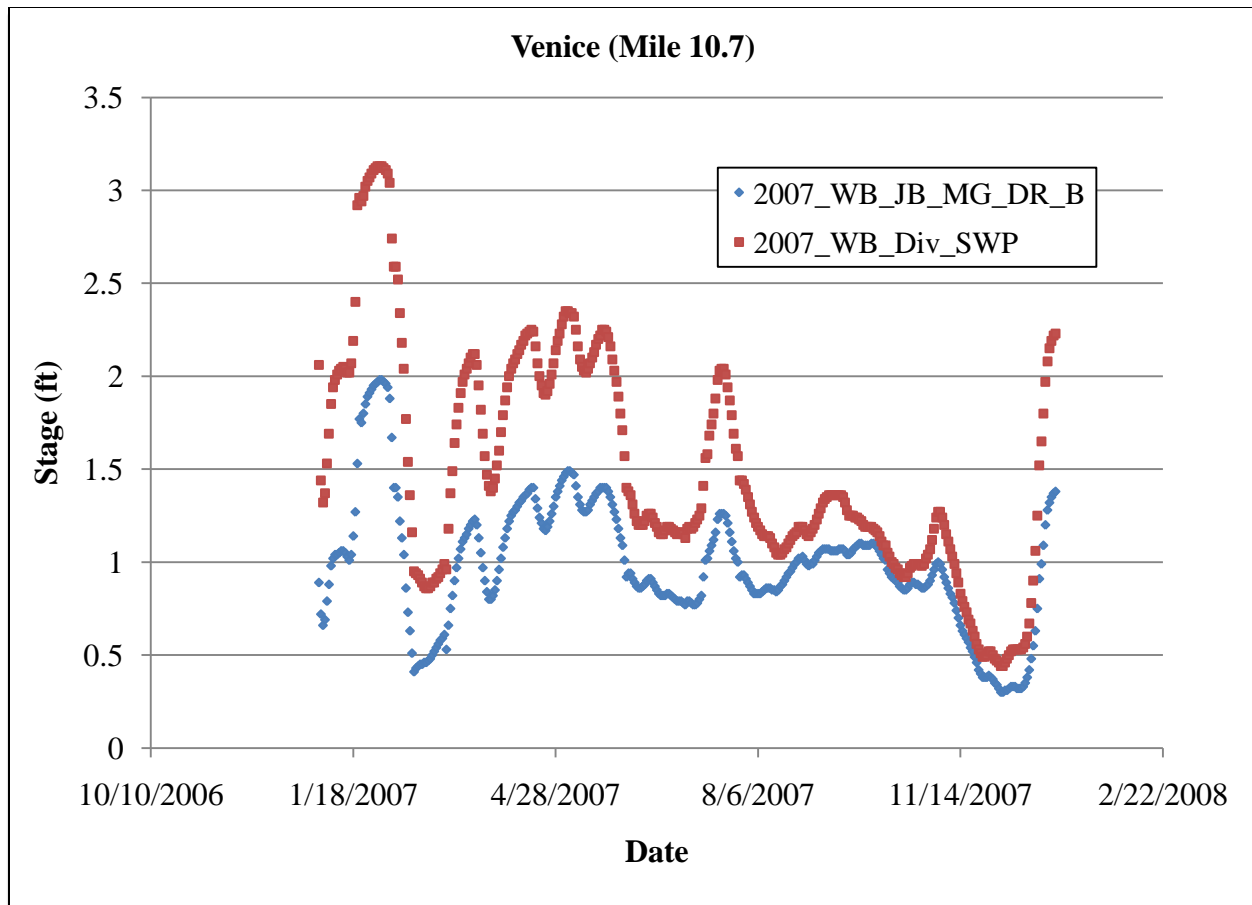


Figure 6-43: Stage Comparison at Venice for the Closure of Southwest Pass and the Addition of the Proposed Diversions (2007\_WB\_Div\_SWP vs. 2007\_WB\_JB\_MG\_DR\_B).

Table 6-13: Mean and Max Difference in Stage for the Closure of Southwest Pass and the Addition of the Proposed Diversions at the Comparison Gages (2007\_WB\_Div\_SWP).

Parameter / Gage	Baton Rouge	Donaldsonville	North of Bonnet Carré	Bonnet Carré	Carrollton	West Pointe a la Hache	Venice
Mean Stage Difference (ft)	0.20	0.30	0.36	0.36	0.39	0.45	0.51
Max Stage Difference (ft)	0.52	1.67	0.85	0.86	0.95	1.25	1.39

**Table 6-14: Average Percent Increase in Flow to the Passes, Fort St. Philip, Bayou Lamoque North, and Bayou Lamoque South due to the Closure of Southwest Pass and the Addition of the Proposed Diversions (2007\_WB\_Div\_SWP).**

Pass	Average Percent Increase	Standard Deviation
Baptiste Collette	35.16%	2.32%
Fort St. Philip	37.22%	7.46%
Grand Pass	36.01%	2.39%
Main Pass	56.70%	1.86%
Pass a Loutr� (dredged to -50 ft)	68.73%	3.39%
South Pass	61.92%	3.25%
Southwest Pass	-	-
Bayou Lamoque North	17.04%	2.28%
Bayou Lamoque South	20.25%	2.35%

The final two simulations for the MLODS proposed diversions and channel modifications were similar to the previous two except both South and Southwest Passes included the closure weirs and Pass a Loutr  was dredged to -50 ft and -40 ft (NAVD 88) (2007\_WB\_Div\_SP\_SWP\_pal50 and 2007\_WB\_Div\_SP\_SWP\_pal40, respectively). Figures 6-44, 6-45, 6-46, 6-47, 6-48, and 6-49 compare the stage at Baton Rouge, Carrollton, and Venice, respectively, for 2007\_WB\_JB\_MG\_DR\_B vs. 2007\_WB\_Div\_SP\_SWP\_pal50 and 2007\_WB\_JB\_MG\_DR\_B vs. 2007\_WB\_Div\_SP\_SWP\_pal40. Tables 6-15 and 6-16 show the average percent increase in flow to the passes, Fort St. Philip, Bayou Lamoque North, and Bayou Lamoque South at the comparison gages.

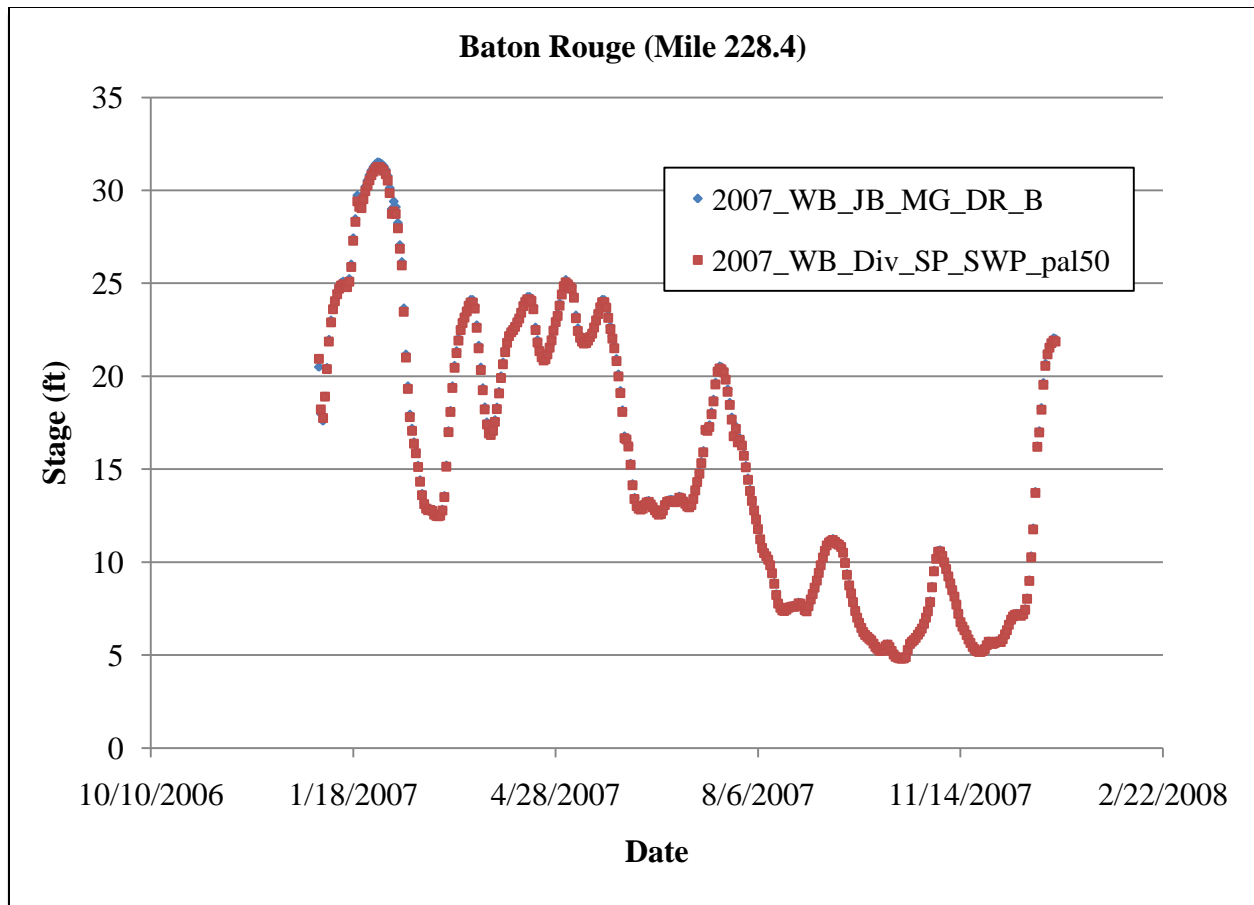


**Figure 6-44: Stage Comparison at Baton Rouge for the Closure of South and Southwest Pass, the Addition of the Proposed Diversions, and the Dredging of Pass a Loutr  to -50 ft (2007\_WB\_Div\_SP\_SWP\_pal50 vs. 2007\_WB\_JB\_MG\_DR\_B).**

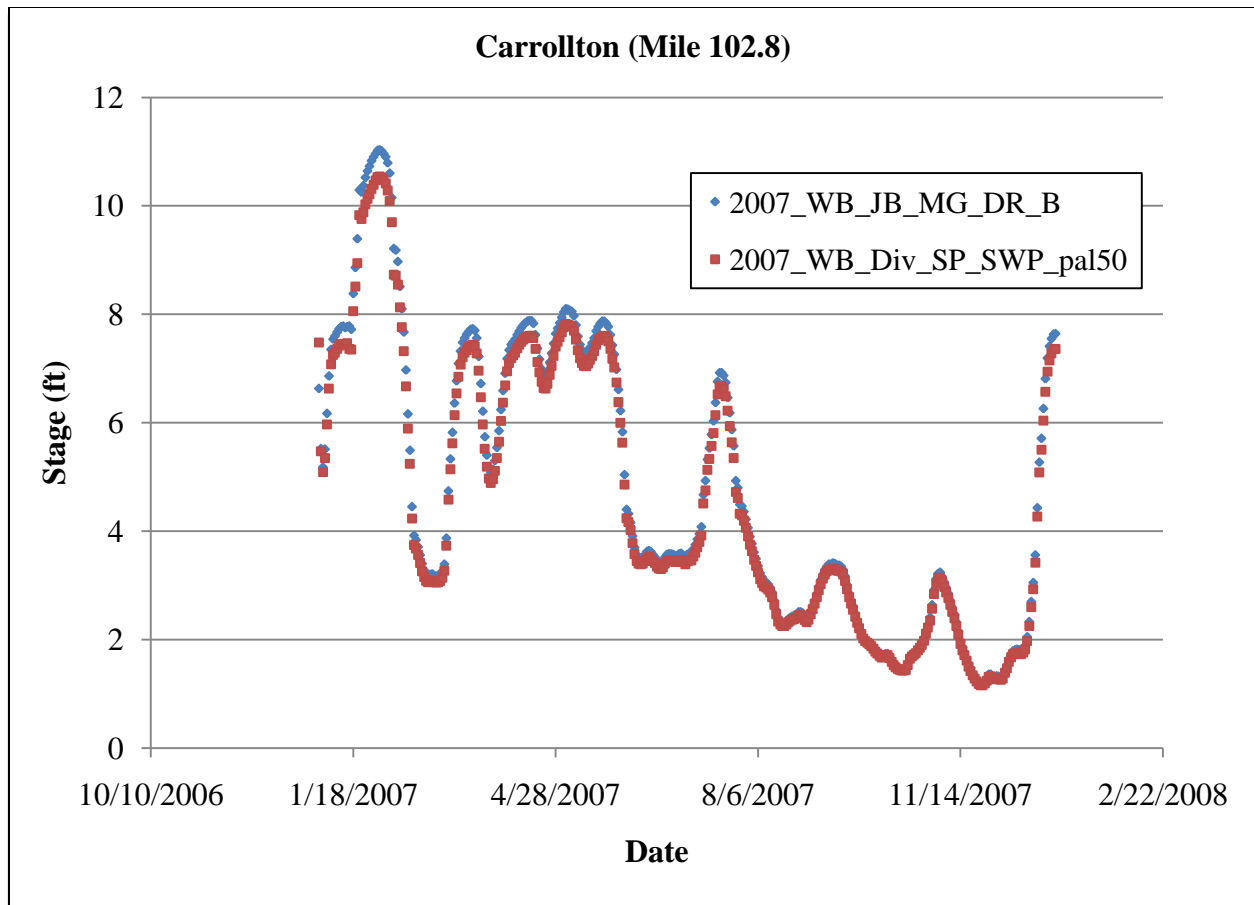


**Figure 6-45: Stage Comparison at Carrollton for the Closure of South and Southwest Pass, the Addition of the Proposed Diversions, and the Dredging of Pass a Loutr  to -50 ft (2007\_WB\_Div\_SP\_SWP\_pal50 vs. 2007\_WB\_JB\_MG\_DR\_B).**

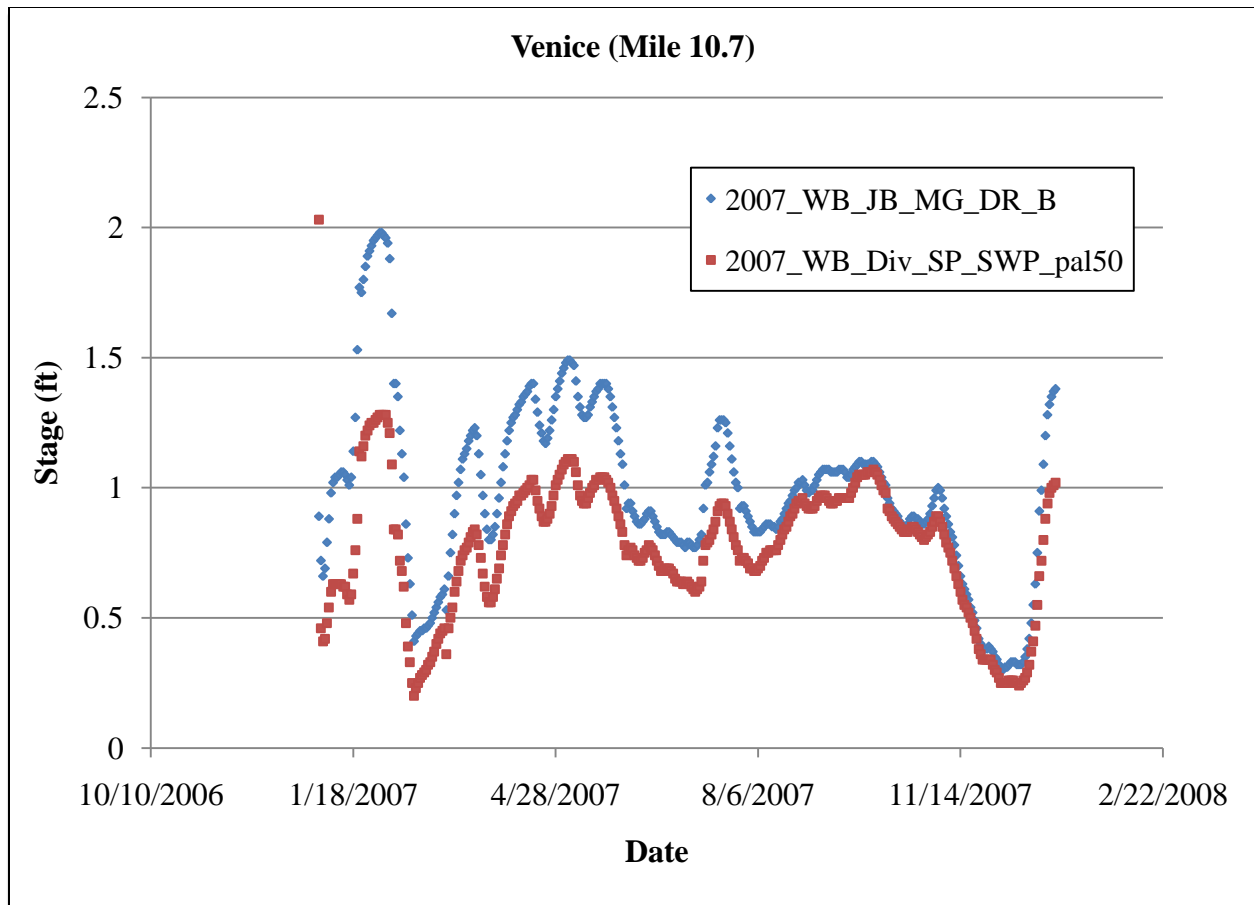


**Figure 6-46: Stage Comparison at Venice for the Closure of South and Southwest Pass, the Addition of the Proposed Diversions, and the Dredging of Pass a Loutr  to -50 ft (2007\_WB\_Div\_SP\_SWP\_pal50 vs. 2007\_WB\_JB\_MG\_DR\_B).**



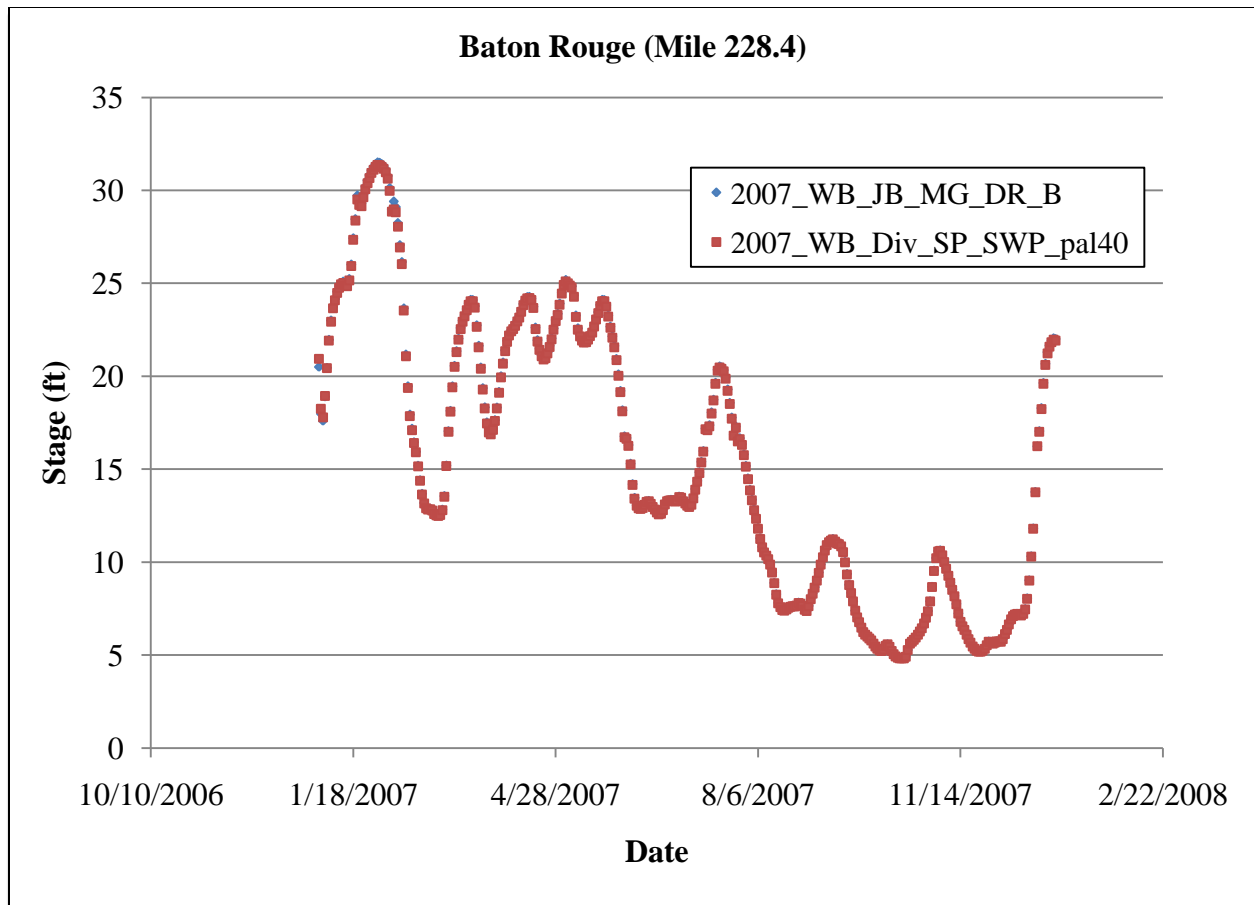


**Figure 6-47: Stage Comparison at Baton Rouge for the Closure of South and Southwest Pass, the Addition of the Proposed Diversions, and the Dredging of Pass a Loutr  to -40 ft (2007\_WB\_Div\_SP\_SWP\_pal40 vs. 2007\_WB\_JB\_MG\_DR\_B).**

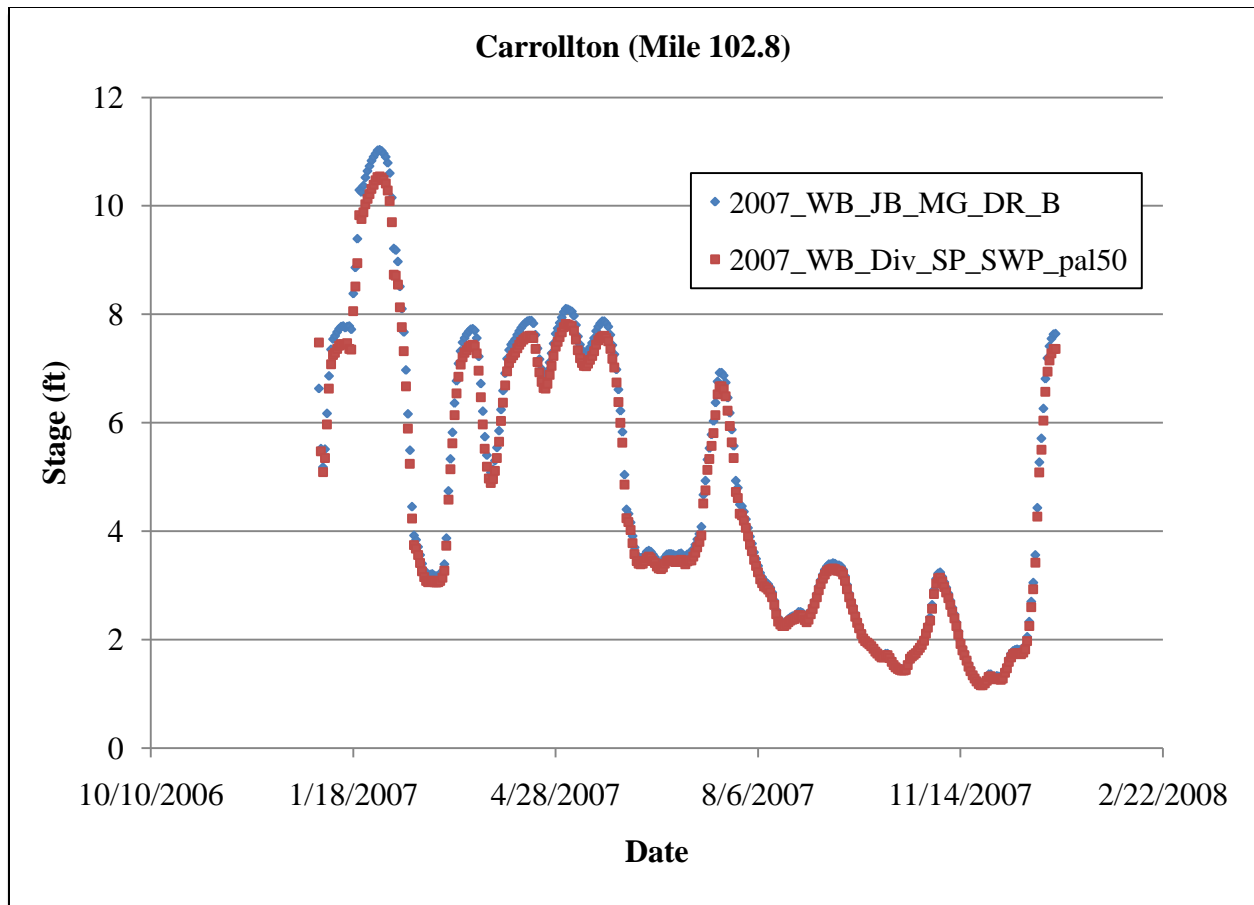


**Figure 6-48: Stage Comparison at Carrollton for the Closure of South and Southwest Pass, the Addition of the Proposed Diversions, and the Dredging of Pass a Loutr  to -40 ft (2007\_WB\_Div\_SP\_SWP\_pal40 vs. 2007\_WB\_JB\_MG\_DR\_B).**

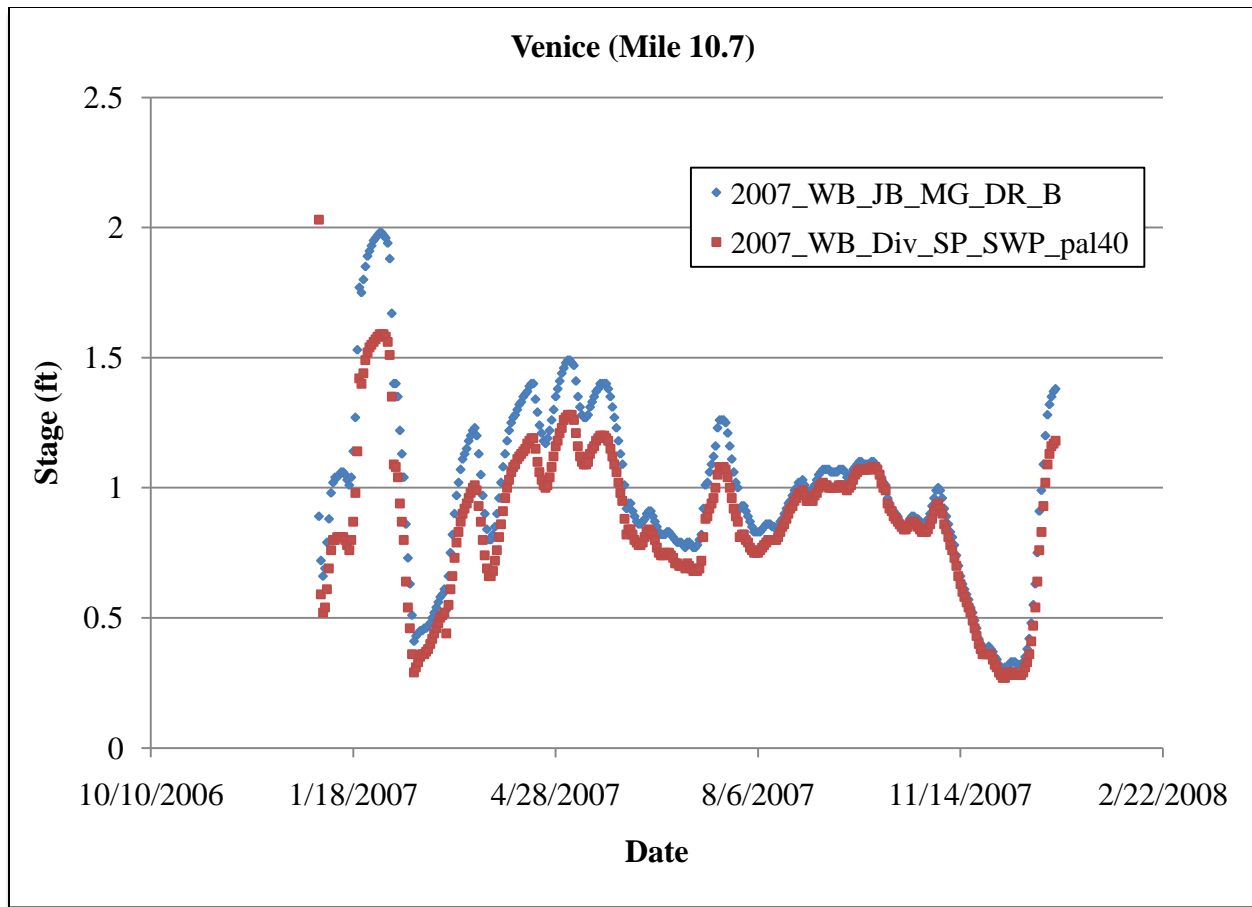


**Figure 6-49: Stage Comparison at Venice for the Closure of South and Southwest Pass, the Addition of the Proposed Diversions, and the Dredging of Pass a Loutr  to -40 ft (2007\_WB\_Div\_SP\_SWP\_pal40 vs. 2007\_WB\_JB\_MG\_DR\_B).**

**Table 6-15: Average Percent Increase in Flow to the Passes, Fort St. Philip, Bayou Lamoque North, and Bayou Lamoque South due to the Addition of the Proposed Diversions, the Closure of South Pass, Southwest Pass, and West Bay and the Dredging of Pass a Loutr  to -50 ft (2007\_WB\_SP\_SWP\_pal50).**

Pass	Average Percent Increase	Standard Deviation
Baptiste Collette	-17.87%	0.37%
Fort St. Philip	-15.40%	2.67%
Grand Pass	-18.47%	0.39%
Main Pass	-33.93%	0.70%
Pass a Loutr� (dredged to -50 ft)	777.80%	43.18%
South Pass	-	-
Southwest Pass	-	-
Bayou Lamoque North	-7.96%	1.31%
Bayou Lamoque South	-9.18%	0.57%

**Table 6-16: Average Percent Increase in Flow to the Passes, Fort St. Philip, Bayou Lamoque North, and Bayou Lamoque South due to the Addition of the Proposed Diversions, the Closure of South Pass, Southwest Pass, and West Bay and the Dredging of Pass a Loutr  to -40 ft (2007\_WB\_SP\_SWP\_pal40).**

Pass	Average Percent Increase	Standard Deviation
Baptiste Collette	-9.65%	0.28%
Fort St. Philip	-8.62%	1.62%
Grand Pass	-9.95%	0.30%
Main Pass	-17.43%	0.54%
Pass a Loutr� (dredged to -40 ft)	715.38%	39.60%
South Pass	-	-
Southwest Pass	-	-
Bayou Lamoque North	-4.33%	0.79%
Bayou Lamoque South	-5.09%	0.35%

## Chapter 7: Discussion

In order to predict the response of the Mississippi River (MR) to natural and man-made stimuli, a 1-D numerical model was created. This model was the first of its kind to extend from Tarbert Landing, MS (RM 306) to the Gulf of Mexico (GOM), as well as to include the Barataria Basin drainage network and the existing passes. The 2007 mean stage calibration root mean square error (RMSE) was approximately 0.77 ft, the mean bias error was less than 0.5 ft, and the mean RMSE per average depth was 1.46%. The 2003 mean stage validation RMSE was approximately 1.08 ft, the mean bias error was less than 0.5 ft, and the mean RMSE per average depth was 2.14%. The 1999-2000 mean stage validation RMSE was approximately 0.79 ft, the mean bias error was less than 0.5 ft, and the RMSE per average depth was 1.57%. These relatively small errors indicate that the model can be used for various applications involving changes to the river channels and/or the introduction of new diversions.

### *7.1 Relative Sea Level Rise Study*

For the relative sea level rise study (RSLR), the values of 1.64, 3.28, and 4.92 ft are used to represent the possible change over the next 50 years in the GOM stage relative to the present (2010) datum where the Lower MR enters the GOM. The values are quite high, but are consistent with annual RSLR rates of 9 to 200 mm/year between New Orleans and Lower Plaquemines Parish. The term “relative” takes into account the effects of land subsidence and sea level rise from the GOM.

The flow rate in a channel is a function of the cross-sectional area and velocity in the channel. As the water surface level increases, the cross-sectional area increases. However, in the model, to maintain the same flow rate as depicted by the initial conditions, the velocity must decrease. This velocity reduction lowers the energy gradient of the channel, which reduces the energy slope of the channel. Therefore, the bed shear stress, which is directly proportional to the energy slope, decreases as well; this affect was observed in the shear stress results. The decrease in shear stress directly affects the sediment transport potential of the river because if there is not enough shear stress from the water near the bed, then less sediment and particulates are removed near the bed. Therefore, the bed material transport capacity is reduced as the water surface level rises.

The rating curves were also analyzed for the three cases of relative sea level rise. The results indicated that as the flow rate and stage increased, the four curves (Original, RSLR 0.5, RSLR 1.0, and RSLR 1.5) converged together, which suggests that at peak flows the stage in the river will reach a peaking limit. Also, the locations furthest from the GOM, such as Violet (RM 83.9) and Belle Chasse (RM 76), showed a stronger tendency to converge at peak flows than the locations nearest to the GOM. This behavior shows that the farther upstream from the GOM a location is, the less likely that location is to be affected by the rise in the water surface elevation.

### *7.2 West Bay Closure Study*

For the West Bay closure study, the West Bay channel was removed entirely from the model to coincide with the decommissioning of the diversion. The flow rates in the passes and other nearby channels were analyzed to determine the distribution of flow. On average, the passes and

Fort St. Philip received approximately 5% more flow capacity than the original flow distribution. Also, the effects of the diversion closure were observed all the way up to Bayou Lamoque North and South (RM 32.7 and 32.4, respectively), which received an average of 2.09% increase in flow.

### ***7.3 Proposed Diversions Study***

For the proposed diversions study, diversion channels and structures were created to simulate the Multiple Lines of Defense Strategy (MLODS) proposed diversions at Buras, Jesuit Bend, Myrtle Grove, and Deer Range. The diversion at Buras was designed as a crevasse-type diversion with uncontrolled discharge at all times. The diversions at Jesuit Bend, Myrtle Grove, and Deer Range were designed as channels with gated structures, which were opened for 6 months at a time. The stage results showed that the removal of flow from the MR reduces the stage in the river. However, the extent of this reduction does not transfer throughout the river. For example, the mean stage difference was averaged for all of the diversion simulations and was found to be -0.32 ft at Carrollton and -0.16 ft at Baton Rouge, which indicates that the diversions would mostly have a local impact on the river rather than a global impact.

### ***7.4 Changes to the Delta Distributaries Study***

For the channel modifications in the Delta study, several simulations were performed for scenarios of closing certain passes, such as South Pass and Southwest Pass, and dredging Pass a Loutr  to variable depths. A similar study was conducted using the proposed diversions from the MLODS. For both studies, the discharge results showed that closing South Pass or Southwest Pass would increase the amount of flow entering the other passes and local channels. In addition, the average percent increase in flow for the diversion simulations was reduced on average by 1.23% with South Pass closed and 4.5% with Southwest Pass closed, which indicates that the proposed diversions would remove the water that would be diverted to the passes and local channels if either pass was removed.

For both studies, two simulations were performed, which consisted of removing South Pass and Southwest Pass and dredging the Pass a Loutr  channel to (i) -50 ft and (ii) -40 ft. The discharge results for each of these simulations show that the flow in the larger Pass a Loutr  channel was increased by over 700% of its original flow because of its extra capacity. Also, the amount of flow in the other passes and local channels was reduced below their original percentages. The amount of flow in the Pass a Loutr  channel did decrease when the depth was decreased to -40 ft and when the proposed diversions were included.

### ***7.5 Sources of Error***

This model is an unsteady hydrodynamic model in that the boundary conditions change over time and the continuity and momentum equations are solved at each time step. It is not, however, a true unsteady model because the channel bed does not change over time. The U.S. Army Corps of Engineers (USACE) surveys the MR and its tributaries once every 10 years with the most recent survey being the 2003-2004 Hydrographic Survey (USACE NOD, 2007). Therefore, it was not possible to update the channels' bathymetry on a yearly or daily basis and constant

channel data were used for every simulation. Also, information on the hydrology of the modeled reach, such as precipitation, surface runoff, infiltration, groundwater table elevation, and evaporation, was not taken into account in the model. This may account for some of the differences in the observed and modeled river stages. For example, a heavy rain event could increase the stage by a few inches. Also, the effective roughness in the model varies with the bed forms, which change dynamically with the flow and bed shear stress; the model does not capture this process. Although HEC-RAS has a sediment transport sub-model, it operates in a quasi-unsteady mode and therefore fails to capture the full dynamic wave in the river.

The low flow period for the 2007 calibration showed some discontinuity between the observed and calculated stage values at the downstream gages. The calculated stage was lower than the observed stage, which could be due to tropical surges at that time or an underestimation of the influence of saltwater intrusion from the GOM.

For the 2003 and 1999-2000 validation simulations, the downstream boundary condition was set as the 2007 GOM salinity stage hydrograph because of the lack of stage and salinity data for those periods. The stage comparison for the 1999-2000 simulation had good agreement between the observed and calculated values with a mean RMSE of 0.79 ft. However, the mean RMSE of 1.08 ft for the 2003 validation was caused by the boundary conditions. The HEC-RAS program is not capable of creating oscillations or abrupt changes during the simulations because the calculations of momentum and continuity rely on the user-inputted boundary conditions. Therefore, if the upstream or downstream boundary condition does not specify a change in the hydrograph, then the model would not know to consider it. For the 2003 validation, the resulting stage hydrographs along the MR did not agree with the observed values near the end of the year, but the results did retain the curve-shape of the upstream discharge hydrograph and the downstream GOM stage hydrograph. One possible reason for the disagreement between the observed and calculated stage values could be the use of the 2007 GOM stage hydrograph as the downstream boundary condition.

The discontinuities between the observed stage and the calculated stage for the 2007-2008 simulation are due to the time interval of the input data. The boundary condition of the time-series of gate openings was given daily values from the USACE website. However, the unsteady hydrodynamics were computed every 10 minutes. Therefore, there is a “shock” to the system, which appears as an unrealistic transient spike in the river stage when the gates are initially opened or closed. The actual field operations of the spillway involved opening the gates over the course of several minutes to hours, which smoothed out any shock that the stage witnessed. Also, the HEC-RAS model’s method of transitioning from orifice flow to surface weir flow is not continuous and could also cause a shock to the system because the equations for the flow rate include exponents on the energy head that change from 0.5 (orifice flow) to 1.5 (weir flow).

One of the problems with the 2003 LIDAR/bathymetry file was the mesh constraints mentioned earlier. Another problem with the 2003 file was that the Louisiana coastal area underwent tremendous land loss (~ 79 square miles) from Hurricanes Katrina and Rita in 2005 (LPBF, 2008), which was not taken into account in the 2003 data. Therefore, the bathymetry in the passes and diversion receiving areas were not representative of the current channel bathymetry.

The model can be used as a guide for future projects, but should not be considered an accurate representation of the MR and its tributaries.

One issue with modeling the Barataria Basin in HEC-RAS is that the program lacks certain structural options, such as locks. For the ICCW at Harvey and Chalmette, the amount of flow entering the channels is entirely dependent on the operations and schedule of the navigation locks. The flow in these channels varies on an hourly to daily basis. To remedy this oversight in the model, the Manning's  $n$  values were increased near the channel intakes to maintain a constant of 100 cfs each, which is an average flow based on lock operational data. Another issue with the Barataria Basin in HEC-RAS is the limit on the number of channels allowed in confluences and splits. For example, the model only allows two channels to combine to form a third channel, or one channel to split into two channels. However, in the Barataria Basin there are several locations where four channels are connected at one location. To remedy this problem, intermediate channels were created to connect one confluence to one split.

Another issue with the channel bathymetry, besides the lack of available data, is that several gages are referenced to different datums. For instance, the West Pointe a la Hache river gage was updated to NAVD 88 in 2006 (Mississippi River & Passes, 2010); however, the other comparison gages at Baton Rouge, Donaldsonville, North of Bonnet Carré, Bonnet Carré, Carrollton, and Venice are referenced to NGVD 29. Therefore, the observed stage data had to be adjusted to the NAVD 88 datum by subtracting a certain height, which was provided by the website (Mississippi River & Passes, 2010).



## **Chapter 8: Conclusions and Recommendations for Future Research**

A 1-D numerical model was created to simulate the hydrodynamics of the Lower Mississippi River and its existing diversions and distributaries. This river response model was needed to investigate the impacts of proposed freshwater diversions, as well as proposed distributary modifications. The model was calibrated using recorded stage data for the calendar year of 2007. The average 2007 calibration RMSE, bias error, and RMSE per average depth were 0.77 ft, less than 0.5 ft, and 1.46%, respectively. The model was then validated using recorded stage data for the calendar year of 2003. The average 2003 validation RMSE, bias error, and RMSE per average depth were 1.08 ft, less than 0.5 ft, and 2.14%, respectively, which are also relatively small errors. Next, the model was validated for the calendar years of 1999-2000, using recorded stage data. The average 1999-2000 validation RMSE, bias error, and RMSE per average depth were 0.79 ft, less than 0.5 ft, and 1.57%, respectively, which are relatively small errors. Therefore, the model was considered suitable for other applications, such as channel modifications, proposed diversions, and relative sea level rise studies.

The first study involved experimenting with relative sea level rise to determine the potential effects on the bed material transport capacity of the river. The results showed a decrease in this capacity as the water surface level increased, which agrees with the expected theoretical behavior. In order to expand this research on the sediment transport capacity, it is recommended that the model be used with the sediment transport module in HEC-RAS 4.1.0, which was released in 2010.

The second study addressed the decommissioning of the West Bay Sediment Diversion, which was officially announced in 2010. The channel was removed from the model and the flow that would normally have entered that channel was automatically re-distributed by the model to the remaining passes and local distributaries.

The third study focused on the channel modifications described in the Lake Pontchartrain Basin Foundation's (LPBF) Multiple Lines of Defense Strategy (MLODS). These modifications included closing off South Pass and Southwest Pass individually and closing them off together along with dredging Pass a Loutr . Similar to the West Bay Study, the model was capable of re-distributing the flow to the remaining passes and channels as South Pass or Southwest Pass were closed. For the dredging of Pass a Loutr , two alternatives were investigated. The first involved dredging the channel to -50 ft and the second involved dredging the channel to -40 ft. Both of these alternatives increased the capacity of the channel, but also reduced the capacity of the other remaining passes and channels. The decrease in capacity in the other passes and channels contradicts the goal of coastal restoration by limiting the amount of freshwater and sediment that could enter those channels and receiving bodies. Therefore, alternatives with shallower or narrower sections in Pass a Loutr  should be investigated further. In order to maintain Pass a Loutr  at a suitable depth for navigation purposes, jetties could be added along the banks, which would allow a narrowing of the channel that would decrease its capacity.

The fourth study included several of the MLODS proposed diversions in the model. The diversions considered were an uncontrolled crevasse-type diversion at Buras and gated diversions at Jesuit Bend, Myrtle Grove, and Deer Range. The model was capable of diverting

flow through these channels and structures, and continuity was maintained. Also, the results indicated that the gage at Carrollton, which is important for New Orleans, would not be significantly affected by the combined operation of these diversions.

The final study involved operating these MLODS diversions along with modifying the Delta distributaries. The model was capable of re-distributing the flow to the remaining passes and distributaries and the amount of flow was reduced by the presence of the diversions. The results indicated that the stage at Carrollton would be only slightly increased by the combined operation of the MLODS diversions in conjunction with the Pass modifications. Also, a similar situation to the third study arose with the dredging of Pass a Loutr , where that channel's capacity removed flow from the remaining passes and distributaries. One alternative would be to increase the capacity of the proposed diversions in order to reduce the stage in the river and thereby reducing the capacity of Pass a Loutr .

Overall, this model is a good tool for understanding the hydrodynamics of the Lower Mississippi River and can be used for many other applications in the future.

## References

- Andrus, T.M. (2007). "Sediment Flux and Fate in the Mississippi River Diversion at West Bay: Observation Study." Thesis, Louisiana State University and Agricultural and Mechanical College, Baton Rouge, LA.
- Barbé, D.E., Fagot, K., & McCorquodale, J.A. (2000). Effects on Dredging Due to Diversions from the Lower Mississippi River. *Journal of Waterway, Port, Coastal, and Ocean Engineering*, ASCE, Vol. 126(3), 121-129.
- BS-12 White Ditch Diversion Restoration and Outfall Management- General Factsheet. (n.d.). *LaCoast.gov - The Louisiana Coastal Wetlands Conservation and Restoration Task Force Web site*. Retrieved March 31, 2010, from <http://www.lacoast.gov/reports/display.asp?projectNumber=BS-12&reportType=general>
- Chang, H.H. (1984). Modeling of River Channel Changes. *Journal of Hydraulic Engineering*, ASCE, Vol. 110(2), 157-172.
- Chow, V.T. (1959). *Open-Channel Hydraulics*. New York: The Blackburn Press.
- Copeland, R.R., & Thomas, W.A. (1992). "Lower Mississippi River Tarbert Landing to East Jetty Sedimentation Study". *Technical Report HL-92-6*, U.S. Army Corps of Engineers, New Orleans District.
- Danish Hydraulic Institute (DHI). (2003). *MIKE 11: A Modelling System for Rivers and Channels, Short Introduction Tutorial*. April 2003. Danish Hydraulic Institute.
- Davis Pond Freshwater Diversion Project (DPFDP). (2002, March 26). *LaCoast.gov – The Louisiana Coastal Wetlands Conservation and Restoration Task Force Web site*. Retrieved March 31, 2010, from <http://www.lacoast.gov/Programs/DavisPond/Index.htm>
- Georgiou, I.Y., McCorquodale, J.A., Neupane, J., Howes, N., Hughes, Z., FitzGerald, D., & Schindler, J.K. (2010). "Modeling the Hydrodynamics of Diversions into Barataria Basin." Final Report submitted to the Lake Pontchartrain Basin Foundation.
- Guilbeau, D. (n.d.). West Bay Sediment Diversion (MR-03). *LaCoast.gov - The Louisiana Coastal Wetlands Conservation and Restoration Task Force Web site*. Retrieved March 31, 2010, from [lacoast.gov/reports/gpfs/MR-03.pdf](http://lacoast.gov/reports/gpfs/MR-03.pdf)
- HEC-6. (2008, October 21). *Hydrologic Engineering Center Home Page*. Retrieved February 15, 2010, from <http://www.hec.usace.army.mil/software/legacysoftware/hec6/hec6.htm>
- Holly, F.M. Jr., Yang, J.C., Schovarz, P., Scheefer, J., Hsu, S.H., & Einhellig, R. (1990). *CHARIMA: Numerical Simulation of Unsteady Water and Sediment Movement in Multiply Connected Networks of Mobile-Bed Channels*. Iowa Institute of Hydraulic Research, Report No. 343, University of Iowa, Iowa City, IA.

- Ingenierie, S., Department of Civil & Environmental Engineering University of New Orleans, & Coastal Restoration Consultants. (1997). Feasibility Study and Report for the Department of Natural Resources State of Louisiana on the Transport of Sediment by Gravity for Coastal Restoration and Wetland Rehabilitation in Louisiana.
- Krishnappan, B.G. (1985). Modeling of Unsteady Flows in Alluvial Streams. *Journal of Hydraulic Engineering*. ASCE, Vol. 111(2), 257-266.
- Lake Pontchartrain Basin Foundation (LPBF). (2008). "Comprehensive Recommendations Supporting the Use of the Multiple Lines of Defense Strategy to Sustain Coastal Louisiana 2008 Report (Version 1)", Lake Pontchartrain Basin Foundation. Metairie, LA.
- Louisiana Coastal Wetlands Conservation and Restoration Task Force (LCWCRTF). *The 1997 Evaluation Report to the U.S. Congress on the Effectiveness of Louisiana Coastal Wetland Restoration Projects*. (1997). Baton Rouge: Bourque Printing, Inc.
- Mahmood, K., & Yevjevich, V. (1975). *Unsteady Flow in Open Channels*, Volume I. Fort Collins: Water Resources Publications.
- McCorquodale, J.A., & Georgiou, I.Y. (2006). Evaluation of Water Quality Models for Ontario Receiving Waters. University of New Orleans, New Orleans, LA. March 27, 2006.
- McCorquodale, J.A., Georgiou, I.Y., Roblin, R., & Retana, G. (2008). "Assessment of Integrated Hydrodynamic and Transport for Long-term Predictions: Volume II, Water Quality Modeling of the Pontchartrain Estuary." June 30, 2008. FMI Center for Environmental Modeling and Pontchartrain Institute for Environmental Studies.
- Meade, R.H. (1995). "Contaminants in the Mississippi River 1987-92." U.S. Geological Survey Circular 1133.
- Meselhe, E.A., Habib, E., Griborio, A.G., Gautman, S., McCorquodale, J.A., & Georgiou, I.Y. (2005). Hydro-Ecological Modeling of Lower Mississippi River. *Proceedings of the 14<sup>th</sup> Biennial Coastal Zone Conference*, New Orleans, LA.
- Meselhe, E.A., Pereira, J.F, Georgiou, I.Y., Allison, M.A., McCorquodale, J.A., & Davis, M.A. (2010). Numerical Modeling of Mobile-Bed Hydrodynamics in the Lower Mississippi River, *Proc. of World Environmental & Water Resources Congress (EWRI) 2010*, A.S.C.E., Providence, RI. (*To be published*).
- Miller, G. (2008, February 11). West Bay Diversion. *U.S. Army Corps of Engineers New Orleans District*. Retrieved March 31, 2010, from [http://www.mvn.usace.army.mil/west\\_bay\\_diversion.htm](http://www.mvn.usace.army.mil/west_bay_diversion.htm)

- Mississippi River & Passes. (2010, March 31). *RiverGages.com: Water Levels of Rivers and Lakes*. Retrieved March 31, 2010, from [www2.mvr.usace.army.mil/WaterControl/new/layout.cfm](http://www2.mvr.usace.army.mil/WaterControl/new/layout.cfm)
- Mississippi River – Wikipedia, the free encyclopedia. (2010, March 17). *Wikipedia, the free encyclopedia*. Retrieved February 1, 2010, from [http://en.wikipedia.org/wiki/Mississippi\\_River](http://en.wikipedia.org/wiki/Mississippi_River)
- Park, D. (2002). “Hydrodynamics and Freshwater Diversion within Barataria Basin.” Dissertation, Louisiana State University and Agricultural and Mechanical College, Baton Rouge, LA.
- Parker, G., Sequeiros, O., & River Morphodynamics Class of Spring 2006. (2006). Large Scale River Morphodynamics: Application to the Mississippi Delta. *Proceedings, River Flow 2006 Conference*. September 6 – 8, 2006.
- Papanicolaou, A.N., Elhakeem, M., Krallis, G., Prakash, S., & Edinger, J. (2008). Sediment Transport Modeling Review – Current and Future Developments. *Journal of Hydraulic Engineering*. ASCE. January 2008.
- Pereira, J.F., McCorquodale, J.A., Meselhe, E.A., Georgiou, I.Y. & Allison, M.A. (2009). Numerical Simulation of Bed Material Transport in the Lower Mississippi River. *Journal of Coastal Research, Proceedings of the 10<sup>th</sup> International Coastal Symposium (SI 56)*, 1449-1453. Lisbon, Portugal.
- Pereira, J.F., Silva, J.M., & Holly, F.M.. (2007). Numerical Simulation of Unsteady Mobile-Bed Hydrodynamics, with Application to Mondego River. *International Association for Hydraulic Research, Proceedings from the 32<sup>nd</sup> Congress*. Spain.
- Port of New Orleans – Louisiana, USA. (2009, December 21). *Port of New Orleans –Louisiana, USA*. Retrieved February 1, 2010, from [http://www.portno.com/pno\\_pages/about\\_overview.htm](http://www.portno.com/pno_pages/about_overview.htm)
- Pratt, T. (2009). “West Bay Sediment Diversion Work Plan, Task 1: Data Collection and Analysis.” U.S. Army Corps of Engineers, Engineer Research and Development Center, Vicksburg, MS.
- Project Fact Sheet: Mississippi Delta Region, LA, Davis Pond Freshwater Diversion Project. (2003, April). *U.S. Army Corps of Engineers, New Orleans District & Louisiana Department of Natural Resources (USACE NOD & LA DNR)*. Retrieved February 1, 2010, from <http://www.mvn.usace.army.mil/PRJ/davispond/davispond.htm>
- Raphelt, N.K., Martin, S.K., & Little, Jr., C.D. (2008). “Desktop Study of Hydrodynamic and Sediment Processes in the Pass a Loutré Channel of the Lower Mississippi River.” U.S. Army Engineer Research & Development Center, Coastal & Hydraulics Laboratory.

- Roberson, J.A., Cassidy, J.J., & Chaudhry, M.H. (1988). *Hydraulic Engineering*. Boston: Houghton Mifflin Company.
- U.S. Army Corps of Engineers, Hydraulic Engineering Center (USACE HEC). (1993). *HEC-6, Scour and Deposition in Rivers and Reservoirs, User's Manual Version 4.1*. U.S. Army Corps of Engineers, Hydrologic Engineering Center (HEC) Publication.
- U.S. Army Corps of Engineers, Hydrologic Engineering Center (USACE HEC). (2008). *HEC-RAS River Analysis System, User's Manual Version 4.0*. U.S. Army Corps of Engineers, Hydrologic Engineering Center (HEC) Publication.
- U.S. Army Corps of Engineers, Mississippi River Commission (USACE MRC). (1985). "New Orleans Area Map." Mississippi River Commission, Vicksburg, MS.
- U.S. Army Corps of Engineers, New Orleans District (USACE NOD), 1993. Mississippi River Hydrographic Survey: 1991 – 1992; Black Hawk, LA to Head of Passes, LA and South and Southwest Passes and Pass a Loutr . Mississippi River Commission, Vicksburg, MS.
- U.S. Army Corps of Engineers, New Orleans District (USACE NOD). (2007). "Mississippi River Hydrographic Survey: 2003 – 2004; Black Hawk, LA to Gulf of Mexico." Mississippi River Commission, Vicksburg, MS.
- U.S. Army Corps of Engineers, New Orleans District (USACE NOD). (2009). "West Bay Survey Data." Mississippi River Commission, Vicksburg, MS.
- U.S. Army Corps of Engineers New Orleans District (USACE NOD): Spillway Opening and Closing Pace. (2010, March 17). *U.S. Army Corps of Engineers New Orleans District*. Retrieved March 17, 2010, from <http://www.mvn.usace.army.mil/bcarre/2008%20operation.asp>
- Visible Earth: Mississippi River Sediment Plume. (2001, March 15). *Visible Earth: Home*. Retrieved March 17, 2010, from [http://visibleearth.nasa.gov/view\\_rec.php?id=1650](http://visibleearth.nasa.gov/view_rec.php?id=1650)
- Waldron, R. (2008). "Physical Modeling of Flow and Sediment Transport Using Distorted Scale Modeling." Thesis, Louisiana State University and Agricultural and Mechanical College, Baton Rouge, LA

## **Appendix A**

### **Junction Data**

**Table A-1: Junction Data for 2007, 2003, and 2007-2008 simulations.**

River	Reach	Upstream Junction	Downstream Junction
Baptiste Collette	Reach 1	Baptiste Collette	
Barataria Bay	Reach 1	Barataria Bay 1	Barataria Bay 2
Barataria Bay	Reach 2	Barataria Bay 2	Barataria Bay 3
Barataria Bay	Reach 3	Barataria Bay 3	Barataria Bay 4
Barataria Bay	Reach 4		Barataria Bay 4
Barataria Bay	Reach 5	Barataria Bay 4	
Barataria Bay WW	Reach 1	Barataria Bay WW 1	Barataria Bay WW 2
Barataria Bay WW	Reach 2	Barataria Bay WW 2	Barataria Bay WW 3
Barataria Bay WW	Reach 3	Barataria Bay WW 3	Barataria Bay WW 4
Barataria Bay WW	Reach 4	Barataria Bay WW 4	Barataria Bay 1
Bayou Lamoque	Reach 1	Bayous N&S	
Bayou Lamoque N	Reach 1	Bayou Lamoque N	Bayous N&S
Bayou Lamoque S	Reach 1	Bayou Lamoque S	Bayous N&S
Bayou Perot	Reach 1	ICCW2	Bayous P&R 1
Bayou Perot	Reach 2	Bayous P&R 1	Bayou P&R 2
Bayou Rigolettes	Reach 1	Bayous P&R 1	Bayou Rigolettes
Bayou Rigolettes	Reach 2	Bayou Rigolettes	Barataria Bay WW 3
Bayou Rigolettes	Reach 3	Bayou Rigolettes	Bayou P&R 2
Bayous P&R	Reach 1	Bayou P&R 2	Little Lake 1
Caernarvon Diversion	Reach 1	Caernarvon	
Davis Pond Diversion	Reach 1	Davis Pond Diversion	Lake Cataouatche 1
Davis Pond Diversion	Lake Cataouatche Right	Lake Cataouatche 1	Lake Cataouatche 2
Davis Pond Diversion	Lake Cataouatche Left	Lake Cataouatche 1	Lake Cataouatche 2
Davis Pond Diversion	Lake Salvador Center	Lake Cataouatche 2	Lake Salvador 1
Davis Pond Diversion	Lake Salvador Right	Lake Salvador 1	Lake Salvador 2
Davis Pond Diversion	Lake Salvador Left	Lake Salvador 1	Des Allemands 4
Davis Pond Diversion	Reach 4	Des Allemands 4	ICCW1
Davis Pond Diversion	Reach 5	ICCW1	ICCW2
Des Allemands	Reach 2.0		Des Allemands 1
Des Allemands	Reach 1.0		Des Allemands 1
Des Allemands	Reach 3.0	Des Allemands 1	Des Allemands 2
Des Allemands	Reach 4.0	Des Allemands 2	Des Allemands 3
Des Allemands	Reach 5.0	Des Allemands 2	Des Allemands 3
Des Allemands	Reach 6.0	Des Allemands 3	Des Allemands 4
Fort St. Philip	Reach 1	Fort St. Philip	
Grand Pass	Reach 1	Grand Pass	Tiger Pass
Grand Pass	Reach 2	Tiger Pass	



**Table A-1 Continued.**

Head of Passes	Reach 1	Pass a Loutr�	South & Southwest
ICCW	Reach 4	Lake Salvador 2	ICCW1
ICCW	Reach 5		ICCW2
ICCW	Reach 1	ICCW H&C	The Pen 1
ICCW	Reach 2	The Pen 1	Barataria Bay WW 1
ICCW	Reach 3	Lake Salvador 2	Barataria Bay WW 1
ICCW Chalmette	Reach 1	ICCW Chalmette	ICCW H&C
ICCW Harvey	Reach 1	ICCW Harvey	ICCW H&C
Little Lake	Reach 1	Little Lake 1	Little Lake 2
Little Lake	Reach 2	Little Lake 1	Little Lake 2
Little Lake	Reach 3	Little Lake 2	Little Lake 3
Little Lake	Reach 4	Little Lake 3	Barataria Bay 1
Little Lake	Reach 5	Little Lake 3	Barataria Bay 3
Main Pass	Reach 1	Main Pass	
Mississippi	Reach 1		Davis Pond Diversion
Mississippi	Reach 2	Davis Pond Diversion	ICCW Harvey
Mississippi	Reach 3	ICCW Harvey	ICCW Chalmette
Mississippi	Reach 4	ICCW Chalmette	Caernarvon
Mississippi	Reach 5	Caernarvon	Bayou Lamoque N
Mississippi	Reach 6	Bayou Lamoque N	Bayou Lamoque S
Mississippi	Reach 7	Bayou Lamoque S	Fort St. Philip
Mississippi	Reach 8	Fort St. Philip	Baptiste Collette
Mississippi	Reach 9	Baptiste Collette	Grand Pass
Mississippi	Reach 10	Grand Pass	West Bay Diversion
Mississippi	Reach 11	West Bay Diversion	Main Pass
Mississippi	Reach 12	Main Pass	Pass a Loutr�
Pass a Loutr�	Reach 1	Pass a Loutr�	
South Pass	Reach 1	South & Southwest	
Southwest Pass	Reach 1	South & Southwest	
The Pen	Reach 1	The Pen 1	The Pen 2
The Pen	Reach 1.5	Barataria Bay WW 2	The Pen 2
The Pen	Reach 2	The Pen 2	The Pen 3
The Pen	Reach 2.5	Barataria Bay WW 4	The Pen 3
The Pen	Reach 3	The Pen 3	Wilkinson Canal
Tiger Pass	Reach 1	Tiger Pass	
West Bay	Reach 1	West Bay Diversion	
Wilkinson Canal	Reach 1		Wilkinson Canal
Wilkinson Canal	Reach 2	Wilkinson Canal	Barataria Bay 2

**Table A-2: Junction Data for 1999-2000 simulation.**

River	Reach	Upstream Junction	Downstream Junction
Baptiste Collette	Reach 1	Baptiste Collette	
Barataria Bay	Reach 1	Barataria Bay 1	Barataria Bay 2
Barataria Bay	Reach 2	Barataria Bay 2	Barataria Bay 3
Barataria Bay	Reach 3	Barataria Bay 3	Barataria Bay 4
Barataria Bay	Reach 4		Barataria Bay 4
Barataria Bay	Reach 5	Barataria Bay 4	
Barataria Bay WW	Reach 1	Barataria Bay WW 1	Barataria Bay WW 2
Barataria Bay WW	Reach 2	Barataria Bay WW 2	Barataria Bay WW 3
Barataria Bay WW	Reach 3	Barataria Bay WW 3	Barataria Bay WW 4
Barataria Bay WW	Reach 4	Barataria Bay WW 4	Barataria Bay 1
Bayou Lamoque	Reach 1	Bayous N&S	
Bayou Lamoque N	Reach 1	Bayou Lamoque N	Bayous N&S
Bayou Lamoque S	Reach 1	Bayou Lamoque S	Bayous N&S
Bayou Perot	Reach 1	ICCW2	Bayous P&R 1
Bayou Perot	Reach 2	Bayous P&R 1	Bayou P&R 2
Bayou Rigolettes	Reach 1	Bayous P&R 1	Bayou Rigolettes
Bayou Rigolettes	Reach 2	Bayou Rigolettes	Barataria Bay WW 3
Bayou Rigolettes	Reach 3	Bayou Rigolettes	Bayou P&R 2
Bayous P&R	Reach 1	Bayou P&R 2	Little Lake 1
Caernarvon Diversion	Reach 1	Caernarvon	
Davis Pond Diversion	Reach 1		Lake Cataouatche 1
Davis Pond Diversion	Lake Cataouatche Right	Lake Cataouatche 1	Lake Cataouatche 2
Davis Pond Diversion	Lake Cataouatche Left	Lake Cataouatche 1	Lake Cataouatche 2
Davis Pond Diversion	Lake Salvador Center	Lake Cataouatche 2	Lake Salvador 1
Davis Pond Diversion	Lake Salvador Right	Lake Salvador 1	Lake Salvador 2
Davis Pond Diversion	Lake Salvador Left	Lake Salvador 1	Des Allemands 4
Davis Pond Diversion	Reach 4	Des Allemands 4	ICCW1
Davis Pond Diversion	Reach 5	ICCW1	ICCW2
Des Allemands	Reach 2.0		Des Allemands 1
Des Allemands	Reach 1.0		Des Allemands 1
Des Allemands	Reach 3.0	Des Allemands 1	Des Allemands 2
Des Allemands	Reach 4.0	Des Allemands 2	Des Allemands 3
Des Allemands	Reach 5.0	Des Allemands 2	Des Allemands 3
Des Allemands	Reach 6.0	Des Allemands 3	Des Allemands 4
Fort St. Philip	Reach 1	Fort St. Philip	
Grand Pass	Reach 1	Grand Pass	Tiger Pass
Grand Pass	Reach 2	Tiger Pass	

**Table A-2 Continued.**

Head of Passes	Reach 1	Pass a Loutr�	South & Southwest
ICCW	Reach 4	Lake Salvador 2	ICCW1
ICCW	Reach 5		ICCW2
ICCW	Reach 1	ICCW H&C	The Pen 1
ICCW	Reach 2	The Pen 1	Barataria Bay WW 1
ICCW	Reach 3	Lake Salvador 2	Barataria Bay WW 1
ICCW Chalmette	Reach 1	ICCW Chalmette	ICCW H&C
ICCW Harvey	Reach 1	ICCW Harvey	ICCW H&C
Little Lake	Reach 1	Little Lake 1	Little Lake 2
Little Lake	Reach 2	Little Lake 1	Little Lake 2
Little Lake	Reach 3	Little Lake 2	Little Lake 3
Little Lake	Reach 4	Little Lake 3	Barataria Bay 1
Little Lake	Reach 5	Little Lake 3	Barataria Bay 3
Main Pass	Reach 1	Main Pass	
Mississippi	Reach 1		ICCW Harvey
Mississippi	Reach 3	ICCW Harvey	ICCW Chalmette
Mississippi	Reach 4	ICCW Chalmette	Caernarvon
Mississippi	Reach 5	Caernarvon	Bayou Lamoque N
Mississippi	Reach 6	Bayou Lamoque N	Bayou Lamoque S
Mississippi	Reach 7	Bayou Lamoque S	Fort St. Philip
Mississippi	Reach 8	Fort St. Philip	Baptiste Collette
Mississippi	Reach 9	Baptiste Collette	Grand Pass
Mississippi	Reach 10	Grand Pass	Main Pass
Mississippi	Reach 12	Main Pass	Pass a Loutr�
Pass a Loutr�	Reach 1	Pass a Loutr�	
South Pass	Reach 1	South & Southwest	
Southwest Pass	Reach 1	South & Southwest	
The Pen	Reach 1	The Pen 1	The Pen 2
The Pen	Reach 1.5	Barataria Bay WW 2	The Pen 2
The Pen	Reach 2	The Pen 2	The Pen 3
The Pen	Reach 2.5	Barataria Bay WW 4	The Pen 3
The Pen	Reach 3	The Pen 3	Wilkinson Canal
Tiger Pass	Reach 1	Tiger Pass	
Wilkinson Canal	Reach 1		Wilkinson Canal
Wilkinson Canal	Reach 2	Wilkinson Canal	Barataria Bay 2

**Table A-3: Junction Data for 2007 WB, WB\_SP, WB\_SWP, WB\_SP\_SWP\_pal50, and WB\_SP\_SWP\_pal40 simulations.**

River	Reach	Upstream Junction	Downstream Junction
Baptiste Collette	Reach 1	Baptiste Collette	
Barataria Bay	Reach 1	Barataria Bay 1	Barataria Bay 2
Barataria Bay	Reach 2	Barataria Bay 2	Barataria Bay 3
Barataria Bay	Reach 3	Barataria Bay 3	Barataria Bay 4
Barataria Bay	Reach 4		Barataria Bay 4
Barataria Bay	Reach 5	Barataria Bay 4	
Barataria Bay WW	Reach 1	Barataria Bay WW 1	Barataria Bay WW 2
Barataria Bay WW	Reach 2	Barataria Bay WW 2	Barataria Bay WW 3
Barataria Bay WW	Reach 3	Barataria Bay WW 3	Barataria Bay WW 4
Barataria Bay WW	Reach 4	Barataria Bay WW 4	Barataria Bay 1
Bayou Lamoque	Reach 1	Bayous N&S	
Bayou Lamoque N	Reach 1	Bayou Lamoque N	Bayous N&S
Bayou Lamoque S	Reach 1	Bayou Lamoque S	Bayous N&S
Bayou Perot	Reach 1	ICCW2	Bayous P&R 1
Bayou Perot	Reach 2	Bayous P&R 1	Bayou P&R 2
Bayou Rigolettes	Reach 1	Bayous P&R 1	Bayou Rigolettes
Bayou Rigolettes	Reach 2	Bayou Rigolettes	Barataria Bay WW 3
Bayou Rigolettes	Reach 3	Bayou Rigolettes	Bayou P&R 2
Bayous P&R	Reach 1	Bayou P&R 2	Little Lake 1
Caernarvon Diversion	Reach 1	Caernarvon	
Davis Pond Diversion	Reach 1	Davis Pond Diversion	Lake Cataouatche 1
Davis Pond Diversion	Lake Cataouatche Right	Lake Cataouatche 1	Lake Cataouatche 2
Davis Pond Diversion	Lake Cataouatche Left	Lake Cataouatche 1	Lake Cataouatche 2
Davis Pond Diversion	Lake Salvador Center	Lake Cataouatche 2	Lake Salvador 1
Davis Pond Diversion	Lake Salvador Right	Lake Salvador 1	Lake Salvador 2
Davis Pond Diversion	Lake Salvador Left	Lake Salvador 1	Des Allemands 4
Davis Pond Diversion	Reach 4	Des Allemands 4	ICCW1
Davis Pond Diversion	Reach 5	ICCW1	ICCW2
Des Allemands	Reach 2.0		Des Allemands 1
Des Allemands	Reach 1.0		Des Allemands 1
Des Allemands	Reach 3.0	Des Allemands 1	Des Allemands 2
Des Allemands	Reach 4.0	Des Allemands 2	Des Allemands 3
Des Allemands	Reach 5.0	Des Allemands 2	Des Allemands 3
Des Allemands	Reach 6.0	Des Allemands 3	Des Allemands 4
Fort St. Philip	Reach 1	Fort St. Philip	
Grand Pass	Reach 1	Grand Pass	Tiger Pass

**Table A-3 Continued.**

Grand Pass	Reach 2	Tiger Pass	
Head of Passes	Reach 1	Pass a Loutr�	South & Southwest
ICCW	Reach 4	Lake Salvador 2	ICCW1
ICCW	Reach 5		ICCW2
ICCW	Reach 1	ICCW H&C	The Pen 1
ICCW	Reach 2	The Pen 1	Barataria Bay WW 1
ICCW	Reach 3	Lake Salvador 2	Barataria Bay WW 1
ICCW Chalmette	Reach 1	ICCW Chalmette	ICCW H&C
ICCW Harvey	Reach 1	ICCW Harvey	ICCW H&C
Little Lake	Reach 1	Little Lake 1	Little Lake 2
Little Lake	Reach 2	Little Lake 1	Little Lake 2
Little Lake	Reach 3	Little Lake 2	Little Lake 3
Little Lake	Reach 4	Little Lake 3	Barataria Bay 1
Little Lake	Reach 5	Little Lake 3	Barataria Bay 3
Main Pass	Reach 1	Main Pass	
Mississippi	Reach 1		Davis Pond Diversion
Mississippi	Reach 2	Davis Pond Diversion	ICCW Harvey
Mississippi	Reach 3	ICCW Harvey	ICCW Chalmette
Mississippi	Reach 4	ICCW Chalmette	Caernarvon
Mississippi	Reach 5	Caernarvon	Bayou Lamoque N
Mississippi	Reach 6	Bayou Lamoque N	Bayou Lamoque S
Mississippi	Reach 7	Bayou Lamoque S	Fort St. Philip
Mississippi	Reach 8	Fort St. Philip	Baptiste Collette
Mississippi	Reach 9	Baptiste Collette	Grand Pass
Mississippi	Reach 10	Grand Pass	Main Pass
Mississippi	Reach 12	Main Pass	Pass a Loutr�
Pass a Loutr�	Reach 1	Pass a Loutr�	
South Pass	Reach 1	South & Southwest	
Southwest Pass	Reach 1	South & Southwest	
The Pen	Reach 1	The Pen 1	The Pen 2
The Pen	Reach 1.5	Barataria Bay WW 2	The Pen 2
The Pen	Reach 2	The Pen 2	The Pen 3
The Pen	Reach 2.5	Barataria Bay WW 4	The Pen 3
The Pen	Reach 3	The Pen 3	Wilkinson Canal
Tiger Pass	Reach 1	Tiger Pass	
Wilkinson Canal	Reach 1		Wilkinson Canal
Wilkinson Canal	Reach 2	Wilkinson Canal	Barataria Bay 2

**Table A-4: Junction Data for 2007 WB\_B simulation.**

River	Reach	Upstream Junction	Downstream Junction
Baptiste Collette	Reach 1	Baptiste Collette	
Barataria Bay	Reach 1	Barataria Bay 1	Barataria Bay 2
Barataria Bay	Reach 2	Barataria Bay 2	Barataria Bay 3
Barataria Bay	Reach 3	Barataria Bay 3	Barataria Bay 4
Barataria Bay	Reach 4		Barataria Bay 4
Barataria Bay	Reach 5	Barataria Bay 4	
Barataria Bay WW	Reach 1	Barataria Bay WW 1	Barataria Bay WW 2
Barataria Bay WW	Reach 2	Barataria Bay WW 2	Barataria Bay WW 3
Barataria Bay WW	Reach 3	Barataria Bay WW 3	Barataria Bay WW 4
Barataria Bay WW	Reach 4	Barataria Bay WW 4	Barataria Bay 1
Bayou Lamoque	Reach 1	Bayous N&S	
Bayou Lamoque N	Reach 1	Bayou Lamoque N	Bayous N&S
Bayou Lamoque S	Reach 1	Bayou Lamoque S	Bayous N&S
Bayou Perot	Reach 1	ICCW2	Bayous P&R 1
Bayou Perot	Reach 2	Bayous P&R 1	Bayou P&R 2
Bayou Rigolettes	Reach 1	Bayous P&R 1	Bayou Rigolettes
Bayou Rigolettes	Reach 2	Bayou Rigolettes	Barataria Bay WW 3
Bayou Rigolettes	Reach 3	Bayou Rigolettes	Bayou P&R 2
Bayous P&R	Reach 1	Bayou P&R 2	Little Lake 1
Buras	Reach 1	Buras	
Caernarvon Diversion	Reach 1	Caernarvon	
Davis Pond Diversion	Reach 1	Davis Pond Diversion	Lake Cataouatche 1
Davis Pond Diversion	Lake Cataouatche Right	Lake Cataouatche 1	Lake Cataouatche 2
Davis Pond Diversion	Lake Cataouatche Left	Lake Cataouatche 1	Lake Cataouatche 2
Davis Pond Diversion	Lake Salvador Center	Lake Cataouatche 2	Lake Salvador 1
Davis Pond Diversion	Lake Salvador Right	Lake Salvador 1	Lake Salvador 2
Davis Pond Diversion	Lake Salvador Left	Lake Salvador 1	Des Allemands 4
Davis Pond Diversion	Reach 4	Des Allemands 4	ICCW1
Davis Pond Diversion	Reach 5	ICCW1	ICCW2
Des Allemands	Reach 2.0		Des Allemands 1
Des Allemands	Reach 1.0		Des Allemands 1
Des Allemands	Reach 3.0	Des Allemands 1	Des Allemands 2
Des Allemands	Reach 4.0	Des Allemands 2	Des Allemands 3
Des Allemands	Reach 5.0	Des Allemands 2	Des Allemands 3
Des Allemands	Reach 6.0	Des Allemands 3	Des Allemands 4
Fort St. Philip	Reach 1	Fort St. Philip	
Grand Pass	Reach 1	Grand Pass	Tiger Pass

**Tale A-4 Continued.**

Grand Pass	Reach 2	Tiger Pass	
Head of Passes	Reach 1	Pass a Loutr�	South & Southwest
ICCW	Reach 4	Lake Salvador 2	ICCW1
ICCW	Reach 5		ICCW2
ICCW	Reach 1	ICCW H&C	The Pen 1
ICCW	Reach 2	The Pen 1	Barataria Bay WW 1
ICCW	Reach 3	Lake Salvador 2	Barataria Bay WW 1
ICCW Chalmette	Reach 1	ICCW Chalmette	ICCW H&C
ICCW Harvey	Reach 1	ICCW Harvey	ICCW H&C
Little Lake	Reach 1	Little Lake 1	Little Lake 2
Little Lake	Reach 2	Little Lake 1	Little Lake 2
Little Lake	Reach 3	Little Lake 2	Little Lake 3
Little Lake	Reach 4	Little Lake 3	Barataria Bay 1
Little Lake	Reach 5	Little Lake 3	Barataria Bay 3
Main Pass	Reach 1	Main Pass	
Mississippi	Reach 1		Davis Pond Diversion
Mississippi	Reach 2	Davis Pond Diversion	ICCW Harvey
Mississippi	Reach 3	ICCW Harvey	ICCW Chalmette
Mississippi	Reach 4	ICCW Chalmette	Caernarvon
Mississippi	Reach 5	Caernarvon	Bayou Lamoque N
Mississippi	Reach 6	Bayou Lamoque N	Bayou Lamoque S
Mississippi	Reach 7	Bayou Lamoque S	Buras
Mississippi	Buras	Buras	Fort St. Philip
Mississippi	Reach 8	Fort St. Philip	Baptiste Collette
Mississippi	Reach 9	Baptiste Collette	Grand Pass
Mississippi	Reach 10	Grand Pass	Main Pass
Mississippi	Reach 12	Main Pass	Pass a Loutr�
Pass a Loutr�	Reach 1	Pass a Loutr�	
South Pass	Reach 1	South & Southwest	
Southwest Pass	Reach 1	South & Southwest	
The Pen	Reach 1	The Pen 1	The Pen 2
The Pen	Reach 1.5	Barataria Bay WW 2	The Pen 2
The Pen	Reach 2	The Pen 2	The Pen 3
The Pen	Reach 2.5	Barataria Bay WW 4	The Pen 3
The Pen	Reach 3	The Pen 3	Wilkinson Canal
Tiger Pass	Reach 1	Tiger Pass	
Wilkinson Canal	Reach 1		Wilkinson Canal
Wilkinson Canal	Reach 2	Wilkinson Canal	Barataria Bay 2

**Table A-5: Junction Data for 2007 WB\_JB\_B simulation.**

River	Reach	Upstream Junction	Downstream Junction
Baptiste Collette	Reach 1	Baptiste Collette	
Barataria Bay	Reach 1	Barataria Bay 1	Barataria Bay 2
Barataria Bay	Reach 2	Barataria Bay 2	Barataria Bay 3
Barataria Bay	Reach 3	Barataria Bay 3	Barataria Bay 4
Barataria Bay	Reach 4		Barataria Bay 4
Barataria Bay	Reach 5	Barataria Bay 4	
Barataria Bay WW	Reach 1	Barataria Bay WW 1	Barataria Bay WW 2
Barataria Bay WW	Reach 2	Barataria Bay WW 2	Barataria Bay WW 3
Barataria Bay WW	Reach 3	Barataria Bay WW 3	Barataria Bay WW 4
Barataria Bay WW	Reach 4	Barataria Bay WW 4	Barataria Bay 1
Bayou Lamoque	Reach 1	Bayous N&S	
Bayou Lamoque N	Reach 1	Bayou Lamoque N	Bayous N&S
Bayou Lamoque S	Reach 1	Bayou Lamoque S	Bayous N&S
Bayou Perot	Reach 1	ICCW2	Bayous P&R 1
Bayou Perot	Reach 2	Bayous P&R 1	Bayou P&R 2
Bayou Rigolettes	Reach 1	Bayous P&R 1	Bayou Rigolettes
Bayou Rigolettes	Reach 2	Bayou Rigolettes	Barataria Bay WW 3
Bayou Rigolettes	Reach 3	Bayou Rigolettes	Bayou P&R 2
Bayous P&R	Reach 1	Bayou P&R 2	Little Lake 1
Buras	Reach 1	Buras	
Caernarvon Diversion	Reach 1	Caernarvon	
Davis Pond Diversion	Reach 1	Davis Pond Diversion	Lake Cataouatche 1
Davis Pond Diversion	Lake Cataouatche Right	Lake Cataouatche 1	Lake Cataouatche 2
Davis Pond Diversion	Lake Cataouatche Left	Lake Cataouatche 1	Lake Cataouatche 2
Davis Pond Diversion	Lake Salvador Center	Lake Cataouatche 2	Lake Salvador 1
Davis Pond Diversion	Lake Salvador Right	Lake Salvador 1	Lake Salvador 2
Davis Pond Diversion	Lake Salvador Left	Lake Salvador 1	Des Allemands 4
Davis Pond Diversion	Reach 4	Des Allemands 4	ICCW1
Davis Pond Diversion	Reach 5	ICCW1	ICCW2
Des Allemands	Reach 2.0		Des Allemands 1
Des Allemands	Reach 1.0		Des Allemands 1
Des Allemands	Reach 3.0	Des Allemands 1	Des Allemands 2
Des Allemands	Reach 4.0	Des Allemands 2	Des Allemands 3
Des Allemands	Reach 5.0	Des Allemands 2	Des Allemands 3
Des Allemands	Reach 6.0	Des Allemands 3	Des Allemands 4
Fort St. Philip	Reach 1	Fort St. Philip	
Grand Pass	Reach 1	Grand Pass	Tiger Pass



**Table A-5 Continued.**

Grand Pass	Reach 2	Tiger Pass	
Head of Passes	Reach 1	Pass a Loutr�	South & Southwest
ICCW	Reach 4	Lake Salvador 2	ICCW1
ICCW	Reach 5		ICCW2
ICCW	Reach 1	ICCW H&C	The Pen 1
ICCW	Reach 2	The Pen 1	Barataria Bay WW 1
ICCW	Reach 3	Lake Salvador 2	Barataria Bay WW 1
ICCW Chalmette	Reach 1	ICCW Chalmette	ICCW H&C
ICCW Harvey	Reach 1	ICCW Harvey	ICCW H&C
Jesuit Bend	Reach 1	Jesuit Bend1	Jesuit Bend2
Little Lake	Reach 1	Little Lake 1	Little Lake 2
Little Lake	Reach 2	Little Lake 1	Little Lake 2
Little Lake	Reach 3	Little Lake 2	Little Lake 3
Little Lake	Reach 4	Little Lake 3	Barataria Bay 1
Little Lake	Reach 5	Little Lake 3	Barataria Bay 3
Main Pass	Reach 1	Main Pass	
Mississippi	Reach 1		Davis Pond Diversion
Mississippi	Reach 2	Davis Pond Diversion	ICCW Harvey
Mississippi	Reach 3	ICCW Harvey	ICCW Chalmette
Mississippi	Reach 4	ICCW Chalmette	Caernarvon
Mississippi	Reach 5	Caernarvon	Jesuit Bend1
Mississippi	Jesuit Bend	Jesuit Bend1	Bayou Lamoque N
Mississippi	Reach 6	Bayou Lamoque N	Bayou Lamoque S
Mississippi	Reach 7	Bayou Lamoque S	Buras
Mississippi	Buras	Buras	Fort St. Philip
Mississippi	Reach 8	Fort St. Philip	Baptiste Collette
Mississippi	Reach 9	Baptiste Collette	Grand Pass
Mississippi	Reach 10	Grand Pass	Main Pass
Mississippi	Reach 12	Main Pass	Pass a Loutr�
Pass a Loutr�	Reach 1	Pass a Loutr�	
South Pass	Reach 1	South & Southwest	
Southwest Pass	Reach 1	South & Southwest	
The Pen	Reach 1	The Pen 1	Jesuit Bend2
The Pen	Jesuit Bend	Jesuit Bend2	The Pen 2
The Pen	Reach 1.5	Barataria Bay WW 2	The Pen 2
The Pen	Reach 2	The Pen 2	The Pen 3
The Pen	Reach 2.5	Barataria Bay WW 4	The Pen 3
The Pen	Reach 3	The Pen 3	Wilkinson Canal

**Table A-5 Continued.**

Tiger Pass	Reach 1	Tiger Pass	
Wilkinson Canal	Reach 1		Wilkinson Canal
Wilkinson Canal	Reach 2	Wilkinson Canal	Barataria Bay 2

**Table A-6: Junction Data for 2007 WB\_JB\_MG\_B simulation.**

River	Reach	Upstream Junction	Downstream Junction
Baptiste Collette	Reach 1	Baptiste Collette	
Barataria Bay	Reach 1	Barataria Bay 1	Barataria Bay 2
Barataria Bay	Reach 2	Barataria Bay 2	Barataria Bay 3
Barataria Bay	Reach 3	Barataria Bay 3	Barataria Bay 4
Barataria Bay	Reach 4		Barataria Bay 4
Barataria Bay	Reach 5	Barataria Bay 4	
Barataria Bay WW	Reach 1	Barataria Bay WW 1	Barataria Bay WW 2
Barataria Bay WW	Reach 2	Barataria Bay WW 2	Barataria Bay WW 3
Barataria Bay WW	Reach 3	Barataria Bay WW 3	Barataria Bay WW 4
Barataria Bay WW	Reach 4	Barataria Bay WW 4	Barataria Bay 1
Bayou Lamoque	Reach 1	Bayous N&S	
Bayou Lamoque N	Reach 1	Bayou Lamoque N	Bayous N&S
Bayou Lamoque S	Reach 1	Bayou Lamoque S	Bayous N&S
Bayou Perot	Reach 1	ICCW2	Bayous P&R 1
Bayou Perot	Reach 2	Bayous P&R 1	Bayou P&R 2
Bayou Rigolettes	Reach 1	Bayous P&R 1	Bayou Rigolettes
Bayou Rigolettes	Reach 2	Bayou Rigolettes	Barataria Bay WW 3
Bayou Rigolettes	Reach 3	Bayou Rigolettes	Bayou P&R 2
Bayous P&R	Reach 1	Bayou P&R 2	Little Lake 1
Buras	Reach 1	Buras	
Caernarvon Diversion	Reach 1	Caernarvon	
Davis Pond Diversion	Reach 1	Davis Pond Diversion	Lake Cataouatche 1
Davis Pond Diversion	Lake Cataouatche Right	Lake Cataouatche 1	Lake Cataouatche 2
Davis Pond Diversion	Lake Cataouatche Left	Lake Cataouatche 1	Lake Cataouatche 2
Davis Pond Diversion	Lake Salvador Center	Lake Cataouatche 2	Lake Salvador 1
Davis Pond Diversion	Lake Salvador Right	Lake Salvador 1	Lake Salvador 2
Davis Pond Diversion	Lake Salvador Left	Lake Salvador 1	Des Allemands 4
Davis Pond Diversion	Reach 4	Des Allemands 4	ICCW1
Davis Pond Diversion	Reach 5	ICCW1	ICCW2
Des Allemands	Reach 2.0		Des Allemands 1
Des Allemands	Reach 1.0		Des Allemands 1
Des Allemands	Reach 3.0	Des Allemands 1	Des Allemands 2
Des Allemands	Reach 4.0	Des Allemands 2	Des Allemands 3
Des Allemands	Reach 5.0	Des Allemands 2	Des Allemands 3
Des Allemands	Reach 6.0	Des Allemands 3	Des Allemands 4
Fort St. Philip	Reach 1	Fort St. Philip	
Grand Pass	Reach 1	Grand Pass	Tiger Pass

**Table A-6 Continued.**

Grand Pass	Reach 2	Tiger Pass	
Head of Passes	Reach 1	Pass a Loutr�	South & Southwest
ICCW	Reach 4	Lake Salvador 2	ICCW1
ICCW	Reach 5		ICCW2
ICCW	Reach 1	ICCW H&C	The Pen 1
ICCW	Reach 2	The Pen 1	Barataria Bay WW 1
ICCW	Reach 3	Lake Salvador 2	Barataria Bay WW 1
ICCW Chalmette	Reach 1	ICCW Chalmette	ICCW H&C
ICCW Harvey	Reach 1	ICCW Harvey	ICCW H&C
Jesuit Bend	Reach 1	Jesuit Bend1	Jesuit Bend2
Little Lake	Reach 1	Little Lake 1	Little Lake 2
Little Lake	Reach 2	Little Lake 1	Little Lake 2
Little Lake	Reach 3	Little Lake 2	Little Lake 3
Little Lake	Reach 4	Little Lake 3	Barataria Bay 1
Little Lake	Reach 5	Little Lake 3	Barataria Bay 3
Main Pass	Reach 1	Main Pass	
Mississippi	Reach 1		Davis Pond Diversion
Mississippi	Reach 2	Davis Pond Diversion	ICCW Harvey
Mississippi	Reach 3	ICCW Harvey	ICCW Chalmette
Mississippi	Reach 4	ICCW Chalmette	Caernarvon
Mississippi	Reach 5	Caernarvon	Jesuit Bend1
Mississippi	Jesuit Bend	Jesuit Bend1	Myrtle Grove
Mississippi	Myrtle Grove	Myrtle Grove	Bayou Lamoque N
Mississippi	Reach 6	Bayou Lamoque N	Bayou Lamoque S
Mississippi	Reach 7	Bayou Lamoque S	Buras
Mississippi	Buras	Buras	Fort St. Philip
Mississippi	Reach 8	Fort St. Philip	Baptiste Collette
Mississippi	Reach 9	Baptiste Collette	Grand Pass
Mississippi	Reach 10	Grand Pass	Main Pass
Mississippi	Reach 12	Main Pass	Pass a Loutr�
Pass a Loutr�	Reach 1	Pass a Loutr�	
South Pass	Reach 1	South & Southwest	
Southwest Pass	Reach 1	South & Southwest	
The Pen	Reach 1	The Pen 1	Jesuit Bend2
The Pen	Jesuit Bend	Jesuit Bend2	The Pen 2
The Pen	Reach 1.5	Barataria Bay WW 2	The Pen 2
The Pen	Reach 2	The Pen 2	The Pen 3
The Pen	Reach 2.5	Barataria Bay WW 4	The Pen 3

**Table A-6 Continued.**

The Pen	Reach 3	The Pen 3	Wilkinson Canal
Tiger Pass	Reach 1	Tiger Pass	
Wilkinson Canal	Reach 1	Myrtle Grove	Wilkinson Canal
Wilkinson Canal	Reach 2	Wilkinson Canal	Barataria Bay 2

**Table A-7: Junction Data for 2007 WB\_JB\_MG\_DR\_B, WB\_Div\_SP, WB\_Div\_SWP, WB\_Div\_SP\_SWP\_pal50, and WB\_Div\_SP\_SWP\_pal40 simulations.**

River	Reach	Upstream Junction	Downstream Junction
Baptiste Collette	Reach 1	Baptiste Collette	
Barataria Bay	Reach 1	Barataria Bay 1	Barataria Bay 2
Barataria Bay	Reach 2	Barataria Bay 2	Barataria Bay 3
Barataria Bay	Reach 3	Barataria Bay 3	Barataria Bay 4
Barataria Bay	Reach 4		Barataria Bay 4
Barataria Bay	Reach 5	Barataria Bay 4	
Barataria Bay WW	Reach 1	Barataria Bay WW 1	Barataria Bay WW 2
Barataria Bay WW	Reach 2	Barataria Bay WW 2	Barataria Bay WW 3
Barataria Bay WW	Reach 3	Barataria Bay WW 3	Barataria Bay WW 4
Barataria Bay WW	Reach 4	Barataria Bay WW 4	Barataria Bay 1
Bayou Lamoque	Reach 1	Bayous N&S	
Bayou Lamoque N	Reach 1	Bayou Lamoque N	Bayous N&S
Bayou Lamoque S	Reach 1	Bayou Lamoque S	Bayous N&S
Bayou Perot	Reach 1	ICCW2	Bayous P&R 1
Bayou Perot	Reach 2	Bayous P&R 1	Bayou P&R 2
Bayou Rigolettes	Reach 1	Bayous P&R 1	Bayou Rigolettes
Bayou Rigolettes	Reach 2	Bayou Rigolettes	Barataria Bay WW 3
Bayou Rigolettes	Reach 3	Bayou Rigolettes	Bayou P&R 2
Bayous P&R	Reach 1	Bayou P&R 2	Little Lake 1
Buras	Reach 1	Buras	
Caernarvon Diversion	Reach 1	Caernarvon	
Davis Pond Diversion	Reach 1	Davis Pond Diversion	Lake Cataouatche 1
Davis Pond Diversion	Lake Cataouatche Right	Lake Cataouatche 1	Lake Cataouatche 2
Davis Pond Diversion	Lake Cataouatche Left	Lake Cataouatche 1	Lake Cataouatche 2
Davis Pond Diversion	Lake Salvador Center	Lake Cataouatche 2	Lake Salvador 1
Davis Pond Diversion	Lake Salvador Right	Lake Salvador 1	Lake Salvador 2
Davis Pond Diversion	Lake Salvador Left	Lake Salvador 1	Des Allemands 4
Davis Pond Diversion	Reach 4	Des Allemands 4	ICCW1
Davis Pond Diversion	Reach 5	ICCW1	ICCW2
Deer Range	Reach 1	Deer Range	
Des Allemands	Reach 2.0		Des Allemands 1
Des Allemands	Reach 1.0		Des Allemands 1
Des Allemands	Reach 3.0	Des Allemands 1	Des Allemands 2
Des Allemands	Reach 4.0	Des Allemands 2	Des Allemands 3
Des Allemands	Reach 5.0	Des Allemands 2	Des Allemands 3
Des Allemands	Reach 6.0	Des Allemands 3	Des Allemands 4

**Table A-7 Continued.**

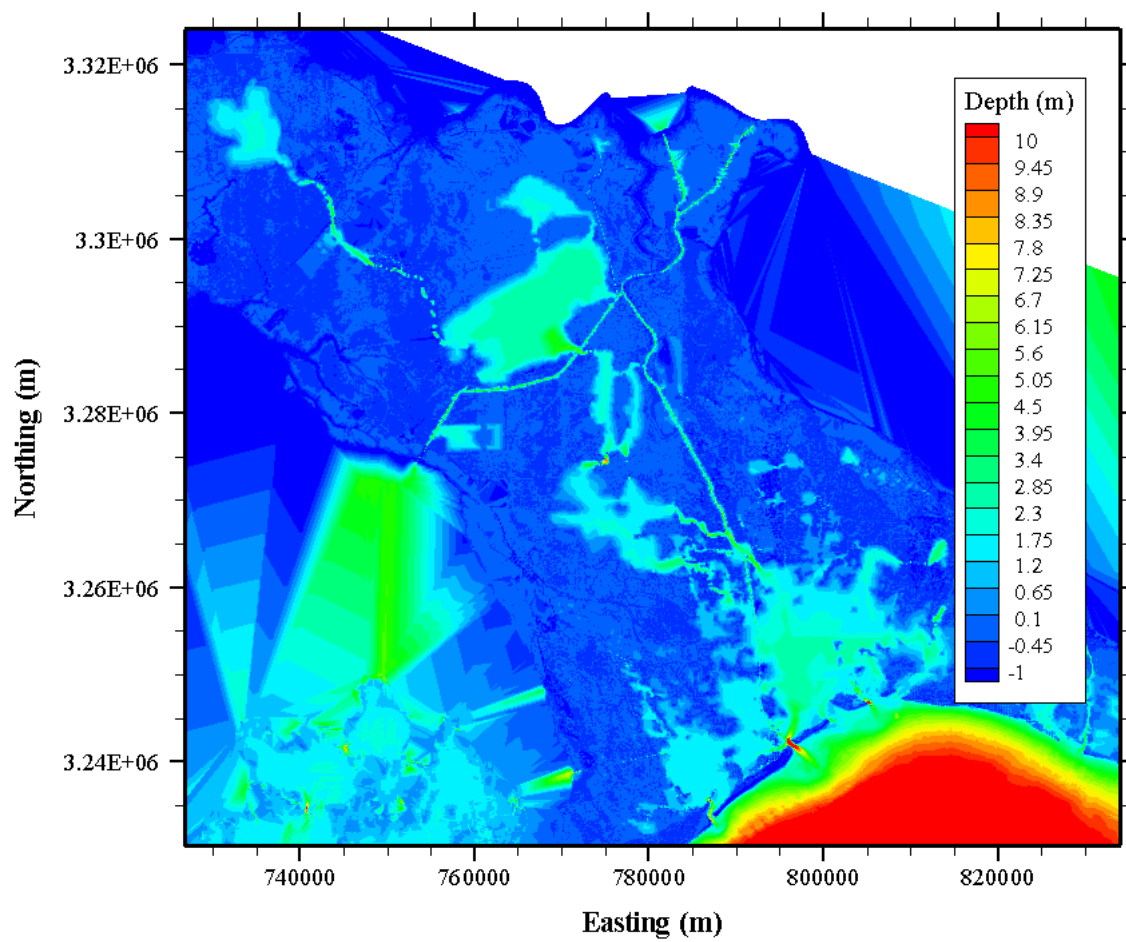
Fort St. Philip	Reach 1	Fort St. Philip	
Grand Pass	Reach 1	Grand Pass	Tiger Pass
Grand Pass	Reach 2	Tiger Pass	
Head of Passes	Reach 1	Pass a Loutr�	South & Southwest
ICCW	Reach 4	Lake Salvador 2	ICCW1
ICCW	Reach 5		ICCW2
ICCW	Reach 1	ICCW H&C	The Pen 1
ICCW	Reach 2	The Pen 1	Barataria WW 1
ICCW	Reach 3	Lake Salvador 2	Barataria WW 1
ICCW Chalmette	Reach 1	ICCW Chalmette	ICCW H&C
ICCW Harvey	Reach 1	ICCW Harvey	ICCW H&C
Jesuit Bend	Reach 1	Jesuit Bend1	Jesuit Bend2
Little Lake	Reach 1	Little Lake 1	Little Lake 2
Little Lake	Reach 2	Little Lake 1	Little Lake 2
Little Lake	Reach 3	Little Lake 2	Little Lake 3
Little Lake	Reach 4	Little Lake 3	Barataria Bay 1
Little Lake	Reach 5	Little Lake 3	Barataria Bay 3
Main Pass	Reach 1	Main Pass	
Mississippi	Reach 1		Davis Pond Diversion
Mississippi	Reach 2	Davis Pond Diversion	ICCW Harvey
Mississippi	Reach 3	ICCW Harvey	ICCW Chalmette
Mississippi	Reach 4	ICCW Chalmette	Caernarvon
Mississippi	Reach 5	Caernarvon	Jesuit Bend1
Mississippi	Jesuit Bend	Jesuit Bend1	Myrtle Grove
Mississippi	Myrtle Grove	Myrtle Grove	Deer Range
Mississippi	Deer Range	Deer Range	Bayou Lamoque N
Mississippi	Reach 6	Bayou Lamoque N	Bayou Lamoque S
Mississippi	Reach 7	Bayou Lamoque S	Buras
Mississippi	Buras	Buras	Fort St. Philip
Mississippi	Reach 8	Fort St. Philip	Baptiste Collette
Mississippi	Reach 9	Baptiste Collette	Grand Pass
Mississippi	Reach 10	Grand Pass	Main Pass
Mississippi	Reach 12	Main Pass	Pass a Loutr�
Pass a Loutr�	Reach 1	Pass a Loutr�	
South Pass	Reach 1	South & Southwest	
Southwest Pass	Reach 1	South & Southwest	
The Pen	Reach 1	The Pen 1	Jesuit Bend2
The Pen	Jesuit Bend	Jesuit Bend2	The Pen 2

**Table A-7 Continued.**

The Pen	Reach 1.5	Barataria Bay WW 2	The Pen 2
The Pen	Reach 2	The Pen 2	The Pen 3
The Pen	Reach 2.5	Barataria Bay WW 4	The Pen 3
The Pen	Reach 3	The Pen 3	Wilkinson Canal
Tiger Pass	Reach 1	Tiger Pass	
Wilkinson Canal	Reach 1	Myrtle Grove	Wilkinson Canal
Wilkinson Canal	Reach 2	Wilkinson Canal	Barataria Bay 2



**Appendix B**  
**2003 Barataria Basin LIDAR/bathymetry Image**



## **Appendix C**

### **Lacey Regime Equations**

The Lacey Regime Equations are used for the design of unlined channels. The Regime Concept states that there is a set of stable channel dimensions for each given flow and silt load. The channel dimensions include a depth, width, and bed slope. The Lacey Regime Equations are as follows:

$$P = 2.67Q^{1/2} \quad (C-1)$$

$$f_s = 8\sqrt{D_{50}} \quad (C-2)$$

$$v = 1.17\sqrt{f_s R} \quad (C-3)$$

$$v = 16R^{2/3} S_0^{1/3} \quad (C-4)$$

$$Q = Av \quad (C-5)$$

$$R = \left[ \frac{Q}{1.17 P f_s^{1/2}} \right]^{2/3} \quad (C-6)$$

$$A = PR \quad (C-7)$$

$$S_0 = \left( \frac{v}{16R^{2/3}} \right)^3 \quad (C-8)$$

where:

- $P$  = representative width [ft]
- $Q$  = flow rate [ft<sup>3</sup>/s]
- $f_s$  = silt factor
- $D_{50}$  = median grain size [in]
- $v$  = velocity [ft/s]
- $R$  = representative depth [ft]
- $S_0$  = bed slope
- $A$  = cross-sectional area [ft<sup>2</sup>]

For the purpose of this study, the avulsion channels were assumed to be rectangular with a top width of  $P$ , which was found using Google Earth Imagery. After finding the top widths, the flow rate was calculated using Equation (C-1). The median grain size for the Mississippi River was assumed to be 0.23 mm, which corresponds to 0.0091 in. Plugging this value into Equation (C-2) yielded a silt factor of 0.763. Entering the flow rate, top width, and silt factor into Equation (C-6), a representative depth was found. The representative cross-sectional area was calculated using Equation (C-7). This area was added to the HEC-RAS area of the immediate cross-section to create an equivalent cross-sectional area. For multiple avulsions at one location, the area for all of the avulsions were summed and then added to the HEC-RAS area. The new top width of the equivalent channel was then calculated by dividing this new area by the hydraulic radius of

the HEC- RAS cross-section. The following example calculates the equivalent channel for Southwest Pass at River Station 26. Figure C-1 shows the original cross section.

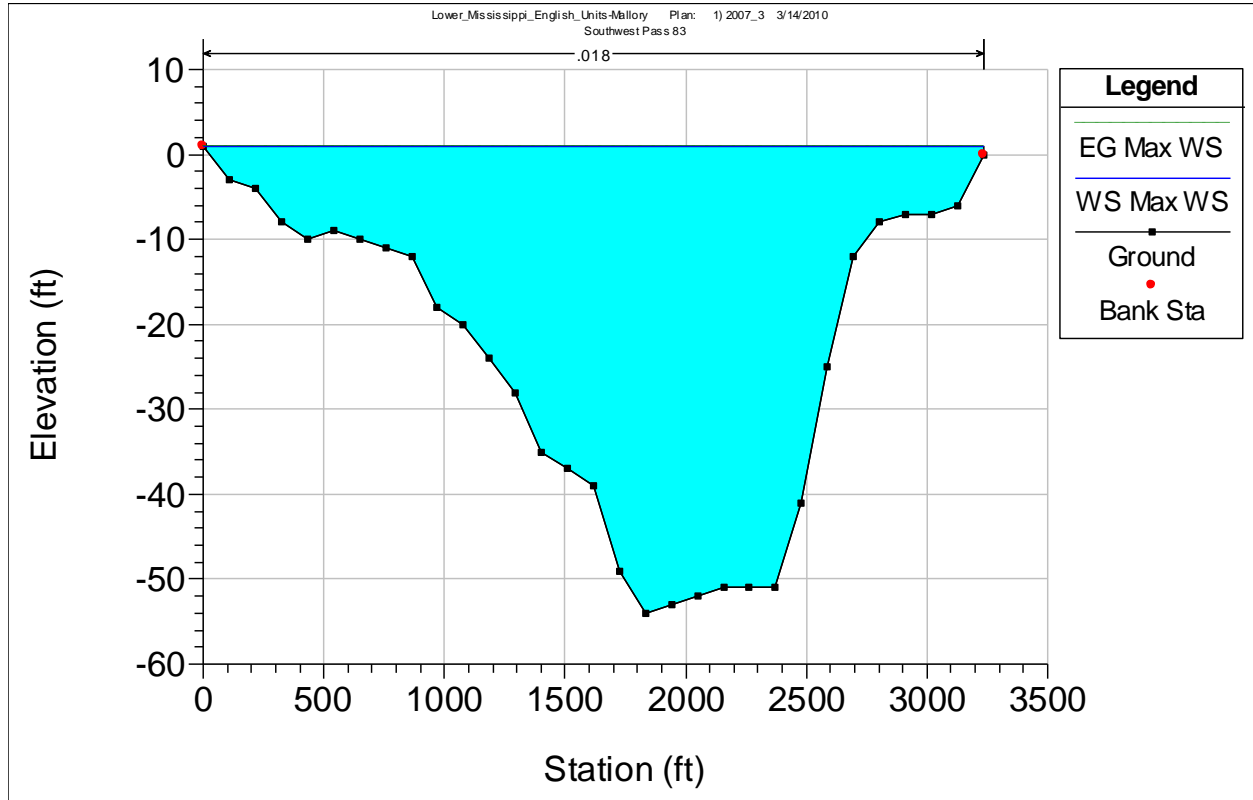


Figure C-1: HEC-RAS Original Cross Section for Southwest Pass River Station 26.

The channel dimensions are a top width of 3235 ft, a hydraulic radius of 25.12 ft, and an area of 80,933 ft<sup>2</sup>. From Google Earth Imagery an avulsion at this location was found to have a top width,  $P'$ , of 1542 ft. Previous avulsions have produced a cumulative area,  $A_c$ , of 15,487 ft<sup>2</sup>. Using Equation (C-1) to solve for the flow rate yields:

$$Q' = \left( \frac{1542 \text{ ft}}{2.67} \right)^2 = 333,539 \text{ cfs}$$

Using the silt factor calculated earlier (0.763), the representative depth was found to be:

$$R' = \left[ \frac{333,539 \text{ cfs}}{1.17 * 1542 \text{ ft} * \sqrt{0.763}} \right]^{2/3} = 35.51 \text{ ft}$$

Plugging  $R'$  and  $P'$  into Equation (C-7) gives a representative area of:

$$A' = 1542 \text{ ft} * 35.51 \text{ ft} = 54,764 \text{ ft}^2$$

Adding this area to the cumulative area and the HEC-RAS-generated area of the original cross-section gives the equivalent channel area,  $A_E$ :

$$A_E = 80,933 \text{ ft}^2 + 15,487 \text{ ft}^2 + 54,764 \text{ ft}^2 = 151,184 \text{ ft}^2$$

Dividing this equivalent area by the HEC-RAS hydraulic radius yields the equivalent top width,  $P_E$ :

$$P_E = \frac{151,184 \text{ ft}^2}{25.12 \text{ ft}} = 6018 \text{ ft}$$

Table C-1 shows the station and elevation data for the original cross-section and the new equivalent cross-section. Figure C-2 shows the equivalent cross-section in HEC-RAS.

**Table C-1: Original and Equivalent Cross-sectional Data for River Station 26.**

Original Cross-Section		Equivalent Cross-Section	
Station (ft)	Elevation (ft)	Station (ft)	Elevation (ft)
0	1	0	1
108	-3	201	-3
216	-4	401	-4
323	-8	602	-8
431	-10	802	-10
539	-9	1003	-9
647	-10	1204	-10
755	-11	1404	-11
863	-12	1605	-12
970	-18	1805	-18
1078	-20	2006	-20
1186	-24	2207	-24
1294	-28	2407	-28
1402	-35	2608	-35
1510	-37	2808	-37
1618	-39	3009	-39
1725	-49	3210	-49
1833	-54	3410	-54
1941	-53	3611	-53
2049	-52	3811	-52
2157	-51	4012	-51
2264	-51	4213	-51
2372	-51	4413	-51
2480	-41	4614	-41
2588	-25	4814	-25
2696	-12	5015	-12
2804	-8	5216	-8
2911	-7	5416	-7

**Table C-1 Continued.**

3019	-7	5617	-7
3127	-6	5817	-6
3235	0	6018	1

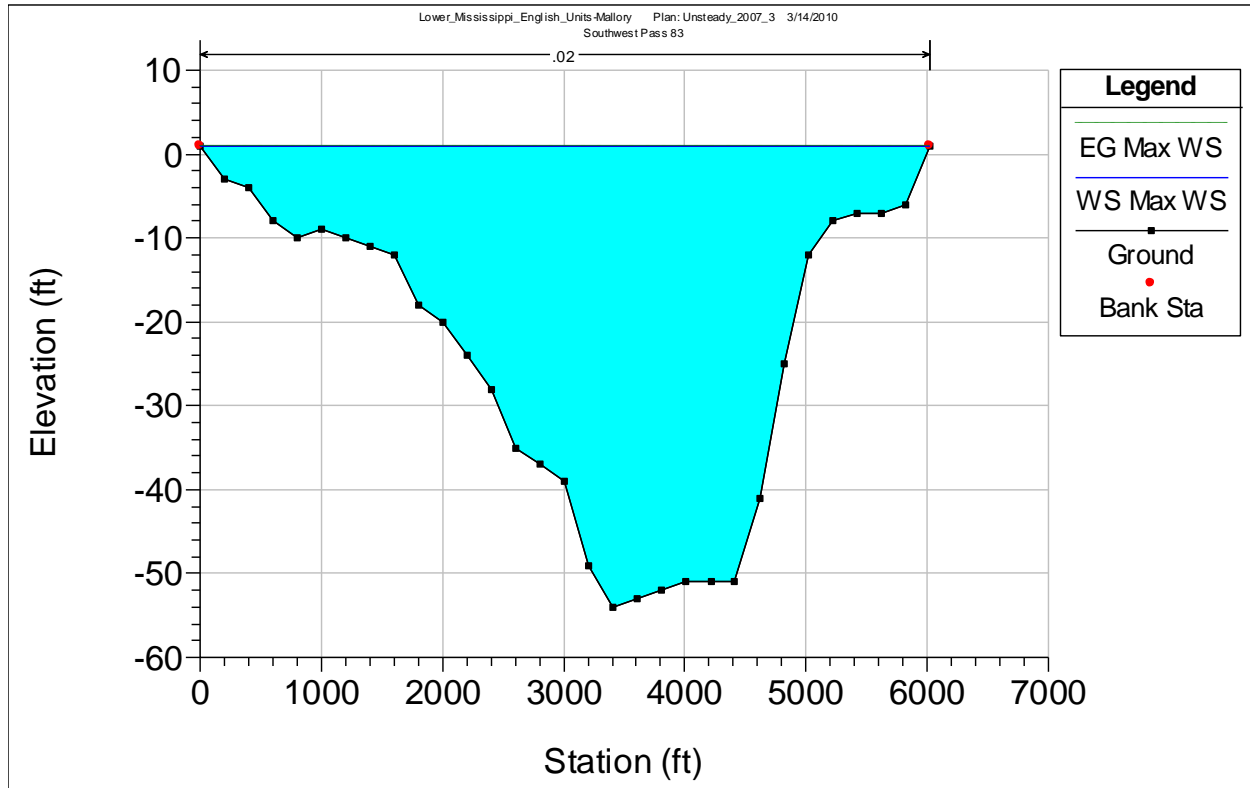


**Figure C-2: HEC-RAS Equivalent Cross Section for Southwest Pass River Station 26.**

## **Appendix D: Initial Conditions**



**Table D-1: Initial Flow Conditions for 2007, 2003, 1999-2000, and 2007-2008 simulations.**

River	Reach	2007	2003	1999-2000	2007-2008
Baptiste Collette	1	66080	110256	67562.73	54475
Barataria Bay	1	1000	1000	196.81	1000
	2	1772	1772	442.07	1772
	3	4900	4900	1050	4900
	4	100	100	100	100
	5	5000	5000	1150	5000
Barataria Bay WW	1	503	503	114.15	503
	2	362	362	82.07	362
	3	672	672	142.31	672
	4	142	142	30.14	142
Bayou Lamoque	1	12000	12000	12000	12000
Bayou Lamoque N	1	4000	4000	4000	4000
Bayou Lamoque S	1	8000	8000	8000	8000
Bayou Perot	1	4296	4296	834.84	4296
	2	3464	3464	673.27	3464
Bayou Rigolettes	1	831	831	161.57	831
	2	310	310	60.25	310
	3	521	521	101.33	521
Bayous P&R	1	3986	3986	774.59	3986
Caernarvon Diversion	1	3000	1200	1200	3000
Davis Pond Diversion	1	4000	4000	150	4000
	Lake Cataouatche Right	2316	2316	86.84	2316
	Lake Cataouatche Left	1684	1684	63.16	1684
	Lake Salvador Center	4000	4000	150	4000
	Lake Salvador Right	852	852	31.94	852
	Lake Salvador Left	3148	3148	118.06	3148
	4	3648	3648	618.06	3648
	5	4096	4096	634.84	4096
Des Allemands	2	250	250	250	250
	1	250	250	250	250
	3	500	500	500	500
	4	60	60	59.59	60
	5	440	440	440.41	440
	6	500	500	500	500
Fort St. Philip	1	6033	10059	4412.91	0
Grand Pass	1	46992	78357	48079.13	38729
	2	32894	54850	33655.39	27110

**Table D-1 Continued.**

Head of Passes	1	212662	354533	220786.1	174263
ICCW	4	448	448	16.78	448
	5	200	200	200	200
	1	200	200	200	200
	2	99	99	98.99	99
	3	404	404	15.16	404
ICCW Chalmette	1	100	100	100	100
ICCW Harvey	1	100	100	100	100
Little Lake	1	1292	1292	251.15	1292
	2	2693	2693	523.44	2693
	3	3986	3986	774.59	3986
	4	3128	3128	607.93	3128
	5	858	858	166.66	858
Main Pass	1	47120	78571	48918.94	39506
Mississippi	1	453811	741692	437818	372845
	2	449811	737692	-	368845
	3	449711	737592	437718	368745
	4	449511	737392	437518	368545
	5	446511	736192	436318	365545
	6	442011	731692	432318	361045
	7	434011	723692	424318	353045
	8	427978	713633	419905.1	353045
	9	361898	603376	352342.4	298570
	10	314906	525020	304263.2	259841
	11	293080	488624	-	241836
	12	245959	410053	255344.3	202330
Pass a Loutr�	1	33297	55521	34558.19	28067
South Pass	1	64710	107901	67226.81	53098
Southwest Pass	1	147952	246632	153559.3	121165
The Pen	1	101	101	101.01	101
	1.5	141	141	32.09	141
	2	242	242	133.1	242
	2.5	530	530	112.17	530
	3	772	772	245.27	772
Tiger Pass	1	14098	23507	14423.74	11619
West Bay	1	21827	36395	-	18005
Wilkinson Canal	1	0	0	0	0
	2	772	772	245.27	772

**Table D-2: Initial Flow Conditions for 2007 WB, WB\_SP, WB\_SWP, WB\_SP\_SWP\_pal50, and WB\_SP\_SWP\_pal40 simulations.**

River	Reach	2007 WB	2007 WB_SP	2007 WB_SWP	2007 WB_SP_SWP_pal50 and 2007 WB_SP_SWP_pal40
Baptiste Collette	1	68827	77147	96422	55627
Barataria Bay	1	1000	1000	1000	1000
	2	1772	1772	1772	1772
	3	4900	4900	4900	4900
	4	100	100	100	100
	5	5000	5000	5000	5000
Barataria WW	1	503	503	503	503
	2	362	362	362	362
	3	672	672	672	672
	4	142	142	142	142
Bayou Lamoque	1	12000	12000	12000	12000
Bayou Lamoque N	1	4000	4000	4000	4000
Bayou Lamoque S	1	8000	8000	8000	8000
Bayou Perot	1	4296	4296	4296	4296
	2	3464	3464	3464	3464
Bayou Rigolettes	1	831	831	831	831
	2	310	310	310	310
	3	521	521	521	521
Bayous P&R	1	3986	3986	3986	3986
Caernarvon Diversion	1	3000	3000	3000	3000
Davis Pond Diversion	1	4000	4000	4000	4000
	Lake Cataouatche Right	2316	2316	2316	2316
	Lake Cataouatche Left	1684	1684	1684	1684
	Lake Salvador Center	4000	4000	4000	4000
	Lake Salvador Right	852	852	852	852

**Table D-2 Continued.**

Davis Pond Diversion	Lake Salvador Left	3148	3148	3148	3148
	4	3648	3648	3648	3648
	5	4096	4096	4096	4096
Des Allemands	2	250	250	250	250
	1	250	250	250	250
	3	500	500	500	500
	4	60	60	60	60
	5	440	440	440	440
	6	500	500	500	500
Fort St. Philip	1	6250	7074	9244	5121
Grand Pass	1	48979	55032	69067	39286
	2	34285	38522	48347	27500
Head of Passes	1	224703	190969	115027	0
ICCW	4	448	448	448	448
	5	200	200	200	200
	1	200	200	200	200
	2	99	99	99	99
	3	404	404	404	404
ICCW Chalmette	1	100	100	100	100
ICCW Harvey	1	100	100	100	100
Little Lake	1	1292	1292	1292	1292
	2	2693	2693	2693	2693
	3	3986	3986	3986	3986
	4	3128	3128	3128	3128
	5	858	858	858	858
Main Pass	1	49920	59857	81725	32338
Mississippi	1	453811	453811	453811	453811
	2	449811	449811	449811	449811
	3	449711	449711	449711	449711
	4	449511	449511	449511	449511
	5	446511	446511	446511	446511
	6	442011	442011	442011	442011
	7	434011	434011	434011	434011
	8	427761	426937	424767	428890
	9	358935	349789	328345	373263
	10	309956	294757	259278	333976
	11	-	-	-	-

**Table D-2 Continued.**

Mississippi	12	260036	234901	177552	301638
Pass a Loutr�	1	35333	43932	62526	301638
South Pass	1	68399	0	115027	0
Southwest Pass	1	156304	190969	0	0
The Pen	1	101	101	101	101
	1.5	141	141	141	141
	2	242	242	242	242
	2.5	530	530	530	530
	3	772	772	772	772
Tiger Pass	1	14694	16510	20720	11786
West Bay	1	-	-	-	-
Wilkinson Canal	1	0	0	0	0
	2	772	772	772	772

**Table D-3: Initial Flow Conditions for 2007 WB\_B, WB\_JB\_B, WB\_JB\_MG\_B, and WB\_JB\_MG\_DR\_B simulations.**

River	Reach	2007 WB_B	2007 WB_JB_B	2007 WB_JB_MG_ B	2007 WB_JB_MG_DR _B
Baptiste Collette	1	59004	58216	55045	53455
Barataria Bay	1	1000	1000	1000	1000
	2	1772	6772	26772	26772
	3	4900	9900	29900	29900
	4	100	100	100	100
	5	5000	10000	30000	30000
Barataria WW	1	503	503	503	503
	2	362	362	362	362
	3	672	672	672	672
	4	142	142	142	142
Bayou Lamoque	1	12000	12000	12000	12000
Bayou Lamoque N	1	4000	4000	4000	4000
Bayou Lamoque S	1	8000	8000	8000	8000
Bayou Perot	1	4296	4296	4296	4296
	2	3464	3464	3464	3464
Bayou Rigolettes	1	831	831	831	831
	2	310	310	310	310
	3	521	521	521	521
Bayous P&R	1	3986	3986	3986	3986
Buras	1	59900	59900	59900	59900
Caernarvon Diversion	1	3000	3000	3000	3000
Davis Pond Diversion	1	4000	4000	4000	4000
	Lake Cataouatche Right	2316	2316	2316	2316
	Lake Cataouatche Left	1684	1684	1684	1684
	Lake Salvador Center	4000	4000	4000	4000
	Lake Salvador Right	852	852	852	852

**Table D-3 Continued.**

Davis Pond Diversion	Lake Salvador Left	3148	3148	3148	3148
	4	3648	3648	3648	3648
	5	4096	4096	4096	4096
Deer Range	1	-	-	-	10000
Des Allemands	2	250	250	250	250
	1	250	250	250	250
	3	500	500	500	500
	4	60	60	60	60
	5	440	440	440	440
	6	500	500	500	500
Fort St. Philip	1	5400	5295	5006	4883
Grand Pass	1	41988	41428	39171	38073
	2	29392	29000	27420	26651
Head of Passes	1	192963	190388	180084	174885
ICCW	4	448	448	448	448
	5	200	200	200	200
	1	200	200	200	200
	2	99	99	99	99
	3	404	404	404	404
ICCW Chalmette	1	100	100	100	100
ICCW Harvey	1	100	100	100	100
Jesuit Bend	1	-	5000	5000	5000
Little Lake	1	1292	1292	1292	1292
	2	2693	2693	2693	2693
	3	3986	3986	3986	3986
	4	3128	3128	3128	3128
	5	858	858	858	858
Main Pass	1	42648	42079	39753	38572
Mississippi	1	453811	453811	453811	453811
	2	449811	449811	449811	449811
	3	449711	449711	449711	449711
	4	449511	449511	449511	449611
	5	446511	446511	446511	446511
	Jesuit Bend	-	441511	441511	441511
	Myrtle Grove	-	-	420511	420011
	Deer Range	-	-	-	410011
	6	440011	435011	415011	405011
	7	432011	427011	407011	397011

**Table D-3 Continued.**

Mississippi	Buras	372111	367111	347111	337111
	8	366711	361816	342105	332228
	9	307707	303600	287060	278772
	10	265719	262172	247889	240699
	12	223070	220093	208137	202127
Pass a Loutr�	1	30107	29705	28053	27243
South Pass	1	58710	57927	54805	53223
Southwest Pass	1	134253	132461	125279	121662
The Pen	1	101	101	101	101
	Jesuit Bend	-	5101	5101	5101
	1.5	141	141	141	141
	2	242	5242	5242	5242
	2.5	530	530	530	530
	3	772	5772	5772	5772
Tiger Pass	1	12597	12428	11751	11422
Wilkinson Canal	1	0	0	20000	20000
	2	772	5772	25772	25772



**Table D-4: Initial Flow Conditions for 2007 WB\_Div\_SP, WB\_Div\_SWP, WB\_Div\_SP\_SWP\_pal50, and WB\_Div\_SP\_SWP\_pal40 simulations.**

River	Reach	2007 WB_Div_SP	2007 WB_Div_SWP	2007 WB_Div_SP_SWP_ pal50 and 2007 WB_Div_SP_SWP_ pal40
Baptiste Collette	1	60007	75389	43160
Barataria Bay	1	1000	1000	1000
	2	26772	26772	26772
	3	29900	29900	29900
	4	100	100	100
	5	30000	30000	30000
Barataria WW	1	503	503	503
	2	362	362	362
	3	672	672	672
	4	142	142	142
Bayou Lamoque	1	12000	12000	12000
Bayou Lamoque N	1	4000	4000	4000
Bayou Lamoque S	1	8000	8000	8000
Bayou Perot	1	4296	4296	4296
	2	3464	3464	3464
Bayou Rigolettes	1	831	831	831
	2	310	310	310
	3	521	521	521
Bayous P&R	1	3986	3986	3986
Buras	1	59900	59900	59900
Caernarvon Diversion	1	3000	3000	3000
Davis Pond Diversion	1	4000	4000	4000
	Lake Cataouatche Right	2316	2316	2316
	Lake Cataouatche Left	1684	1684	1684
	Lake Salvador Center	4000	4000	4000

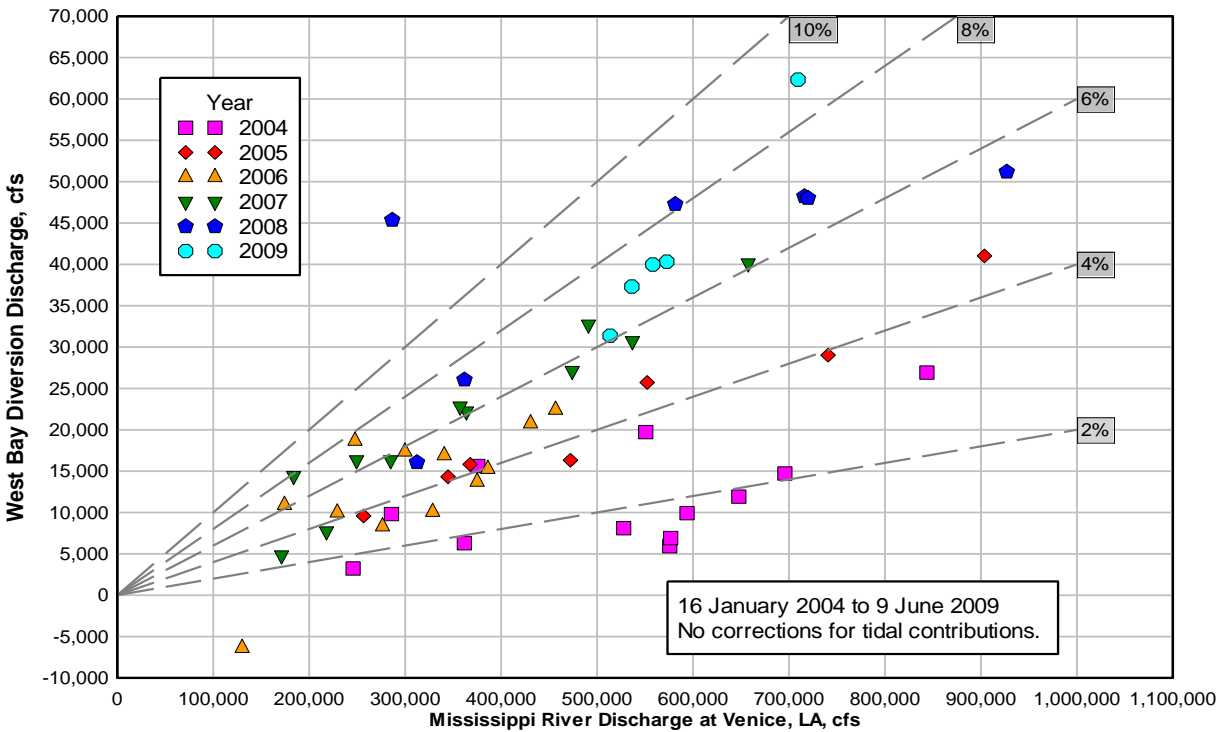
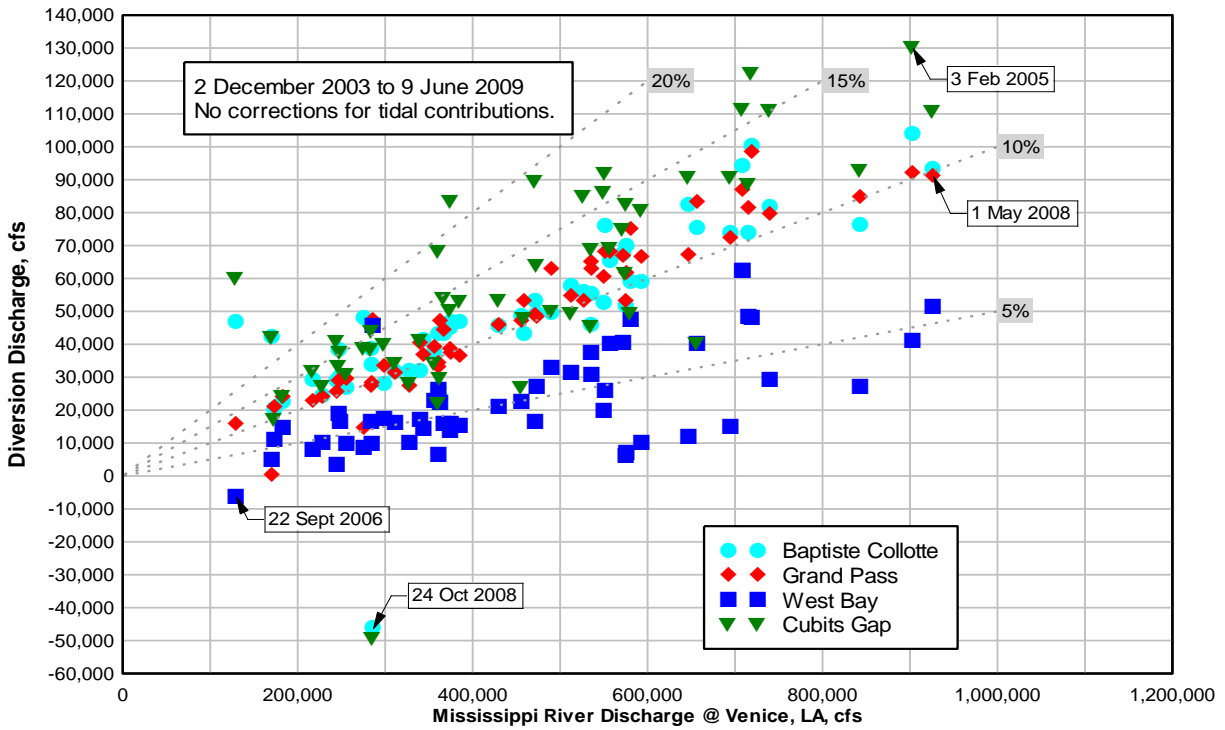
**Table D-4 Continued.**

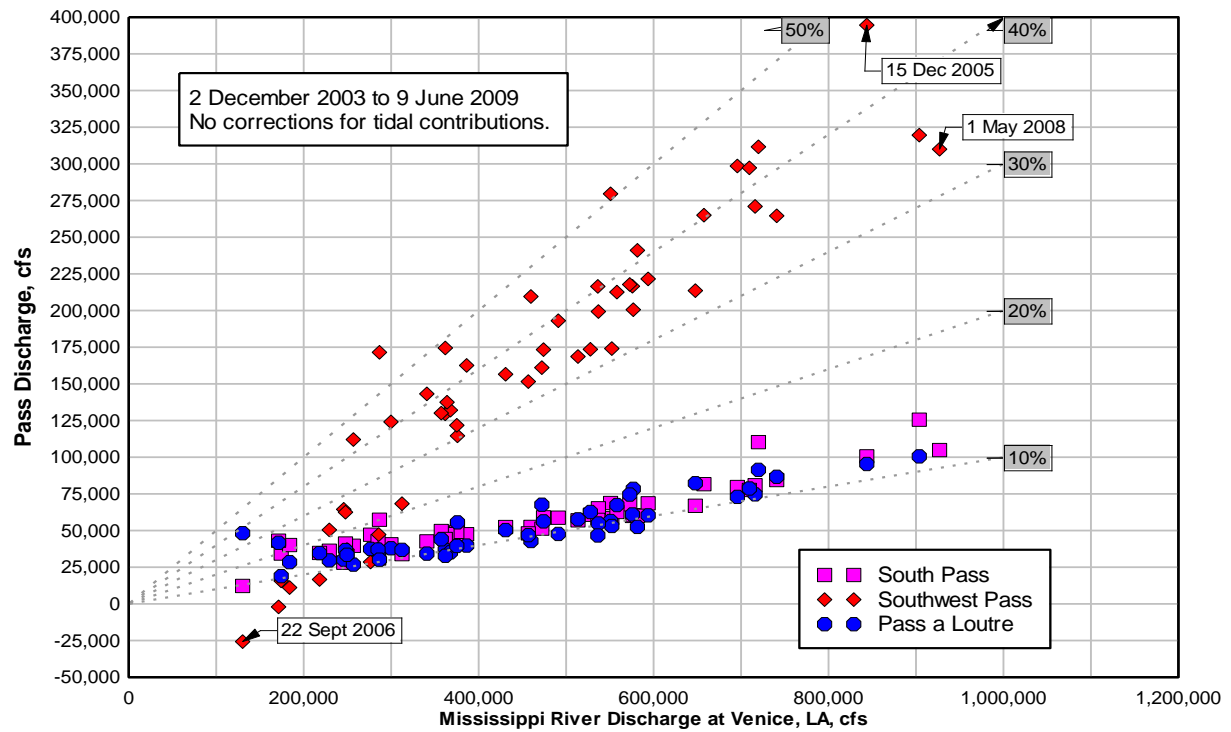
Davis Pond Diversion	Lake Salvador Right	852	852	852
	Lake Salvador Left	3148	3148	3148
	4	3648	3648	3648
	5	4096	4096	4096
Deer Range	1	10000	10000	10000
Des Allemands	2	250	250	250
	1	250	250	250
	3	500	500	500
	4	60	60	60
	5	440	440	440
	6	500	500	500
Fort St. Philip	1	5399	6749	4089
Grand Pass	1	42824	53981	30505
	2	29977	37787	21353
Head of Passes	1	148939	89891	0
ICCW	4	448	448	448
	5	200	200	200
	1	200	200	200
	2	99	99	99
	3	404	404	404
ICCW Chalmette	1	100	100	100
ICCW Harvey	1	100	100	100
Jesuit Bend	1	5000	5000	5000
Little Lake	1	1292	1292	1292
	2	2693	2693	2693
	3	3986	3986	3986
	4	3128	3128	3128
	5	858	858	858
Main Pass	1	46174	63231	25043
Mississippi	1	453811	453811	453811
	2	449811	449811	449811
	3	449711	449711	449711
	4	449611	449611	449611
	5	446511	446511	446511
	Jesuit Bend	441511	441511	441511

**Table D-4 Continued.**

Mississippi	Myrtle Grove	420011	420011	420011
	Deer Range	410011	410011	410011
	6	405011	405011	405011
	7	397011	397011	397011
	Buras	337111	337111	337111
	8	331712	330362	333022
	9	271705	254973	289862
	10	228881	200992	259357
	12	182707	137761	234314
Pass a Loutr�	1	33768	47869	234314
South Pass	1	0	89891	0
Southwest Pass	1	148939	0	0
The Pen	1	101	101	101
	Jesuit Bend	5101.01	5101	5101
	1.5	141	141	141
	2	5242	5242	5242
	2.5	530	530	530
	3	5772	5772	5772
Tiger Pass	1	12847	16194	9151
Wilkinson Canal	1	20000	20000	20000
	2	25772	25772	25772

**Appendix E**  
**Acoustic Doppler Current Profiler Charts, (Pratt, 2009)**





## **Appendix F**

### **Boundary Conditions**

**Table F-1: Time-series Gate Operations for Bayou Lamoque North and South Structures for all simulations.**

Gate Group	North Structure				South Structure			
	1	2	3	4	1	2	3	4
Gate Height (ft)	10	6	0	0	8	0	0	0

**Table F-2: Elevation Controlled Gate Operations for Caernarvon Diversion Structure for all simulations.**

Gate Group	1	2	3	4	5
Stage Difference at which gate begins to open (ft)	2	2	2	2	2
Stage Difference at which gate begins to close (ft)	4	4	4	4	4
Gate Opening Rate (ft/min)	0.1	0.1	0.1	0.1	0.1
Gate Closing Rate (ft/min)	0.1	0.1	0.1	0.1	0.1
Maximum Gate Opening (ft)	5	5	5	5	5
Minimum Gate Opening (ft)	2	2	2	2	2
Initial Gate Opening (ft)	5	5	5	5	5

**Table F-3: Elevation Controlled Gate Operations for Davis Pond Diversion Structure (2003, 2007-2008, & all 2007 simulations).**

Gate Group	1	2	3	4
Stage Difference at which gate begins to open (ft)	4.5	4.5	4.5	4.5
Stage Difference at which gate begins to close (ft)	2	2	2	2
Gate Opening Rate (ft/min)	0.095	0.095	0.095	0.095
Gate Closing Rate (ft/min)	0.095	0.095	0.095	0.095
Maximum Gate Opening (ft)	10	0	10	0
Minimum Gate Opening (ft)	1.75	0	1.75	0
Initial Gate Opening (ft)	6	0	6	0



**Table F-4: Gate Operations for 2008 Opening of the Bonnet Carré Spillway Lateral Structure.**

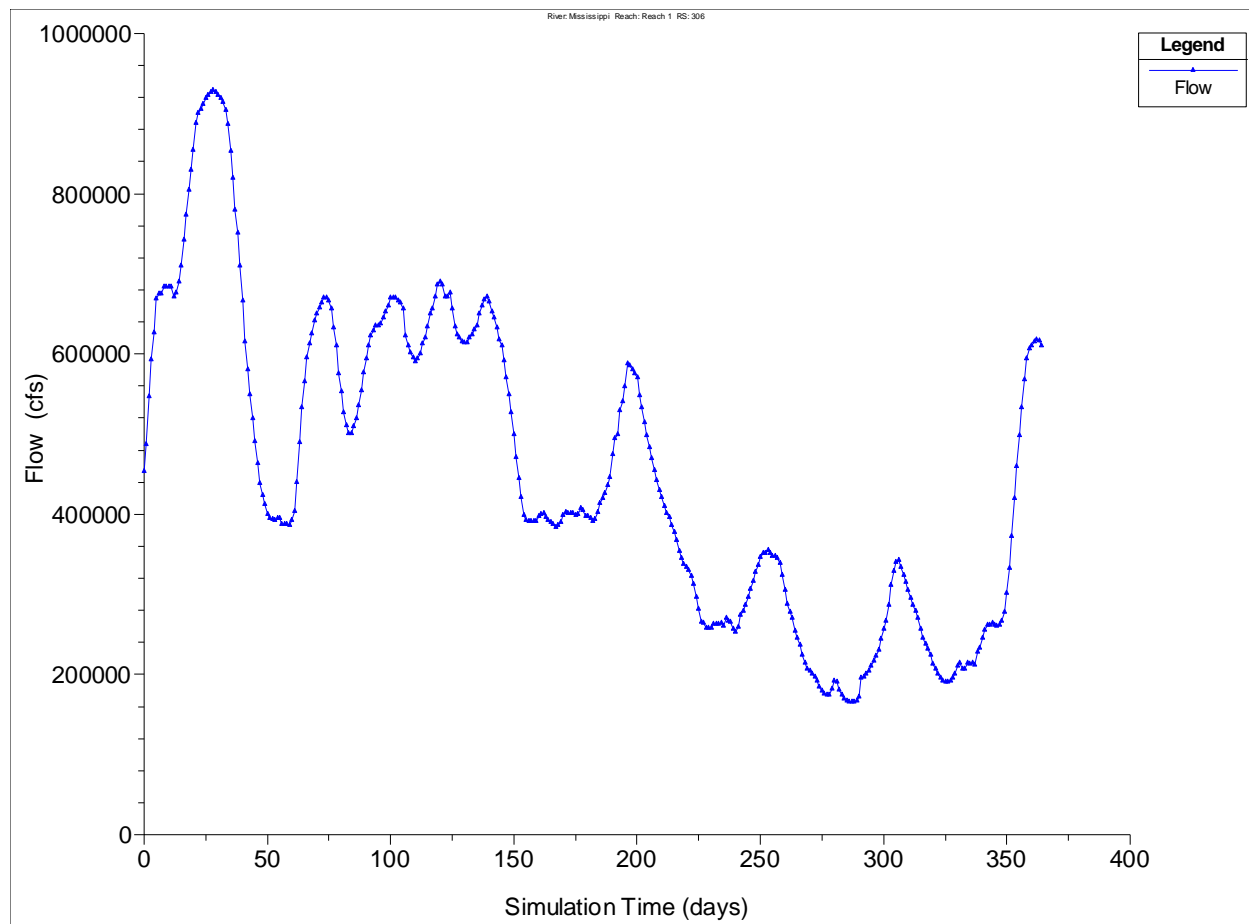
Date/Gate Group	1	2	3	4	5	6	7	8
11-Apr-2008	0.00	0.00	0.00	0.00	0.00	0.00	0.00	10.00
12-Apr-2008	5.00	0.00	5.00	0.00	0.00	0.00	0.00	10.00
13-Apr-2008	10.00	0.00	10.00	0.00	0.00	0.00	0.00	10.00
14-Apr-2008	10.00	0.00	10.00	0.00	0.00	0.00	0.00	10.00
15-Apr-2008	10.00	0.00	10.00	0.00	0.00	0.00	0.00	10.00
16-Apr-2008	10.00	0.00	10.00	0.00	0.00	0.00	0.00	10.00
17-Apr-2008	10.00	0.00	10.00	0.00	4.00	0.00	10.00	10.00
18-Apr-2008	10.00	0.00	10.00	0.00	6.00	0.00	10.00	10.00
19-Apr-2008	10.00	0.00	10.00	0.00	8.00	0.00	10.00	10.00
20-Apr-2008	10.00	0.00	10.00	0.00	8.00	0.00	10.00	10.00
21-Apr-2008	10.00	0.00	10.00	0.00	8.00	0.00	10.00	10.00
22-Apr-2008	10.00	0.00	10.00	0.00	8.00	0.00	10.00	10.00
23-Apr-2008	10.00	0.00	10.00	0.00	8.00	0.00	10.00	10.00
24-Apr-2008	10.00	0.00	9.23	0.00	8.00	0.00	10.00	10.00
25-Apr-2008	10.00	0.00	8.46	0.00	8.00	0.00	10.00	10.00
26-Apr-2008	9.00	0.00	7.69	0.00	7.27	0.00	9.23	10.00
27-Apr-2008	8.00	0.00	6.92	0.00	6.55	0.00	8.46	10.00
28-Apr-2008	7.00	0.00	6.15	0.00	5.82	0.00	7.69	10.00
29-Apr-2008	6.00	0.00	5.38	0.00	5.09	0.00	6.92	10.00
30-Apr-2008	5.00	0.00	4.62	0.00	4.36	0.00	6.15	10.00
1-May-2008	4.00	0.00	3.85	0.00	3.64	0.00	5.38	10.00
2-May-2008	3.00	0.00	3.08	0.00	2.91	0.00	4.62	10.00
3-May-2008	2.00	0.00	2.31	0.00	2.18	0.00	3.85	10.00
4-May-2008	1.00	0.00	1.54	0.00	1.45	0.00	3.08	10.00
5-May-2008	0.00	0.00	0.77	0.00	0.73	0.00	2.31	10.00
6-May-2008	0.00	0.00	0.00	0.00	0.00	0.00	1.54	10.00
7-May-2008	0.00	0.00	0.00	0.00	0.00	0.00	0.77	10.00
8-May-2008	0.00	0.00	0.00	0.00	0.00	0.00	0.00	10.00

**Table F-4 Continued.**

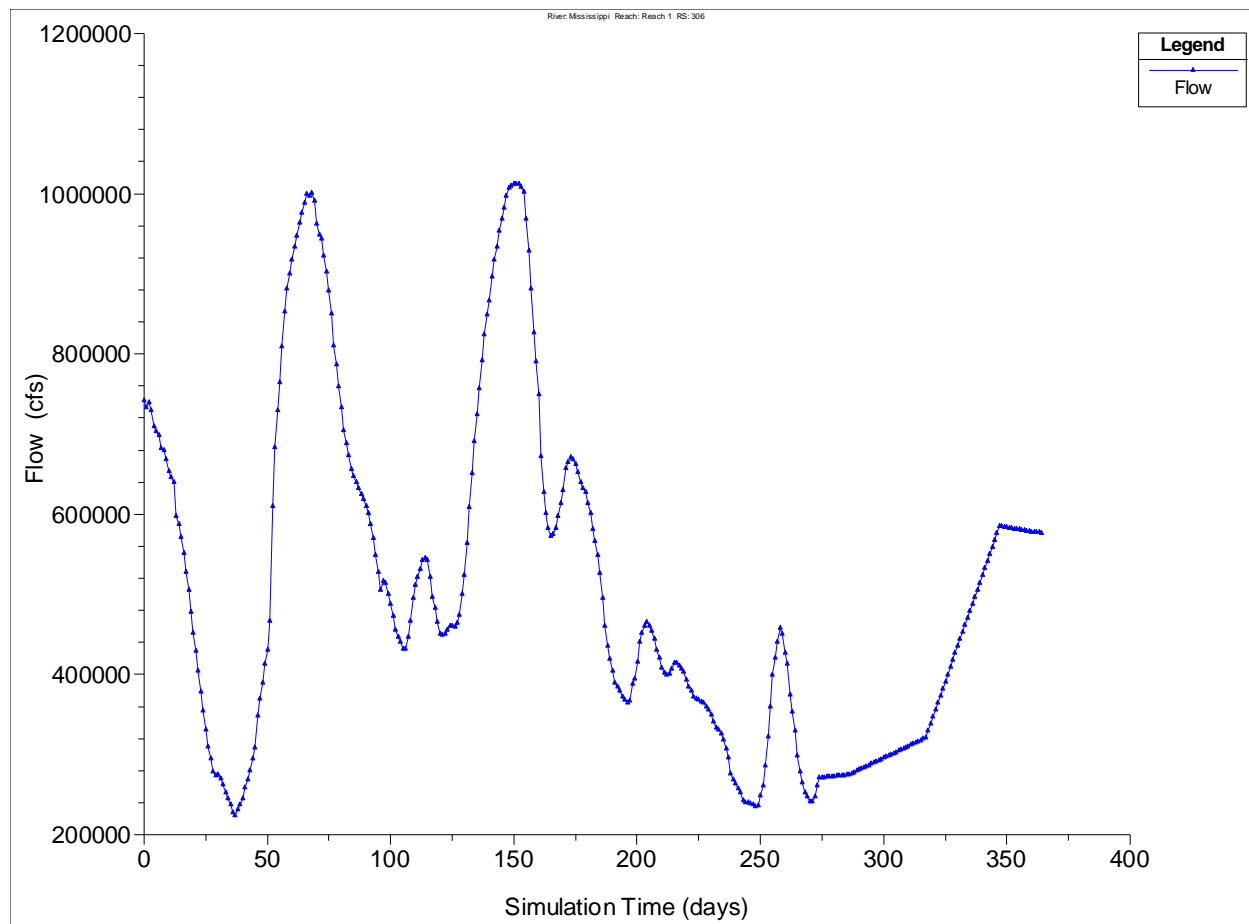
Date/Gate Group	9	10	11	12	13	14	15	16
11-Apr-2008	0.00	0.00	0.00	0.00	0.00	0.00	0.00	0.00
12-Apr-2008	0.00	0.00	0.00	0.00	6.24	10.08	0.00	0.00
13-Apr-2008	0.00	0.00	0.00	0.00	6.24	10.08	0.00	0.00
14-Apr-2008	0.00	0.00	0.00	0.00	6.24	10.08	0.00	0.00
15-Apr-2008	0.00	0.00	0.00	0.00	6.24	10.08	0.00	0.00
16-Apr-2008	0.00	0.00	0.00	2.88	6.24	10.08	0.00	0.00
17-Apr-2008	0.00	0.00	0.00	2.88	6.24	10.08	0.00	0.00
18-Apr-2008	0.00	0.00	0.00	2.88	6.24	10.08	0.00	0.00
19-Apr-2008	0.00	12.00	0.00	2.88	6.24	10.08	0.00	0.00
20-Apr-2008	0.00	12.00	0.00	2.88	6.24	10.08	0.00	0.00
21-Apr-2008	0.00	12.00	0.00	2.88	6.24	10.08	0.00	0.00
22-Apr-2008	0.00	12.00	0.00	2.88	6.24	10.08	0.00	0.00
23-Apr-2008	0.00	12.00	0.00	2.88	6.24	10.08	0.00	0.00
24-Apr-2008	0.00	12.00	0.00	2.88	6.24	10.08	0.00	0.00
25-Apr-2008	0.00	12.00	0.00	2.88	6.24	10.08	0.00	0.00
26-Apr-2008	0.00	11.08	0.00	2.66	5.76	9.30	0.00	0.00
27-Apr-2008	0.00	10.15	0.00	2.44	5.28	8.53	0.00	0.00
28-Apr-2008	0.00	9.23	0.00	2.22	4.80	7.75	0.00	0.00
29-Apr-2008	0.00	8.31	0.00	1.99	4.32	6.98	0.00	0.00
30-Apr-2008	0.00	7.38	0.00	1.77	3.84	6.20	0.00	0.00
1-May-2008	0.00	6.46	0.00	1.55	3.36	5.43	0.00	0.00
2-May-2008	0.00	5.54	0.00	1.33	2.88	4.65	0.00	0.00
3-May-2008	0.00	4.62	0.00	1.11	2.40	3.88	0.00	0.00
4-May-2008	0.00	3.69	0.00	0.89	1.92	3.10	0.00	0.00
5-May-2008	0.00	2.77	0.00	0.66	1.44	2.33	0.00	0.00
6-May-2008	0.00	1.85	0.00	0.44	0.96	1.55	0.00	0.00
7-May-2008	0.00	0.92	0.00	0.22	0.48	0.78	0.00	0.00
8-May-2008	0.00	0.00	0.00	0.00	0.00	0.00	0.00	0.00

**Table F-5: Time-series Gate Operations for Jesuit Bend, Deer Range, and Myrtle Grove Diversion Structures for all simulations.**

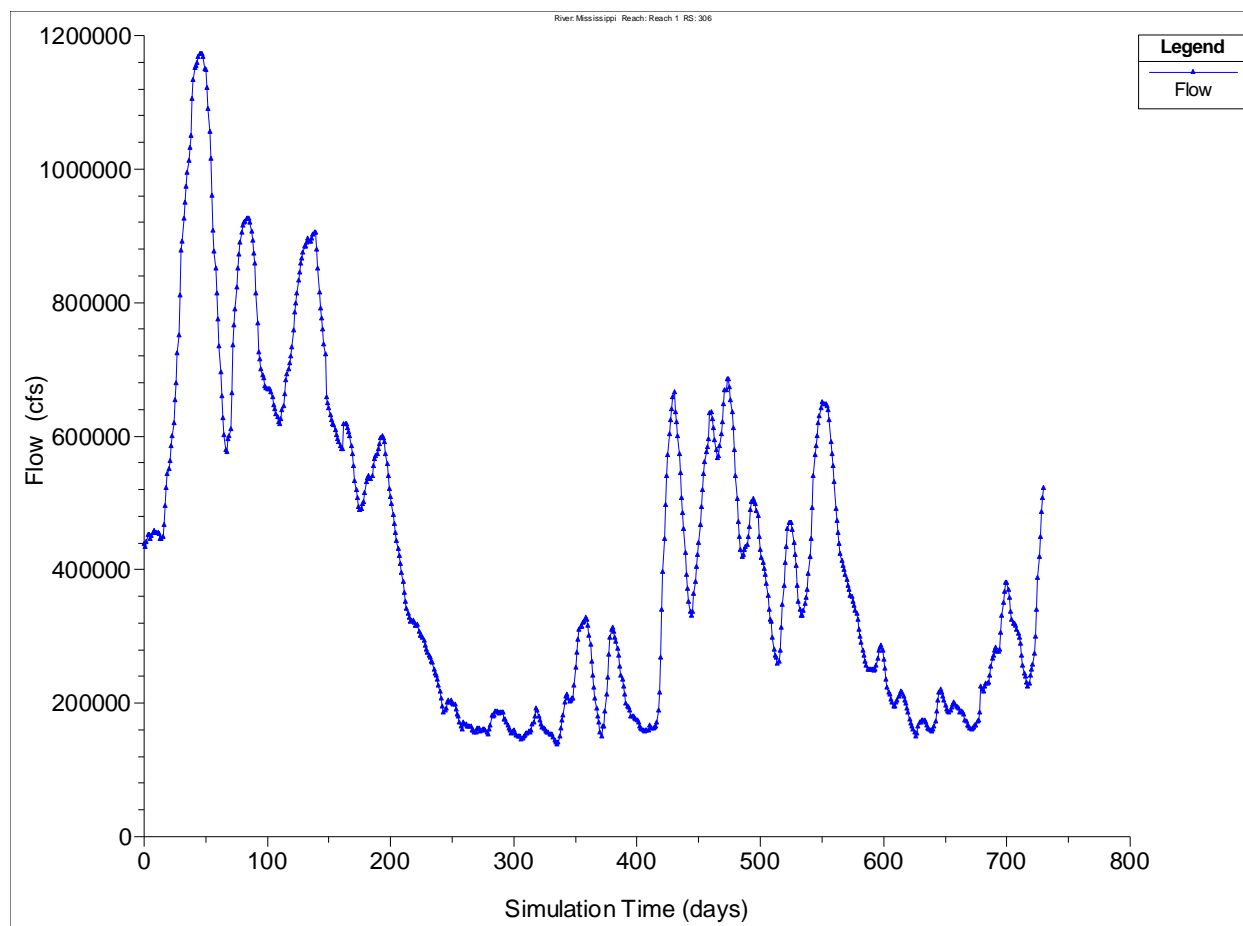
Diversion Structure	Jesuit Bend		Deer Range					Myrtle Grove					
Gate Number	1	2	1	2	3	4	5	1	2	3	4	5	6
Gate Height (ft)	14	14	14	14	14	14	14	15	15	15	15	15	15



**Figure F-1: 2007 Upstream Flow Hydrograph for Mississippi Reach 1.**



**Figure F-2: 2003 Upstream Flow Hydrograph for Mississippi Reach 1.**



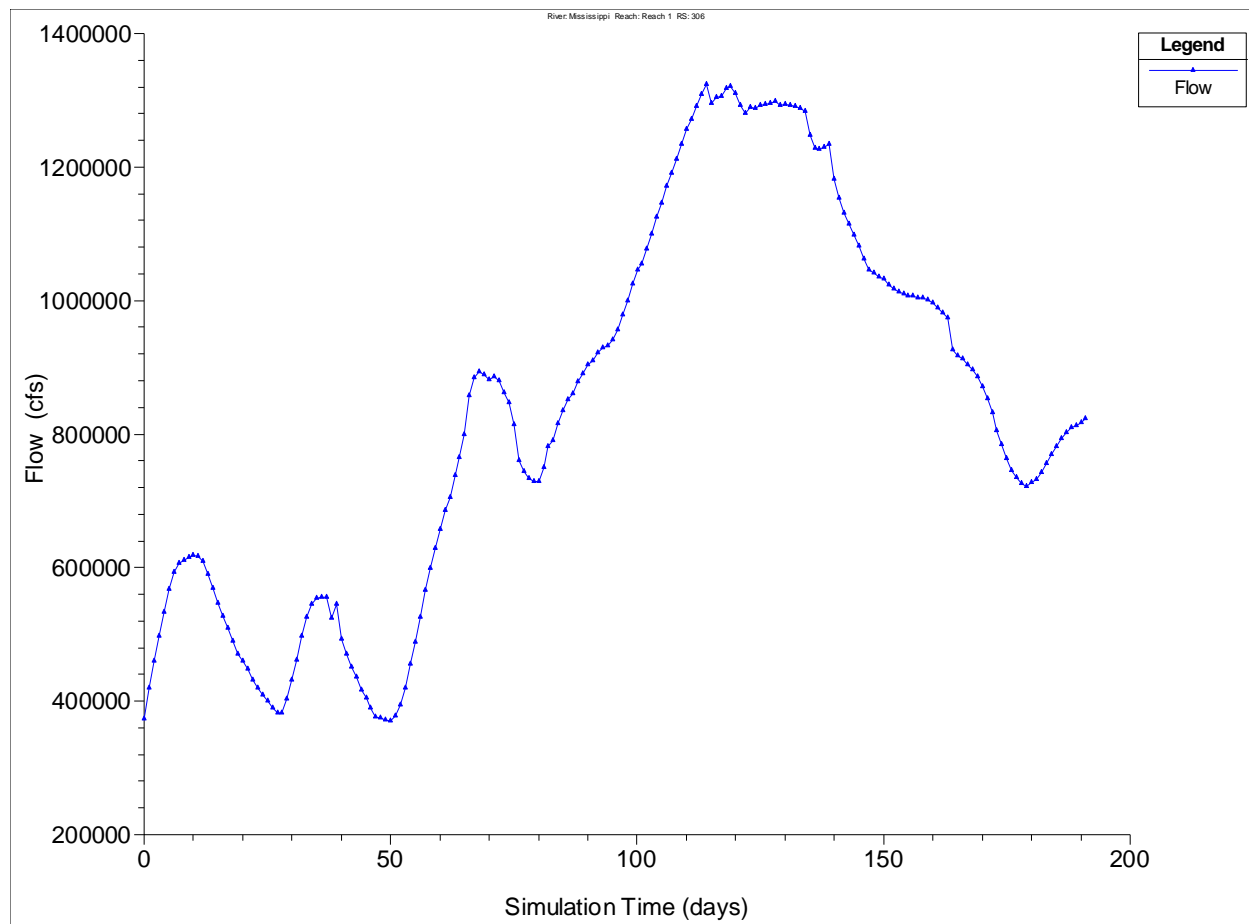


**Figure F-4: 2007-2008 Upstream Flow Hydrograph for Mississippi Reach 1.**

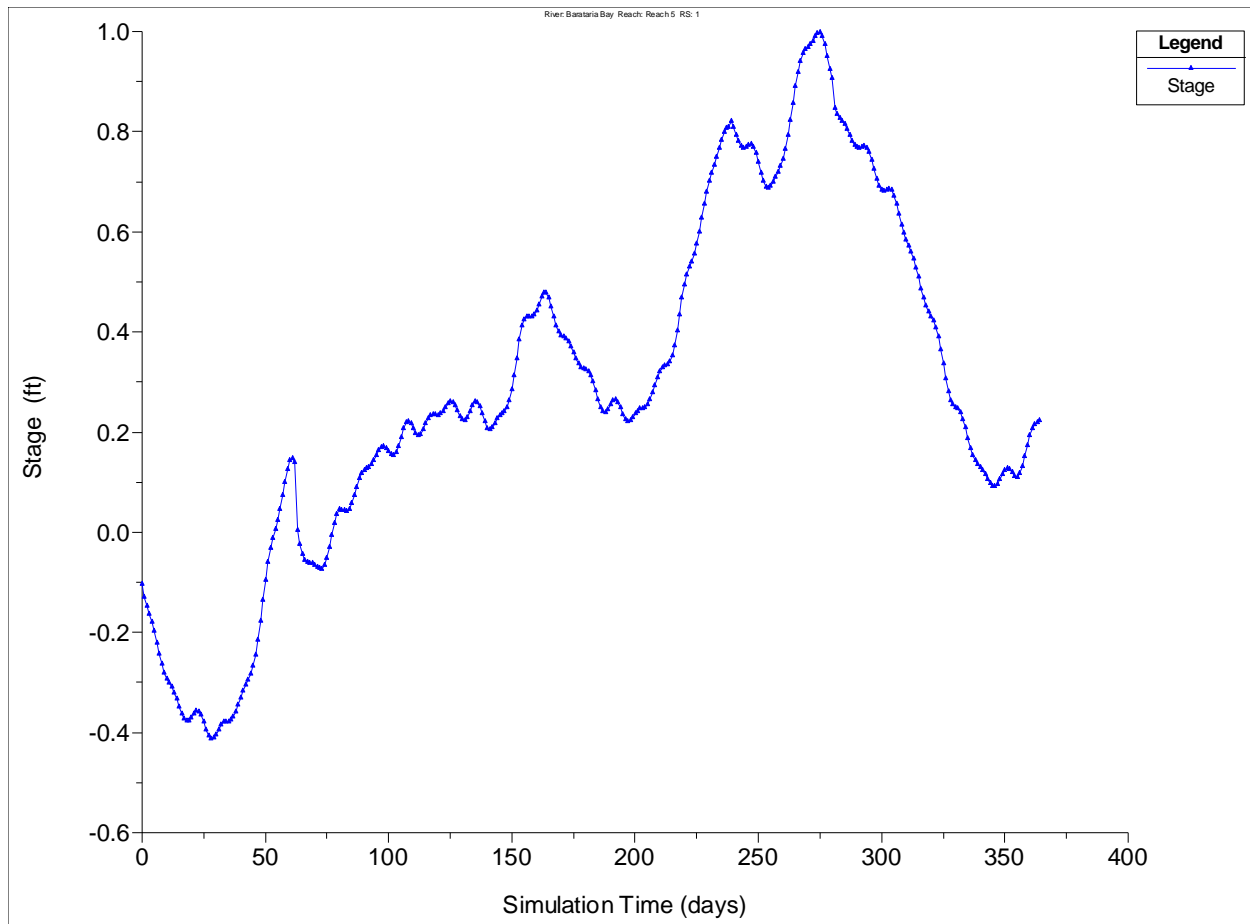


**Figure F-5: 2007, 2003, and 1999-2000 Downstream Stage Hydrograph for the Gulf of Mexico (excluding the Sea Level Rise Study Stage Hydrographs).**

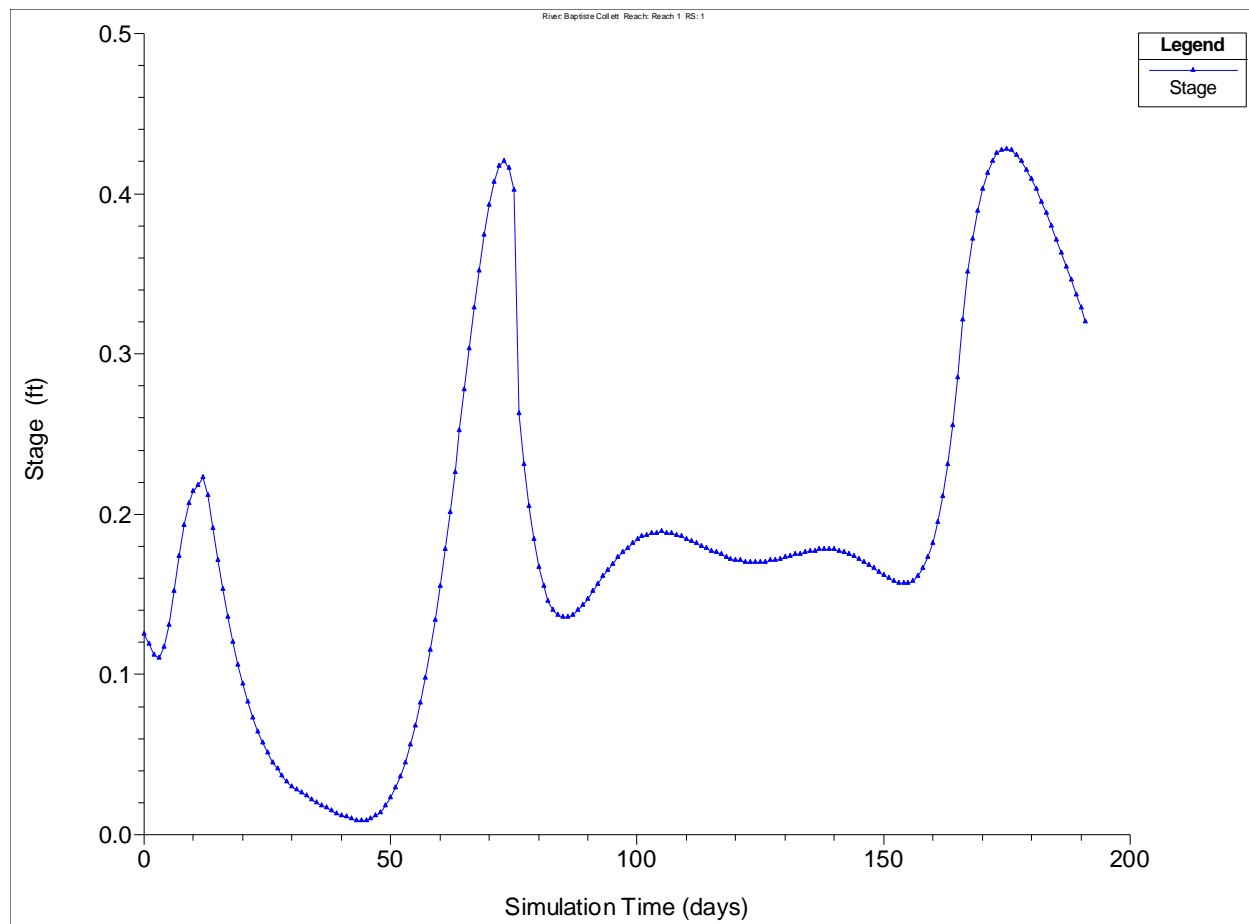


**Figure F-6: 2007-2008 Downstream Stage Hydrograph for the Gulf of Mexico.**



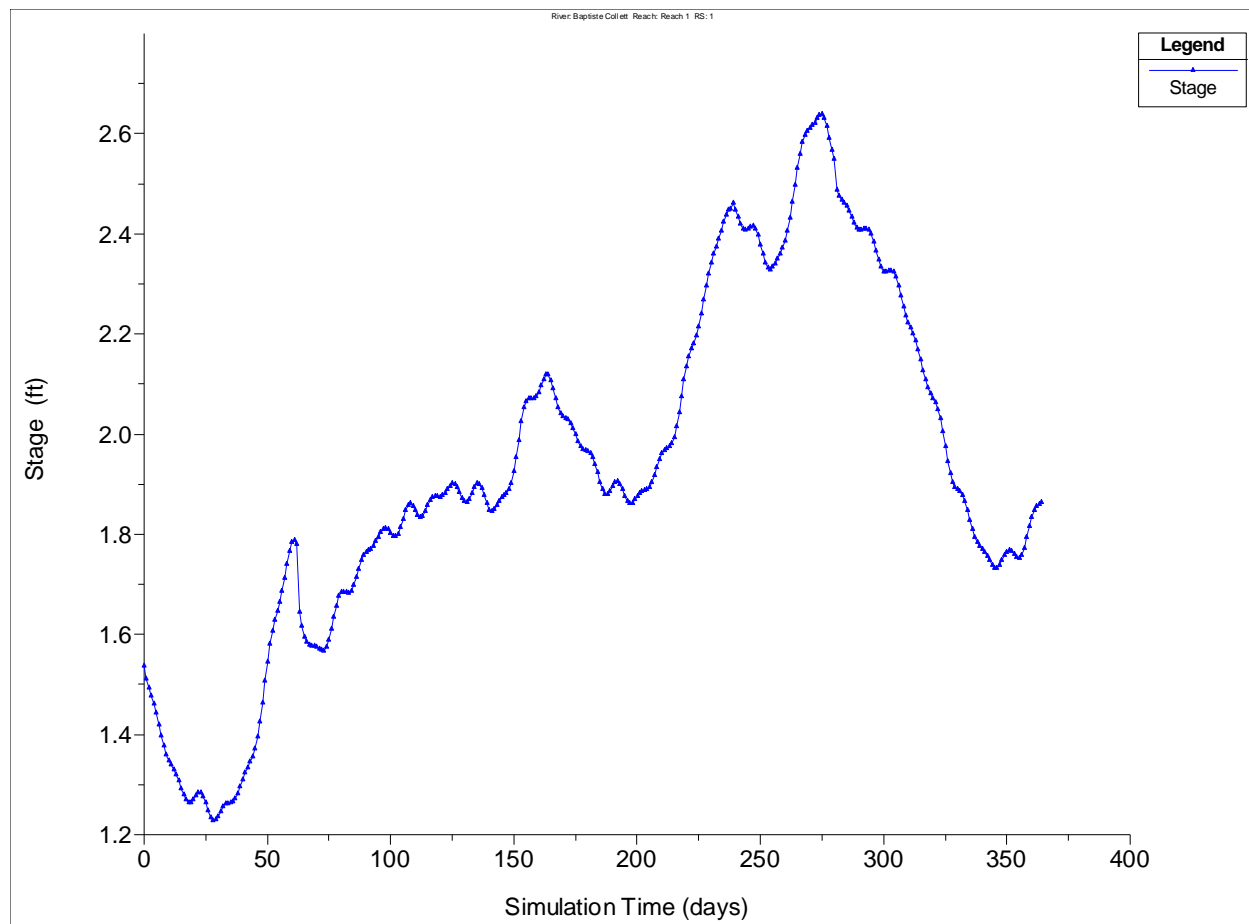


**Figure F-7: 2007 Downstream Stage Hydrograph for the Gulf of Mexico for Relative Sea Level Rise of 1.64 ft (0.5 m).**

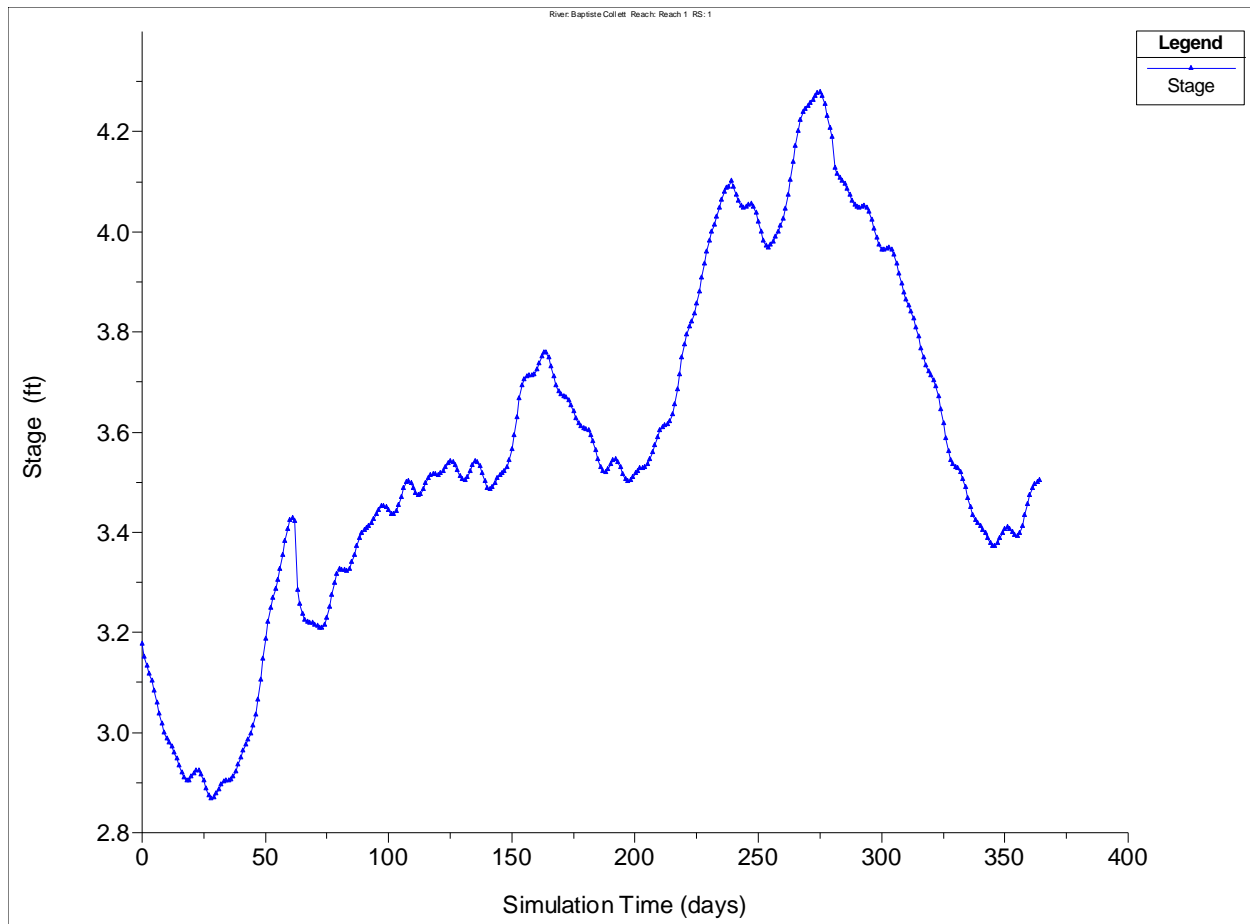


**Figure F-8: 2007 Downstream Stage Hydrograph for the Gulf of Mexico for Relative Sea Level Rise of 3.28 ft (1.0 m).**

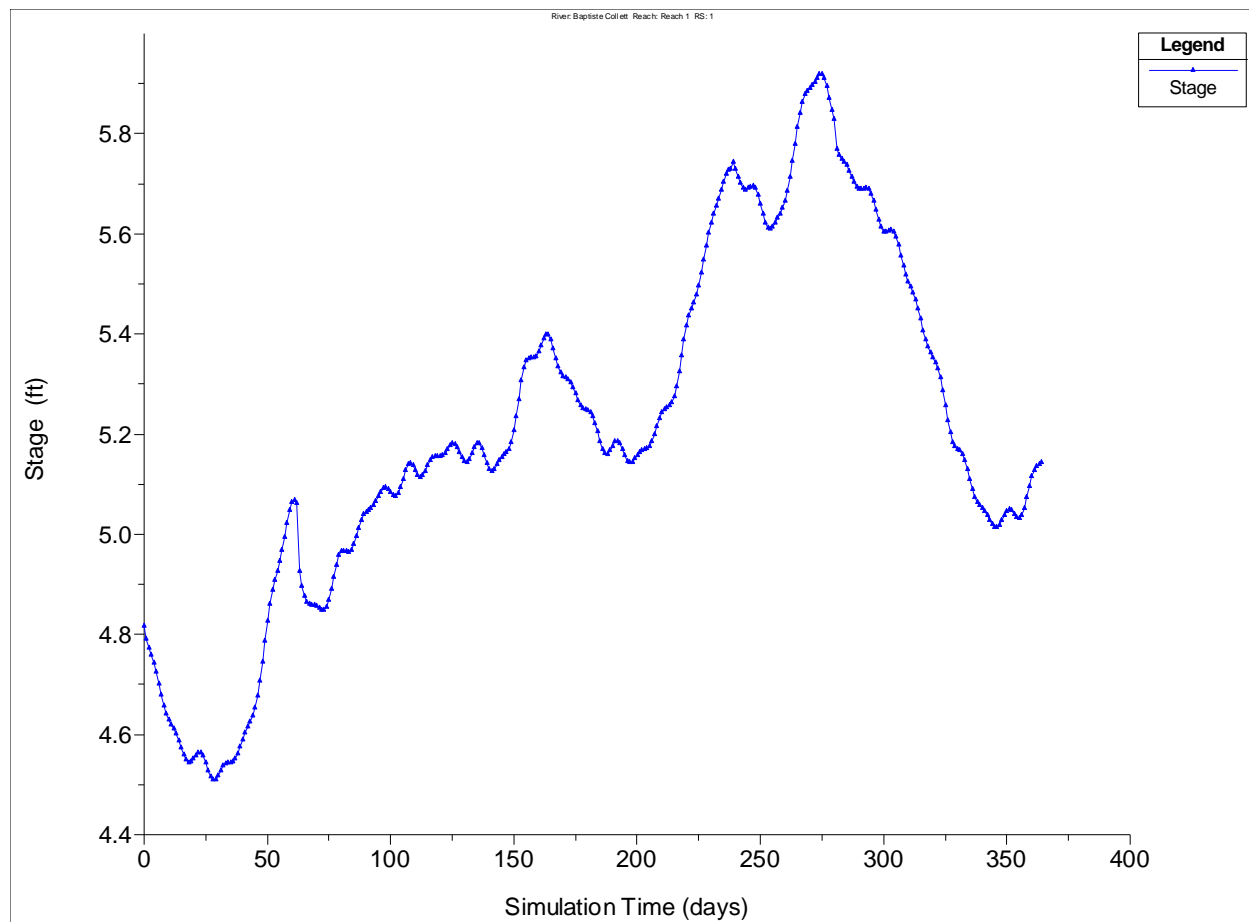


**Figure F-9: 2007 Downstream Stage Hydrograph for the Gulf of Mexico for Relative Sea Level Rise of 4.92 ft (1.5 m).**

## **Appendix G**

### **Manning's $n$ Values<sup>17</sup>**

---

<sup>17</sup> River Stations that were interpolated in HEC-RAS are denoted with an “\*”.

**Table G-1: Manning's  $n$  Values for Baptiste Collette.**

Baptiste Collette						
Number	Reach	River Station	Friction ( $n/K$ )	Left Overbank	Channel	Right Overbank
1	Reach 1	35	$n$	0.024	0.022	0.024
2	Reach 1	34	$n$	0.024	0.022	0.024
3	Reach 1	33	$n$	0.024	0.022	0.024
4	Reach 1	32	$n$	0.024	0.022	0.024
5	Reach 1	31	$n$	0.024	0.022	0.024
6	Reach 1	30	$n$	0.024	0.022	0.024
7	Reach 1	29	$n$	0.024	0.022	0.024
8	Reach 1	28	$n$	0.024	0.022	0.024
9	Reach 1	27	$n$	0.024	0.022	0.024
10	Reach 1	26	$n$	0.024	0.022	0.024
11	Reach 1	25	$n$	0.024	0.022	0.024
12	Reach 1	24	$n$	0.024	0.022	0.024
13	Reach 1	23	$n$	0.024	0.022	0.024
14	Reach 1	22	$n$	0.024	0.022	0.024
15	Reach 1	21	$n$	0.024	0.022	0.024
16	Reach 1	20	$n$	0.024	0.022	0.024
17	Reach 1	19	$n$	0.024	0.022	0.024
18	Reach 1	18	$n$	0.024	0.022	0.024
19	Reach 1	17	$n$	0.024	0.022	0.024
20	Reach 1	16	$n$	0.024	0.022	0.024
21	Reach 1	15	$n$	0.024	0.022	0.024
22	Reach 1	14	$n$	0.024	0.022	0.024
23	Reach 1	13	$n$	0.024	0.022	0.024
24	Reach 1	12	$n$	0.024	0.022	0.024
25	Reach 1	11	$n$	0.024	0.022	0.024
26	Reach 1	10	$n$	0.024	0.022	0.024
27	Reach 1	9	$n$	0.024	0.022	0.024
28	Reach 1	8	$n$	0.024	0.022	0.024
29	Reach 1	7	$n$	0.024	0.022	0.024
30	Reach 1	6	$n$	0.024	0.022	0.024
31	Reach 1	5	$n$	0.024	0.022	0.024
32	Reach 1	4	$n$	0.024	0.022	0.024
33	Reach 1	3	$n$	0.024	0.022	0.024
34	Reach 1	2	$n$	0.024	0.022	0.024
35	Reach 1	1	$n$	0.024	0.022	0.024

**Table G-2: Manning's  $n$  Values for Barataria Bay.**

Barataria Bay						
Number	Reach	River Station	Friction ( $n/K$ )	Left Overbank	Channel	Right Overbank
1	Reach 1	5	$n$	0.03	0.03	0.03
2	Reach 1	4	$n$	0.03	0.03	0.03
3	Reach 1	3	$n$	0.03	0.03	0.03
4	Reach 1	2	$n$	0.03	0.03	0.03
5	Reach 1	1	$n$	0.03	0.03	0.03
6	Reach 2	2	$n$	0.03	0.03	0.03
7	Reach 2	1	$n$	0.03	0.03	0.03
8	Reach 3	3	$n$	0.03	0.03	0.03
9	Reach 3	2	$n$	0.03	0.03	0.03
10	Reach 3	1	$n$	0.03	0.03	0.03
11	Reach 4	10	$n$	0.03	0.03	0.03
12	Reach 4	9	$n$	0.03	0.03	0.03
13	Reach 4	8	$n$	0.03	0.03	0.03
14	Reach 4	7	$n$	0.03	0.03	0.03
15	Reach 4	6	$n$	0.03	0.03	0.03
16	Reach 4	5	$n$	0.03	0.03	0.03
17	Reach 4	4	$n$	0.03	0.03	0.03
18	Reach 4	3	$n$	0.03	0.03	0.03
19	Reach 4	2	$n$	0.03	0.03	0.03
20	Reach 4	1	$n$	0.03	0.03	0.03
21	Reach 5	7	$n$	0.03	0.03	0.03
22	Reach 5	6	$n$	0.03	0.03	0.03
23	Reach 5	5	$n$	0.03	0.03	0.03
24	Reach 5	4	$n$	0.03	0.03	0.03
25	Reach 5	3	$n$	0.03	0.03	0.03
26	Reach 5	2	$n$	0.03	0.03	0.03
27	Reach 5	1	$n$	0.03	0.03	0.03

**Table G-3: Manning's  $n$  Values for Barataria Bay Waterway.**

Barataria Bay Waterway						
Number	Reach	River Station	Friction ( $n/K$ )	Left Overbank	Channel	Right Overbank
1	Reach 1	35	$n$	0.03	0.03	0.03
2	Reach 1	34	$n$	0.03	0.03	0.03
3	Reach 1	33	$n$	0.03	0.03	0.03
4	Reach 1	32	$n$	0.03	0.03	0.03
5	Reach 1	31	$n$	0.03	0.03	0.03
6	Reach 1	30	$n$	0.03	0.03	0.03
7	Reach 1	29	$n$	0.03	0.03	0.03
8	Reach 1	28	$n$	0.03	0.03	0.03
9	Reach 2	27	$n$	0.03	0.03	0.03
10	Reach 2	26	$n$	0.03	0.03	0.03
11	Reach 2	25	$n$	0.03	0.03	0.03
12	Reach 2	24	$n$	0.03	0.03	0.03
13	Reach 3	23	$n$	0.03	0.03	0.03
14	Reach 3	22	$n$	0.03	0.03	0.03
15	Reach 3	21	$n$	0.03	0.03	0.03
16	Reach 3	20	$n$	0.03	0.03	0.03
17	Reach 3	19	$n$	0.03	0.03	0.03
18	Reach 4	18	$n$	0.03	0.03	0.03
19	Reach 4	17	$n$	0.03	0.03	0.03
20	Reach 4	16	$n$	0.03	0.03	0.03
21	Reach 4	15	$n$	0.03	0.03	0.03
22	Reach 4	14	$n$	0.03	0.03	0.03
23	Reach 4	13	$n$	0.03	0.03	0.03
24	Reach 4	12	$n$	0.03	0.03	0.03
25	Reach 4	11	$n$	0.03	0.03	0.03
26	Reach 4	10	$n$	0.03	0.03	0.03
27	Reach 4	9	$n$	0.03	0.03	0.03
28	Reach 4	8	$n$	0.03	0.03	0.03
29	Reach 4	7	$n$	0.03	0.03	0.03
30	Reach 4	6	$n$	0.03	0.03	0.03
31	Reach 4	5	$n$	0.03	0.03	0.03
32	Reach 4	4	$n$	0.03	0.03	0.03
33	Reach 4	3	$n$	0.03	0.03	0.03
34	Reach 4	2	$n$	0.03	0.03	0.03
35	Reach 4	1	$n$	0.03	0.03	0.03

**Table G-4: Manning's  $n$  Values for Bayou Lamoque.**

Bayou Lamoque						
Number	Reach	River Station	Friction ( $n/K$ )	Left Overbank	Channel	Right Overbank
1	Reach 1	21	$n$	0.025	0.022	0.025
2	Reach 1	20	$n$	0.025	0.022	0.025
3	Reach 1	19	$n$	0.025	0.022	0.025
4	Reach 1	18	$n$	0.025	0.022	0.025
5	Reach 1	17	$n$	0.025	0.022	0.025
6	Reach 1	16	$n$	0.025	0.022	0.025
7	Reach 1	15	$n$	0.025	0.022	0.025
8	Reach 1	14	$n$	0.025	0.022	0.025
9	Reach 1	13	$n$	0.025	0.022	0.025
10	Reach 1	12	$n$	0.025	0.022	0.025
11	Reach 1	11	$n$	0.025	0.022	0.025
12	Reach 1	10	$n$	0.025	0.022	0.025
13	Reach 1	9	$n$	0.025	0.022	0.025
14	Reach 1	8	$n$	0.025	0.022	0.025
15	Reach 1	7	$n$	0.025	0.022	0.025
16	Reach 1	6	$n$	0.025	0.022	0.025
17	Reach 1	5	$n$	0.025	0.022	0.025
18	Reach 1	4	$n$	0.025	0.022	0.025
19	Reach 1	3	$n$	0.025	0.022	0.025
20	Reach 1	2	$n$	0.025	0.022	0.025
21	Reach 1	1	$n$	0.025	0.022	0.025



**Table G-5: Manning's  $n$  Values for Bayou Lamoque North.**

Bayou Lamoque North						
Number	Reach	River Station	Friction ( $n/K$ )	Left Overbank	Channel	Right Overbank
1	Reach 1	15	$n$	0.025	0.023	0.025
2	Reach 1	14	$n$	0.025	0.023	0.025
3	Reach 1	13	$n$	0.025	0.023	0.025
4	Reach 1	12	$n$	0.025	0.023	0.025
5	Reach 1	11.5	Inline Structure			
6	Reach 1	11.25	$n$	0.025	0.023	0.025
7	Reach 1	11	$n$	0.025	0.023	0.025
8	Reach 1	10	$n$	0.025	0.023	0.025
9	Reach 1	9	$n$	0.025	0.023	0.025
10	Reach 1	8	$n$	0.025	0.023	0.025
11	Reach 1	7	$n$	0.025	0.023	0.025
12	Reach 1	6	$n$	0.025	0.023	0.025
13	Reach 1	5	$n$	0.025	0.023	0.025
14	Reach 1	4	$n$	0.025	0.023	0.025
15	Reach 1	3	$n$	0.025	0.023	0.025
16	Reach 1	2	$n$	0.025	0.023	0.025
17	Reach 1	1	$n$	0.025	0.023	0.025

**Table G-6: Manning's  $n$  Values for Bayou Lamoque South.**

Bayou Lamoque South						
Number	Reach	River Station	Friction ( $n/K$ )	Left Overbank	Channel	Right Overbank
1	Reach 1	15	$n$	0.025	0.023	0.025
2	Reach 1	14	$n$	0.025	0.023	0.025
3	Reach 1	13	$n$	0.025	0.023	0.025
4	Reach 1	12	$n$	0.025	0.023	0.025
5	Reach 1	11.5	Inline Structure			
6	Reach 1	11.25	$n$	0.025	0.023	0.025
7	Reach 1	11	$n$	0.025	0.023	0.025
8	Reach 1	10	$n$	0.025	0.023	0.025
9	Reach 1	9	$n$	0.025	0.023	0.025
10	Reach 1	8	$n$	0.025	0.023	0.025
11	Reach 1	7	$n$	0.025	0.023	0.025
12	Reach 1	6	$n$	0.025	0.023	0.025
13	Reach 1	5	$n$	0.025	0.023	0.025
14	Reach 1	4	$n$	0.025	0.023	0.025
15	Reach 1	3	$n$	0.025	0.023	0.025
16	Reach 1	2	$n$	0.025	0.023	0.025
17	Reach 1	1	$n$	0.025	0.023	0.025

**Table G-7: Manning's  $n$  Values for Bayou Perot.**

Bayou Perot						
Number	Reach	River Station	Friction ( $n/K$ )	Left Overbank	Channel	Right Overbank
1	Reach 1	16	$n$	0.03	0.03	0.03
2	Reach 1	15	$n$	0.03	0.03	0.03
3	Reach 1	14	$n$	0.03	0.03	0.03
4	Reach 1	13	$n$	0.03	0.03	0.03
5	Reach 1	12	$n$	0.03	0.03	0.03
6	Reach 1	11	$n$	0.03	0.03	0.03
7	Reach 1	10	$n$	0.03	0.03	0.03
8	Reach 1	9	$n$	0.03	0.03	0.03
9	Reach 1	8	$n$	0.03	0.03	0.03
10	Reach 2	7	$n$	0.03	0.03	0.03
11	Reach 2	6	$n$	0.03	0.03	0.03
12	Reach 2	5	$n$	0.03	0.03	0.03
13	Reach 2	4	$n$	0.03	0.03	0.03
14	Reach 2	3	$n$	0.03	0.03	0.03
15	Reach 2	2	$n$	0.03	0.03	0.03
16	Reach 2	1	$n$	0.03	0.03	0.03

**Table G-8: Manning's  $n$  Values for Bayou Rigolettes.**

Bayou Rigolettes						
Number	Reach	River Station	Friction ( $n/K$ )	Left Overbank	Channel	Right Overbank
1	Reach 1	2	$n$	0.03	0.03	0.03
2	Reach 1	1	$n$	0.03	0.03	0.03
3	Reach 2	4	$n$	0.03	0.03	0.03
4	Reach 2	3	$n$	0.03	0.03	0.03
5	Reach 2	2	$n$	0.03	0.03	0.03
6	Reach 2	1	$n$	0.03	0.03	0.03
7	Reach 3	7	$n$	0.03	0.03	0.03
8	Reach 3	6	$n$	0.03	0.03	0.03
9	Reach 3	5	$n$	0.03	0.03	0.03
10	Reach 3	4	$n$	0.03	0.03	0.03
11	Reach 3	3	$n$	0.03	0.03	0.03
12	Reach 3	2	$n$	0.03	0.03	0.03
13	Reach 3	1	$n$	0.03	0.03	0.03

**Table G-9: Manning's  $n$  Values for Bayous P&R.**

Bayous P&R						
Number	Reach	River Station	Friction ( $n/K$ )	Left Overbank	Channel	Right Overbank
1	Reach 1	2	$n$	0.03	0.03	0.03
2	Reach 1	1	$n$	0.03	0.03	0.03

**Table G-10: Manning's  $n$  for Buras.**

Buras						
Number	Reach	River Station	Friction ( $n/K$ )	Left Overbank	Channel	Right Overbank
1	Reach 1	22	$n$	0.2	0.2	0.2
2	Reach 1	21	$n$	0.2	0.2	0.2
3	Reach 1	20	$n$	0.2	0.2	0.2
4	Reach 1	19	$n$	0.2	0.2	0.2
5	Reach 1	18	$n$	0.2	0.2	0.2
6	Reach 1	17	$n$	0.2	0.2	0.2
7	Reach 1	16	$n$	0.2	0.2	0.2
8	Reach 1	15	$n$	0.2	0.2	0.2
9	Reach 1	14	$n$	0.2	0.2	0.2
10	Reach 1	13	$n$	0.2	0.2	0.2
11	Reach 1	12	$n$	0.06	0.03	0.06
12	Reach 1	11	$n$	0.06	0.03	0.06
13	Reach 1	10	$n$	0.06	0.03	0.06
14	Reach 1	9	$n$	0.06	0.03	0.06
15	Reach 1	8	$n$	0.06	0.03	0.06
16	Reach 1	7	$n$	0.06	0.03	0.06
17	Reach 1	6	$n$	0.06	0.03	0.06
18	Reach 1	5	$n$	0.06	0.03	0.06
19	Reach 1	4	$n$	0.06	0.03	0.06
20	Reach 1	3	$n$	0.06	0.03	0.06
21	Reach 1	2	$n$	0.06	0.03	0.06
22	Reach 1	1	$n$	0.06	0.03	0.06

**Table G-11: Manning's  $n$  Values for Caernarvon<sup>18</sup>.**

Caernarvon						
Number	Reach	River Station	Friction ( $n/K$ )	Left Overbank	Channel	Right Overbank
1	Reach 1	20	$n$	0.06	0.03	0.06
2	Reach 1	19	$n$	0.014	0.014	0.014
3	Reach 1	18.5	Inline Structure			
4	Reach 1	18	$n$	0.014	0.014	0.014
5	Reach 1	17	$n$	0.06	0.03	0.06
6	Reach 1	16	$n$	0.06	0.03	0.06
7	Reach 1	15	$n$	0.06	0.03	0.06
8	Reach 1	14	$n$	0.06	0.03	0.06
9	Reach 1	13	$n$	0.06	0.03	0.06
10	Reach 1	12	$n$	0.06	0.03	0.06
11	Reach 1	11	$n$	0.06	0.03	0.06
12	Reach 1	10	$n$	0.06	0.03	0.06
13	Reach 1	9	$n$	0.06	0.03	0.06
14	Reach 1	8	$n$	0.06	0.03	0.06
15	Reach 1	7	$n$	0.06	0.03	0.06
16	Reach 1	6	$n$	0.06	0.03	0.06
17	Reach 1	5	$n$	0.06	0.03	0.06
18	Reach 1	4	$n$	0.06	0.03	0.06
19	Reach 1	3	$n$	0.06	0.03	0.06
20	Reach 1	2	$n$	0.06	0.03	0.06
21	Reach 1	1	$n$	0.06	0.03	0.06

<sup>18</sup> For the Caernarvon Diversion, the guide walls for the structure are made of concrete. As a result, a Manning's  $n$  value of 0.014 was used to emulate this change in roughness.

**Table G-12: Manning's  $n$  Values for Davis Pond.**

Davis Pond						
Number	Reach	River Station	Friction ( $n/K$ )	Left Overbank	Channel	Right Overbank
1	Reach 1	24	$n$	0.2	0.2	0.2
2	Reach 1	23	$n$	0.2	0.2	0.2
3	Reach 1	22	$n$	0.2	0.2	0.2
4	Reach 1	21	$n$	0.2	0.2	0.2
5	Reach 1	20.5	Inline Structure			
6	Reach 1	20	$n$	0.2	0.2	0.2
7	Reach 1	19	$n$	0.2	0.2	0.2
8	Reach 1	18	$n$	0.03	0.03	0.03
9	Reach 1	17	$n$	0.03	0.03	0.03
10	Reach 1	16	$n$	0.03	0.03	0.03
11	Reach 1	15	$n$	0.03	0.03	0.03
12	Reach 1	14	$n$	0.03	0.03	0.03
13	Reach 1	13	$n$	0.03	0.03	0.03
14	Reach 1	12	$n$	0.03	0.03	0.03
15	Reach 1	11.8*	$n$	0.03	0.03	0.03
16	Reach 1	11.6*	$n$	0.03	0.03	0.03
17	Reach 1	11.4*	$n$	0.03	0.03	0.03
18	Reach 1	11.2*	$n$	0.03	0.03	0.03
19	Reach 1	11	$n$	0.03	0.03	0.03
20	Reach 1	10	$n$	0.03	0.03	0.03
21	Reach 1	9	$n$	0.03	0.03	0.03
22	Reach 1	8.8*	$n$	0.03	0.03	0.03
23	Reach 1	8.6*	$n$	0.03	0.03	0.03
24	Reach 1	8.4*	$n$	0.03	0.03	0.03
25	Reach 1	8.2*	$n$	0.03	0.03	0.03
26	Reach 1	8	$n$	0.03	0.03	0.03
27	Reach 1	7.75*	$n$	0.03	0.03	0.03
28	Reach 1	7.5*	$n$	0.03	0.03	0.03
29	Reach 1	7.25*	$n$	0.03	0.03	0.03
30	Reach 1	7	$n$	0.03	0.03	0.03
31	Reach 1	6	$n$	0.03	0.03	0.03
32	Reach 1	5	$n$	0.03	0.03	0.03
33	Reach 1	4	$n$	0.03	0.03	0.03
34	Reach 1	3	$n$	0.03	0.03	0.03
35	Reach 1	2	$n$	0.03	0.03	0.03

**Table G-12 Continued.**

36	Reach 1	1	<i>n</i>	0.03	0.03	0.03
37	L. C. Right	4	<i>n</i>	0.03	0.03	0.03
38	L. C. Right	3	<i>n</i>	0.03	0.03	0.03
39	L. C. Right	2	<i>n</i>	0.03	0.03	0.03
40	L. C. Right	1	<i>n</i>	0.03	0.03	0.03
41	L. C. Left	3	<i>n</i>	0.03	0.03	0.03
42	L. C. Left	2	<i>n</i>	0.03	0.03	0.03
43	L. C. Left	1	<i>n</i>	0.03	0.03	0.03
44	L. S. Center	10	<i>n</i>	0.03	0.03	0.03
45	L. S. Center	9	<i>n</i>	0.03	0.03	0.03
46	L. S. Center	8	<i>n</i>	0.03	0.03	0.03
47	L. S. Center	7	<i>n</i>	0.03	0.03	0.03
48	L. S. Center	6	<i>n</i>	0.03	0.03	0.03
49	L. S. Center	5	<i>n</i>	0.03	0.03	0.03
50	L. S. Center	4	<i>n</i>	0.03	0.03	0.03
51	L. S. Center	3	<i>n</i>	0.03	0.03	0.03
52	L. S. Center	2	<i>n</i>	0.03	0.03	0.03
53	L. S. Center	1	<i>n</i>	0.03	0.03	0.03
54	L. S. Right	3	<i>n</i>	0.03	0.03	0.03
55	L. S. Right	2	<i>n</i>	0.03	0.03	0.03
56	L. S. Right	1	<i>n</i>	0.03	0.03	0.03
57	L. S. Left	2	<i>n</i>	0.03	0.03	0.03
58	L. S. Left	1	<i>n</i>	0.03	0.03	0.03
59	Reach 4	2	<i>n</i>	0.03	0.03	0.03
60	Reach 4	1	<i>n</i>	0.03	0.03	0.03
61	Reach 5	2	<i>n</i>	0.03	0.03	0.03
62	Reach 5	1	<i>n</i>	0.03	0.03	0.03

**Table G-13: Manning's  $n$  Values for Deer Range.**

Deer Range						
Number	Reach	River Station	Friction ( $n/K$ )	Left Overbank	Channel	Right Overbank
1	Reach 1	21	$n$	0.06	0.03	0.06
2	Reach 1	20	$n$	0.06	0.03	0.06
3	Reach 1	19.5	Inline Structure			
4	Reach 1	19	$n$	0.06	0.03	0.06
5	Reach 1	18	$n$	0.06	0.03	0.06
6	Reach 1	17	$n$	0.06	0.03	0.06
7	Reach 1	16	$n$	0.06	0.03	0.06
8	Reach 1	15	$n$	0.06	0.03	0.06
9	Reach 1	14	$n$	0.06	0.03	0.06
10	Reach 1	13	$n$	0.06	0.03	0.06
11	Reach 1	12	$n$	0.06	0.03	0.06
12	Reach 1	11	$n$	0.06	0.03	0.06
13	Reach 1	10	$n$	0.06	0.03	0.06
14	Reach 1	9	$n$	0.06	0.03	0.06
15	Reach 1	8	$n$	0.06	0.03	0.06
16	Reach 1	7	$n$	0.06	0.03	0.06
17	Reach 1	6	$n$	0.06	0.03	0.06
18	Reach 1	5	$n$	0.06	0.03	0.06
19	Reach 1	4	$n$	0.06	0.03	0.06
20	Reach 1	3	$n$	0.06	0.03	0.06
21	Reach 1	2	$n$	0.06	0.03	0.06
22	Reach 1	1	$n$	0.06	0.03	0.06



**Table G-14: Manning's  $n$  Values for Des Allemands.**

Des Allemands						
Number	Reach	River Station	Friction ( $n/K$ )	Left Overbank	Channel	Right Overbank
1	Reach 2.0	5	$n$	0.03	0.03	0.03
2	Reach 2.0	4	$n$	0.03	0.03	0.03
3	Reach 2.0	3	$n$	0.03	0.03	0.03
4	Reach 2.0	2	$n$	0.03	0.03	0.03
5	Reach 2.0	1	$n$	0.03	0.03	0.03
6	Reach 1.0	5	$n$	0.03	0.03	0.03
7	Reach 1.0	4	$n$	0.03	0.03	0.03
8	Reach 1.0	3	$n$	0.03	0.03	0.03
9	Reach 1.0	2	$n$	0.03	0.03	0.03
10	Reach 1.0	1	$n$	0.03	0.03	0.03
11	Reach 3.0	38	$n$	0.03	0.03	0.03
12	Reach 3.0	37	$n$	0.03	0.03	0.03
13	Reach 3.0	36	$n$	0.03	0.03	0.03
14	Reach 3.0	35	$n$	0.03	0.03	0.03
15	Reach 3.0	34	$n$	0.03	0.03	0.03
16	Reach 3.0	33	$n$	0.03	0.03	0.03
17	Reach 3.0	32	$n$	0.03	0.03	0.03
18	Reach 3.0	31	$n$	0.03	0.03	0.03
19	Reach 3.0	30	$n$	0.03	0.03	0.03
20	Reach 3.0	29	$n$	0.03	0.03	0.03
21	Reach 3.0	28	$n$	0.03	0.03	0.03
22	Reach 3.0	27	$n$	0.03	0.03	0.03
23	Reach 3.0	26	$n$	0.03	0.03	0.03
24	Reach 3.0	25	$n$	0.03	0.03	0.03
25	Reach 3.0	24	$n$	0.03	0.03	0.03
26	Reach 3.0	23	$n$	0.03	0.03	0.03
27	Reach 3.0	22	$n$	0.03	0.03	0.03
28	Reach 3.0	21	$n$	0.03	0.03	0.03
29	Reach 3.0	20	$n$	0.03	0.03	0.03
30	Reach 3.0	19	$n$	0.03	0.03	0.03
31	Reach 3.0	18	$n$	0.03	0.03	0.03
32	Reach 3.0	17	$n$	0.03	0.03	0.03
33	Reach 3.0	16	$n$	0.03	0.03	0.03
34	Reach 3.0	15	$n$	0.03	0.03	0.03
35	Reach 3.0	14	$n$	0.03	0.03	0.03
36	Reach 3.0	13	$n$	0.03	0.03	0.03
37	Reach 3.0	12	$n$	0.03	0.03	0.03
38	Reach 3.0	11	$n$	0.03	0.03	0.03
39	Reach 3.0	10	$n$	0.03	0.03	0.03
40	Reach 3.0	9	$n$	0.03	0.03	0.03

**Table G-14 Continued.**

41	Reach 3.0	8	<i>n</i>	0.03	0.03	0.03
42	Reach 3.0	7	<i>n</i>	0.03	0.03	0.03
43	Reach 3.0	6	<i>n</i>	0.03	0.03	0.03
44	Reach 3.0	5	<i>n</i>	0.03	0.03	0.03
45	Reach 3.0	4	<i>n</i>	0.03	0.03	0.03
46	Reach 3.0	3	<i>n</i>	0.03	0.03	0.03
47	Reach 3.0	2	<i>n</i>	0.03	0.03	0.03
48	Reach 3.0	1	<i>n</i>	0.03	0.03	0.03
49	Reach 4.0	5	<i>n</i>	0.03	0.03	0.03
50	Reach 4.0	4	<i>n</i>	0.03	0.03	0.03
51	Reach 4.0	3	<i>n</i>	0.03	0.03	0.03
52	Reach 4.0	2	<i>n</i>	0.03	0.03	0.03
53	Reach 4.0	1	<i>n</i>	0.03	0.03	0.03
54	Reach 5.0	5	<i>n</i>	0.03	0.03	0.03
55	Reach 5.0	4	<i>n</i>	0.03	0.03	0.03
56	Reach 5.0	3	<i>n</i>	0.03	0.03	0.03
57	Reach 5.0	2	<i>n</i>	0.03	0.03	0.03
58	Reach 5.0	1	<i>n</i>	0.03	0.03	0.03
59	Reach 6.0	12	<i>n</i>	0.03	0.03	0.03
60	Reach 6.0	11	<i>n</i>	0.03	0.03	0.03
61	Reach 6.0	10	<i>n</i>	0.03	0.03	0.03
62	Reach 6.0	9	<i>n</i>	0.03	0.03	0.03
63	Reach 6.0	8	<i>n</i>	0.03	0.03	0.03
64	Reach 6.0	7	<i>n</i>	0.03	0.03	0.03
65	Reach 6.0	6	<i>n</i>	0.03	0.03	0.03
66	Reach 6.0	5	<i>n</i>	0.03	0.03	0.03
67	Reach 6.0	4	<i>n</i>	0.03	0.03	0.03
68	Reach 6.0	3	<i>n</i>	0.03	0.03	0.03
69	Reach 6.0	2	<i>n</i>	0.03	0.03	0.03
70	Reach 6.0	1	<i>n</i>	0.03	0.03	0.03

**Table G-15: Manning's  $n$  Values for Fort St. Philip.**

Fort St. Philip						
Number	Reach	River Station	Friction ( $n/K$ )	Left Overbank	Channel	Right Overbank
1	Reach 1	16	$n$	0.2	0.2	0.2
2	Reach 1	15.75*	$n$	0.2	0.2	0.2
3	Reach 1	15.5*	$n$	0.2	0.2	0.2
4	Reach 1	15.25*	$n$	0.2	0.2	0.2
5	Reach 1	15	$n$	0.2	0.2	0.2
6	Reach 1	14.75*	$n$	0.2	0.2	0.2
7	Reach 1	14.5*	$n$	0.2	0.2	0.2
8	Reach 1	14.25*	$n$	0.2	0.2	0.2
9	Reach 1	14	$n$	0.2	0.2	0.2
10	Reach 1	13.75*	$n$	0.2	0.2	0.2
11	Reach 1	13.5*	$n$	0.2	0.2	0.2
12	Reach 1	13.25*	$n$	0.2	0.2	0.2
13	Reach 1	13	$n$	0.2	0.2	0.2
14	Reach 1	12.75*	$n$	0.2	0.2	0.2
15	Reach 1	12.5*	$n$	0.2	0.2	0.2
16	Reach 1	12.25*	$n$	0.2	0.2	0.2
17	Reach 1	12	$n$	0.2	0.2	0.2
18	Reach 1	11.75*	$n$	0.2	0.2	0.2
19	Reach 1	11.5*	$n$	0.2	0.2	0.2
20	Reach 1	11.25*	$n$	0.2	0.2	0.2
21	Reach 1	11	$n$	0.2	0.2	0.2
22	Reach 1	10.75*	$n$	0.2	0.2	0.2
23	Reach 1	10.5*	$n$	0.2	0.2	0.2
24	Reach 1	10.25*	$n$	0.2	0.2	0.2
25	Reach 1	10	$n$	0.2	0.2	0.2
26	Reach 1	9.75*	$n$	0.2	0.2	0.2
27	Reach 1	9.5*	$n$	0.2	0.2	0.2
28	Reach 1	9.25*	$n$	0.2	0.2	0.2
29	Reach 1	9	$n$	0.2	0.2	0.2
30	Reach 1	8.75*	$n$	0.2	0.2	0.2
31	Reach 1	8.5*	$n$	0.2	0.2	0.2
32	Reach 1	8.25*	$n$	0.2	0.2	0.2
33	Reach 1	8	$n$	0.2	0.2	0.2
34	Reach 1	7.75*	$n$	0.2	0.2	0.2
35	Reach 1	7.5*	$n$	0.2	0.2	0.2
36	Reach 1	7.25*	$n$	0.2	0.2	0.2
37	Reach 1	7	$n$	0.2	0.2	0.2
38	Reach 1	6.75*	$n$	0.2	0.2	0.2
39	Reach 1	6.5*	$n$	0.2	0.2	0.2
40	Reach 1	6.25*	$n$	0.2	0.2	0.2

**Table G-15 Continued.**

41	Reach 1	6	<i>n</i>	0.2	0.2	0.2
42	Reach 1	5.75*	<i>n</i>	0.2	0.2	0.2
43	Reach 1	5.5*	<i>n</i>	0.2	0.2	0.2
44	Reach 1	5.25*	<i>n</i>	0.2	0.2	0.2
45	Reach 1	5	<i>n</i>	0.2	0.2	0.2
46	Reach 1	4.75*	<i>n</i>	0.2	0.2	0.2
47	Reach 1	4.5*	<i>n</i>	0.2	0.2	0.2
48	Reach 1	4.25*	<i>n</i>	0.2	0.2	0.2
49	Reach 1	4	<i>n</i>	0.2	0.2	0.2
50	Reach 1	3.75*	<i>n</i>	0.2	0.2	0.2
51	Reach 1	3.5*	<i>n</i>	0.2	0.2	0.2
52	Reach 1	3.25*	<i>n</i>	0.2	0.2	0.2
53	Reach 1	3	<i>n</i>	0.2	0.2	0.2
54	Reach 1	2.75*	<i>n</i>	0.2	0.2	0.2
55	Reach 1	2.5*	<i>n</i>	0.2	0.2	0.2
56	Reach 1	2.25*	<i>n</i>	0.2	0.2	0.2
57	Reach 1	2	<i>n</i>	0.2	0.2	0.2
58	Reach 1	1.75*	<i>n</i>	0.2	0.2	0.2
59	Reach 1	1.5*	<i>n</i>	0.2	0.2	0.2
60	Reach 1	1.25*	<i>n</i>	0.2	0.2	0.2
61	Reach 1	1	<i>n</i>	0.2	0.2	0.2

**Table G-16: Manning's  $n$  Values for Grand Pass.**

Grand Pass						
Number	Reach	River Station	Friction ( $n/K$ )	Left Overbank	Channel	Right Overbank
1	Reach 1	34	$n$	0.024	0.02	0.024
2	Reach 1	33	$n$	0.024	0.02	0.024
3	Reach 1	32	$n$	0.024	0.02	0.024
4	Reach 1	31	$n$	0.024	0.02	0.024
5	Reach 1	30	$n$	0.024	0.02	0.024
6	Reach 2	29	$n$	0.024	0.02	0.024
7	Reach 2	28	$n$	0.024	0.02	0.024
8	Reach 2	27	$n$	0.024	0.02	0.024
9	Reach 2	26	$n$	0.024	0.02	0.024
10	Reach 2	25	$n$	0.024	0.02	0.024
11	Reach 2	24	$n$	0.024	0.02	0.024
12	Reach 2	23	$n$	0.024	0.02	0.024
13	Reach 2	22	$n$	0.024	0.02	0.024
14	Reach 2	21	$n$	0.024	0.02	0.024
15	Reach 2	20	$n$	0.024	0.02	0.024
16	Reach 2	19	$n$	0.024	0.02	0.024
17	Reach 2	18	$n$	0.024	0.02	0.024
18	Reach 2	17	$n$	0.024	0.02	0.024
19	Reach 2	16	$n$	0.024	0.02	0.024
20	Reach 2	15	$n$	0.024	0.02	0.024
21	Reach 2	14	$n$	0.024	0.02	0.024
22	Reach 2	13	$n$	0.024	0.02	0.024
23	Reach 2	12	$n$	0.024	0.02	0.024
24	Reach 2	11	$n$	0.024	0.02	0.024
25	Reach 2	10	$n$	0.024	0.02	0.024
26	Reach 2	9	$n$	0.024	0.02	0.024
27	Reach 2	8	$n$	0.024	0.02	0.024
28	Reach 2	7	$n$	0.024	0.02	0.024
29	Reach 2	6	$n$	0.024	0.02	0.024
30	Reach 2	5	$n$	0.024	0.02	0.024
31	Reach 2	4	$n$	0.024	0.02	0.024
32	Reach 2	3	$n$	0.024	0.02	0.024
33	Reach 2	2	$n$	0.024	0.02	0.024
34	Reach 2	1	$n$	0.024	0.02	0.024

**Table G-17: Manning's  $n$  Values for Head of Passes.**

Head of Passes						
Number	Reach	River Station	Friction ( $n/K$ )	Left Overbank	Channel	Right Overbank
1	Reach 1	2	$n$	0.02	0.0195	0.02
2	Reach 1	1	$n$	0.02	0.0195	0.02

**Table G-18: Manning's  $n$  Values for ICCW.**

ICCW						
Number	Reach	River Station	Friction ( $n/K$ )	Left Overbank	Channel	Right Overbank
1	Reach 4	34	$n$	0.03	0.03	0.03
2	Reach 4	33	$n$	0.03	0.03	0.03
3	Reach 4	32	$n$	0.03	0.03	0.03
4	Reach 4	31	$n$	0.03	0.03	0.03
5	Reach 4	30	$n$	0.03	0.03	0.03
6	Reach 4	29	$n$	0.03	0.03	0.03
7	Reach 4	28	$n$	0.03	0.03	0.03
8	Reach 4	27	$n$	0.03	0.03	0.03
9	Reach 4	26	$n$	0.03	0.03	0.03
10	Reach 5	52	$n$	0.03	0.03	0.03
11	Reach 5	51	$n$	0.03	0.03	0.03
12	Reach 5	50	$n$	0.03	0.03	0.03
13	Reach 5	49	$n$	0.03	0.03	0.03
14	Reach 5	48.5	Lateral Structure			
15	Reach 5	48	$n$	0.03	0.03	0.03
16	Reach 5	47	$n$	0.03	0.03	0.03
17	Reach 5	46	$n$	0.03	0.03	0.03
18	Reach 5	45	$n$	0.03	0.03	0.03
19	Reach 5	44	$n$	0.03	0.03	0.03
20	Reach 5	43	$n$	0.03	0.03	0.03
21	Reach 5	42	$n$	0.03	0.03	0.03
22	Reach 5	41	$n$	0.03	0.03	0.03
23	Reach 5	40	$n$	0.03	0.03	0.03
24	Reach 5	39	$n$	0.03	0.03	0.03
25	Reach 5	38	$n$	0.03	0.03	0.03
26	Reach 5	37	$n$	0.03	0.03	0.03
27	Reach 5	36	$n$	0.03	0.03	0.03
28	Reach 5	35	$n$	0.03	0.03	0.03
29	Reach 5	34	$n$	0.03	0.03	0.03
30	Reach 5	33	$n$	0.03	0.03	0.03
31	Reach 5	32	$n$	0.03	0.03	0.03
32	Reach 5	31	$n$	0.03	0.03	0.03
33	Reach 5	30	$n$	0.03	0.03	0.03
34	Reach 5	29	$n$	0.03	0.03	0.03
35	Reach 5	28	$n$	0.03	0.03	0.03
36	Reach 1	52	$n$	0.03	0.03	0.03
37	Reach 1	51	$n$	0.03	0.03	0.03
38	Reach 1	50	$n$	0.03	0.03	0.03
39	Reach 1	49	$n$	0.03	0.03	0.03
40	Reach 1	48	$n$	0.03	0.03	0.03

**Table G-18 Continued.**

41	Reach 1	47	<i>n</i>	0.03	0.03	0.03
42	Reach 1	46	<i>n</i>	0.03	0.03	0.03
43	Reach 2	45	<i>n</i>	0.03	0.03	0.03
44	Reach 2	44	<i>n</i>	0.03	0.03	0.03
45	Reach 2	43	<i>n</i>	0.03	0.03	0.03
46	Reach 2	42	<i>n</i>	0.03	0.03	0.03
47	Reach 2	41	<i>n</i>	0.03	0.03	0.03
48	Reach 2	40	<i>n</i>	0.03	0.03	0.03
49	Reach 2	39	<i>n</i>	0.03	0.03	0.03
50	Reach 2	38	<i>n</i>	0.03	0.03	0.03
51	Reach 3	37	<i>n</i>	0.03	0.03	0.03
52	Reach 3	36	<i>n</i>	0.03	0.03	0.03
53	Reach 3	35	<i>n</i>	0.03	0.03	0.03

**Table G-19: Manning's *n* Values for ICCW Chalmette.**

ICCW Chalmette						
Number	Reach	River Station	Friction ( <i>n/K</i> )	Left Overbank	Channel	Right Overbank
1	Reach 1	15	<i>n</i>	0.7	0.7	0.7
2	Reach 1	14	<i>n</i>	0.7	0.7	0.7
3	Reach 1	13	<i>n</i>	0.7	0.7	0.7
4	Reach 1	12	<i>n</i>	0.03	0.03	0.03
5	Reach 1	11	<i>n</i>	0.03	0.03	0.03
6	Reach 1	10	<i>n</i>	0.03	0.03	0.03
7	Reach 1	9	<i>n</i>	0.03	0.03	0.03
8	Reach 1	8	<i>n</i>	0.03	0.03	0.03
9	Reach 1	7	<i>n</i>	0.03	0.03	0.03
10	Reach 1	6	<i>n</i>	0.03	0.03	0.03
11	Reach 1	5	<i>n</i>	0.03	0.03	0.03
12	Reach 1	4	<i>n</i>	0.03	0.03	0.03
13	Reach 1	3	<i>n</i>	0.03	0.03	0.03
14	Reach 1	2	<i>n</i>	0.03	0.03	0.03
15	Reach 1	1	<i>n</i>	0.03	0.03	0.03

**Table G-20: Manning's  $n$  Values for ICCW Harvey.**

ICCW Harvey						
Number	Reach	River Station	Friction ( $n/K$ )	Left Overbank	Channel	Right Overbank
1	Reach 1	13	$n$	0.7	0.7	0.7
2	Reach 1	12	$n$	0.7	0.7	0.7
3	Reach 1	11	$n$	0.7	0.7	0.7
4	Reach 1	10	$n$	0.03	0.03	0.03
5	Reach 1	9	$n$	0.03	0.03	0.03
6	Reach 1	8	$n$	0.03	0.03	0.03
7	Reach 1	7	$n$	0.03	0.03	0.03
8	Reach 1	6	$n$	0.03	0.03	0.03
9	Reach 1	5	$n$	0.03	0.03	0.03
10	Reach 1	4	$n$	0.03	0.03	0.03
11	Reach 1	3	$n$	0.03	0.03	0.03
12	Reach 1	2	$n$	0.03	0.03	0.03
13	Reach 1	1	$n$	0.03	0.03	0.03

**Table G-21: Manning's  $n$  Values for Jesuit Bend.**

Jesuit Bend						
Number	Reach	River Station	Friction ( $n/K$ )	Left Overbank	Channel	Right Overbank
1	Reach 1	11	$n$	0.06	0.03	0.06
2	Reach 1	10	$n$	0.06	0.03	0.06
3	Reach 1	9.5	Inline Structure			
4	Reach 1	9	$n$	0.06	0.03	0.06
5	Reach 1	8	$n$	0.06	0.03	0.06
6	Reach 1	7	$n$	0.06	0.03	0.06
7	Reach 1	6	$n$	0.06	0.03	0.06
8	Reach 1	5	$n$	0.06	0.03	0.06
9	Reach 1	4	$n$	0.06	0.03	0.06
10	Reach 1	3	$n$	0.06	0.03	0.06
11	Reach 1	2	$n$	0.06	0.03	0.06
12	Reach 1	1	$n$	0.06	0.03	0.06



**Table G-22: Manning's  $n$  Values for Little Lake.**

Little Lake						
Number	Reach	River Station	Friction ( $n/K$ )	Left Overbank	Channel	Right Overbank
1	Reach 1	9	$n$	0.03	0.03	0.03
2	Reach 1	8	$n$	0.03	0.03	0.03
3	Reach 1	7	$n$	0.03	0.03	0.03
4	Reach 1	6	$n$	0.03	0.03	0.03
5	Reach 1	5	$n$	0.03	0.03	0.03
6	Reach 1	4	$n$	0.03	0.03	0.03
7	Reach 1	3	$n$	0.03	0.03	0.03
8	Reach 1	2	$n$	0.03	0.03	0.03
9	Reach 1	1	$n$	0.03	0.03	0.03
10	Reach 2	8	$n$	0.03	0.03	0.03
11	Reach 2	7	$n$	0.03	0.03	0.03
12	Reach 2	6	$n$	0.03	0.03	0.03
13	Reach 2	5	$n$	0.03	0.03	0.03
14	Reach 2	4	$n$	0.03	0.03	0.03
15	Reach 2	3	$n$	0.03	0.03	0.03
16	Reach 2	2	$n$	0.03	0.03	0.03
17	Reach 2	1	$n$	0.03	0.03	0.03
18	Reach 3	4	$n$	0.03	0.03	0.03
19	Reach 3	3	$n$	0.03	0.03	0.03
20	Reach 3	2	$n$	0.03	0.03	0.03
21	Reach 3	1	$n$	0.03	0.03	0.03
22	Reach 4	6	$n$	0.03	0.03	0.03
23	Reach 4	5	$n$	0.03	0.03	0.03
24	Reach 4	4	$n$	0.03	0.03	0.03
25	Reach 4	3	$n$	0.03	0.03	0.03
26	Reach 4	2	$n$	0.03	0.03	0.03
27	Reach 4	1	$n$	0.03	0.03	0.03
28	Reach 5	24	$n$	0.03	0.03	0.03
29	Reach 5	23	$n$	0.03	0.03	0.03
30	Reach 5	22	$n$	0.03	0.03	0.03
31	Reach 5	21	$n$	0.03	0.03	0.03
32	Reach 5	20	$n$	0.03	0.03	0.03
33	Reach 5	19	$n$	0.03	0.03	0.03
34	Reach 5	18	$n$	0.03	0.03	0.03
35	Reach 5	17	$n$	0.03	0.03	0.03
36	Reach 5	16	$n$	0.03	0.03	0.03
37	Reach 5	15	$n$	0.03	0.03	0.03
38	Reach 5	14	$n$	0.03	0.03	0.03
39	Reach 5	13	$n$	0.03	0.03	0.03
40	Reach 5	12	$n$	0.03	0.03	0.03

**Table G-22 Continued.**

41	Reach 5	11	<i>n</i>	0.03	0.03	0.03
42	Reach 5	10	<i>n</i>	0.03	0.03	0.03
43	Reach 5	9	<i>n</i>	0.03	0.03	0.03
44	Reach 5	8	<i>n</i>	0.03	0.03	0.03
45	Reach 5	7	<i>n</i>	0.03	0.03	0.03
46	Reach 5	6	<i>n</i>	0.03	0.03	0.03
47	Reach 5	5	<i>n</i>	0.03	0.03	0.03
48	Reach 5	4	<i>n</i>	0.03	0.03	0.03
49	Reach 5	3	<i>n</i>	0.03	0.03	0.03
50	Reach 5	2	<i>n</i>	0.03	0.03	0.03
51	Reach 5	1	<i>n</i>	0.03	0.03	0.03

**Table G-23: Manning's  $n$  Values for Main Pass.**

Main Pass						
Number	Reach	River Station	Friction ( $n/K$ )	Left Overbank	Channel	Right Overbank
1	Reach 1	56	$n$	0.023	0.02	0.023
2	Reach 1	55	$n$	0.023	0.02	0.023
3	Reach 1	54	$n$	0.023	0.02	0.023
4	Reach 1	53	$n$	0.023	0.02	0.023
5	Reach 1	52	$n$	0.023	0.02	0.023
6	Reach 1	51	$n$	0.023	0.02	0.023
7	Reach 1	50	$n$	0.023	0.02	0.023
8	Reach 1	49	$n$	0.023	0.02	0.023
9	Reach 1	48	$n$	0.023	0.02	0.023
10	Reach 1	47	$n$	0.023	0.02	0.023
11	Reach 1	46	$n$	0.023	0.02	0.023
12	Reach 1	45	$n$	0.023	0.02	0.023
13	Reach 1	44	$n$	0.023	0.02	0.023
14	Reach 1	43	$n$	0.023	0.02	0.023
15	Reach 1	42	$n$	0.023	0.02	0.023
16	Reach 1	41	$n$	0.023	0.02	0.023
17	Reach 1	40	$n$	0.023	0.02	0.023
18	Reach 1	39	$n$	0.023	0.02	0.023
19	Reach 1	38	$n$	0.023	0.02	0.023
20	Reach 1	37	$n$	0.023	0.02	0.023
21	Reach 1	36	$n$	0.023	0.02	0.023
22	Reach 1	35	$n$	0.023	0.02	0.023
23	Reach 1	34	$n$	0.023	0.02	0.023
24	Reach 1	33	$n$	0.023	0.02	0.023
25	Reach 1	32	$n$	0.023	0.02	0.023
26	Reach 1	31	$n$	0.023	0.02	0.023
27	Reach 1	30	$n$	0.023	0.02	0.023
28	Reach 1	29	$n$	0.023	0.02	0.023
29	Reach 1	28	$n$	0.023	0.02	0.023
30	Reach 1	27	$n$	0.023	0.02	0.023
31	Reach 1	26	$n$	0.023	0.02	0.023
32	Reach 1	25	$n$	0.023	0.02	0.023
33	Reach 1	24	$n$	0.023	0.02	0.023
34	Reach 1	23	$n$	0.023	0.02	0.023
35	Reach 1	22	$n$	0.023	0.02	0.023
36	Reach 1	21	$n$	0.023	0.02	0.023
37	Reach 1	20	$n$	0.023	0.02	0.023
38	Reach 1	19	$n$	0.023	0.02	0.023
39	Reach 1	18	$n$	0.023	0.02	0.023
40	Reach 1	17	$n$	0.023	0.02	0.023

**Table G-23 Continued.**

41	Reach 1	16	<i>n</i>	0.023	0.02	0.023
42	Reach 1	15	<i>n</i>	0.023	0.02	0.023
43	Reach 1	14	<i>n</i>	0.023	0.02	0.023
44	Reach 1	13	<i>n</i>	0.023	0.02	0.023
45	Reach 1	12	<i>n</i>	0.023	0.02	0.023
46	Reach 1	11	<i>n</i>	0.023	0.02	0.023
47	Reach 1	10	<i>n</i>	0.023	0.02	0.023
48	Reach 1	9	<i>n</i>	0.023	0.02	0.023
49	Reach 1	8	<i>n</i>	0.023	0.02	0.023
50	Reach 1	7.5	<i>n</i>	0.023	0.02	0.023

**Table G-24: Manning's  $n$  Values for Mississippi.**

Mississippi						
Number	Reach	River Station	Friction ( $n/K$ )	Left Overbank	Channel	Right Overbank
1	Reach 1	306	$n$	0.026	0.024	0.026
2	Reach 1	305.8	$n$	0.026	0.024	0.026
3	Reach 1	305.6	$n$	0.026	0.024	0.026
4	Reach 1	305.4	$n$	0.026	0.024	0.026
5	Reach 1	305.2	$n$	0.026	0.024	0.026
6	Reach 1	305	$n$	0.026	0.024	0.026
7	Reach 1	304.8	$n$	0.026	0.024	0.026
8	Reach 1	304.5	$n$	0.026	0.024	0.026
9	Reach 1	304.2	$n$	0.026	0.024	0.026
10	Reach 1	303.7	$n$	0.026	0.024	0.026
11	Reach 1	303.2	$n$	0.026	0.024	0.026
12	Reach 1	302.7	$n$	0.026	0.024	0.026
13	Reach 1	302.3	$n$	0.026	0.024	0.026
14	Reach 1	302	$n$	0.026	0.024	0.026
15	Reach 1	301.7	$n$	0.026	0.024	0.026
16	Reach 1	301.2	$n$	0.026	0.024	0.026
17	Reach 1	300.9	$n$	0.026	0.024	0.026
18	Reach 1	300.5	$n$	0.026	0.024	0.026
19	Reach 1	300.1	$n$	0.026	0.024	0.026
20	Reach 1	299.7	$n$	0.026	0.024	0.026
21	Reach 1	299.4	$n$	0.026	0.024	0.026
22	Reach 1	299	$n$	0.026	0.024	0.026
23	Reach 1	298.5	$n$	0.026	0.024	0.026
24	Reach 1	298.1	$n$	0.026	0.024	0.026
25	Reach 1	297.6	$n$	0.026	0.024	0.026
26	Reach 1	297.3	$n$	0.026	0.024	0.026
27	Reach 1	296.9	$n$	0.026	0.024	0.026
28	Reach 1	296.6	$n$	0.026	0.024	0.026
29	Reach 1	296.5	Lateral Structure			
30	Reach 1	296.3	$n$	0.026	0.024	0.026
31	Reach 1	296	$n$	0.026	0.024	0.026
32	Reach 1	295.7	$n$	0.026	0.024	0.026
33	Reach 1	295.3	$n$	0.026	0.024	0.026
34	Reach 1	295	$n$	0.026	0.024	0.026

**Table G-24 Continued.**

35	Reach 1	294.7	<i>n</i>	0.026	0.024	0.026
36	Reach 1	294.3	<i>n</i>	0.026	0.024	0.026
37	Reach 1	293.9	<i>n</i>	0.026	0.024	0.026
38	Reach 1	293.5	<i>n</i>	0.026	0.024	0.026
39	Reach 1	293.1	<i>n</i>	0.026	0.024	0.026
40	Reach 1	292.7	<i>n</i>	0.026	0.024	0.026
41	Reach 1	292.3	<i>n</i>	0.026	0.024	0.026
42	Reach 1	292	<i>n</i>	0.026	0.024	0.026
43	Reach 1	291.7	<i>n</i>	0.026	0.024	0.026
44	Reach 1	291.3	<i>n</i>	0.026	0.024	0.026
45	Reach 1	290.9	<i>n</i>	0.026	0.024	0.026
46	Reach 1	290.6	<i>n</i>	0.026	0.024	0.026
47	Reach 1	290.2	<i>n</i>	0.026	0.024	0.026
48	Reach 1	289.9	<i>n</i>	0.026	0.024	0.026
49	Reach 1	289.5	<i>n</i>	0.026	0.024	0.026
50	Reach 1	289.2	<i>n</i>	0.026	0.024	0.026
51	Reach 1	289	<i>n</i>	0.026	0.024	0.026
52	Reach 1	288.7	<i>n</i>	0.026	0.024	0.026
53	Reach 1	288.4	<i>n</i>	0.026	0.024	0.026
54	Reach 1	288.1	<i>n</i>	0.026	0.024	0.026
55	Reach 1	287.8	<i>n</i>	0.026	0.024	0.026
56	Reach 1	287.5	<i>n</i>	0.026	0.024	0.026
57	Reach 1	287.2	<i>n</i>	0.026	0.024	0.026
58	Reach 1	287	<i>n</i>	0.026	0.024	0.026
59	Reach 1	286.8	<i>n</i>	0.026	0.024	0.026
60	Reach 1	286.6	<i>n</i>	0.026	0.024	0.026
61	Reach 1	286.2	<i>n</i>	0.026	0.024	0.026
62	Reach 1	285.9	<i>n</i>	0.026	0.024	0.026
63	Reach 1	285.6	<i>n</i>	0.026	0.024	0.026
64	Reach 1	285.3	<i>n</i>	0.026	0.024	0.026
65	Reach 1	285	<i>n</i>	0.026	0.024	0.026
66	Reach 1	284.6	<i>n</i>	0.026	0.024	0.026
67	Reach 1	284.3	<i>n</i>	0.026	0.024	0.026
68	Reach 1	284	<i>n</i>	0.026	0.024	0.026
69	Reach 1	283.6	<i>n</i>	0.026	0.024	0.026
70	Reach 1	283.3	<i>n</i>	0.026	0.024	0.026
71	Reach 1	282.9	<i>n</i>	0.026	0.024	0.026
72	Reach 1	282.5	<i>n</i>	0.026	0.024	0.026

**Table G-24 Continued.**

73	Reach 1	282.1	<i>n</i>	0.026	0.024	0.026
74	Reach 1	281.8	<i>n</i>	0.026	0.024	0.026
75	Reach 1	281.4	<i>n</i>	0.026	0.024	0.026
76	Reach 1	281.2	<i>n</i>	0.026	0.024	0.026
77	Reach 1	280.8	<i>n</i>	0.026	0.024	0.026
78	Reach 1	280.5	<i>n</i>	0.026	0.024	0.026
79	Reach 1	280.1	<i>n</i>	0.026	0.024	0.026
80	Reach 1	279.8	<i>n</i>	0.026	0.024	0.026
81	Reach 1	279.4	<i>n</i>	0.026	0.024	0.026
82	Reach 1	279.1	<i>n</i>	0.026	0.024	0.026
83	Reach 1	278.8	<i>n</i>	0.026	0.024	0.026
84	Reach 1	278.5	<i>n</i>	0.026	0.024	0.026
85	Reach 1	278.2	<i>n</i>	0.026	0.024	0.026
86	Reach 1	277.9	<i>n</i>	0.026	0.024	0.026
87	Reach 1	277.6	<i>n</i>	0.026	0.024	0.026
88	Reach 1	277.3	<i>n</i>	0.026	0.024	0.026
89	Reach 1	277	<i>n</i>	0.026	0.024	0.026
90	Reach 1	276.7	<i>n</i>	0.026	0.024	0.026
91	Reach 1	276.4	<i>n</i>	0.026	0.024	0.026
92	Reach 1	276.1	<i>n</i>	0.026	0.024	0.026
93	Reach 1	275.8	<i>n</i>	0.026	0.024	0.026
94	Reach 1	275.5	<i>n</i>	0.026	0.024	0.026
95	Reach 1	275.2	<i>n</i>	0.026	0.024	0.026
96	Reach 1	274.9	<i>n</i>	0.026	0.024	0.026
97	Reach 1	274.6	<i>n</i>	0.026	0.024	0.026
98	Reach 1	274.3	<i>n</i>	0.026	0.024	0.026
99	Reach 1	274.1	<i>n</i>	0.026	0.024	0.026
100	Reach 1	273.7	<i>n</i>	0.026	0.024	0.026
101	Reach 1	273.5	<i>n</i>	0.026	0.024	0.026
102	Reach 1	273.2	<i>n</i>	0.026	0.024	0.026
103	Reach 1	272.9	<i>n</i>	0.026	0.024	0.026
104	Reach 1	272.6	<i>n</i>	0.026	0.024	0.026
105	Reach 1	272.3	<i>n</i>	0.026	0.024	0.026
106	Reach 1	271.8	<i>n</i>	0.026	0.024	0.026
107	Reach 1	271.4	<i>n</i>	0.026	0.024	0.026
108	Reach 1	271	<i>n</i>	0.026	0.024	0.026
109	Reach 1	270.6	<i>n</i>	0.026	0.024	0.026
110	Reach 1	270.2	<i>n</i>	0.026	0.024	0.026

**Table G-24 Continued.**

111	Reach 1	269.9	<i>n</i>	0.026	0.024	0.026
112	Reach 1	269.6	<i>n</i>	0.026	0.024	0.026
113	Reach 1	269.3	<i>n</i>	0.026	0.024	0.026
114	Reach 1	269	<i>n</i>	0.026	0.024	0.026
115	Reach 1	268.7	<i>n</i>	0.026	0.024	0.026
116	Reach 1	268.4	<i>n</i>	0.026	0.024	0.026
117	Reach 1	268.1	<i>n</i>	0.026	0.024	0.026
118	Reach 1	267.8	<i>n</i>	0.026	0.024	0.026
119	Reach 1	267.4	<i>n</i>	0.026	0.024	0.026
120	Reach 1	267.1	<i>n</i>	0.026	0.024	0.026
121	Reach 1	266.8	<i>n</i>	0.026	0.024	0.026
122	Reach 1	266.4	<i>n</i>	0.026	0.024	0.026
123	Reach 1	266	<i>n</i>	0.026	0.024	0.026
124	Reach 1	265.6	<i>n</i>	0.026	0.024	0.026
125	Reach 1	265.1	<i>n</i>	0.026	0.024	0.026
126	Reach 1	264.6	<i>n</i>	0.026	0.024	0.026
127	Reach 1	264.2	<i>n</i>	0.026	0.024	0.026
128	Reach 1	263.8	<i>n</i>	0.026	0.024	0.026
129	Reach 1	263.4	<i>n</i>	0.026	0.024	0.026
130	Reach 1	263.1	<i>n</i>	0.026	0.024	0.026
131	Reach 1	262.7	<i>n</i>	0.026	0.024	0.026
132	Reach 1	262.3	<i>n</i>	0.026	0.024	0.026
133	Reach 1	261.9	<i>n</i>	0.026	0.024	0.026
134	Reach 1	261.5	<i>n</i>	0.026	0.024	0.026
135	Reach 1	261.2	<i>n</i>	0.026	0.024	0.026
136	Reach 1	260.9	<i>n</i>	0.026	0.024	0.026
137	Reach 1	260.6	<i>n</i>	0.026	0.024	0.026
138	Reach 1	260.3	<i>n</i>	0.026	0.024	0.026
139	Reach 1	260	<i>n</i>	0.026	0.024	0.026
140	Reach 1	259.7	<i>n</i>	0.026	0.024	0.026
141	Reach 1	259.3	<i>n</i>	0.026	0.024	0.026
142	Reach 1	259.1	<i>n</i>	0.026	0.024	0.026
143	Reach 1	258.7	<i>n</i>	0.026	0.024	0.026
144	Reach 1	258.4	<i>n</i>	0.026	0.024	0.026
145	Reach 1	258	<i>n</i>	0.026	0.024	0.026
146	Reach 1	257.6	<i>n</i>	0.026	0.024	0.026
147	Reach 1	257.3	<i>n</i>	0.026	0.024	0.026
148	Reach 1	257	<i>n</i>	0.026	0.024	0.026



**Table G-24 Continued.**

149	Reach 1	256.6	<i>n</i>	0.026	0.024	0.026
150	Reach 1	256.2	<i>n</i>	0.026	0.024	0.026
151	Reach 1	255.9	<i>n</i>	0.026	0.024	0.026
152	Reach 1	255.6	<i>n</i>	0.026	0.024	0.026
153	Reach 1	255.2	<i>n</i>	0.026	0.024	0.026
154	Reach 1	254.8	<i>n</i>	0.026	0.024	0.026
155	Reach 1	254.5	<i>n</i>	0.026	0.024	0.026
156	Reach 1	254.2	<i>n</i>	0.026	0.024	0.026
157	Reach 1	253.6	<i>n</i>	0.026	0.024	0.026
158	Reach 1	253.3	<i>n</i>	0.026	0.024	0.026
159	Reach 1	253	<i>n</i>	0.026	0.024	0.026
160	Reach 1	252.7	<i>n</i>	0.026	0.024	0.026
161	Reach 1	252.4	<i>n</i>	0.026	0.024	0.026
162	Reach 1	251.9	<i>n</i>	0.026	0.024	0.026
163	Reach 1	251.1	<i>n</i>	0.026	0.024	0.026
164	Reach 1	250.6	<i>n</i>	0.026	0.024	0.026
165	Reach 1	250.2	<i>n</i>	0.026	0.024	0.026
166	Reach 1	249.8	<i>n</i>	0.026	0.024	0.026
167	Reach 1	249.3	<i>n</i>	0.026	0.024	0.026
168	Reach 1	248.8	<i>n</i>	0.026	0.024	0.026
169	Reach 1	248.3	<i>n</i>	0.026	0.024	0.026
170	Reach 1	247.8	<i>n</i>	0.026	0.024	0.026
171	Reach 1	247.5	<i>n</i>	0.026	0.024	0.026
172	Reach 1	247.1	<i>n</i>	0.026	0.024	0.026
173	Reach 1	246.8	<i>n</i>	0.026	0.024	0.026
174	Reach 1	246.5	<i>n</i>	0.026	0.024	0.026
175	Reach 1	246.2	<i>n</i>	0.026	0.024	0.026
176	Reach 1	245.8	<i>n</i>	0.026	0.024	0.026
177	Reach 1	245.6	<i>n</i>	0.026	0.024	0.026
178	Reach 1	245.3	<i>n</i>	0.026	0.024	0.026
179	Reach 1	245.1	<i>n</i>	0.026	0.024	0.026
180	Reach 1	244.9	<i>n</i>	0.026	0.024	0.026
181	Reach 1	244.7	<i>n</i>	0.026	0.024	0.026
182	Reach 1	244.5	<i>n</i>	0.026	0.024	0.026
183	Reach 1	244.2	<i>n</i>	0.026	0.024	0.026
184	Reach 1	244.1	<i>n</i>	0.026	0.024	0.026
185	Reach 1	243.9	<i>n</i>	0.026	0.024	0.026
186	Reach 1	243.7	<i>n</i>	0.026	0.024	0.026

**Table G-24 Continued.**

187	Reach 1	243.5	<i>n</i>	0.026	0.024	0.026
188	Reach 1	243.2	<i>n</i>	0.026	0.024	0.026
189	Reach 1	242.9	<i>n</i>	0.026	0.024	0.026
190	Reach 1	242.6	<i>n</i>	0.026	0.024	0.026
191	Reach 1	242.3	<i>n</i>	0.026	0.024	0.026
192	Reach 1	242.1	<i>n</i>	0.026	0.024	0.026
193	Reach 1	241.8	<i>n</i>	0.026	0.024	0.026
194	Reach 1	241.6	<i>n</i>	0.026	0.024	0.026
195	Reach 1	241.4	<i>n</i>	0.026	0.024	0.026
196	Reach 1	241.1	<i>n</i>	0.026	0.024	0.026
197	Reach 1	240.9	<i>n</i>	0.026	0.024	0.026
198	Reach 1	240.6	<i>n</i>	0.026	0.024	0.026
199	Reach 1	240.4	<i>n</i>	0.026	0.024	0.026
200	Reach 1	240.3	<i>n</i>	0.026	0.024	0.026
201	Reach 1	240	<i>n</i>	0.026	0.024	0.026
202	Reach 1	239.8	<i>n</i>	0.026	0.024	0.026
203	Reach 1	239.6	<i>n</i>	0.026	0.024	0.026
204	Reach 1	239.4	<i>n</i>	0.026	0.024	0.026
205	Reach 1	239.1	<i>n</i>	0.026	0.024	0.026
206	Reach 1	238.9	<i>n</i>	0.026	0.024	0.026
207	Reach 1	238.6	<i>n</i>	0.026	0.024	0.026
208	Reach 1	238.3	<i>n</i>	0.026	0.024	0.026
209	Reach 1	238.1	<i>n</i>	0.026	0.024	0.026
210	Reach 1	237.8	<i>n</i>	0.026	0.024	0.026
211	Reach 1	237.5	<i>n</i>	0.026	0.024	0.026
212	Reach 1	237.2	<i>n</i>	0.026	0.024	0.026
213	Reach 1	236.9	<i>n</i>	0.026	0.024	0.026
214	Reach 1	236.5	<i>n</i>	0.026	0.024	0.026
215	Reach 1	236.2	<i>n</i>	0.026	0.024	0.026
216	Reach 1	235.9	<i>n</i>	0.026	0.024	0.026
217	Reach 1	235.7	<i>n</i>	0.026	0.024	0.026
218	Reach 1	235.4	<i>n</i>	0.026	0.024	0.026
219	Reach 1	235.1	<i>n</i>	0.026	0.024	0.026
220	Reach 1	234.8	<i>n</i>	0.026	0.024	0.026
221	Reach 1	234.6	<i>n</i>	0.026	0.024	0.026
222	Reach 1	234.4	<i>n</i>	0.026	0.024	0.026
223	Reach 1	234.2	<i>n</i>	0.026	0.024	0.026
224	Reach 1	234	<i>n</i>	0.026	0.024	0.026

**Table G-24 Continued.**

225	Reach 1	233.8	<i>n</i>	0.026	0.024	0.026
226	Reach 1	233.6	<i>n</i>	0.026	0.024	0.026
227	Reach 1	233.4	<i>n</i>	0.026	0.024	0.026
228	Reach 1	233.2	<i>n</i>	0.026	0.024	0.026
229	Reach 1	233	<i>n</i>	0.026	0.024	0.026
230	Reach 1	232.8	<i>n</i>	0.026	0.024	0.026
231	Reach 1	232.5	<i>n</i>	0.026	0.024	0.026
232	Reach 1	232.3	<i>n</i>	0.026	0.024	0.026
233	Reach 1	232	<i>n</i>	0.026	0.024	0.026
234	Reach 1	231.8	<i>n</i>	0.026	0.024	0.026
235	Reach 1	231.5	<i>n</i>	0.026	0.024	0.026
236	Reach 1	231.2	<i>n</i>	0.026	0.024	0.026
237	Reach 1	230.9	<i>n</i>	0.026	0.024	0.026
238	Reach 1	230.6	<i>n</i>	0.026	0.024	0.026
239	Reach 1	230.4	<i>n</i>	0.026	0.024	0.026
240	Reach 1	230.1	<i>n</i>	0.026	0.024	0.026
241	Reach 1	229.8	<i>n</i>	0.026	0.024	0.026
242	Reach 1	229.6	<i>n</i>	0.026	0.024	0.026
243	Reach 1	229.4	<i>n</i>	0.026	0.024	0.026
244	Reach 1	229.2	<i>n</i>	0.026	0.024	0.026
245	Reach 1	229	<i>n</i>	0.026	0.024	0.026
246	Reach 1	228.7	<i>n</i>	0.026	0.024	0.026
247	Reach 1	228.5	<i>n</i>	0.026	0.024	0.026
248	Reach 1	228.3	<i>n</i>	0.026	0.024	0.026
249	Reach 1	228.1	<i>n</i>	0.026	0.024	0.026
250	Reach 1	227.8	<i>n</i>	0.026	0.024	0.026
251	Reach 1	227.6	<i>n</i>	0.026	0.024	0.026
252	Reach 1	227.4	<i>n</i>	0.026	0.024	0.026
253	Reach 1	227.2	<i>n</i>	0.026	0.024	0.026
254	Reach 1	226.9	<i>n</i>	0.026	0.024	0.026
255	Reach 1	226.6	<i>n</i>	0.026	0.024	0.026
256	Reach 1	226.4	<i>n</i>	0.026	0.024	0.026
257	Reach 1	226.1	<i>n</i>	0.026	0.024	0.026
258	Reach 1	225.8	<i>n</i>	0.026	0.024	0.026
259	Reach 1	225.5	<i>n</i>	0.026	0.024	0.026
260	Reach 1	225.2	<i>n</i>	0.026	0.024	0.026
261	Reach 1	225	<i>n</i>	0.026	0.024	0.026
262	Reach 1	224.7	<i>n</i>	0.026	0.024	0.026

**Table G-24 Continued.**

263	Reach 1	224.5	<i>n</i>	0.026	0.024	0.026
264	Reach 1	224.2	<i>n</i>	0.026	0.024	0.026
265	Reach 1	223.9	<i>n</i>	0.026	0.024	0.026
266	Reach 1	223.6	<i>n</i>	0.026	0.024	0.026
267	Reach 1	223.3	<i>n</i>	0.026	0.024	0.026
268	Reach 1	223.1	<i>n</i>	0.026	0.024	0.026
269	Reach 1	222.9	<i>n</i>	0.026	0.024	0.026
270	Reach 1	222.6	<i>n</i>	0.026	0.024	0.026
271	Reach 1	222.4	<i>n</i>	0.026	0.024	0.026
272	Reach 1	222.1	<i>n</i>	0.026	0.024	0.026
273	Reach 1	221.8	<i>n</i>	0.026	0.024	0.026
274	Reach 1	221.5	<i>n</i>	0.026	0.024	0.026
275	Reach 1	221.2	<i>n</i>	0.026	0.024	0.026
276	Reach 1	220.9	<i>n</i>	0.026	0.024	0.026
277	Reach 1	220.6	<i>n</i>	0.026	0.024	0.026
278	Reach 1	220.3	<i>n</i>	0.026	0.024	0.026
279	Reach 1	220	<i>n</i>	0.026	0.024	0.026
280	Reach 1	219.7	<i>n</i>	0.026	0.024	0.026
281	Reach 1	219.4	<i>n</i>	0.026	0.024	0.026
282	Reach 1	219.1	<i>n</i>	0.026	0.024	0.026
283	Reach 1	218.8	<i>n</i>	0.026	0.024	0.026
284	Reach 1	218.6	<i>n</i>	0.026	0.024	0.026
285	Reach 1	218.3	<i>n</i>	0.026	0.024	0.026
286	Reach 1	217.9	<i>n</i>	0.026	0.024	0.026
287	Reach 1	217.6	<i>n</i>	0.026	0.024	0.026
288	Reach 1	217.3	<i>n</i>	0.026	0.024	0.026
289	Reach 1	216.9	<i>n</i>	0.026	0.024	0.026
290	Reach 1	216.6	<i>n</i>	0.026	0.024	0.026
291	Reach 1	216.4	<i>n</i>	0.026	0.024	0.026
292	Reach 1	216.1	<i>n</i>	0.026	0.024	0.026
293	Reach 1	215.8	<i>n</i>	0.026	0.024	0.026
294	Reach 1	215.5	<i>n</i>	0.026	0.024	0.026
295	Reach 1	215.3	<i>n</i>	0.026	0.024	0.026
296	Reach 1	215.1	<i>n</i>	0.026	0.024	0.026
297	Reach 1	214.9	<i>n</i>	0.026	0.024	0.026
298	Reach 1	214.7	<i>n</i>	0.026	0.024	0.026
299	Reach 1	214.5	<i>n</i>	0.026	0.024	0.026
300	Reach 1	214.2	<i>n</i>	0.026	0.024	0.026

**Table G-24 Continued.**

301	Reach 1	214	<i>n</i>	0.026	0.024	0.026
302	Reach 1	213.7	<i>n</i>	0.026	0.024	0.026
303	Reach 1	213.5	<i>n</i>	0.026	0.024	0.026
304	Reach 1	213.2	<i>n</i>	0.026	0.024	0.026
305	Reach 1	212.9	<i>n</i>	0.026	0.024	0.026
306	Reach 1	212.5	<i>n</i>	0.026	0.024	0.026
307	Reach 1	212.1	<i>n</i>	0.026	0.024	0.026
308	Reach 1	211.8	<i>n</i>	0.026	0.024	0.026
309	Reach 1	211.5	<i>n</i>	0.026	0.024	0.026
310	Reach 1	211.2	<i>n</i>	0.026	0.024	0.026
311	Reach 1	210.9	<i>n</i>	0.026	0.024	0.026
312	Reach 1	210.6	<i>n</i>	0.026	0.024	0.026
313	Reach 1	210.3	<i>n</i>	0.026	0.024	0.026
314	Reach 1	210	<i>n</i>	0.026	0.024	0.026
315	Reach 1	209.7	<i>n</i>	0.026	0.024	0.026
316	Reach 1	209.4	<i>n</i>	0.026	0.024	0.026
317	Reach 1	209.2	<i>n</i>	0.026	0.024	0.026
318	Reach 1	208.9	<i>n</i>	0.026	0.024	0.026
319	Reach 1	208.7	<i>n</i>	0.026	0.024	0.026
320	Reach 1	208.5	<i>n</i>	0.026	0.024	0.026
321	Reach 1	208.2	<i>n</i>	0.026	0.024	0.026
322	Reach 1	208	<i>n</i>	0.026	0.024	0.026
323	Reach 1	207.7	<i>n</i>	0.026	0.024	0.026
324	Reach 1	207.4	<i>n</i>	0.026	0.024	0.026
325	Reach 1	207.1	<i>n</i>	0.026	0.024	0.026
326	Reach 1	206.8	<i>n</i>	0.026	0.024	0.026
327	Reach 1	206.6	<i>n</i>	0.026	0.024	0.026
328	Reach 1	206.4	<i>n</i>	0.026	0.024	0.026
329	Reach 1	206.2	<i>n</i>	0.026	0.024	0.026
330	Reach 1	205.9	<i>n</i>	0.026	0.024	0.026
331	Reach 1	205.6	<i>n</i>	0.026	0.024	0.026
332	Reach 1	205.4	<i>n</i>	0.026	0.024	0.026
333	Reach 1	205.1	<i>n</i>	0.026	0.024	0.026
334	Reach 1	204.8	<i>n</i>	0.026	0.024	0.026
335	Reach 1	204.5	<i>n</i>	0.026	0.024	0.026
336	Reach 1	204.3	<i>n</i>	0.026	0.024	0.026
337	Reach 1	203.9	<i>n</i>	0.026	0.024	0.026
338	Reach 1	203.6	<i>n</i>	0.026	0.024	0.026

**Table G-24 Continued.**

339	Reach 1	203.3	<i>n</i>	0.026	0.024	0.026
340	Reach 1	203	<i>n</i>	0.026	0.024	0.026
341	Reach 1	202.7	<i>n</i>	0.026	0.024	0.026
342	Reach 1	202.4	<i>n</i>	0.026	0.024	0.026
343	Reach 1	202.1	<i>n</i>	0.026	0.024	0.026
344	Reach 1	201.9	<i>n</i>	0.026	0.024	0.026
345	Reach 1	201.6	<i>n</i>	0.026	0.024	0.026
346	Reach 1	201.3	<i>n</i>	0.026	0.024	0.026
347	Reach 1	201	<i>n</i>	0.026	0.024	0.026
348	Reach 1	200.7	<i>n</i>	0.026	0.024	0.026
349	Reach 1	200.5	<i>n</i>	0.026	0.024	0.026
350	Reach 1	200.3	<i>n</i>	0.026	0.024	0.026
351	Reach 1	200.1	<i>n</i>	0.026	0.024	0.026
352	Reach 1	199.9	<i>n</i>	0.026	0.024	0.026
353	Reach 1	199.6	<i>n</i>	0.026	0.024	0.026
354	Reach 1	199.4	<i>n</i>	0.026	0.024	0.026
355	Reach 1	199.1	<i>n</i>	0.026	0.024	0.026
356	Reach 1	198.8	<i>n</i>	0.026	0.024	0.026
357	Reach 1	198.5	<i>n</i>	0.026	0.024	0.026
358	Reach 1	198.2	<i>n</i>	0.026	0.024	0.026
359	Reach 1	197.9	<i>n</i>	0.026	0.024	0.026
360	Reach 1	197.6	<i>n</i>	0.026	0.024	0.026
361	Reach 1	197.3	<i>n</i>	0.026	0.024	0.026
362	Reach 1	197.1	<i>n</i>	0.026	0.024	0.026
363	Reach 1	196.9	<i>n</i>	0.026	0.024	0.026
364	Reach 1	196.6	<i>n</i>	0.026	0.024	0.026
365	Reach 1	196.4	<i>n</i>	0.026	0.024	0.026
366	Reach 1	196.1	<i>n</i>	0.026	0.024	0.026
367	Reach 1	195.9	<i>n</i>	0.026	0.024	0.026
368	Reach 1	195.6	<i>n</i>	0.026	0.024	0.026
369	Reach 1	195.4	<i>n</i>	0.026	0.024	0.026
370	Reach 1	195.1	<i>n</i>	0.026	0.024	0.026
371	Reach 1	194.9	<i>n</i>	0.026	0.024	0.026
372	Reach 1	194.6	<i>n</i>	0.026	0.024	0.026
373	Reach 1	194.4	<i>n</i>	0.026	0.024	0.026
374	Reach 1	194.1	<i>n</i>	0.026	0.024	0.026
375	Reach 1	193.9	<i>n</i>	0.026	0.024	0.026
376	Reach 1	193.7	<i>n</i>	0.026	0.024	0.026

**Table G-24 Continued.**

377	Reach 1	193.4	<i>n</i>	0.026	0.024	0.026
378	Reach 1	193.3	<i>n</i>	0.026	0.024	0.026
379	Reach 1	193	<i>n</i>	0.026	0.024	0.026
380	Reach 1	192.8	<i>n</i>	0.026	0.024	0.026
381	Reach 1	192.5	<i>n</i>	0.026	0.024	0.026
382	Reach 1	192.2	<i>n</i>	0.026	0.024	0.026
383	Reach 1	191.9	<i>n</i>	0.026	0.024	0.026
384	Reach 1	191.6	<i>n</i>	0.026	0.024	0.026
385	Reach 1	191.3	<i>n</i>	0.026	0.024	0.026
386	Reach 1	191	<i>n</i>	0.026	0.024	0.026
387	Reach 1	190.7	<i>n</i>	0.026	0.024	0.026
388	Reach 1	190.4	<i>n</i>	0.026	0.024	0.026
389	Reach 1	190.1	<i>n</i>	0.026	0.024	0.026
390	Reach 1	189.8	<i>n</i>	0.026	0.024	0.026
391	Reach 1	189.5	<i>n</i>	0.026	0.024	0.026
392	Reach 1	189.3	<i>n</i>	0.026	0.024	0.026
393	Reach 1	189	<i>n</i>	0.026	0.024	0.026
394	Reach 1	188.7	<i>n</i>	0.026	0.024	0.026
395	Reach 1	188.5	<i>n</i>	0.026	0.024	0.026
396	Reach 1	188.2	<i>n</i>	0.026	0.024	0.026
397	Reach 1	187.9	<i>n</i>	0.026	0.024	0.026
398	Reach 1	187.6	<i>n</i>	0.026	0.024	0.026
399	Reach 1	187.2	<i>n</i>	0.026	0.024	0.026
400	Reach 1	186.9	<i>n</i>	0.026	0.024	0.026
401	Reach 1	186.6	<i>n</i>	0.026	0.024	0.026
402	Reach 1	186.3	<i>n</i>	0.026	0.024	0.026
403	Reach 1	185.9	<i>n</i>	0.026	0.024	0.026
404	Reach 1	185.6	<i>n</i>	0.026	0.024	0.026
405	Reach 1	185.3	<i>n</i>	0.026	0.024	0.026
406	Reach 1	185	<i>n</i>	0.026	0.024	0.026
407	Reach 1	184.7	<i>n</i>	0.026	0.024	0.026
408	Reach 1	184.5	<i>n</i>	0.026	0.024	0.026
409	Reach 1	184.2	<i>n</i>	0.026	0.024	0.026
410	Reach 1	184	<i>n</i>	0.026	0.024	0.026
411	Reach 1	183.7	<i>n</i>	0.026	0.024	0.026
412	Reach 1	183.4	<i>n</i>	0.026	0.024	0.026
413	Reach 1	183.1	<i>n</i>	0.026	0.024	0.026
414	Reach 1	182.8	<i>n</i>	0.026	0.024	0.026

**Table G-24 Continued.**

415	Reach 1	182.5	<i>n</i>	0.026	0.024	0.026
416	Reach 1	182.3	<i>n</i>	0.026	0.024	0.026
417	Reach 1	182	<i>n</i>	0.026	0.024	0.026
418	Reach 1	181.8	<i>n</i>	0.026	0.024	0.026
419	Reach 1	181.5	<i>n</i>	0.026	0.024	0.026
420	Reach 1	181.3	<i>n</i>	0.026	0.024	0.026
421	Reach 1	181.1	<i>n</i>	0.026	0.024	0.026
422	Reach 1	180.9	<i>n</i>	0.026	0.024	0.026
423	Reach 1	180.6	<i>n</i>	0.026	0.024	0.026
424	Reach 1	180.3	<i>n</i>	0.026	0.024	0.026
425	Reach 1	179.9	<i>n</i>	0.026	0.024	0.026
426	Reach 1	179.7	<i>n</i>	0.026	0.024	0.026
427	Reach 1	179.4	<i>n</i>	0.026	0.024	0.026
428	Reach 1	179.1	<i>n</i>	0.026	0.024	0.026
429	Reach 1	178.7	<i>n</i>	0.026	0.024	0.026
430	Reach 1	178.5	<i>n</i>	0.026	0.024	0.026
431	Reach 1	178.2	<i>n</i>	0.026	0.024	0.026
432	Reach 1	178	<i>n</i>	0.026	0.024	0.026
433	Reach 1	177.8	<i>n</i>	0.026	0.024	0.026
434	Reach 1	177.5	<i>n</i>	0.026	0.024	0.026
435	Reach 1	177.2	<i>n</i>	0.026	0.024	0.026
436	Reach 1	176.9	<i>n</i>	0.026	0.024	0.026
437	Reach 1	176.7	<i>n</i>	0.026	0.024	0.026
438	Reach 1	176.5	<i>n</i>	0.026	0.024	0.026
439	Reach 1	176.3	<i>n</i>	0.026	0.024	0.026
440	Reach 1	176	<i>n</i>	0.026	0.024	0.026
441	Reach 1	175.8	<i>n</i>	0.026	0.024	0.026
442	Reach 1	175.5	<i>n</i>	0.026	0.024	0.026
443	Reach 1	175.2	<i>n</i>	0.026	0.024	0.026
444	Reach 1	174.9	<i>n</i>	0.026	0.024	0.026
445	Reach 1	174.6	<i>n</i>	0.026	0.024	0.026
446	Reach 1	174.3	<i>n</i>	0.026	0.024	0.026
447	Reach 1	174	<i>n</i>	0.026	0.024	0.026
448	Reach 1	173.7	<i>n</i>	0.026	0.024	0.026
449	Reach 1	173.4	<i>n</i>	0.026	0.024	0.026
450	Reach 1	173.2	<i>n</i>	0.026	0.024	0.026
451	Reach 1	172.9	<i>n</i>	0.026	0.024	0.026
452	Reach 1	172.7	<i>n</i>	0.026	0.024	0.026



**Table G-24 Continued.**

453	Reach 1	172.5	<i>n</i>	0.026	0.024	0.026
454	Reach 1	172.3	<i>n</i>	0.026	0.024	0.026
455	Reach 1	172.1	<i>n</i>	0.026	0.024	0.026
456	Reach 1	171.9	<i>n</i>	0.026	0.024	0.026
457	Reach 1	171.7	<i>n</i>	0.026	0.024	0.026
458	Reach 1	171.5	<i>n</i>	0.026	0.024	0.026
459	Reach 1	171.1	<i>n</i>	0.026	0.024	0.026
460	Reach 1	170.9	<i>n</i>	0.026	0.024	0.026
461	Reach 1	170.7	<i>n</i>	0.026	0.024	0.026
462	Reach 1	170.5	<i>n</i>	0.026	0.024	0.026
463	Reach 1	170.2	<i>n</i>	0.026	0.024	0.026
464	Reach 1	169.9	<i>n</i>	0.026	0.024	0.026
465	Reach 1	169.7	<i>n</i>	0.026	0.024	0.026
466	Reach 1	169.5	<i>n</i>	0.026	0.024	0.026
467	Reach 1	169.3	<i>n</i>	0.026	0.024	0.026
468	Reach 1	169.1	<i>n</i>	0.026	0.024	0.026
469	Reach 1	168.8	<i>n</i>	0.026	0.024	0.026
470	Reach 1	168.6	<i>n</i>	0.026	0.024	0.026
471	Reach 1	168.4	<i>n</i>	0.026	0.024	0.026
472	Reach 1	168.1	<i>n</i>	0.026	0.024	0.026
473	Reach 1	167.8	<i>n</i>	0.026	0.024	0.026
474	Reach 1	167.5	<i>n</i>	0.026	0.024	0.026
475	Reach 1	167.3	<i>n</i>	0.026	0.024	0.026
476	Reach 1	167	<i>n</i>	0.026	0.024	0.026
477	Reach 1	166.8	<i>n</i>	0.026	0.024	0.026
478	Reach 1	166.6	<i>n</i>	0.026	0.024	0.026
479	Reach 1	166.3	<i>n</i>	0.026	0.024	0.026
480	Reach 1	166.1	<i>n</i>	0.026	0.024	0.026
481	Reach 1	165.8	<i>n</i>	0.026	0.024	0.026
482	Reach 1	165.5	<i>n</i>	0.026	0.024	0.026
483	Reach 1	165.2	<i>n</i>	0.026	0.024	0.026
484	Reach 1	164.9	<i>n</i>	0.026	0.024	0.026
485	Reach 1	164.6	<i>n</i>	0.026	0.024	0.026
486	Reach 1	164.3	<i>n</i>	0.026	0.024	0.026
487	Reach 1	164	<i>n</i>	0.026	0.024	0.026
488	Reach 1	163.7	<i>n</i>	0.026	0.024	0.026
489	Reach 1	163.5	<i>n</i>	0.026	0.024	0.026
490	Reach 1	163.2	<i>n</i>	0.026	0.024	0.026

**Table G-24 Continued.**

491	Reach 1	162.9	<i>n</i>	0.026	0.024	0.026
492	Reach 1	162.6	<i>n</i>	0.026	0.024	0.026
493	Reach 1	162.3	<i>n</i>	0.026	0.024	0.026
494	Reach 1	161.9	<i>n</i>	0.026	0.024	0.026
495	Reach 1	161.7	<i>n</i>	0.026	0.024	0.026
496	Reach 1	161.3	<i>n</i>	0.026	0.024	0.026
497	Reach 1	161	<i>n</i>	0.026	0.024	0.026
498	Reach 1	160.8	<i>n</i>	0.026	0.024	0.026
499	Reach 1	160.6	<i>n</i>	0.026	0.024	0.026
500	Reach 1	160.4	<i>n</i>	0.026	0.024	0.026
501	Reach 1	160.1	<i>n</i>	0.026	0.024	0.026
502	Reach 1	159.9	<i>n</i>	0.026	0.024	0.026
503	Reach 1	159.6	<i>n</i>	0.026	0.024	0.026
504	Reach 1	159.4	<i>n</i>	0.026	0.024	0.026
505	Reach 1	159.1	<i>n</i>	0.026	0.024	0.026
506	Reach 1	158.9	<i>n</i>	0.026	0.024	0.026
507	Reach 1	158.6	<i>n</i>	0.026	0.024	0.026
508	Reach 1	158.3	<i>n</i>	0.026	0.024	0.026
509	Reach 1	158	<i>n</i>	0.026	0.024	0.026
510	Reach 1	157.8	<i>n</i>	0.026	0.024	0.026
511	Reach 1	157.5	<i>n</i>	0.026	0.024	0.026
512	Reach 1	157.2	<i>n</i>	0.026	0.024	0.026
513	Reach 1	156.9	<i>n</i>	0.026	0.024	0.026
514	Reach 1	156.7	<i>n</i>	0.026	0.024	0.026
515	Reach 1	156.4	<i>n</i>	0.026	0.024	0.026
516	Reach 1	156.1	<i>n</i>	0.026	0.024	0.026
517	Reach 1	155.8	<i>n</i>	0.026	0.024	0.026
518	Reach 1	155.5	<i>n</i>	0.026	0.024	0.026
519	Reach 1	155.1	<i>n</i>	0.026	0.024	0.026
520	Reach 1	154.8	<i>n</i>	0.026	0.024	0.026
521	Reach 1	154.5	<i>n</i>	0.026	0.024	0.026
522	Reach 1	154.2	<i>n</i>	0.026	0.024	0.026
523	Reach 1	153.9	<i>n</i>	0.026	0.024	0.026
524	Reach 1	153.5	<i>n</i>	0.026	0.024	0.026
525	Reach 1	153.2	<i>n</i>	0.026	0.024	0.026
526	Reach 1	152.8	<i>n</i>	0.026	0.024	0.026
527	Reach 1	152.5	<i>n</i>	0.026	0.024	0.026
528	Reach 1	152.1	<i>n</i>	0.026	0.024	0.026

**Table G-24 Continued.**

529	Reach 1	151.9	<i>n</i>	0.026	0.024	0.026
530	Reach 1	151.6	<i>n</i>	0.026	0.024	0.026
531	Reach 1	151.4	<i>n</i>	0.026	0.024	0.026
532	Reach 1	151.1	<i>n</i>	0.026	0.024	0.026
533	Reach 1	150.8	<i>n</i>	0.026	0.024	0.026
534	Reach 1	150.5	<i>n</i>	0.026	0.024	0.026
535	Reach 1	150.2	<i>n</i>	0.026	0.024	0.026
536	Reach 1	149.9	<i>n</i>	0.026	0.024	0.026
537	Reach 1	149.6	<i>n</i>	0.026	0.024	0.026
538	Reach 1	149.3	<i>n</i>	0.026	0.024	0.026
539	Reach 1	149	<i>n</i>	0.026	0.024	0.026
540	Reach 1	148.8	<i>n</i>	0.026	0.024	0.026
541	Reach 1	148.5	<i>n</i>	0.026	0.024	0.026
542	Reach 1	148.2	<i>n</i>	0.026	0.024	0.026
543	Reach 1	147.9	<i>n</i>	0.026	0.024	0.026
544	Reach 1	147.6	<i>n</i>	0.026	0.024	0.026
545	Reach 1	147.3	<i>n</i>	0.026	0.024	0.026
546	Reach 1	146.9	<i>n</i>	0.026	0.024	0.026
547	Reach 1	146.6	<i>n</i>	0.026	0.024	0.026
548	Reach 1	146.4	<i>n</i>	0.026	0.024	0.026
549	Reach 1	146.1	<i>n</i>	0.026	0.024	0.026
550	Reach 1	145.8	<i>n</i>	0.026	0.024	0.026
551	Reach 1	145.5	<i>n</i>	0.026	0.024	0.026
552	Reach 1	145.2	<i>n</i>	0.026	0.024	0.026
553	Reach 1	144.9	<i>n</i>	0.026	0.024	0.026
554	Reach 1	144.6	<i>n</i>	0.026	0.024	0.026
555	Reach 1	144.3	<i>n</i>	0.026	0.024	0.026
556	Reach 1	144	<i>n</i>	0.026	0.024	0.026
557	Reach 1	143.7	<i>n</i>	0.026	0.024	0.026
558	Reach 1	143.3	<i>n</i>	0.026	0.024	0.026
559	Reach 1	143	<i>n</i>	0.026	0.024	0.026
560	Reach 1	142.7	<i>n</i>	0.026	0.024	0.026
561	Reach 1	142.3	<i>n</i>	0.026	0.024	0.026
562	Reach 1	142.1	<i>n</i>	0.026	0.024	0.026
563	Reach 1	141.7	<i>n</i>	0.026	0.024	0.026
564	Reach 1	141.4	<i>n</i>	0.026	0.024	0.026
565	Reach 1	141.1	<i>n</i>	0.026	0.024	0.026
566	Reach 1	140.7	<i>n</i>	0.026	0.024	0.026

**Table G-24 Continued.**

567	Reach 1	140.4	<i>n</i>	0.026	0.024	0.026
568	Reach 1	140	<i>n</i>	0.026	0.024	0.026
569	Reach 1	139.7	<i>n</i>	0.026	0.024	0.026
570	Reach 1	139.4	<i>n</i>	0.026	0.024	0.026
571	Reach 1	139.1	<i>n</i>	0.026	0.024	0.026
572	Reach 1	138.7	<i>n</i>	0.026	0.024	0.026
573	Reach 1	138.4	<i>n</i>	0.026	0.024	0.026
574	Reach 1	138.1	<i>n</i>	0.026	0.024	0.026
575	Reach 1	137.8	<i>n</i>	0.026	0.024	0.026
576	Reach 1	137.4	<i>n</i>	0.026	0.024	0.026
577	Reach 1	137.1	<i>n</i>	0.026	0.024	0.026
578	Reach 1	136.8	<i>n</i>	0.026	0.024	0.026
579	Reach 1	136.5	<i>n</i>	0.026	0.024	0.026
580	Reach 1	136.1	<i>n</i>	0.026	0.024	0.026
581	Reach 1	135.8	<i>n</i>	0.026	0.024	0.026
582	Reach 1	135.6	<i>n</i>	0.026	0.024	0.026
583	Reach 1	135.3	<i>n</i>	0.026	0.024	0.026
584	Reach 1	135	<i>n</i>	0.026	0.024	0.026
585	Reach 1	134.7	<i>n</i>	0.026	0.024	0.026
586	Reach 1	134.4	<i>n</i>	0.026	0.024	0.026
587	Reach 1	134.1	<i>n</i>	0.026	0.024	0.026
588	Reach 1	133.8	<i>n</i>	0.026	0.024	0.026
589	Reach 1	133.4	<i>n</i>	0.026	0.024	0.026
590	Reach 1	133.1	<i>n</i>	0.026	0.024	0.026
591	Reach 1	132.8	<i>n</i>	0.026	0.024	0.026
592	Reach 1	132.5	<i>n</i>	0.026	0.024	0.026
593	Reach 1	132.2	<i>n</i>	0.026	0.024	0.026
594	Reach 1	131.9	<i>n</i>	0.026	0.024	0.026
595	Reach 1	131.5	<i>n</i>	0.026	0.024	0.026
596	Reach 1	131.3	<i>n</i>	0.026	0.024	0.026
597	Reach 1	131	<i>n</i>	0.026	0.024	0.026
598	Reach 1	130.7	<i>n</i>	0.026	0.024	0.026
599	Reach 1	130.5	<i>n</i>	0.026	0.024	0.026
600	Reach 1	130.2	<i>n</i>	0.026	0.024	0.026
601	Reach 1	130	<i>n</i>	0.026	0.024	0.026
602	Reach 1	129.7	<i>n</i>	0.026	0.024	0.026
603	Reach 1	129.5	<i>n</i>	0.026	0.024	0.026
604	Reach 1	129.2	<i>n</i>	0.026	0.024	0.026

**Table G-24 Continued.**

605	Reach 1	129	<i>n</i>	0.026	0.024	0.026
606	Reach 1	128.7	<i>n</i>	0.026	0.024	0.026
607	Reach 1	128.6	Lateral Structure			
608	Reach 1	128.4	<i>n</i>	0.026	0.024	0.026
609	Reach 1	128.1	<i>n</i>	0.026	0.024	0.026
610	Reach 1	127.8	<i>n</i>	0.026	0.024	0.026
611	Reach 1	127.5	<i>n</i>	0.026	0.024	0.026
612	Reach 1	127.2	<i>n</i>	0.026	0.024	0.026
613	Reach 1	126.9	<i>n</i>	0.026	0.024	0.026
614	Reach 1	126.6	<i>n</i>	0.026	0.024	0.026
615	Reach 1	126.3	<i>n</i>	0.026	0.024	0.026
616	Reach 1	126	<i>n</i>	0.026	0.024	0.026
617	Reach 1	125.8	<i>n</i>	0.026	0.024	0.026
618	Reach 1	125.5	<i>n</i>	0.026	0.024	0.026
619	Reach 1	125.2	<i>n</i>	0.026	0.024	0.026
620	Reach 1	125	<i>n</i>	0.026	0.024	0.026
621	Reach 1	124.7	<i>n</i>	0.026	0.024	0.026
622	Reach 1	124.5	<i>n</i>	0.026	0.024	0.026
623	Reach 1	124.2	<i>n</i>	0.026	0.024	0.026
624	Reach 1	124	<i>n</i>	0.026	0.024	0.026
625	Reach 1	123.8	<i>n</i>	0.026	0.024	0.026
626	Reach 1	123.5	<i>n</i>	0.026	0.024	0.026
627	Reach 1	123.3	<i>n</i>	0.026	0.024	0.026
628	Reach 1	123.1	<i>n</i>	0.026	0.024	0.026
629	Reach 1	122.8	<i>n</i>	0.026	0.024	0.026
630	Reach 1	122.5	<i>n</i>	0.026	0.024	0.026
631	Reach 1	122.2	<i>n</i>	0.026	0.024	0.026
632	Reach 1	121.9	<i>n</i>	0.026	0.024	0.026
633	Reach 1	121.6	<i>n</i>	0.026	0.024	0.026
634	Reach 1	121.3	<i>n</i>	0.026	0.024	0.026
635	Reach 1	120.9	<i>n</i>	0.026	0.024	0.026
636	Reach 1	120.6	<i>n</i>	0.026	0.024	0.026
637	Reach 1	120.2	<i>n</i>	0.026	0.024	0.026
638	Reach 1	119.9	<i>n</i>	0.026	0.024	0.026
639	Reach 1	119.7	<i>n</i>	0.026	0.024	0.026
640	Reach 1	119.4	<i>n</i>	0.026	0.024	0.026
641	Reach 1	119	<i>n</i>	0.026	0.024	0.026

**Table G-24 Continued.**

642	Reach 1	118.7	<i>n</i>	0.026	0.024	0.026
643	Reach 1	118.5	<i>n</i>	0.026	0.024	0.026
644	Reach 2	118.2	<i>n</i>	0.025	0.024	0.025
645	Reach 2	117.9	<i>n</i>	0.025	0.024	0.025
646	Reach 2	117.6	<i>n</i>	0.025	0.024	0.025
647	Reach 2	117.3	<i>n</i>	0.025	0.024	0.025
648	Reach 2	117.1	<i>n</i>	0.025	0.024	0.025
649	Reach 2	116.8	<i>n</i>	0.025	0.024	0.025
650	Reach 2	116.6	<i>n</i>	0.025	0.024	0.025
651	Reach 2	116.3	<i>n</i>	0.025	0.024	0.025
652	Reach 2	116	<i>n</i>	0.025	0.024	0.025
653	Reach 2	115.6	<i>n</i>	0.025	0.024	0.025
654	Reach 2	115.3	<i>n</i>	0.025	0.024	0.025
655	Reach 2	115	<i>n</i>	0.025	0.024	0.025
656	Reach 2	114.8	<i>n</i>	0.025	0.024	0.025
657	Reach 2	114.5	<i>n</i>	0.025	0.024	0.025
658	Reach 2	114.2	<i>n</i>	0.025	0.024	0.025
659	Reach 2	113.8	<i>n</i>	0.025	0.024	0.025
660	Reach 2	113.5	<i>n</i>	0.025	0.024	0.025
661	Reach 2	113.1	<i>n</i>	0.025	0.024	0.025
662	Reach 2	112.8	<i>n</i>	0.025	0.024	0.025
663	Reach 2	112.4	<i>n</i>	0.025	0.024	0.025
664	Reach 2	112.1	<i>n</i>	0.025	0.024	0.025
665	Reach 2	111.9	<i>n</i>	0.025	0.024	0.025
666	Reach 2	111.6	<i>n</i>	0.025	0.024	0.025
667	Reach 2	111.3	<i>n</i>	0.025	0.024	0.025
668	Reach 2	111	<i>n</i>	0.025	0.024	0.025
669	Reach 2	110.7	<i>n</i>	0.025	0.024	0.025
670	Reach 2	110.4	<i>n</i>	0.025	0.024	0.025
671	Reach 2	110.2	<i>n</i>	0.025	0.024	0.025
672	Reach 2	109.9	<i>n</i>	0.025	0.024	0.025
673	Reach 2	109.7	<i>n</i>	0.025	0.024	0.025
674	Reach 2	109.5	<i>n</i>	0.025	0.024	0.025
675	Reach 2	109.2	<i>n</i>	0.025	0.024	0.025
676	Reach 2	109	<i>n</i>	0.025	0.024	0.025
677	Reach 2	108.8	<i>n</i>	0.025	0.024	0.025
678	Reach 2	108.6	<i>n</i>	0.025	0.024	0.025
679	Reach 2	108.4	<i>n</i>	0.025	0.024	0.025

**Table G-24 Continued.**

680	Reach 2	108.2	<i>n</i>	0.025	0.024	0.025
681	Reach 2	107.9	<i>n</i>	0.025	0.024	0.025
682	Reach 2	107.6	<i>n</i>	0.025	0.024	0.025
683	Reach 2	107.4	<i>n</i>	0.025	0.024	0.025
684	Reach 2	107.1	<i>n</i>	0.025	0.024	0.025
685	Reach 2	106.9	<i>n</i>	0.025	0.024	0.025
686	Reach 2	106.6	<i>n</i>	0.025	0.024	0.025
687	Reach 2	106.3	<i>n</i>	0.025	0.024	0.025
688	Reach 2	106	<i>n</i>	0.025	0.024	0.025
689	Reach 2	105.7	<i>n</i>	0.025	0.024	0.025
690	Reach 2	105.5	<i>n</i>	0.025	0.024	0.025
691	Reach 2	105.2	<i>n</i>	0.025	0.024	0.025
692	Reach 2	105	<i>n</i>	0.025	0.024	0.025
693	Reach 2	104.8	<i>n</i>	0.025	0.024	0.025
694	Reach 2	104.6	<i>n</i>	0.025	0.024	0.025
695	Reach 2	104.4	<i>n</i>	0.025	0.024	0.025
696	Reach 2	104.2	<i>n</i>	0.025	0.024	0.025
697	Reach 2	103.9	<i>n</i>	0.025	0.024	0.025
698	Reach 2	103.7	<i>n</i>	0.025	0.024	0.025
699	Reach 2	103.5	<i>n</i>	0.025	0.024	0.025
700	Reach 2	103.3	<i>n</i>	0.025	0.024	0.025
701	Reach 2	103.1	<i>n</i>	0.025	0.024	0.025
702	Reach 2	102.8	<i>n</i>	0.025	0.024	0.025
703	Reach 2	102.7	<i>n</i>	0.025	0.024	0.025
704	Reach 2	102.4	<i>n</i>	0.025	0.024	0.025
705	Reach 2	102.2	<i>n</i>	0.025	0.024	0.025
706	Reach 2	102	<i>n</i>	0.025	0.024	0.025
707	Reach 2	101.8	<i>n</i>	0.025	0.024	0.025
708	Reach 2	101.6	<i>n</i>	0.025	0.024	0.025
709	Reach 2	101.4	<i>n</i>	0.025	0.024	0.025
710	Reach 2	101.3	<i>n</i>	0.025	0.024	0.025
711	Reach 2	101.1	<i>n</i>	0.025	0.024	0.025
712	Reach 2	100.9	<i>n</i>	0.025	0.024	0.025
713	Reach 2	100.7	<i>n</i>	0.025	0.024	0.025
714	Reach 2	100.6	<i>n</i>	0.025	0.024	0.025
715	Reach 2	100.4	<i>n</i>	0.025	0.024	0.025
716	Reach 2	100.1	<i>n</i>	0.025	0.024	0.025
717	Reach 2	99.9	<i>n</i>	0.025	0.024	0.025

**Table G-24 Continued.**

718	Reach 2	99.6	<i>n</i>	0.025	0.024	0.025
719	Reach 2	99.3	<i>n</i>	0.025	0.024	0.025
720	Reach 2	99	<i>n</i>	0.025	0.024	0.025
721	Reach 2	98.7	<i>n</i>	0.025	0.024	0.025
722	Reach 2	98.5	<i>n</i>	0.025	0.024	0.025
723	Reach 2	98.2	<i>n</i>	0.025	0.024	0.025
724	Reach 3	97.9	<i>n</i>	0.025	0.024	0.025
725	Reach 3	97.7	<i>n</i>	0.025	0.024	0.025
726	Reach 3	97.4	<i>n</i>	0.025	0.024	0.025
727	Reach 3	97.1	<i>n</i>	0.025	0.024	0.025
728	Reach 3	96.9	<i>n</i>	0.025	0.024	0.025
729	Reach 3	96.7	<i>n</i>	0.025	0.024	0.025
730	Reach 3	96.5	<i>n</i>	0.025	0.024	0.025
731	Reach 3	96.3	<i>n</i>	0.025	0.024	0.025
732	Reach 3	96.2	<i>n</i>	0.025	0.024	0.025
733	Reach 3	96	<i>n</i>	0.025	0.024	0.025
734	Reach 3	95.8	<i>n</i>	0.025	0.024	0.025
735	Reach 3	95.6	<i>n</i>	0.025	0.024	0.025
736	Reach 3	95.5	<i>n</i>	0.025	0.024	0.025
737	Reach 3	95.4	<i>n</i>	0.025	0.024	0.025
738	Reach 3	95.2	<i>n</i>	0.025	0.024	0.025
739	Reach 3	95.1	<i>n</i>	0.025	0.024	0.025
740	Reach 3	94.9	<i>n</i>	0.025	0.024	0.025
741	Reach 3	94.7	<i>n</i>	0.025	0.024	0.025
742	Reach 3	94.6	<i>n</i>	0.025	0.024	0.025
743	Reach 3	94.4	<i>n</i>	0.025	0.024	0.025
744	Reach 3	94.2	<i>n</i>	0.025	0.024	0.025
745	Reach 3	94	<i>n</i>	0.025	0.024	0.025
746	Reach 3	93.8	<i>n</i>	0.025	0.024	0.025
747	Reach 3	93.6	<i>n</i>	0.025	0.024	0.025
748	Reach 3	93.4	<i>n</i>	0.025	0.024	0.025
749	Reach 3	93.1	<i>n</i>	0.025	0.024	0.025
750	Reach 3	92.9	<i>n</i>	0.025	0.024	0.025
751	Reach 3	92.6	<i>n</i>	0.025	0.024	0.025
752	Reach 3	92.3	<i>n</i>	0.025	0.024	0.025
753	Reach 3	92	<i>n</i>	0.025	0.024	0.025
754	Reach 3	91.8	<i>n</i>	0.025	0.024	0.025
755	Reach 3	91.5	<i>n</i>	0.025	0.024	0.025



**Table G-24 Continued.**

756	Reach 3	91.2	<i>n</i>	0.025	0.024	0.025
757	Reach 3	90.9	<i>n</i>	0.025	0.024	0.025
758	Reach 3	90.6	<i>n</i>	0.025	0.024	0.025
759	Reach 3	90.4	<i>n</i>	0.025	0.024	0.025
760	Reach 3	90.1	<i>n</i>	0.025	0.024	0.025
761	Reach 3	89.9	<i>n</i>	0.025	0.024	0.025
762	Reach 3	89.5	<i>n</i>	0.025	0.024	0.025
763	Reach 3	89.3	<i>n</i>	0.025	0.024	0.025
764	Reach 3	88.9	<i>n</i>	0.025	0.024	0.025
765	Reach 3	88.6	<i>n</i>	0.025	0.024	0.025
766	Reach 3	88.3	<i>n</i>	0.025	0.024	0.025
767	Reach 3	88.1	<i>n</i>	0.025	0.024	0.025
768	Reach 3	87.8	<i>n</i>	0.025	0.024	0.025
769	Reach 4	87.5	<i>n</i>	0.025	0.024	0.025
770	Reach 4	87.2	<i>n</i>	0.025	0.024	0.025
771	Reach 4	87	<i>n</i>	0.025	0.024	0.025
772	Reach 4	86.7	<i>n</i>	0.025	0.024	0.025
773	Reach 4	86.3	<i>n</i>	0.025	0.024	0.025
774	Reach 4	86	<i>n</i>	0.025	0.024	0.025
775	Reach 4	85.7	<i>n</i>	0.025	0.024	0.025
776	Reach 4	85.4	<i>n</i>	0.025	0.024	0.025
777	Reach 4	85.1	<i>n</i>	0.025	0.024	0.025
778	Reach 4	84.8	<i>n</i>	0.025	0.024	0.025
779	Reach 4	84.6	<i>n</i>	0.025	0.024	0.025
780	Reach 4	84.2	<i>n</i>	0.025	0.024	0.025
781	Reach 4	83.9	<i>n</i>	0.025	0.024	0.025
782	Reach 4	83.6	<i>n</i>	0.025	0.024	0.025
783	Reach 4	83.3	<i>n</i>	0.025	0.024	0.025
784	Reach 4	83.1	<i>n</i>	0.025	0.024	0.025
785	Reach 4	82.8	<i>n</i>	0.025	0.024	0.025
786	Reach 4	82.6	<i>n</i>	0.025	0.024	0.025
787	Reach 4	82.4	<i>n</i>	0.025	0.024	0.025
788	Reach 4	82.2	<i>n</i>	0.025	0.024	0.025
789	Reach 4	82	<i>n</i>	0.025	0.024	0.025
790	Reach 4	81.8	<i>n</i>	0.025	0.024	0.025
791	Reach 4	81.5	<i>n</i>	0.025	0.024	0.025
792	Reach 5	81.2	<i>n</i>	0.025	0.024	0.025
793	Reach 5	80.9	<i>n</i>	0.025	0.024	0.025

**Table G-24 Continued.**

794	Reach 5	80.6	<i>n</i>	0.025	0.024	0.025
795	Reach 5	80.3	<i>n</i>	0.025	0.024	0.025
796	Reach 5	80	<i>n</i>	0.025	0.024	0.025
797	Reach 5	79.7	<i>n</i>	0.025	0.024	0.025
798	Reach 5	79.5	<i>n</i>	0.025	0.024	0.025
799	Reach 5	79.2	<i>n</i>	0.025	0.024	0.025
800	Reach 5	78.9	<i>n</i>	0.025	0.024	0.025
801	Reach 5	78.6	<i>n</i>	0.025	0.024	0.025
802	Reach 5	78.4	<i>n</i>	0.025	0.024	0.025
803	Reach 5	78.1	<i>n</i>	0.025	0.024	0.025
804	Reach 5	77.9	<i>n</i>	0.025	0.024	0.025
805	Reach 5	77.7	<i>n</i>	0.025	0.024	0.025
806	Reach 5	77.5	<i>n</i>	0.025	0.024	0.025
807	Reach 5	77.2	<i>n</i>	0.025	0.024	0.025
808	Reach 5	76.9	<i>n</i>	0.025	0.024	0.025
809	Reach 5	76.7	<i>n</i>	0.025	0.024	0.025
810	Reach 5	76.5	<i>n</i>	0.025	0.024	0.025
811	Reach 5	76.3	<i>n</i>	0.025	0.024	0.025
812	Reach 5	76.2	<i>n</i>	0.025	0.024	0.025
813	Reach 5	76	<i>n</i>	0.025	0.024	0.025
814	Reach 5	75.7	<i>n</i>	0.025	0.024	0.025
815	Reach 5	75.5	<i>n</i>	0.025	0.024	0.025
816	Reach 5	75.3	<i>n</i>	0.025	0.024	0.025
817	Reach 5	75.1	<i>n</i>	0.025	0.024	0.025
818	Reach 5	74.9	<i>n</i>	0.025	0.024	0.025
819	Reach 5	74.6	<i>n</i>	0.025	0.024	0.025
820	Reach 5	74.4	<i>n</i>	0.025	0.024	0.025
821	Reach 5	74.1	<i>n</i>	0.025	0.024	0.025
822	Reach 5	73.8	<i>n</i>	0.025	0.024	0.025
823	Reach 5	73.6	<i>n</i>	0.025	0.024	0.025
824	Reach 5	73.3	<i>n</i>	0.025	0.024	0.025
825	Reach 5	73.2	<i>n</i>	0.025	0.024	0.025
826	Reach 5	73	<i>n</i>	0.025	0.024	0.025
827	Reach 5	72.8	<i>n</i>	0.025	0.024	0.025
828	Reach 5	72.6	<i>n</i>	0.025	0.024	0.025
829	Reach 5	72.3	<i>n</i>	0.025	0.024	0.025
830	Reach 5	72.2	<i>n</i>	0.025	0.024	0.025
831	Reach 5	71.9	<i>n</i>	0.025	0.024	0.025

**Table G-24 Continued.**

832	Reach 5	71.7	<i>n</i>	0.025	0.024	0.025
833	Reach 5	71.5	<i>n</i>	0.025	0.024	0.025
834	Reach 5	71.2	<i>n</i>	0.025	0.024	0.025
835	Reach 5	71	<i>n</i>	0.025	0.024	0.025
836	Reach 5	70.8	<i>n</i>	0.025	0.024	0.025
837	Reach 5	70.6	<i>n</i>	0.025	0.024	0.025
838	Reach 5	70.3	<i>n</i>	0.025	0.024	0.025
839	Reach 5	70.1	<i>n</i>	0.025	0.024	0.025
840	Reach 5	69.9	<i>n</i>	0.025	0.024	0.025
841	Reach 5	69.7	<i>n</i>	0.025	0.024	0.025
842	Reach 5	69.4	<i>n</i>	0.025	0.024	0.025
843	Reach 5	69.1	<i>n</i>	0.025	0.024	0.025
844	Reach 5	68.9	<i>n</i>	0.025	0.024	0.025
845	Reach 5	68.6	<i>n</i>	0.025	0.024	0.025
846	Reach 5	68.4	<i>n</i>	0.025	0.024	0.025
847	Reach 5	68.2	<i>n</i>	0.025	0.024	0.025
848	Reach 5	68	<i>n</i>	0.025	0.024	0.025
849	Reach 5	67.8	<i>n</i>	0.025	0.024	0.025
850	Reach 5	67.5	<i>n</i>	0.025	0.024	0.025
851	Reach 5	67.3	<i>n</i>	0.025	0.024	0.025
852	Reach 5	67.1	<i>n</i>	0.025	0.024	0.025
853	Reach 5	66.9	<i>n</i>	0.025	0.024	0.025
854	Reach 5	66.6	<i>n</i>	0.025	0.024	0.025
855	Reach 5	66.4	<i>n</i>	0.025	0.024	0.025
856	Reach 5	66.1	<i>n</i>	0.025	0.024	0.025
857	Reach 5	65.8	<i>n</i>	0.025	0.024	0.025
858	Reach 5	65.6	<i>n</i>	0.025	0.024	0.025
859	Reach 5	65.3	<i>n</i>	0.025	0.024	0.025
860	Reach 5	65	<i>n</i>	0.025	0.024	0.025
861	Reach 5	64.7	<i>n</i>	0.025	0.024	0.025
862	Reach 5	64.5	<i>n</i>	0.025	0.024	0.025
863	Reach 5	64.2	<i>n</i>	0.025	0.024	0.025
864	Reach 5	63.9	<i>n</i>	0.025	0.024	0.025
865	Reach 5	63.6	<i>n</i>	0.025	0.024	0.025
866	Reach 5	63.4	<i>n</i>	0.025	0.024	0.025
867	Reach 5	63.1	<i>n</i>	0.025	0.024	0.025
868	Reach 5	62.9	<i>n</i>	0.025	0.024	0.025
869	Reach 5	62.6	<i>n</i>	0.025	0.024	0.025

**Table G-24 Continued.**

870	Reach 5	62.3	<i>n</i>	0.025	0.024	0.025
871	Reach 5	62.1	<i>n</i>	0.025	0.024	0.025
872	Reach 5	61.9	<i>n</i>	0.025	0.024	0.025
873	Reach 5	61.6	<i>n</i>	0.025	0.024	0.025
874	Reach 5	61.3	<i>n</i>	0.025	0.024	0.025
875	Reach 5	61	<i>n</i>	0.025	0.024	0.025
876	Reach 5	60.8	<i>n</i>	0.025	0.024	0.025
877	Reach 5	60.6	<i>n</i>	0.025	0.024	0.025
878	Reach 5	60.4	<i>n</i>	0.025	0.024	0.025
879	Reach 5	60.2	<i>n</i>	0.025	0.024	0.025
880	Reach 5	60	<i>n</i>	0.025	0.024	0.025
881	Reach 5	59.7	<i>n</i>	0.025	0.024	0.025
882	Reach 5	59.5	<i>n</i>	0.025	0.024	0.025
883	Reach 5	59.3	<i>n</i>	0.025	0.024	0.025
884	Reach 5	59.1	<i>n</i>	0.025	0.024	0.025
885	Reach 5	58.8	<i>n</i>	0.025	0.024	0.025
886	Reach 5	58.4	<i>n</i>	0.025	0.023	0.025
887	Reach 5	58.2	<i>n</i>	0.025	0.023	0.025
888	Reach 5	57.9	<i>n</i>	0.025	0.023	0.025
889	Reach 5	57.6	<i>n</i>	0.025	0.023	0.025
890	Reach 5	57.3	<i>n</i>	0.025	0.023	0.025
891	Reach 5	56.9	<i>n</i>	0.025	0.023	0.025
892	Reach 5	56.5	<i>n</i>	0.025	0.023	0.025
893	Reach 5	56.2	<i>n</i>	0.025	0.023	0.025
894	Reach 5	55.8	<i>n</i>	0.025	0.023	0.025
895	Reach 5	55.4	<i>n</i>	0.025	0.023	0.025
896	Reach 5	55.1	<i>n</i>	0.025	0.023	0.025
897	Reach 5	54.8	<i>n</i>	0.025	0.023	0.025
898	Reach 5	54.5	<i>n</i>	0.025	0.023	0.025
899	Reach 5	54.2	<i>n</i>	0.025	0.023	0.025
900	Reach 5	53.9	<i>n</i>	0.025	0.023	0.025
901	Reach 5	53.6	<i>n</i>	0.025	0.023	0.025
902	Reach 5	53.3	<i>n</i>	0.025	0.023	0.025
903	Reach 5	53	<i>n</i>	0.025	0.023	0.025
904	Reach 5	52.6	<i>n</i>	0.025	0.023	0.025
905	Reach 5	52.3	<i>n</i>	0.025	0.023	0.025
906	Reach 5	51.9	<i>n</i>	0.025	0.023	0.025
907	Reach 5	51.6	<i>n</i>	0.025	0.023	0.025

**Table G-24 Continued.**

908	Reach 5	51.2	<i>n</i>	0.025	0.023	0.025
909	Reach 5	50.9	<i>n</i>	0.025	0.023	0.025
910	Reach 5	50.5	<i>n</i>	0.025	0.023	0.025
911	Reach 5	50.2	<i>n</i>	0.025	0.023	0.025
912	Reach 5	49.8	<i>n</i>	0.025	0.023	0.025
913	Reach 5	49.5	<i>n</i>	0.025	0.023	0.025
914	Reach 5	49.1	<i>n</i>	0.025	0.023	0.025
915	Reach 5	48.8	<i>n</i>	0.025	0.023	0.025
916	Reach 5	48.5	<i>n</i>	0.025	0.023	0.025
917	Reach 5	48.2	<i>n</i>	0.025	0.023	0.025
918	Reach 5	47.9	<i>n</i>	0.025	0.023	0.025
919	Reach 5	47.6	<i>n</i>	0.025	0.023	0.025
920	Reach 5	47.2	<i>n</i>	0.025	0.023	0.025
921	Reach 5	46.9	<i>n</i>	0.025	0.023	0.025
922	Reach 5	46.5	<i>n</i>	0.025	0.023	0.025
923	Reach 5	46.1	<i>n</i>	0.025	0.023	0.025
924	Reach 5	45.7	<i>n</i>	0.025	0.023	0.025
925	Reach 5	45.3	<i>n</i>	0.025	0.021	0.025
926	Reach 5	45	<i>n</i>	0.025	0.021	0.025
927	Reach 5	44.7	<i>n</i>	0.025	0.021	0.025
928	Reach 5	44.4	<i>n</i>	0.025	0.021	0.025
929	Reach 5	44.1	<i>n</i>	0.025	0.021	0.025
930	Reach 5	43.8	<i>n</i>	0.025	0.021	0.025
931	Reach 5	43.5	<i>n</i>	0.025	0.021	0.025
932	Reach 5	43.2	<i>n</i>	0.025	0.021	0.025
933	Reach 5	42.9	<i>n</i>	0.025	0.021	0.025
934	Reach 5	42.6	<i>n</i>	0.025	0.021	0.025
935	Reach 5	42.3	<i>n</i>	0.025	0.021	0.025
936	Reach 5	42	<i>n</i>	0.025	0.021	0.025
937	Reach 5	41.6	<i>n</i>	0.025	0.021	0.025
938	Reach 5	41.3	<i>n</i>	0.025	0.021	0.025
939	Reach 5	41	<i>n</i>	0.025	0.021	0.025
940	Reach 5	40.7	<i>n</i>	0.025	0.021	0.025
941	Reach 5	40.4	<i>n</i>	0.025	0.021	0.025
942	Reach 5	40.1	<i>n</i>	0.025	0.021	0.025
943	Reach 5	39.8	<i>n</i>	0.025	0.021	0.025
944	Reach 5	39.5	<i>n</i>	0.025	0.021	0.025
945	Reach 5	39.3	<i>n</i>	0.025	0.021	0.025

**Table G-24 Continued.**

946	Reach 5	39	<i>n</i>	0.025	0.021	0.025
947	Reach 5	38.7	<i>n</i>	0.025	0.021	0.025
948	Reach 5	38.6	Lateral Structure			
949	Reach 5	38.4	<i>n</i>	0.025	0.021	0.025
950	Reach 5	38.1	<i>n</i>	0.025	0.021	0.025
951	Reach 5	37.8	<i>n</i>	0.025	0.021	0.025
952	Reach 5	37.5	<i>n</i>	0.025	0.021	0.025
953	Reach 5	37.2	<i>n</i>	0.025	0.021	0.025
954	Reach 5	36.9	<i>n</i>	0.025	0.021	0.025
955	Reach 5	36.6	<i>n</i>	0.025	0.021	0.025
956	Reach 5	36.4	<i>n</i>	0.025	0.021	0.025
957	Reach 5	36.1	<i>n</i>	0.025	0.021	0.025
958	Reach 5	35.8	<i>n</i>	0.025	0.021	0.025
959	Reach 5	35.5	<i>n</i>	0.025	0.021	0.025
960	Reach 5	35.2	<i>n</i>	0.025	0.021	0.025
961	Reach 5	34.9	<i>n</i>	0.025	0.021	0.025
962	Reach 5	34.7	<i>n</i>	0.025	0.021	0.025
963	Reach 5	34.3	<i>n</i>	0.025	0.021	0.025
964	Reach 5	33.9	<i>n</i>	0.025	0.021	0.025
965	Reach 5	33.6	<i>n</i>	0.025	0.021	0.025
966	Reach 5	33.3	<i>n</i>	0.025	0.021	0.025
967	Reach 5	32.9	<i>n</i>	0.025	0.021	0.025
968	Reach 5	32.7	<i>n</i>	0.025	0.021	0.025
969	Reach 6	32.71	<i>n</i>	0.025	0.021	0.025
970	Reach 6	32.7	<i>n</i>	0.025	0.021	0.025
971	Reach 6	32.6	Lateral Structure			
972	Reach 6	32.41	<i>n</i>	0.025	0.02	0.025
973	Reach 6	32.4	<i>n</i>	0.025	0.02	0.025
974	Reach 7	32.41	<i>n</i>	0.025	0.02	0.025
975	Reach 7	32.4	<i>n</i>	0.025	0.02	0.025
976	Reach 7	32.3	Lateral Structure			
977	Reach 7	32.1	<i>n</i>	0.025	0.02	0.025
978	Reach 7	31.9	<i>n</i>	0.025	0.02	0.025
979	Reach 7	31.6	<i>n</i>	0.025	0.02	0.025
980	Reach 7	31.4	<i>n</i>	0.025	0.02	0.025

**Table G-24 Continued.**

981	Reach 7	31.2	<i>n</i>	0.025	0.02	0.025
982	Reach 7	31	<i>n</i>	0.025	0.02	0.025
983	Reach 7	30.8	<i>n</i>	0.025	0.02	0.025
984	Reach 7	30.6	<i>n</i>	0.025	0.02	0.025
985	Reach 7	30.4	<i>n</i>	0.025	0.02	0.025
986	Reach 7	30.1	<i>n</i>	0.025	0.02	0.025
987	Reach 7	29.9	<i>n</i>	0.025	0.02	0.025
988	Reach 7	29.6	<i>n</i>	0.025	0.02	0.025
989	Reach 7	29.5	<i>n</i>	0.025	0.02	0.025
990	Reach 7	29.2	<i>n</i>	0.025	0.02	0.025
991	Reach 7	29	<i>n</i>	0.025	0.02	0.025
992	Reach 7	28.8	<i>n</i>	0.025	0.02	0.025
993	Reach 7	28.5	<i>n</i>	0.025	0.02	0.025
994	Reach 7	28.3	<i>n</i>	0.025	0.02	0.025
995	Reach 7	28	<i>n</i>	0.025	0.02	0.025
996	Reach 7	27.7	<i>n</i>	0.025	0.02	0.025
997	Reach 7	27.4	<i>n</i>	0.025	0.02	0.025
998	Reach 7	27.1	<i>n</i>	0.025	0.02	0.025
999	Reach 7	26.7	<i>n</i>	0.025	0.02	0.025
1000	Reach 7	26.4	<i>n</i>	0.025	0.02	0.025
1001	Reach 7	26	<i>n</i>	0.025	0.02	0.025
1002	Reach 7	25.6	<i>n</i>	0.025	0.02	0.025
1003	Reach 7	25.2	<i>n</i>	0.025	0.02	0.025
1004	Reach 7	24.9	<i>n</i>	0.025	0.02	0.025
1005	Reach 7	24.6	<i>n</i>	0.025	0.02	0.025
1006	Reach 7	24.2	<i>n</i>	0.025	0.02	0.025
1007	Reach 7	23.8	<i>n</i>	0.025	0.02	0.025
1008	Reach 7	23.5	<i>n</i>	0.025	0.02	0.025
1009	Reach 7	23.1	<i>n</i>	0.025	0.02	0.025
1010	Reach 7	22.7	<i>n</i>	0.025	0.02	0.025
1011	Reach 7	22.4	<i>n</i>	0.025	0.02	0.025
1012	Reach 7	22	<i>n</i>	0.025	0.02	0.025
1013	Reach 7	21.7	<i>n</i>	0.025	0.02	0.025
1014	Reach 7	21.3	<i>n</i>	0.025	0.02	0.025
1015	Reach 7	21	<i>n</i>	0.025	0.02	0.025
1016	Reach 7	20.7	<i>n</i>	0.025	0.02	0.025
1017	Reach 7	20.5	<i>n</i>	0.025	0.02	0.025
1018	Reach 7	20.1	<i>n</i>	0.025	0.02	0.025

**Table G-24 Continued.**

1019	Reach 7	19.9	<i>n</i>	0.025	0.02	0.025
1020	Reach 7	19.6	<i>n</i>	0.025	0.02	0.025
1021	Reach 8	19.4	<i>n</i>	0.025	0.02	0.025
1022	Reach 8	19.1	<i>n</i>	0.025	0.02	0.025
1023	Reach 8	18.8	<i>n</i>	0.025	0.02	0.025
1024	Reach 8	18.6	<i>n</i>	0.025	0.02	0.025
1025	Reach 8	18.3	<i>n</i>	0.025	0.02	0.025
1026	Reach 8	18	<i>n</i>	0.025	0.02	0.025
1027	Reach 8	17.7	<i>n</i>	0.025	0.019	0.025
1028	Reach 8	17.4	<i>n</i>	0.025	0.019	0.025
1029	Reach 8	17.1	<i>n</i>	0.025	0.019	0.025
1030	Reach 8	16.8	<i>n</i>	0.025	0.019	0.025
1031	Reach 8	16.5	<i>n</i>	0.025	0.019	0.025
1032	Reach 8	16.2	<i>n</i>	0.025	0.019	0.025
1033	Reach 8	15.8	<i>n</i>	0.025	0.019	0.025
1034	Reach 8	15.6	<i>n</i>	0.025	0.019	0.025
1035	Reach 8	15.3	<i>n</i>	0.025	0.019	0.025
1036	Reach 8	15	<i>n</i>	0.025	0.019	0.025
1037	Reach 8	14.7	<i>n</i>	0.025	0.019	0.025
1038	Reach 8	14.5	<i>n</i>	0.025	0.019	0.025
1039	Reach 8	14.2	<i>n</i>	0.025	0.019	0.025
1040	Reach 8	13.8	<i>n</i>	0.025	0.019	0.025
1041	Reach 8	13.5	<i>n</i>	0.025	0.019	0.025
1042	Reach 8	13.2	<i>n</i>	0.025	0.019	0.025
1043	Reach 8	13	<i>n</i>	0.025	0.019	0.025
1044	Reach 8	12.8	<i>n</i>	0.025	0.019	0.025
1045	Reach 8	12.5	<i>n</i>	0.025	0.019	0.025
1046	Reach 8	12.2	<i>n</i>	0.025	0.019	0.025
1047	Reach 8	12	<i>n</i>	0.025	0.019	0.025
1048	Reach 8	11.7	<i>n</i>	0.025	0.019	0.025
1049	Reach 8	11.4	<i>n</i>	0.025	0.019	0.025
1050	Reach 9	11.2	<i>n</i>	0.025	0.019	0.025
1051	Reach 9	11.1	<i>n</i>	0.025	0.019	0.025
1052	Reach 9	10.8	<i>n</i>	0.025	0.019	0.025
1053	Reach 9	10.6	<i>n</i>	0.025	0.019	0.025
1054	Reach 9	10.4	<i>n</i>	0.025	0.019	0.025
1055	Reach 10	10.2	<i>n</i>	0.025	0.019	0.025
1056	Reach 10	9.97	<i>n</i>	0.025	0.019	0.025



**Table G-24 Continued.**

1057	Reach 10	9.7	<i>n</i>	0.025	0.019	0.025
1058	Reach 10	9.4	<i>n</i>	0.025	0.019	0.025
1059	Reach 10	9.1	<i>n</i>	0.025	0.019	0.025
1060	Reach 10	8.9	<i>n</i>	0.025	0.019	0.025
1061	Reach 10	8.7	<i>n</i>	0.025	0.019	0.025
1062	Reach 10	8.4	<i>n</i>	0.025	0.019	0.025
1063	Reach 10	8.1	<i>n</i>	0.025	0.019	0.025
1064	Reach 10	7.94	<i>n</i>	0.025	0.019	0.025
1065	Reach 10	7.5	<i>n</i>	0.025	0.019	0.025
1066	Reach 10	7.3	<i>n</i>	0.025	0.019	0.025
1067	Reach 10	6.9	<i>n</i>	0.025	0.019	0.025
1068	Reach 10	6.7	<i>n</i>	0.025	0.019	0.025
1069	Reach 10	6.5	<i>n</i>	0.025	0.019	0.025
1070	Reach 10	6.2	<i>n</i>	0.025	0.019	0.025
1071	Reach 10	6	<i>n</i>	0.025	0.019	0.025
1072	Reach 10	5.8	<i>n</i>	0.025	0.019	0.025
1073	Reach 10	5.5	<i>n</i>	0.025	0.019	0.025
1074	Reach 10	5.3	<i>n</i>	0.025	0.019	0.025
1075	Reach 10	5.1	<i>n</i>	0.025	0.019	0.025
1076	Reach 10	4.9	<i>n</i>	0.025	0.019	0.025
1077	Reach 10	4.7	<i>n</i>	0.025	0.019	0.025
1078	Reach 11	4.46	<i>n</i>	0.025	0.019	0.025
1079	Reach 11	4.26	<i>n</i>	0.025	0.019	0.025
1080	Reach 11	4.04	<i>n</i>	0.025	0.019	0.025
1081	Reach 11	3.83	<i>n</i>	0.025	0.019	0.025
1082	Reach 11	3.6	<i>n</i>	0.025	0.019	0.025
1083	Reach 11	3.36	<i>n</i>	0.025	0.019	0.025
1084	Reach 11	3.15	<i>n</i>	0.025	0.019	0.025
1085	Reach 12	2.95	<i>n</i>	0.02	0.0195	0.02
1086	Reach 12	2.75	<i>n</i>	0.02	0.0195	0.02
1087	Reach 12	2.65	<i>n</i>	0.02	0.0195	0.02
1088	Reach 12	2.46	<i>n</i>	0.02	0.0195	0.02
1089	Reach 12	2.28	<i>n</i>	0.02	0.0195	0.02
1090	Reach 12	2.08	<i>n</i>	0.02	0.0195	0.02
1091	Reach 12	1.7	<i>n</i>	0.02	0.0195	0.02
1092	Reach 12	1.53	<i>n</i>	0.02	0.0195	0.02
1093	Reach 12	1.4	<i>n</i>	0.02	0.0195	0.02
1094	Reach 12	1.25	<i>n</i>	0.02	0.0195	0.02

**Table G-24 Continued.**

1095	Reach 12	1.1	<i>n</i>	0.02	0.0195	0.02
1096	Reach 12	0.98	<i>n</i>	0.02	0.0195	0.02
1097	Reach 12	0.7	<i>n</i>	0.02	0.0195	0.02
1098	Reach 12	0.58	<i>n</i>	0.02	0.0195	0.02
1099	Reach 12	0.35	<i>n</i>	0.02	0.0195	0.02
1100	Reach 12	0.2	<i>n</i>	0.02	0.0195	0.02
1101	Reach 12	0.07	<i>n</i>	0.02	0.0195	0.02

**Table G-25: Manning's  $n$  Values for Pass a Loutré.**

Pass a Loutré						
Number	Reach	River Station	Friction ( $n/K$ )	Left Overbank	Channel	Right Overbank
1	Reach 1	29	$n$	0.024	0.02	0.024
2	Reach 1	28	$n$	0.024	0.02	0.024
3	Reach 1	27	$n$	0.024	0.02	0.024
4	Reach 1	26	$n$	0.024	0.02	0.024
5	Reach 1	25	$n$	0.024	0.02	0.024
6	Reach 1	24	$n$	0.024	0.02	0.024
7	Reach 1	23	$n$	0.024	0.02	0.024
8	Reach 1	22	$n$	0.024	0.02	0.024
9	Reach 1	21	$n$	0.024	0.02	0.024
10	Reach 1	20	$n$	0.024	0.02	0.024
11	Reach 1	19	$n$	0.024	0.02	0.024
12	Reach 1	18	$n$	0.024	0.02	0.024
13	Reach 1	17	$n$	0.024	0.02	0.024
14	Reach 1	16	$n$	0.024	0.02	0.024
15	Reach 1	15	$n$	0.024	0.02	0.024
16	Reach 1	14	$n$	0.024	0.02	0.024
17	Reach 1	13	$n$	0.024	0.02	0.024
18	Reach 1	12	$n$	0.024	0.02	0.024
19	Reach 1	11	$n$	0.024	0.02	0.024
20	Reach 1	10	$n$	0.024	0.02	0.024
21	Reach 1	9	$n$	0.024	0.02	0.024
22	Reach 1	8	$n$	0.024	0.02	0.024
23	Reach 1	7	$n$	0.024	0.02	0.024
24	Reach 1	6	$n$	0.024	0.02	0.024
25	Reach 1	5	$n$	0.024	0.02	0.024
26	Reach 1	4	$n$	0.024	0.02	0.024
27	Reach 1	3	$n$	0.024	0.02	0.024
28	Reach 1	2	$n$	0.024	0.02	0.024
29	Reach 1	1	$n$	0.024	0.02	0.024

**Table G-26: Manning's  $n$  Values for South Pass.**

South Pass						
Number	Reach	River Station	Friction ( $n/K$ )	Left Overbank	Channel	Right Overbank
1	Reach 1	79	$n$	0.024	0.02	0.024
2	Reach 1	78	$n$	0.024	0.02	0.024
3	Reach 1	77	$n$	0.024	0.02	0.024
4	Reach 1	76	$n$	0.024	0.02	0.024
5	Reach 1	75	$n$	0.024	0.02	0.024
6	Reach 1	74	$n$	0.024	0.02	0.024
7	Reach 1	73	$n$	0.024	0.02	0.024
8	Reach 1	72	$n$	0.024	0.02	0.024
9	Reach 1	71	$n$	0.024	0.02	0.024
10	Reach 1	70	$n$	0.024	0.02	0.024
11	Reach 1	69	$n$	0.024	0.02	0.024
12	Reach 1	68	$n$	0.024	0.02	0.024
13	Reach 1	67	$n$	0.024	0.02	0.024
14	Reach 1	66	$n$	0.024	0.02	0.024
15	Reach 1	65	$n$	0.024	0.02	0.024
16	Reach 1	64	$n$	0.024	0.02	0.024
17	Reach 1	63	$n$	0.024	0.02	0.024
18	Reach 1	62	$n$	0.024	0.02	0.024
19	Reach 1	61	$n$	0.024	0.02	0.024
20	Reach 1	60	$n$	0.024	0.02	0.024
21	Reach 1	59	$n$	0.024	0.02	0.024
22	Reach 1	58	$n$	0.024	0.02	0.024
23	Reach 1	57	$n$	0.024	0.02	0.024
24	Reach 1	56	$n$	0.024	0.02	0.024
25	Reach 1	55	$n$	0.024	0.02	0.024
26	Reach 1	54	$n$	0.024	0.02	0.024
27	Reach 1	53	$n$	0.024	0.02	0.024
28	Reach 1	52	$n$	0.024	0.02	0.024
29	Reach 1	51	$n$	0.024	0.02	0.024
30	Reach 1	50	$n$	0.024	0.02	0.024
31	Reach 1	49	$n$	0.024	0.02	0.024
32	Reach 1	48	$n$	0.024	0.02	0.024
33	Reach 1	47	$n$	0.024	0.02	0.024
34	Reach 1	46	$n$	0.024	0.02	0.024
35	Reach 1	45	$n$	0.024	0.02	0.024

**Table G-26 Continued.**

36	Reach 1	44	<i>n</i>	0.024	0.02	0.024
37	Reach 1	43	<i>n</i>	0.024	0.02	0.024
38	Reach 1	42	<i>n</i>	0.024	0.02	0.024
39	Reach 1	41	<i>n</i>	0.024	0.02	0.024
40	Reach 1	40	<i>n</i>	0.024	0.02	0.024
41	Reach 1	39	<i>n</i>	0.024	0.02	0.024
42	Reach 1	38	<i>n</i>	0.024	0.02	0.024
43	Reach 1	37	<i>n</i>	0.024	0.02	0.024
44	Reach 1	36	<i>n</i>	0.024	0.02	0.024
45	Reach 1	35	<i>n</i>	0.024	0.02	0.024
46	Reach 1	34	<i>n</i>	0.024	0.02	0.024
47	Reach 1	33	<i>n</i>	0.024	0.02	0.024
48	Reach 1	32	<i>n</i>	0.024	0.02	0.024
49	Reach 1	31	<i>n</i>	0.024	0.02	0.024
50	Reach 1	30	<i>n</i>	0.024	0.02	0.024
51	Reach 1	29	<i>n</i>	0.024	0.02	0.024
52	Reach 1	28	<i>n</i>	0.024	0.02	0.024
53	Reach 1	27	<i>n</i>	0.024	0.02	0.024
54	Reach 1	26	<i>n</i>	0.024	0.02	0.024
55	Reach 1	25	<i>n</i>	0.024	0.02	0.024
56	Reach 1	24	<i>n</i>	0.024	0.02	0.024
57	Reach 1	23	<i>n</i>	0.024	0.02	0.024
58	Reach 1	22	<i>n</i>	0.024	0.02	0.024
59	Reach 1	21	<i>n</i>	0.024	0.02	0.024
60	Reach 1	20	<i>n</i>	0.024	0.02	0.024
61	Reach 1	19	<i>n</i>	0.024	0.02	0.024
62	Reach 1	18	<i>n</i>	0.024	0.02	0.024
63	Reach 1	17	<i>n</i>	0.024	0.02	0.024
64	Reach 1	16	<i>n</i>	0.024	0.02	0.024
65	Reach 1	15	<i>n</i>	0.024	0.02	0.024
66	Reach 1	14	<i>n</i>	0.024	0.02	0.024
67	Reach 1	13	<i>n</i>	0.024	0.02	0.024
68	Reach 1	12	<i>n</i>	0.024	0.02	0.024
69	Reach 1	11	<i>n</i>	0.024	0.02	0.024
70	Reach 1	10	<i>n</i>	0.024	0.02	0.024
71	Reach 1	9	<i>n</i>	0.024	0.02	0.024
72	Reach 1	8	<i>n</i>	0.024	0.02	0.024
73	Reach 1	7	<i>n</i>	0.024	0.02	0.024

**Table G-26 Continued.**

74	Reach 1	6	<i>n</i>	0.024	0.02	0.024
75	Reach 1	5	<i>n</i>	0.024	0.02	0.024
76	Reach 1	4	<i>n</i>	0.024	0.02	0.024
77	Reach 1	3	<i>n</i>	0.024	0.02	0.024
78	Reach 1	2	<i>n</i>	0.024	0.02	0.024
79	Reach 1	1	<i>n</i>	0.024	0.02	0.024

**Table G-27: Manning's  $n$  Values for Southwest Pass.**

Southwest Pass						
Number	Reach	River Station	Friction ( $n/K$ )	Left Overbank	Channel	Right Overbank
1	Reach 1	108	$n$	0.024	0.02	0.024
2	Reach 1	107	$n$	0.024	0.02	0.024
3	Reach 1	106	$n$	0.024	0.02	0.024
4	Reach 1	105	$n$	0.024	0.02	0.024
5	Reach 1	104	$n$	0.024	0.02	0.024
6	Reach 1	103	$n$	0.024	0.02	0.024
7	Reach 1	102	$n$	0.024	0.02	0.024
8	Reach 1	101	$n$	0.024	0.02	0.024
9	Reach 1	100	$n$	0.024	0.02	0.024
10	Reach 1	99	$n$	0.024	0.02	0.024
11	Reach 1	98	$n$	0.024	0.02	0.024
12	Reach 1	97	$n$	0.024	0.02	0.024
13	Reach 1	96	$n$	0.024	0.02	0.024
14	Reach 1	95	$n$	0.024	0.02	0.024
15	Reach 1	94	$n$	0.024	0.02	0.024
16	Reach 1	93	$n$	0.024	0.02	0.024
17	Reach 1	92	$n$	0.024	0.02	0.024
18	Reach 1	91	$n$	0.024	0.02	0.024
19	Reach 1	90	$n$	0.024	0.02	0.024
20	Reach 1	89	$n$	0.024	0.02	0.024
21	Reach 1	88	$n$	0.024	0.02	0.024
22	Reach 1	87	$n$	0.024	0.02	0.024
23	Reach 1	86	$n$	0.024	0.02	0.024
24	Reach 1	85	$n$	0.024	0.02	0.024
25	Reach 1	84	$n$	0.024	0.02	0.024
26	Reach 1	83	$n$	0.024	0.02	0.024
27	Reach 1	82	$n$	0.024	0.02	0.024
28	Reach 1	81	$n$	0.024	0.02	0.024
29	Reach 1	80	$n$	0.024	0.02	0.024
30	Reach 1	79	$n$	0.024	0.02	0.024
31	Reach 1	78	$n$	0.024	0.02	0.024
32	Reach 1	77	$n$	0.024	0.02	0.024
33	Reach 1	76	$n$	0.024	0.02	0.024
34	Reach 1	75	$n$	0.024	0.02	0.024
35	Reach 1	74	$n$	0.024	0.02	0.024

**Table G-27 Continued.**

36	Reach 1	73	<i>n</i>	0.024	0.02	0.024
37	Reach 1	72	<i>n</i>	0.024	0.02	0.024
38	Reach 1	71	<i>n</i>	0.024	0.02	0.024
39	Reach 1	70	<i>n</i>	0.024	0.02	0.024
40	Reach 1	69	<i>n</i>	0.024	0.02	0.024
41	Reach 1	68	<i>n</i>	0.024	0.02	0.024
42	Reach 1	67	<i>n</i>	0.024	0.02	0.024
43	Reach 1	66	<i>n</i>	0.024	0.02	0.024
44	Reach 1	65	<i>n</i>	0.024	0.02	0.024
45	Reach 1	64	<i>n</i>	0.024	0.02	0.024
46	Reach 1	63	<i>n</i>	0.024	0.02	0.024
47	Reach 1	62	<i>n</i>	0.024	0.02	0.024
48	Reach 1	61	<i>n</i>	0.024	0.02	0.024
49	Reach 1	60	<i>n</i>	0.024	0.02	0.024
50	Reach 1	59	<i>n</i>	0.024	0.02	0.024
51	Reach 1	58	<i>n</i>	0.024	0.02	0.024
52	Reach 1	57	<i>n</i>	0.024	0.02	0.024
53	Reach 1	56	<i>n</i>	0.024	0.02	0.024
54	Reach 1	55	<i>n</i>	0.024	0.02	0.024
55	Reach 1	54	<i>n</i>	0.024	0.02	0.024
56	Reach 1	53	<i>n</i>	0.024	0.02	0.024
57	Reach 1	52	<i>n</i>	0.024	0.02	0.024
58	Reach 1	51	<i>n</i>	0.024	0.02	0.024
59	Reach 1	50	<i>n</i>	0.024	0.02	0.024
60	Reach 1	49	<i>n</i>	0.024	0.02	0.024
61	Reach 1	48	<i>n</i>	0.024	0.02	0.024
62	Reach 1	47	<i>n</i>	0.024	0.02	0.024
63	Reach 1	46	<i>n</i>	0.024	0.02	0.024
64	Reach 1	45	<i>n</i>	0.024	0.02	0.024
65	Reach 1	44	<i>n</i>	0.024	0.02	0.024
66	Reach 1	43	<i>n</i>	0.024	0.02	0.024
67	Reach 1	42	<i>n</i>	0.024	0.02	0.024
68	Reach 1	41	<i>n</i>	0.024	0.02	0.024
69	Reach 1	40	<i>n</i>	0.024	0.02	0.024
70	Reach 1	39	<i>n</i>	0.024	0.02	0.024
71	Reach 1	38	<i>n</i>	0.024	0.02	0.024
72	Reach 1	37	<i>n</i>	0.024	0.02	0.024
73	Reach 1	36	<i>n</i>	0.024	0.02	0.024



**Table G-27 Continued.**

74	Reach 1	35	<i>n</i>	0.024	0.02	0.024
75	Reach 1	34	<i>n</i>	0.024	0.02	0.024
76	Reach 1	33	<i>n</i>	0.024	0.02	0.024
77	Reach 1	32	<i>n</i>	0.024	0.02	0.024
78	Reach 1	31	<i>n</i>	0.024	0.02	0.024
79	Reach 1	30	<i>n</i>	0.024	0.02	0.024
80	Reach 1	29	<i>n</i>	0.024	0.02	0.024
81	Reach 1	28	<i>n</i>	0.024	0.02	0.024
82	Reach 1	27	<i>n</i>	0.024	0.02	0.024
83	Reach 1	26	<i>n</i>	0.024	0.02	0.024
84	Reach 1	25	<i>n</i>	0.024	0.02	0.024
85	Reach 1	24	<i>n</i>	0.024	0.02	0.024
86	Reach 1	23	<i>n</i>	0.024	0.02	0.024
87	Reach 1	22	<i>n</i>	0.024	0.02	0.024
88	Reach 1	21	<i>n</i>	0.024	0.02	0.024
89	Reach 1	20	<i>n</i>	0.024	0.02	0.024
90	Reach 1	19	<i>n</i>	0.024	0.02	0.024
91	Reach 1	18	<i>n</i>	0.024	0.02	0.024
92	Reach 1	17	<i>n</i>	0.024	0.02	0.024
93	Reach 1	16	<i>n</i>	0.024	0.02	0.024
94	Reach 1	15	<i>n</i>	0.024	0.02	0.024
95	Reach 1	14	<i>n</i>	0.024	0.02	0.024
96	Reach 1	13	<i>n</i>	0.024	0.02	0.024
97	Reach 1	12	<i>n</i>	0.024	0.02	0.024
98	Reach 1	11	<i>n</i>	0.024	0.02	0.024
99	Reach 1	10	<i>n</i>	0.024	0.02	0.024
100	Reach 1	9	<i>n</i>	0.024	0.02	0.024
101	Reach 1	8	<i>n</i>	0.024	0.02	0.024
102	Reach 1	7	<i>n</i>	0.024	0.02	0.024
103	Reach 1	6	<i>n</i>	0.024	0.02	0.024
104	Reach 1	5	<i>n</i>	0.024	0.02	0.024
105	Reach 1	4	<i>n</i>	0.024	0.02	0.024
106	Reach 1	3	<i>n</i>	0.024	0.02	0.024
107	Reach 1	2	<i>n</i>	0.024	0.02	0.024
108	Reach 1	1	<i>n</i>	0.024	0.02	0.024

**Table G-28: Manning's  $n$  Values for The Pen.**

The Pen						
Number	Reach	River Station	Friction ( $n/K$ )	Left Overbank	Channel	Right Overbank
1	Reach 1	20	$n$	0.03	0.03	0.03
2	Reach 1	19	$n$	0.03	0.03	0.03
3	Reach 1	18	$n$	0.03	0.03	0.03
4	Reach 1	17	$n$	0.03	0.03	0.03
5	Reach 1	16	$n$	0.03	0.03	0.03
6	Reach 1	15	$n$	0.03	0.03	0.03
7	Reach 1	14	$n$	0.03	0.03	0.03
8	Reach 1	13	$n$	0.03	0.03	0.03
9	Reach 1.5	2	$n$	0.03	0.03	0.03
10	Reach 1.5	1	$n$	0.03	0.03	0.03
11	Reach 2	12	$n$	0.03	0.03	0.03
12	Reach 2	11	$n$	0.03	0.03	0.03
13	Reach 2	10	$n$	0.03	0.03	0.03
14	Reach 2	9	$n$	0.03	0.03	0.03
15	Reach 2	8	$n$	0.03	0.03	0.03
16	Reach 2.5	2	$n$	0.03	0.03	0.03
17	Reach 2.5	1	$n$	0.03	0.03	0.03
18	Reach 3	7	$n$	0.03	0.03	0.03
19	Reach 3	6	$n$	0.03	0.03	0.03
20	Reach 3	5	$n$	0.03	0.03	0.03
21	Reach 3	4	$n$	0.03	0.03	0.03
22	Reach 3	3	$n$	0.03	0.03	0.03
23	Reach 3	2	$n$	0.03	0.03	0.03
24	Reach 3	1	$n$	0.03	0.03	0.03

**Table G-29: Manning's  $n$  Values for Tiger Pass.**

Tiger Pass						
Number	Reach	River Station	Friction ( $n/K$ )	Left Overbank	Channel	Right Overbank
1	Reach 1	17	$n$	0.02	0.019	0.02
2	Reach 1	16	$n$	0.02	0.019	0.02
3	Reach 1	15	$n$	0.02	0.019	0.02
4	Reach 1	14	$n$	0.02	0.019	0.02
5	Reach 1	13	$n$	0.02	0.019	0.02
6	Reach 1	12	$n$	0.02	0.019	0.02
7	Reach 1	11	$n$	0.02	0.019	0.02
8	Reach 1	10	$n$	0.02	0.019	0.02
9	Reach 1	9	$n$	0.02	0.019	0.02
10	Reach 1	8	$n$	0.02	0.019	0.02
11	Reach 1	7	$n$	0.02	0.019	0.02
12	Reach 1	6	$n$	0.02	0.019	0.02
13	Reach 1	5	$n$	0.02	0.019	0.02
14	Reach 1	4	$n$	0.02	0.019	0.02
15	Reach 1	3	$n$	0.02	0.019	0.02
16	Reach 1	2	$n$	0.02	0.019	0.02
17	Reach 1	1	$n$	0.02	0.019	0.02

**Table G-30: Manning's  $n$  Values for West Bay.**

West Bay						
Number	Reach	River Station	Friction ( $n/K$ )	Left Overbank	Channel	Right Overbank
1	Reach 1	13	$n$	0.2	0.2	0.2
2	Reach 1	12	$n$	0.2	0.2	0.2
3	Reach 1	11	$n$	0.2	0.2	0.2
4	Reach 1	10	$n$	0.2	0.2	0.2
5	Reach 1	9	$n$	0.2	0.2	0.2
6	Reach 1	8	$n$	0.2	0.2	0.2
7	Reach 1	7	$n$	0.2	0.2	0.2
8	Reach 1	6	$n$	0.2	0.2	0.2
9	Reach 1	5	$n$	0.2	0.2	0.2
10	Reach 1	4	$n$	0.023	0.021	0.023
11	Reach 1	3	$n$	0.023	0.021	0.023
12	Reach 1	2	$n$	0.023	0.021	0.023
13	Reach 1	1	$n$	0.023	0.021	0.023

**Table G-31: Manning's  $n$  Values for Wilkinson Canal<sup>19</sup>.**

Wilkinson Canal						
Number	Reach	River Station	Friction ( $n/K$ )	Left Overbank	Channel	Right Overbank
1	Reach 1	16	$n$	0.06	0.03	0.06
2	Reach 1	15	$n$	0.06	0.03	0.06
3	Reach 1	14	$n$	0.06	0.03	0.06
4	Reach 1	13	$n$	0.06	0.03	0.06
5	Reach 1	12	$n$	0.06	0.03	0.06
6	Reach 2	11	$n$	0.06	0.03	0.06
7	Reach 2	10	$n$	0.06	0.03	0.06
8	Reach 2	9	$n$	0.06	0.03	0.06
9	Reach 2	8	$n$	0.06	0.03	0.06
10	Reach 2	7	$n$	0.06	0.03	0.06
11	Reach 2	6	$n$	0.06	0.03	0.06
12	Reach 2	5	$n$	0.06	0.03	0.06
13	Reach 2	4	$n$	0.06	0.03	0.06
14	Reach 2	3	$n$	0.06	0.03	0.06
15	Reach 2	2	$n$	0.06	0.03	0.06
16	Reach 2	1	$n$	0.06	0.03	0.06

<sup>19</sup> The Manning's  $n$  values were the same for Wilkinson Canal for the simulations when it was connected at Myrtle Grove. An additional River Station (RS 9.5) was created to give a location for the inline structure.

**Appendix H**  
**Passes Discharge Records**

**Table H-1: Discharge Record for West Bay.**

Date	Mississippi River			West Bay Diversion Canal		New Orleans Stage (8:00 am) FT NGVD
	at Tarbert Landing <sup>20</sup>	at Venice <sup>21</sup>	above West Bay <sup>21</sup>	at entrance	% Venice Flow	
2-Dec-2003	564,000	459,000	355,000	not taken		5.92
16-Jan-2004	568,000	527,000	393,000	8,180	1.6%	7.36
13-Feb-2004	575,000	593,000	not taken	10,000	1.7%	8.60
20-Mar-2004	838,000	695,000	547,000	14,800	2.1%	12.24
16-Apr-2004	575,000	575,000	392,000	6,000	1.0%	7.57
12-May-2004	700,000	576,000	443,000	6,990	1.2%	10.66
23-Jun-2004	835,000	647,000	479,000	12,000	1.9%	11.46
4-Aug-2004	383,000	361,000	266,000	6,360	1.8%	4.36
1-Sep-2004	243,000	245,000	176,000	3,310	1.4%	2.58
29-Sep-2004	394,000	375,000	312,000	15,700	4.2%	4.33
27-Oct-2004	256,000	285,000	205,000	9,890	3.5%	2.58
17-Nov-2004	611,000	550,000	445,000	19,800	3.6%	7.73
15-Dec-2004	927,000	843,000	686,000	27,000	3.2%	12.82
3-Feb-2005	1,220,000	903,000	754,000	41,100	4.6%	15.73
1-Mar-2005	801,000	740,000	571,500	29,100	3.9%	11.72
5-Apr-2005	490,000	471,500	367,000	16,400	3.5%	6.41
27-Apr-2005	720,000	551,500	386,500	25,800	4.7%	9.97
18-May-2005	466,000	367,000	291,500	15,900	4.3%	5.38
29-Jun-2005	416,000	344,000	291,500	14,400	4.2%	2.80
27-Jul-2005	281,000	256,000	203,000	9,660	3.8%	2.86
19-Jan-2006	296,000	328,000	251,500	10,150	3.1%	2.60
16-Feb-2006	484,000	456,000	329,000	22,500	4.9%	5.97
16-Mar-2006	270,000	247,000	175,000	18,750	7.6%	2.65
25-Apr-2006	434,000	385,500	297,500	15,350	4.0%	4.96
22-May-2006	500,000	430,000	343,000	20,850	4.8%	5.73
19-Jun-2006	312,000	299,000	242,000	17,450	5.8%	3.31
17-Jul-2006	224,000	228,500	178,000	10,080	4.4%	2.52
28-Aug-2006	166,000	173,500	118,500	11,000	6.3%	1.99
22-Sep-2006	179,000	129,400	99,600	-6,300	-4.9%	2.50
19-Oct-2006	265,000	275,650	199,700	8,400	3.0%	3.80
16-Nov-2006	430,000	374,300	289,400	13,800	3.7%	4.17
27-Dec-2006	362,000	340,000	290,000	17,000	5.0%	3.50
25-Jan-2007	901,000	656,800	515,900	40,200	6.1%	12.10
2-Mar-2007	387,000	363,100	301,600	22,300	6.1%	4.70
27-Apr-2007	620,000	536,100	413,000	30,800	5.7%	9.00
25-May-2007	645,000	490,300	392,800	32,800	6.7%	8.98

<sup>20</sup> The discharge at Tarbert Landing includes a 2-day lag from the daily computed discharges.<sup>21</sup> The discharges do not account for tidal contributions.

**Table H-1 Continued.**

22-Jun-2007	399,000	356,500	315,000	22,900	6.4%	4.56
20-Jul-2007	580,000	473,400	377,600	27,200	5.7%	6.94
30-Aug-2007	257,000	217,300	144,700	7,800	3.6%	2.65
26-Sep-2007	237,000	183,100	116,200	14,500	7.9%	2.97
23-Oct-2007	201,000	170,500	126,100	4,900	2.9%	2.90
6-Nov-2007	334,000	284,200	194,100	16,400	5.8%	3.20
18-Dec-2007	278,000	248,700	180,700	16,400	6.6%	2.27
21-Mar-2008	910,000	715,300	512,100	48,300	6.8%	12.10
17-Apr-2008	1,425,000	719,100	633,800	48,098	6.7%	16.69
1-May-2008	1,310,000	926,205	627,681	51,270	5.5%	16.47
26-Jun-2008	810,000	580,730	447,753	47,364	8.2%	11.70
22-Aug-2008	420,000	361,079	295,977	26,137	7.2%	4.50
24-Oct-2008	259,000	285,828	274,190	45,449	15.9%	4.40
19-Dec-2008	310,000	311,576	227,982	16,140	5.2%	3.00
16-Jan-2009	632,487	535,499	411,878	37,395	7.0%	9.10

**Table H-2: Discharge Record for Baptiste Collette.**

Date	Mississippi River			Baptiste Collette		New Orleans Stage
	at Tarbert Landing <sup>20</sup>	at Venice <sup>21</sup>	above West Bay <sup>21</sup>	at entrance	% Venice Flow	(8:00 am) FT NGVD
2-Dec-2003	564,000	459,000	355,000	43,300	9.4%	5.92
16-Jan-2004	568,000	527,000	393,000	55,900	10.6%	7.36
13-Feb-2004	575,000	593,000	not taken	58,900	9.9%	8.60
20-Mar-2004	838,000	695,000	547,000	73,900	10.6%	12.24
16-Apr-2004	575,000	575,000	392,000	51,600	9.0%	7.57
12-May-2004	700,000	576,000	443,000	69,800	12.1%	10.66
23-Jun-2004	835,000	647,000	479,000	82,300	12.7%	11.46
4-Aug-2004	383,000	361,000	266,000	43,200	12.0%	4.36
1-Sep-2004	243,000	245,000	176,000	28,800	11.8%	2.58
29-Sep-2004	394,000	375,000	312,000	46,700	12.5%	4.33
27-Oct-2004	256,000	285,000	205,000	33,700	11.8%	2.58
17-Nov-2004	611,000	550,000	445,000	52,600	9.6%	7.73
15-Dec-2004	927,000	843,000	686,000	76,200	9.0%	12.82
3-Feb-2005	1,220,000	903,000	754,000	104,000	11.5%	15.73
1-Mar-2005	801,000	740,000	571,500	81,650	11.0%	11.72
5-Apr-2005	490,000	471,500	367,000	53,250	11.3%	6.41
27-Apr-2005	720,000	551,500	386,500	76,000	13.8%	9.97
18-May-2005	466,000	367,000	291,500	43,250	11.8%	5.38
29-Jun-2005	416,000	344,000	291,500	41,350	12.0%	2.80
27-Jul-2005	281,000	256,000	203,000	26,900	10.5%	2.86
19-Jan-2006	296,000	328,000	251,500	32,050	9.8%	2.60
16-Feb-2006	484,000	456,000	329,000	48,700	10.7%	5.97
16-Mar-2006	270,000	247,000	175,000	38,200	15.5%	2.65
25-Apr-2006	434,000	385,500	297,500	46,650	12.1%	4.96
22-May-2006	500,000	430,000	343,000	45,700	10.6%	5.73
19-Jun-2006	312,000	299,000	242,000	28,050	9.4%	3.31
17-Jul-2006	224,000	228,500	178,000	24,350	10.7%	2.52
28-Aug-2006	166,000	173,500	118,500	20,300	11.7%	1.99
22-Sep-2006	179,000	129,400	99,600	46,700	36.1%	2.50
19-Oct-2006	265,000	275,650	199,700	48,000	17.4%	3.80
16-Nov-2006	430,000	374,300	289,400	45,049	12.0%	4.17
27-Dec-2006	362,000	340,000	290,000	31,834	9.4%	3.50
25-Jan-2007	901,000	656,800	515,900	75,236	11.5%	12.10
2-Mar-2007	387,000	363,100	301,600	23,780	6.5%	4.70
27-Apr-2007	620,000	536,100	413,000	55,188	10.3%	9.00
25-May-2007	645,000	490,300	392,800	49,607	10.1%	8.98
22-Jun-2007	399,000	356,500	315,000	37,736	10.6%	4.56
20-Jul-2007	580,000	473,400	377,600	49,229	10.4%	6.94
30-Aug-2007	257,000	217,300	144,700	29,325	13.5%	2.65



**Table H-2 Continued.**

26-Sep-2007	237,000	183,100	116,200	22,350	12.2%	2.97
23-Oct-2007	201,000	170,500	126,100	42,300	24.8%	2.90
6-Nov-2007	334,000	284,200	194,100	38,640	13.6%	3.20
18-Dec-2007	278,000	248,700	180,700	29,956	12.0%	2.27
21-Mar-2008	910,000	715,300	512,100	73,779	10.3%	12.10
17-Apr-2008	1,425,000	719,100	633,800	100,173	13.9%	16.69
1-May-2008	1,310,000	926,205	627,681	93,384	10.1%	16.47
26-Jun-2008	810,000	580,730	447,753	58,933	10.1%	11.70
22-Aug-2008	420,000	361,079	295,977	26,399	7.3%	4.50
24-Oct-2008	259,000	285,828	274,190	-46,219	-16.2%	4.40
19-Dec-2008	310,000	311,576	227,982	31,488	10.1%	3.00
16-Jan-2009	632,487	535,499	411,878	46,014	8.6%	9.10

**Table H-3: Discharge Record for Grand Pass.**

Date	Mississippi River			Grand Pass		New Orleans Stage
	at Tarbert Landing <sup>20</sup>	at Venice <sup>21</sup>	above West Bay <sup>21</sup>	at entrance	% Venice Flow	(8:00 am) FT NGVD
2-Dec-2003	564,000	459,000	355,000	53,300	11.6%	5.92
16-Jan-2004	568,000	527,000	393,000	53,300	10.1%	7.36
13-Feb-2004	575,000	593,000	not taken	66,600	11.2%	8.60
20-Mar-2004	838,000	695,000	547,000	72,400	10.4%	12.24
16-Apr-2004	575,000	575,000	392,000	53,300	9.3%	7.57
12-May-2004	700,000	576,000	443,000	61,600	10.7%	10.66
23-Jun-2004	835,000	647,000	479,000	67,200	10.4%	11.46
4-Aug-2004	383,000	361,000	266,000	34,400	9.5%	4.36
1-Sep-2004	243,000	245,000	176,000	25,500	10.4%	2.58
29-Sep-2004	394,000	375,000	312,000	37,500	10.0%	4.33
27-Oct-2004	256,000	285,000	205,000	28,200	9.9%	2.58
17-Nov-2004	611,000	550,000	445,000	60,600	11.0%	7.73
15-Dec-2004	927,000	843,000	686,000	84,900	10.1%	12.82
3-Feb-2005	1,220,000	903,000	754,000	92,000	10.2%	15.73
1-Mar-2005	801,000	740,000	571,500	79,500	10.7%	11.72
5-Apr-2005	490,000	471,500	367,000	48,800	10.3%	6.41
27-Apr-2005	720,000	551,500	386,500	68,150	12.4%	9.97
18-May-2005	466,000	367,000	291,500	44,300	12.1%	5.38
29-Jun-2005	416,000	344,000	291,500	36,850	10.7%	2.80
27-Jul-2005	281,000	256,000	203,000	29,500	11.5%	2.86
19-Jan-2006	296,000	328,000	251,500	27,350	8.3%	2.60
16-Feb-2006	484,000	456,000	329,000	47,200	10.4%	5.97
16-Mar-2006	270,000	247,000	175,000	28,750	11.6%	2.65
25-Apr-2006	434,000	385,500	297,500	36,550	9.5%	4.96
22-May-2006	500,000	430,000	343,000	45,950	10.7%	5.73
19-Jun-2006	312,000	299,000	242,000	33,350	11.2%	3.31
17-Jul-2006	224,000	228,500	178,000	24,000	10.5%	2.52
28-Aug-2006	166,000	173,500	118,500	21,000	12.1%	1.99
22-Sep-2006	179,000	129,400	99,600	15,750	12.2%	2.50
19-Oct-2006	265,000	275,650	199,700	14,700	5.3%	3.80
16-Nov-2006	430,000	374,300	289,400	38,668	10.3%	4.17
27-Dec-2006	362,000	340,000	290,000	40,495	11.9%	3.50
25-Jan-2007	901,000	656,800	515,900	83,160	12.7%	12.10
2-Mar-2007	387,000	363,100	301,600	47,207	13.0%	4.70
27-Apr-2007	620,000	536,100	413,000	62,759	11.7%	9.00
25-May-2007	645,000	490,300	392,800	62,880	12.8%	8.98
22-Jun-2007	399,000	356,500	315,000	39,286	11.0%	4.56
20-Jul-2007	580,000	473,400	377,600	48,380	10.2%	6.94
30-Aug-2007	257,000	217,300	144,700	22,816	10.5%	2.65

**Table H-3 Continued.**

26-Sep-2007	237,000	183,100	116,200	24,166	13.2%	2.97
23-Oct-2007	201,000	170,500	126,100	450	0.3%	2.90
6-Nov-2007	334,000	284,200	194,100	27,500	9.7%	3.20
18-Dec-2007	278,000	248,700	180,700	29,243	11.8%	2.27
21-Mar-2008	910,000	715,300	512,100	81,294	11.4%	12.10
17-Apr-2008	1,425,000	719,100	633,800	98,413	13.7%	16.69
1-May-2008	1,310,000	926,205	627,681	91,099	9.8%	16.47
26-Jun-2008	810,000	580,730	447,753	75,168	12.9%	11.70
22-Aug-2008	420,000	361,079	295,977	33,121	9.2%	4.50
24-Oct-2008	259,000	285,828	274,190	47,390	16.6%	4.40
19-Dec-2008	310,000	311,576	227,982	31,231	10.0%	3.00
16-Jan-2009	632,487	535,499	411,878	65,016	12.1%	9.10

**Table H-4: Discharge Record for Main Pass.**

Date	Mississippi River			Cubits Gap (Main Pass)		New Orleans Stage (8:00 am) FT NGVD
	at Tarbert Landing <sup>20</sup>	at Venice <sup>21</sup>	above West Bay <sup>21</sup>	at entrance	% Venice Flow	
2-Dec-2003	564,000	459,000	355,000	47,900	10.4%	5.92
16-Jan-2004	568,000	527,000	393,000	84,800	16.1%	7.36
13-Feb-2004	575,000	593,000	not taken	80,600	13.6%	8.60
20-Mar-2004	838,000	695,000	547,000	90,500	13.0%	12.24
16-Apr-2004	575,000	575,000	392,000	61,500	10.7%	7.57
12-May-2004	700,000	576,000	443,000	82,300	14.3%	10.66
23-Jun-2004	835,000	647,000	479,000	90,600	14.0%	11.46
4-Aug-2004	383,000	361,000	266,000	68,300	18.9%	4.36
1-Sep-2004	243,000	245,000	176,000	40,900	16.7%	2.58
29-Sep-2004	394,000	375,000	312,000	83,400	22.2%	4.33
27-Oct-2004	256,000	285,000	205,000	43,800	15.4%	2.58
17-Nov-2004	611,000	550,000	445,000	86,100	15.7%	7.73
15-Dec-2004	927,000	843,000	686,000	92,700	11.0%	12.82
3-Feb-2005	1,220,000	903,000	754,000	130,000	14.4%	15.73
1-Mar-2005	801,000	740,000	571,500	111,000	15.0%	11.72
5-Apr-2005	490,000	471,500	367,000	89,400	19.0%	6.41
27-Apr-2005	720,000	551,500	386,500	91,850	16.7%	9.97
18-May-2005	466,000	367,000	291,500	53,900	14.7%	5.38
29-Jun-2005	416,000	344,000	291,500		0.0%	2.80
27-Jul-2005	281,000	256,000	203,000	30,650	12.0%	2.86
19-Jan-2006	296,000	328,000	251,500	28,100	8.6%	2.60
16-Feb-2006	484,000	456,000	329,000	26,700	5.9%	5.97
16-Mar-2006	270,000	247,000	175,000	33,250	13.5%	2.65
25-Apr-2006	434,000	385,500	297,500	53,050	13.8%	4.96
22-May-2006	500,000	430,000	343,000	53,400	12.4%	5.73
19-Jun-2006	312,000	299,000	242,000	40,000	13.4%	3.31
17-Jul-2006	224,000	228,500	178,000	27,050	11.8%	2.52
28-Aug-2006	166,000	173,500	118,500	17,200	9.9%	1.99
22-Sep-2006	179,000	129,400	99,600	60,100	46.4%	2.50
19-Oct-2006	265,000	275,650	199,700	38,600	14.0%	3.80
16-Nov-2006	430,000	374,300	289,400	50,141	13.4%	4.17
27-Dec-2006	362,000	340,000	290,000	41,254	12.1%	3.50
25-Jan-2007	901,000	656,800	515,900	40,191	6.1%	12.10
2-Mar-2007	387,000	363,100	301,600	29,531	8.1%	4.70
27-Apr-2007	620,000	536,100	413,000	68,753	12.8%	9.00
25-May-2007	645,000	490,300	392,800	49,791	10.2%	8.98
22-Jun-2007	399,000	356,500	315,000	34,141	9.6%	4.56
20-Jul-2007	580,000	473,400	377,600	63,775	13.5%	6.94
30-Aug-2007	257,000	217,300	144,700	31,816	14.6%	2.65

**Table H-4 Continued.**

26-Sep-2007	237,000	183,100	116,200	24,202	13.2%	2.97
23-Oct-2007	201,000	170,500	126,100	41,900	24.6%	2.90
6-Nov-2007	334,000	284,200	194,100	38,300	13.5%	3.20
18-Dec-2007	278,000	248,700	180,700	37,420	15.0%	2.27
21-Mar-2008	910,000	715,300	512,100	88,376	12.4%	12.10
17-Apr-2008	1,425,000	719,100	633,800	122,222	17.0%	16.69
1-May-2008	1,310,000	926,205	627,681	110,793	12.0%	16.47
26-Jun-2008	810,000	580,730	447,753	49,190	8.5%	11.70
22-Aug-2008	420,000	361,079	295,977	21,857	6.1%	4.50
24-Oct-2008	259,000	285,828	274,190	-49,377	-17.3%	4.40
19-Dec-2008	310,000	311,576	227,982	34,038	10.9%	3.00
16-Jan-2009	632,487	535,499	411,878	45,432	8.5%	9.10

**Table H-5: Discharge Record for Pass a Loutr .**

Date	Mississippi River			Pass a Loutr�		New Orleans Stage
	at Tarbert Landing <sup>20</sup>	at Venice <sup>21</sup>	above West Bay <sup>21</sup>	at entrance	% Venice Flow	(8:00 am) FT NGVD
2-Dec-2003	564,000	459,000	355,000	43,300	9.4%	5.92
16-Jan-2004	568,000	527,000	393,000	63,100	12.0%	7.36
13-Feb-2004	575,000	593,000	not taken	60,800	10.3%	8.60
20-Mar-2004	838,000	695,000	547,000	73,400	10.6%	12.24
16-Apr-2004	575,000	575,000	392,000	61,400	10.7%	7.57
12-May-2004	700,000	576,000	443,000	78,900	13.7%	10.66
23-Jun-2004	835,000	647,000	479,000	82,700	12.8%	11.46
4-Aug-2004	383,000	361,000	266,000	37,200	10.3%	4.36
1-Sep-2004	243,000	245,000	176,000	30,600	12.5%	2.58
29-Sep-2004	394,000	375,000	312,000	56,000	14.9%	4.33
27-Oct-2004	256,000	285,000	205,000	35,900	12.6%	2.58
17-Nov-2004	611,000	550,000	445,000	56,900	10.3%	7.73
15-Dec-2004	927,000	843,000	686,000	95,800	11.4%	12.82
3-Feb-2005	1,220,000	903,000	754,000	101,000	11.2%	15.73
1-Mar-2005	801,000	740,000	571,500	87,100	11.8%	11.72
5-Apr-2005	490,000	471,500	367,000	68,050	14.4%	6.41
27-Apr-2005	720,000	551,500	386,500	53,550	9.7%	9.97
18-May-2005	466,000	367,000	291,500	35,600	9.7%	5.38
29-Jun-2005	416,000	344,000	291,500		0.0%	2.80
27-Jul-2005	281,000	256,000	203,000	27,200	10.6%	2.86
19-Jan-2006	296,000	328,000	251,500		0.0%	2.60
16-Feb-2006	484,000	456,000	329,000	47,300	10.4%	5.97
16-Mar-2006	270,000	247,000	175,000	37,150	15.0%	2.65
25-Apr-2006	434,000	385,500	297,500	40,200	10.4%	4.96
22-May-2006	500,000	430,000	343,000	50,750	11.8%	5.73
19-Jun-2006	312,000	299,000	242,000	38,350	12.8%	3.31
17-Jul-2006	224,000	228,500	178,000	30,100	13.2%	2.52
28-Aug-2006	166,000	173,500	118,500	19,350	11.2%	1.99
22-Sep-2006	179,000	129,400	99,600	48,625	37.6%	2.50
19-Oct-2006	265,000	275,650	199,700	37,900	13.7%	3.80
16-Nov-2006	430,000	374,300	289,400	39,933	10.7%	4.17
27-Dec-2006	362,000	340,000	290,000	34,712	10.2%	3.50
25-Jan-2007	901,000	656,800	515,900		0.0%	12.10
2-Mar-2007	387,000	363,100	301,600		0.0%	4.70
27-Apr-2007	620,000	536,100	413,000	55,272	10.3%	9.00
25-May-2007	645,000	490,300	392,800	48,119	9.8%	8.98
22-Jun-2007	399,000	356,500	315,000	44,490	12.5%	4.56
20-Jul-2007	580,000	473,400	377,600	56,677	12.0%	6.94
30-Aug-2007	257,000	217,300	144,700	35,043	16.1%	2.65

**Table H-5 Continued.**

26-Sep-2007	237,000	183,100	116,200	28,884	15.8%	2.97
23-Oct-2007	201,000	170,500	126,100	42,100	24.7%	2.90
6-Nov-2007	334,000	284,200	194,100	37,500	13.2%	3.20
18-Dec-2007	278,000	248,700	180,700	33,932	13.6%	2.27
21-Mar-2008	910,000	715,300	512,100	75,112	10.5%	12.10
17-Apr-2008	1,425,000	719,100	633,800	91,830	12.8%	16.69
26-Jun-2008	810,000	580,730	447,753	52,940	9.1%	11.70
22-Aug-2008	420,000	361,079	295,977	33,245	9.2%	4.50
24-Oct-2008	259,000	285,828	274,190	30,576	10.7%	4.40
19-Dec-2008	310,000	311,576	227,982	37,289	12.0%	3.00
16-Jan-2009	632,487	535,499	411,878	47,087	8.8%	9.10

**Table H-6: Discharge Record for South Pass.**

Date	Mississippi River			South Pass		New Orleans Stage (8:00 am) FT NGVD
	at Tarbert Landing <sup>20</sup>	at Venice <sup>21</sup>	above West Bay <sup>21</sup>	at entrance	% Venice Flow	
2-Dec-2003	564,000	459,000	355,000	52,900	11.5%	5.92
16-Jan-2004	568,000	527,000	393,000	61,200	11.6%	7.36
13-Feb-2004	575,000	593,000	not taken	69,000	11.6%	8.60
20-Mar-2004	838,000	695,000	547,000	80,100	11.5%	12.24
16-Apr-2004	575,000	575,000	392,000	60,400	10.5%	7.57
12-May-2004	700,000	576,000	443,000	60,900	10.6%	10.66
23-Jun-2004	835,000	647,000	479,000	67,300	10.4%	11.46
4-Aug-2004	383,000	361,000	266,000	44,500	12.3%	4.36
1-Sep-2004	243,000	245,000	176,000	28,500	11.6%	2.58
29-Sep-2004	394,000	375,000	312,000	52,700	14.1%	4.33
27-Oct-2004	256,000	285,000	205,000	31,400	11.0%	2.58
17-Nov-2004	611,000	550,000	445,000	69,200	12.6%	7.73
15-Dec-2004	927,000	843,000	686,000	101,000	12.0%	12.82
3-Feb-2005	1,220,000	903,000	754,000	126,000	14.0%	15.73
1-Mar-2005	801,000	740,000	571,500	84,850	11.5%	11.72
5-Apr-2005	490,000	471,500	367,000	51,750	11.0%	6.41
27-Apr-2005	720,000	551,500	386,500	58,950	10.7%	9.97
18-May-2005	466,000	367,000	291,500	48,800	13.3%	5.38
29-Jun-2005	416,000	344,000	291,500		0.0%	2.80
27-Jul-2005	281,000	256,000	203,000	40,050	15.6%	2.86
19-Jan-2006	296,000	328,000	251,500		0.0%	2.60
16-Feb-2006	484,000	456,000	329,000	48,500	10.6%	5.97
16-Mar-2006	270,000	247,000	175,000	41,600	16.8%	2.65
25-Apr-2006	434,000	385,500	297,500	47,950	12.4%	4.96
22-May-2006	500,000	430,000	343,000	52,850	12.3%	5.73
19-Jun-2006	312,000	299,000	242,000	41,050	13.7%	3.31
17-Jul-2006	224,000	228,500	178,000	36,650	16.0%	2.52
28-Aug-2006	166,000	173,500	118,500	34,750	20.0%	1.99
22-Sep-2006	179,000	129,400	99,600	12,650	9.8%	2.50
19-Oct-2006	265,000	275,650	199,700	47,600	17.3%	3.80
16-Nov-2006	430,000	374,300	289,400	49,577	13.2%	4.17
27-Dec-2006	362,000	340,000	290,000	43,043	12.7%	3.50
25-Jan-2007	901,000	656,800	515,900	82,045	12.5%	12.10
2-Mar-2007	387,000	363,100	301,600	47,964	13.2%	4.70
27-Apr-2007	620,000	536,100	413,000	65,598	12.2%	9.00
25-May-2007	645,000	490,300	392,800	59,199	12.1%	8.98
22-Jun-2007	399,000	356,500	315,000	50,141	14.1%	4.56
20-Jul-2007	580,000	473,400	377,600	59,416	12.6%	6.94
30-Aug-2007	257,000	217,300	144,700	35,179	16.2%	2.65



**Table H-6 Continued.**

26-Sep-2007	237,000	183,100	116,200	40,569	22.2%	2.97
23-Oct-2007	201,000	170,500	126,100	43,500	25.5%	2.90
6-Nov-2007	334,000	284,200	194,100	43,200	15.2%	3.20
18-Dec-2007	278,000	248,700	180,700	32,787	13.2%	2.27
21-Mar-2008	910,000	715,300	512,100	81,327	11.4%	12.10
17-Apr-2008	1,425,000	719,100	633,800	110,720	15.4%	16.69
1-May-2008	1,310,000	926,205	627,681	105,315	11.4%	16.47
26-Jun-2008	810,000	580,730	447,753	60,491	10.4%	11.70
22-Aug-2008	420,000	361,079	295,977	44,709	12.4%	4.50
24-Oct-2008	259,000	285,828	274,190	57,813	20.2%	4.40
19-Dec-2008	310,000	311,576	227,982	34,362	11.0%	3.00
16-Jan-2009	632,487	535,499	411,878	57,712	10.8%	9.10

**Table H-7: Discharge Record for Southwest Pass.**

Date	Mississippi River			Southwest Pass		New Orleans Stage (8:00 am) FT NGVD
	at Tarbert Landing <sup>20</sup>	at Venice <sup>21</sup>	above West Bay <sup>21</sup>	at entrance	% Venice Flow	
2-Dec-2003	564,000	459,000	355,000	210000	45.8%	5.92
16-Jan-2004	568,000	527,000	393,000	174000	33.0%	7.36
13-Feb-2004	575,000	593,000	not taken	222,000	37.4%	8.60
20-Mar-2004	838,000	695,000	547,000	299,000	43.0%	12.24
16-Apr-2004	575,000	575,000	392,000	217,000	37.7%	7.57
12-May-2004	700,000	576,000	443,000	201,000	34.9%	10.66
23-Jun-2004	835,000	647,000	479,000	214,000	33.1%	11.46
4-Aug-2004	383,000	361,000	266,000	130,000	36.0%	4.36
1-Sep-2004	243,000	245,000	176,000	64,900	26.5%	2.58
29-Sep-2004	394,000	375,000	312,000	115,000	30.7%	4.33
27-Oct-2004	256,000	285,000	205,000	47,700	16.7%	2.58
17-Nov-2004	611,000	550,000	445,000	280,000	50.9%	7.73
15-Dec-2004	927,000	843,000	686,000	395,000	46.9%	12.82
3-Feb-2005	1,220,000	903,000	754,000	320,000	35.4%	15.73
1-Mar-2005	801,000	740,000	571,500	265,000	35.8%	11.72
5-Apr-2005	490,000	471,500	367,000	161,500	34.3%	6.41
27-Apr-2005	720,000	551,500	386,500	174,500	31.6%	9.97
18-May-2005	466,000	367,000	291,500	132,500	36.1%	5.38
29-Jun-2005	416,000	344,000	291,500		0.0%	2.80
27-Jul-2005	281,000	256,000	203,000	112,500	43.9%	2.86
19-Jan-2006	296,000	328,000	251,500		0.0%	2.60
16-Feb-2006	484,000	456,000	329,000	152,000	33.3%	5.97
16-Mar-2006	270,000	247,000	175,000	62,950	25.5%	2.65
25-Apr-2006	434,000	385,500	297,500	163,000	42.3%	4.96
22-May-2006	500,000	430,000	343,000	157,000	36.5%	5.73
19-Jun-2006	312,000	299,000	242,000	124,500	41.6%	3.31
17-Jul-2006	224,000	228,500	178,000	50,900	22.3%	2.52
28-Aug-2006	166,000	173,500	118,500	16,100	9.3%	1.99
22-Sep-2006	179,000	129,400	99,600	-25,300	-19.6%	2.50
19-Oct-2006	265,000	275,650	199,700	29,000	10.5%	3.80
16-Nov-2006	430,000	374,300	289,400	122,167	32.6%	4.17
27-Dec-2006	362,000	340,000	290,000	143,600	42.2%	3.50
25-Jan-2007	901,000	656,800	515,900	265,447	40.4%	12.10
2-Mar-2007	387,000	363,100	301,600	137,904	38.0%	4.70
27-Apr-2007	620,000	536,100	413,000	199,734	37.3%	9.00
25-May-2007	645,000	490,300	392,800	193,490	39.5%	8.98
22-Jun-2007	399,000	356,500	315,000	130,516	36.6%	4.56
20-Jul-2007	580,000	473,400	377,600	173,779	36.7%	6.94
30-Aug-2007	257,000	217,300	144,700	17,046	7.8%	2.65

**Table H-7 Continued.**

26-Sep-2007	237,000	183,100	116,200	11,576	6.3%	2.97
23-Oct-2007	201,000	170,500	126,100	-1,600	-0.9%	2.90
6-Nov-2007	334,000	284,200	194,100	38,100	13.4%	3.20
18-Dec-2007	278,000	248,700	180,700	37,492	15.1%	2.27
21-Mar-2008	910,000	715,300	512,100	271,406	37.9%	12.10
17-Apr-2008	1,425,000	719,100	633,800	312,051	43.4%	16.69
1-May-2008	1,310,000	926,205	627,681	310,417	33.5%	16.47
26-Jun-2008	810,000	580,730	447,753	241,466	41.6%	11.70
22-Aug-2008	420,000	361,079	295,977	174,904	48.4%	4.50
24-Oct-2008	259,000	285,828	274,190	171,928	60.2%	4.40
19-Dec-2008	310,000	311,576	227,982	68,752	22.1%	3.00
16-Jan-2009	632,487	535,499	411,878	216,882	40.5%	9.10

## **Appendix I**

### **Flow Roughness Factors**

**Table I-1: Flow Roughness Factors for Mississippi River (all simulations).**

Flow / RS	Roughness Factor					
	306-188.5	188.2-157.8	157.5-118.5	118.2-98.2	81.2-32.7	11.2-10.4
0	-	-	-	1.2	-	-
50000	-	-	-	1.2	1.3	1.5
100000	1	1.2	1.3	1.55	1.3	1.5
150000	1	1.2	1.5	1.6	1.3	1.5
200000	0.9	0.9	1.5	1.6	1.3	1.5
250000	0.9	0.7	1.2	1.6	1.3	1.5
300000	0.9	0.7	1.2	1.65	1.3	1.2
350000	0.9	0.7	1.2	1.6	1.2	1.2
400000	1	0.8	1.1	1.2	1.2	1.2
450000	1.1	0.9	1.15	1.2	1.2	1.2
500000	0.9	0.85	1.1	1.2	1.2	1.2
550000	0.9	0.9	1.15	1.1	1.2	1.2
600000	0.9	0.9	1.15	1.1	1.2	1.2
650000	0.9	0.9	1.15	1.1	1.1	1.2
700000	1.1	0.85	1	1.1	1.1	1.1
750000	1.1	0.8	0.9	1.1	1	1
800000	1.1	0.8	0.9	1.1	1	1
850000	0.9	0.8	0.9	0.9	0.9	1
900000	0.9	0.8	0.9	0.9	0.9	1
950000	0.9	0.8	0.9	0.9	0.9	1
1000000	0.9	0.8	0.9	0.9	0.9	1
1050000	0.9	0.8	0.8	0.9	0.9	1
1100000	0.9	0.9	0.8	0.9	0.9	1
1150000	0.9	0.9	0.8	1	-	-
1200000	0.9	0.9	0.8	1	-	-
1250000	0.9	0.9	0.8	-	-	-
1300000	0.85	-	-	-	-	-
1350000	0.85	-	-	-	-	-

## **Vita**

Mallory Anne Davis was born in Meraux, Louisiana in 1986. She received her B.S. from the University of New Orleans in December 2008. She is currently a candidate for an M.S. in Civil and Environmental Engineering, which will be awarded May 2010.